Water and Urban Initiative Report

Future Outlook of Urban Water Environment in Asian Cities

United Nations University
Institute for the Advanced Study of Sustainability

THE GLOBAL GOALS
For Sustainable Development

Please cite this publication as follows:
"Y. Masago, B. K. Mishra, S. M. Jalilov, M. Kefi, P. Kumar, M. Dilley, K. Fukushi. (2018). Future Outlook of Urban Water Environment in Asian Cities. United Nations University – Institute for the Advanced Study of Sustainability, Tokyo."

This document summarizes the key findings from the Water and Urban Initiative Project. The full report can be accessed from here: http://www.water-urban.org/

This Project and the research leading to these results has received funding from the Ministry of the Environment, Japan, through the Low Carbon Urban Water Environment Project, and the Japan Society for the Promotion of Science through Grant-in-Aid for JSPS Research Fellow.

Designed by MORI DESIGN INC., Tokyo
Printed in Japan

ISBN978-92-808-4593-8

Water and Urban Initiative Report

Future Outlook of Urban Water Environment in Asian Cities

Authors

Yoshifumi Masago
Binaya Kumar Mishra
Shokhrukh-Mirzo Jalilov
Mohamed Kefi
Pankaj Kumar
Misato Dilley
Kensuke Fukushi

Advisor

Chongrak Polprasert
Professor, Thammasat University

UNITED NATIONS
UNIVERSITY

UNU-IAS

United Nations University
Institute for the Advanced Study of Sustainability

5-53-70 Jingumae, Shibuya-ku, Tokyo 150-8925 Japan
Tel: +81 3 5467 1212 Fax: +81 3 3499 2828
ias.wui@unu.edu

ias.unu.edu

Executive Summary

Worldwide, scarce freshwater resources are increasingly being used to satisfy the demands of a rapidly increasing population and a growing global economy. One-third of the world's river basins have reached their capacity for exploitation, and half of the global population is directly affected by water scarcity. Furthermore, the increasing rate of uncontrolled and unplanned urbanization in developing countries in Asia, Africa, and South America is likely one of the most important factors in the decline of the quality of urban water bodies and the increasing health and other associated risks for urban residents.

Many of the largest river systems in the world are in Asia, including the Ganges, Brahmaputra, and Mekong, but according to the water availability per capita, Asia is behind Europe and North and South America (UN Water, 2008). Currently, South and Southeast Asia are affected by clean water scarcity because most domestic wastewater (speculated to be more than 80% by the World Water Assessment Programme, UNESCO, in the "2017 UN World Water Development Report, Wastewater: The Untapped Resource") is directly discharged untreated into oceans, lakes, rivers, and streams. Recent rapid industrial expansion and economic development has affected local water bodies and resulted in unfavorable hydrological, ecological, and environmental changes in many river systems. One of the reasons for such situations is that rapid industrialization and urbanization have not been followed by the development of solid waste and wastewater treatment facilities and other infrastructure. In addition to the contamination of water bodies through toxic industrial chemicals, the lack of household sewerage systems has also contributed to the low water quality in many parts of Asia.

To enhance the capacity of local governments and to increase the understanding of the latest urban water management techniques, United Nations University Institute for the Advanced Study of Sustainability initiated a 4-year project entitled the "Water and Urban Initiative (WUI)" (http://www.water-urban.org/) that aims to contribute to sustainable urban development by creating scientific tools to forecast the future state of urban water environments. The project also seeks to contribute to capacity development aimed at improving urban water environments in developing countries in Asia by focusing on population growth, urbanization, and low-carbon measures. The research findings generated through the interdisciplinary approach of WUI will fill an important gap in the understanding of urban water environments globally and contribute to improved policymaking in this key area.

The purpose of this report is to highlight several cities in Asia where WUI has applied the integrated analysis framework to address and promote sustainable urban water management. Eight cities were chosen from a long list of developing urban areas in Asia to provide a range of geographical, cultural, economic, and hydrological contexts. The main dimensions of the interdisciplinary approach for addressing issues confronting Asian cities and, consequently, those of the initiated research program can be outlined as follows:

Flood risk prevention, management and assessment;
Water quality assessment;
Water-related health risk assessment; and
Economic evaluation of water quality improvement.

Systems analysis is the core of the research under the project with the aim of integrating outcomes from different components and analyzing the results with respect to a comprehensive set of goals and objectives, and the work included studies of technical models and future scenarios affecting water infrastructure in a city. Our case studies highlighted a number of results, lessons, and practical recommendations as important in successfully implementing future sustainable water management strategies and improving decision-making processes in water-related sectors in those countries.

Table of Contents

List of abbreviations

AR5	Fifth Assessment Report
BOD	biochemical oxygen demand
CDF	cumulative distribution function
CDM	Clean Development Mechanism
CMIP5	Coupled Model Intercomparison Project Phase 5
COD	chemical oxygen demand
CVM	contingent valuation method
DEM	digital elevation model
DENR	Department of Environment and Natural Resources
DKI Jakarta	Special Capital City District of Jakarta
DO	dissolved oxygen
FAO	Food and Agriculture Organization of the United Nations
GCM	global climate model
GHG	greenhouse gas
GIS	geographic information system
GPS	global positioning system
IAM	integrated assessment model
IDF	inverse distribution function
IPCC	Intergovernmental Panel on Climate Change
JCM	Joint Crediting Mechanism
LIPI	Lembaga Ilmu Pengetahuan Indonesia
LULC	land use and land cover
MDGs	Millennium Development Goals
MWSS	Metropolitan Waterworks and Sewerage System
NCR	National Capital Region
PAGASA	Philippine Atmospheric, Geophysical and Astronomical Service Administration
PMMoV	Pepper Mild Mottle Virus
QMRA	quantitative microbial risk assessment
RCP	representative concentration pathway
SDGs	Sustainable Development Goals
UASB	upflow anaerobic sludge blanket
UN	United Nations
UN DESA	United Nations Department of Economic and Social Affairs
UNU-IAS	United Nations University - Institute for the Advanced Study of Sustainability
WEAP	Water Evaluation and Planning
WMS	Watershed Modeling System
WSUD	water-sensitive urban design
WTP	willingness to pay
WUI	Water and Urban Initiative
WWTP	wastewater treatment plant

1 Background

1.1 Urbanizing Asian cities

The process of urbanization is defined as the population shift from rural to urban areas that results in increasing populations in cities and towns. The main cause of this process is industrialization and economic development, which lead to greater labor specialization and division when industries absorb the surplus labor force that cannot be employed in agriculture. Cities provide job opportunities for masses of people that move away from the countryside; these migrants provide emerging industries with a cheap, abundant, and productive labor force.

The rate of urbanization is increasing worldwide, especially in developing countries. According to the United Nations (UN), the global population was evenly split between urban and rural areas for the first time in 2008. By 2050, it is expected that 70% of the global population will be living in urban areas and that urban growth will mostly occur in less developed countries (UN DESA, 2015).

The urbanization in the developing countries of Asia has specific characteristics that are different from those of urbanization in developed and developing countries in other parts of the globe. While the cause of urbanization in developed countries is mainly migration from rural to urban areas, that in developing countries is also influenced by natural population growth (births exceeding deaths), which is substantial in some cases. In addition, a large portion of rural-to-urban migration takes place because of economic hardship, as the rural and landless people of the countryside move to cities and towns in the hope of a better life and employment. However, in the absence of clear and effective governance policies, cities cannot satisfy and accommodate the needs of an ever-increasing number of such migrants. For instance, in cities such as Chennai, Metro Manila, and Jakarta, many of the wealthiest people, business leaders, and the middle class live alongside many people that occupy officially defined slums.

The population growth in urban areas is often associated with a lack of appropriate infrastructure and adequate residential areas, which results in an expansion of informal settlements. Due to rapid urbanization combined with a high rate of economic development, cities are experiencing the degradation and depletion of natural resources, including water, with detrimental impacts on human health, economic productivity, the quality of freshwater resources, and ecosystems. In recognition of these challenges associated with urbanization, the New Urban Agenda, which was adopted at the UN Conference on Housing and Sustainable Urban Development (Habitat III) in 2016, called for action to promote sustainable urbanization.

Therefore, it is important to remember that “urban” does not automatically mean a developed city with literate people who have access to basic utilities such as electricity, water and sanitation. Many Asian cities still lack good roads as well as adequate and accessible schools, hospitals, government services, etc., and in many cases, these deficiencies make the cities little different from the places the migrants left in seeking a good life.

1.2 Climate change

Climate change is triggered by many factors, including oceanic processes (such as oceanic circulation), biotic processes, variations in the solar radiation reaching the Earth, plate tectonics, volcanic eruptions, and anthropogenic alterations of the natural world. Human activities, primarily the burning of fossil fuels and changes in land cover/use, are believed to be increasing the concentrations of greenhouse gases (GHGs), which alters energy balances and leads to atmospheric warming that results in climate change. Global climate change is largely attributed to disruptions in the ways that people live and interact with their environment, and its impacts include alteration of ecosystems, interruption of food production and water supply, damage to infrastructure, increases in human morbidity and mortality, and consequences for mental health and human well-being (IPCC, 2014). The consequences of climate change are already becoming evident in the changes in the amount, intensity and frequency of precipitation as well as temperature in many parts of the world that are likely to increase the frequency of disastrous floods. Traditional flood management practices, which are based on structural solutions assuming floods of a given, constant return period, would definitely not be valid in the context of climate change. For countries at all levels of economic and technological development, these effects will be exacerbated by a significant lack of adaptation to current climate variability in many sectors. Among the problems caused and aggravated by climate change, the impact to the water sector is one of the critical issues; precipitation will have an especially important influence due to climate change. Asia has been affected by more hydrometeorological events, such as floods and storms, than any other region of the world (EM-DAT, 2010), and in recognition of the economic significance of water resources, many studies have sought to examine the effects of climate change on precipitation patterns and hydrologic regimes (Dore 2005, Kleinn et al., 2005, Abbs et al., 2007). These studies suggest clear regional precipitation trends that may increase in the future due to climate change. In particular, wet regions are increasingly experiencing higher levels of precipitation, whereas arid areas are witnessing reduced levels and becoming drier. The risk of climate change is expected to exacerbate the current flooding trends and introduce new, hitherto unknown challenges to flood management in most countries in South and Southeast Asia as well as China, which are the most populous regions.

Climate change is projected to increase the global temperature and intensify the global water cycle, increasing both extreme events and the number of non-rainy days, causing multiple stresses from floods and droughts, respectively. It is difficult to precisely predict the future climate due to uncertainties in climate models and various other sources, but understanding climate change and variability is important for impact assessment and adaptation. Climate projections are the main tools used to understand the expected impact of climate change on different sectors in a country. These projections are synthetic time series of climate variables with the goal that the time-series models will match the real-world data, and they can be for past, present and future conditions. The Intergovernmental Panel on Climate Change (IPCC) Fifth Assessment Report (AR5) concludes that the warming of the climate system is unequivocal and that limiting climate change requires substantial and sustained reductions in GHG emissions.

Global climate models (GCMs) simulate the response of GHGs concentrations and provide estimates of climate variables such as temperature, precipitation, etc. (Mishra and Herath, 2011). Such coupled climate–carbon cycle models simulate the natural exchange of terrestrial and oceanic carbon with the atmosphere, thus providing a predictive link between emissions and atmospheric concentrations of CO_2. These models calculate changes in atmospheric CO_2 concentrations given an emissions scenario that is required to follow a prescribed concentration pathway. GCMs are currently the most credible tools for simulating the response of the global climate system to increasing GHGs concentrations, and they provide climatic variables such as temperature and precipitation. The GCM output is used for climate predictions and to study climate variability and change. The approach is a combination of numerical models that can simulate important global climate features at the continental scale, such as the atmospheric circulation cells, intertropical convergence zones, and jet streams, and they can also simulate oceanic circulation reasonably well, including the conveyor belt and thermohaline circulation (Zorita and Storch 1999). The models calculate interactions based on the predefined physical laws within and across different grids (based on resolution) to represent climate behavior over time, and those with higher resolution potentially enable better representation of local features.

The GCM outputs are based on coarse-resolution information (e.g., topography and land surface), which is used to generate climatic variables, but the forcing and circulation that affect local (basin-level) climate generally occur at a much finer scale. Therefore, directly using GCM outputs is not suitable for impact assessment. To bridge the gaps between the scale of GCMs and local scales and to account for inaccuracies in describing rainfall extremes, downscaling methods are commonly used in climate change studies. Downscaling is the process of deriving local-level climate projections from the GCM outputs. There are various downscaling techniques to convert GCM outputs into locally applicable climate data that are broadly classified as either dynamical or statistical methods (Mishra and Herath, 2011). Dynamic downscaling includes nesting high-resolution Regional Climate Models within GCMs, which ensures consistency between climatological variables, but this approach is computationally demanding. On the other hand, statistical downscaling methods use statistical relationships between large-scale and local-scale climate variables. Spatial downscaling is the process of deriving finer-resolution (i.e., local) climate data from the coarse GCM output for studies of climate change impacts at the local level. The GCM outputs are typically at a course spatial resolution of hundreds of kilometers, whereas the resolution required for impact assessments is like that of daily temperature and rainfall.

The latest generation of the state-of-the-art Earth system GCMs has recently been used to carry out simulations for Coupled Model Intercomparison Project Phase 5 (CMIP5) (Taylor et al., 2012; Moss et al., 2010) that include a new set of four future socioeconomic scenarios referred to as representative concentration pathways (RCPs): RCP 2.6, RCP 4.5, RCP 6.0, and RCP 8.5 (Moss et al., 2010). These future scenarios include a CO_2 concentration pathway computed to be consistent with anthropogenic carbon emissions as generated by four integrated assessment models (IAMs). The RCPs are labeled according to the approximate global radiative-forcing level in the year 2100.

1.3 Urban flood risk

Urban flooding results in economic loss as well as social discomfort for the people who live in and commute to cities. The causes of urban flooding are very complicated due to the conditions of the drainage system, urban flood control facilities, geography of the urban area, rainfall intensity and so on, so urban areas can be more or less vulnerable to flooding depending on the case. To deal with urban flooding, it is necessary to consider the interactions among the components of the entire system. Southeast and South Asia are known as hot spots of natural disasters, of which flooding has been the most common form and responsible for damages to human lives/settlements, agriculture, infrastructure and other properties. Flooding in the region results from a wide range of factors and processes, including concentrated precipitation, cloudbursts, snow melt, and glacial lake outburst. In addition, the tropical monsoon climate and fragile geology and physiography of the region create conditions that result in flood events of catastrophic magnitude. Urban areas, where impervious materials cover much of the land surface, are characterized by reduced infiltration and accelerated runoff, so they suffer from floods even in non-floodplain areas. Historically, riverine flooding and flash flooding along floodplains have received considerable attention (Parker, 1980). Complexities in the urban environment and drainage infrastructure have an inherent influence on surface runoff, which generates urban flooding and poses challenges for modeling urban flood hazard and risk.

Rapid urbanization and climate change are the most important challenges facing the region, posing unprecedented multidimensional challenges for all countries and communities in Monsoon Asia. These changes will affect water resources in both quantity and quality, so water, storm water, and wastewater infrastructure will face greater risk of damage. The effects of unplanned urbanization and climate change will manifest as difficulties in operations to disrupted services, thus increasing the cost of water and wastewater services. Therefore, governments, planners, and water managers must re-examine processes for the development of municipal water and wastewater services as well as adaptation strategies to incorporate land use and climate change into infrastructure design, capital investment projects, service planning, and operation and maintenance.

Construction of drainage networks generally shortens the time for the concentration and increases direct runoff, resulting in more rapid rise in streamflow and depletion of the water table (Willems et al., 2012). Additionally, natural water bodies, such as lakes, wetlands, and waterways, which can hold a considerable amount of floodwater, have been largely reduced or filled, increasing the incidence of flooding. Rapid land use changes in developing countries and an increase in extreme rainfall events could potentially result in elevated flood risk, particularly in megacities, due to inadequate drainage systems (Rafiei Emam et al., 2016, Mishra et. al., 2017).

Urbanization changes hydrological behavior by reducing infiltration, base flow, and lag time while increasing surface runoff, peak flow, flow volumes, and flooding frequency. Therefore, land use changes coupled with climate change may have adverse effects on hydrological behavior and flooding or drought frequencies. However, some elements of the water cycle can be ignored due to the time scale of urban floods. Transpiration, evaporation, and groundwater flow are very slow processes, so these elements have no significant influence on urban flooding. Therefore, rainfall,

infiltration, vegetal interception, depression storage, and surface runoff are the important components for consideration.

Changes in climate patterns affect water availability and run-off, which alter the flood regimes of rivers. Urbanization is occurring at a high rate in developing countries, and the IPCC report (2014) stated that a greater number of regions are likely to experience extremely heavy precipitation and flood events in the future. Under an energized global water cycle, the future climate may be characterized by increased rainfall intensities as well as longer non-rainy days, so an increase in intense rainfall events as well as prolonged periods of water scarcity are two of the most pressing problems associated with climate change in Monsoon Asia. The expected impacts of climate change, the increased rainfall intensities and the resulting increase in direct runoff and thus the rapid rise in stream flow and the depletion of the groundwater table, are similar to the impacts of urbanization on the water cycle.

The increasing frequency of urban flood disaster events has threatened human lives and infrastructure, causing greater economic losses. Disasters are recognized as a factor constraining development and contributing to poverty (Moench et al., 2007). In 2016, the occurrence of hydrological disasters such as floods and landslides rose compared to the previous decade (2006 – 2015), and hydrological events represented 51.7% of the total natural disasters that occurred in 2016 compared to 50.5% for the 2006–2015 period. Additionally, the total cost due to hydrological disasters in 2016 was estimated to be 59 billion USD, representing 74% of the annual average for the period (2006 - 2015) (Guha-Sapir et al., 2016). Among the damages caused by hydrological disasters, flooding was estimated to account for 98.8% of the total in 2016 (Guha-Sapir et al., 2016). It has been shown that the impact of a natural disaster will affect the GDP of a country, not only during the year of a given event but in successive years as well (ADB, 2013). Due to various factors (e.g., geographic location, climate, rapid urbanization), Asian regions are considered the most exposed to flood hazards in the world. The occurrence of natural disasters has risen considerably, and the risk in Asia is higher than that in Europe and Africa. The increase in potential damage and the vulnerability of the people has led local decision makers and governments to adopt and implement flood control measures to attenuate disasters in urban areas. Three international frameworks, namely, the Sustainable Development Goals (SDGs), the Paris Agreement on Climate Change, and the Sendai Framework for Disaster Risk Reduction, were adopted in 2015. Disaster risk reduction is expected to contribute to achieving development objectives and the response to the increasing hazards that are projected due to global warming (Moench et al., 2007). Additionally, the quantification and valuation of flood damage are important factors in decision-making strategies for specific flood risk management measures.

1.4 Water pollution

Water is the most vital natural resource that has both social and economic value for human beings (Hanemann et al., 2006). The average water availability per capita is currently sufficient, but the spatiotemporal asymmetry is great. At present, more than 1.1 billion people around the globe do

not have adequate access to clean drinking water (Pink, 2016). On the other hand, rapid population growth, urbanization, economic development, and climate change exert constant and tremendous pressure on water resources and the associated ecosystems, resulting in severe water quality crises and water scarcity (Mukate et al., 2017). Degradation of the urban water environment is a challenging issue in developing nations despite the adoption of a number of countermeasures (Ismail and Abed, 2013). Asian economies have shown rapid growth and urbanization, and the accompanying demands on the water, land, and ecosystems as resources pose significant challenges for the delivery of commodities such as food, energy, and water for municipal and industrial purposes. The discussion regarding water in South Asia, in particular, is vociferous, antagonistic, and increasingly associated with national security. Renewable water resources in the region have fallen dramatically on a per capita basis since the 1960s and reached the level of water stress of countries such as India, Pakistan, and Afghanistan by 2015 (Gareth et al., 2014). The expected impacts of climate change will further exacerbate the challenges facing planners and providers of such services, so the delivery of sustainable water and sanitation services in growing towns and cities remains an issue. Considering the current water stress and scarcity, the UN has called for sustainable water resource management to achieve water security, which means securing sufficient water of good quality, for all by the year 2030 as the main agenda of the SDGs (Bos et al., 2016).

1.5 Sustainable Development Goals

In September 2015, world leaders adopted the 2030 Agenda for Sustainable Development and SDGs to end poverty, flight inequality, tackle climate change and ensure prosperity for all in 15 years. The SDGs are built on the success of the Millennium Development Goals (MDGs), and the 17 goals have a total of 169 specific identified targets for achievement. It is argued that the SDGs are unique in that the goals require actions by all countries, so a holistic approach is necessary. Indeed, the 17 goals are complementary; for example, Goal 1of eradicating poverty will not be realized unless the issue of climate change (Goal 13) is addressed.

The same applies to the achievement of sustainable water management. The world has met the target of halving the proportion of people without access to improved sources of water five years ahead of schedule according to the MDGs. However, almost 840 million people remained without access to an improved source of drinking water in 2017, and 2.5 billion people in developing countries still lack access to basic sanitation (WHO and UNICEF, 2017). Hence, the SDGs recognize access to water and sanitation as a human right. In particular, Goal 6, "Ensure availability and sustainable management of water and sanitation for all" is dedicated to water. However, there are many other SDGs with water-related targets, including Goal 3 "Ensure healthy lives and promote well-being for all at all ages", Goal 11 "Make cities and human settlements inclusive, safe, resilient and sustainable", Goal 12 "Ensure sustainable consumption and production patterns", Goal 14 "Conserve and sustainably use the oceans, seas and marine resources for sustainable development", and Goal 15 "Protect, restore and promote sustainable use of terrestrial ecosystems, sustainably manage forests, combat desertification, and halt and reverse land degradation and halt biodiversity

loss." Therefore, it could be argued that tackling the issue of water is essential to the overall success of the SDGs.

References

Abbs, D.; McInnes, K.; Rafter, T. *The impact of climate change on extreme rainfall and coastal sea levels over south-east Queensland. Part 2: A High-Resolution Modelling Study of the Effect of Climate Change on the Intensity of Extreme Rainfall Events*; Division of Marine and Atmospheric Research, Commonwealth Scientific and Industrial Research Organization: Aspendale, Australia, 2007.

Asian Development Bank. *The Rise of Natural Disasters in Asia and the Pacific: Learning from ADB's Experience*; Asian Development Bank: Mandaluyong, Philippines, 2013.

Bos, R.; Alves, D.; Latorre, C.; Macleod, N.; Payen, G.; Roaf, V.; Rouse, M. *Manual on the human right to safe drinking water and sanitation for practitioners*; IWA Publishing: London, UK, 2016.

Dore, M.H.I. Climate change and changes in global precipitation patterns: What do we know?; *Environ. Int.*, 2005, 31(8): 1167–1181.

EM-DAT. *The Emergency Events Database*, Université Catholique de Louvain, Brussels, Belgium, 2010.

Gareth, P. *Attitudes to water in South Asia*. Chatham House: London, UK, 2014.

Guha-Sapir, D.; Hoyois, P.; Wallemacq, P.; Below, R. *Annual Disaster Statistical Review 2016: The Numbers and Trends*; Université Catholique de Louvain: Brussels, Belgium, 2016.

Hanemann W.M. The economic conception of water. In *Water Crisis: myth or reality?*; Rogers, P.P., Llamas, M.R., Martinez-Cortina, L., Eds.; Taylor & Francis, London, UK, 2006.

Intergovernmental Panel on Climate Change. *Climate Change 2014: Synthesis Report*. Core Writing Team; Pachauri, R.K., Meyer, L.A., Eds.; IPCC, Geneva, Switzerland, 2014.

Ismail, A.H.; Abed G.A. BOD and DO modeling for Tigris River at Baghdad city portion using QUAL2K model, *Journal of Kerbala University* **2013**, 11(3): 257-273.

Kleinn, J.; Frei, C.; Gurtz, J.; Luthi, D.; Vidale, P. L.; Schar, C. Hydrological simulations in the Rhine basin by a regional climate model. *J. Geophys. Res.* **2005**, 110, D04102.

Mishra, B.; Herath, S. Climate projections downscaling and impact assessment on precipitation over upper Bagmati River Basin, In *Proceedings of Third International Conference on Addressing Climate Change for Sustainable Development Through Up-scaling Renewable Energy Technologies*, Tribhuvan Univ., Kathmandu, Nepal, 2011, pp. 275–281.

Mishra, B.K.; Rafiei-Emam, A.; Masago, Y.; Kumar, P.; Regmi, R.K.; Fukushi, K. Assessment of future flood inundations under climate and land use change scenarios in the Ciliwung River Basin, Jakarta. *J. Flood Risk Manag.* **2018**, 11(S2): S1105-S1115.

Moench, M.; Mechler, R.; Stapelton, S. *The costs and benefits of disaster risk management and cost benefit analysis*; United Nations International Strategy for Disaster Reduction: Geneva, Switzerland, 2007. https://www.unisdr.org/files/1084_InfoNote3HLdialogueCostsandBenefits.pdf [Accessed on 25 November 2017]

Moss, R.,H.; Edmonds, J.A.; Hibbard, K.A.; Manning, M.R.; Rose, S.K.; van Vuuren, D.P.; Carter, T.R.; Emori, S.; Kainuma, M.; Kram, T.; Meehl, G.A.; Mitchell, J.F.; Nakicenovic, N.; Riahi, K.; Smith, S.J.; Stouffer, R.J.; Thomson, A.M.; Weyant, J.P.; Wilbanks, T.J. The next generation of scenarios for climate change research and assessment. *Nature* **2010**, 463(7282): 747-56.

Mukate, S.; Panaskar, D.; Wagh, V.; Muley, A.; Jangam, C.; Pawar, R.; Impact of anthropogenic inputs on water quality in Chincholi Industrial area of Solapur, Maharashtra, India. *Groundwater Sustain. Dev.* 2017, Article in press.

Ward, R. *Floods - A Geographical Perspective*; Macmillan: London, UK, 1978.

Pink, R.M. *Water Rights in Southeast Asia and India*; Palgrave Macmillan: Basingstoke, UK, 2016.

Rafiei Emam A.; Mishra B.K.; Kumar P.; Masago Y.; Fukushi K. Impact assessment of climate and land-use changes on flooding behavior in the upper Ciliwung River, Jakarta, Indonesia. *Water* **2016**, 8: 559.

Taylor, K.E.; Stouffer, R.J.; Meehl, G.A. An overview of CMIP5 and the experiment design. *Bull. Am. Meteorol. Soc.* **2012**, 93: 485–498.

United Nations Department of Economic and Social Affairs, Population Division *World Urbanization Prospects: The 2014 Revision*; ST/ESA/SER.A/366; United Nations: New York, NY, 2015.

Willems, P.; Olsson, J.; Arnbjerg-Nielsen, K.; Beecham, S.; Pathirana, A.; Gregersen, I.B.; Nguyen, V.T.V. *Impacts of climate change on rainfall extremes and urban drainage systems*; IWA Publishing: London, UK, 2012.

World Health Organization and (WHO) and the United Nations Children's Fund (UNICEF) *Progress on drinking water, sanitation and hygiene: 2017 update and SDG baselines*; World Health Organization and (WHO) and the United Nations Children's Fund (UNICEF): Geneva, Switzerland, 2017.

Zorita, E.; von Storch, H. The Analog method as a simple statistical downscaling technique: Comparison with more complicated methods. *J. Clim.* **1999**, 12(8): 2474–2489.

2 Aims and strategies

2.1 Research framework

The growing recognition of complexity requires systems approaches to solve urban water management issues. Integrated systems approaches involve interdisciplinarity, as complex city infrastructures comprise diverse and intersecting natural, technical, and institutional dimensions (Mark et al., 2015). Therefore, properly understanding these issues and finding the ways to solve them requires researchers and professionals from different academic and professional disciplines to provide input, exchange opinions, and learn from each other to discover new, creative solutions. In this work, an integrated approach is applied to interrelate the abovementioned four services of urban water management (Figure 2.1).

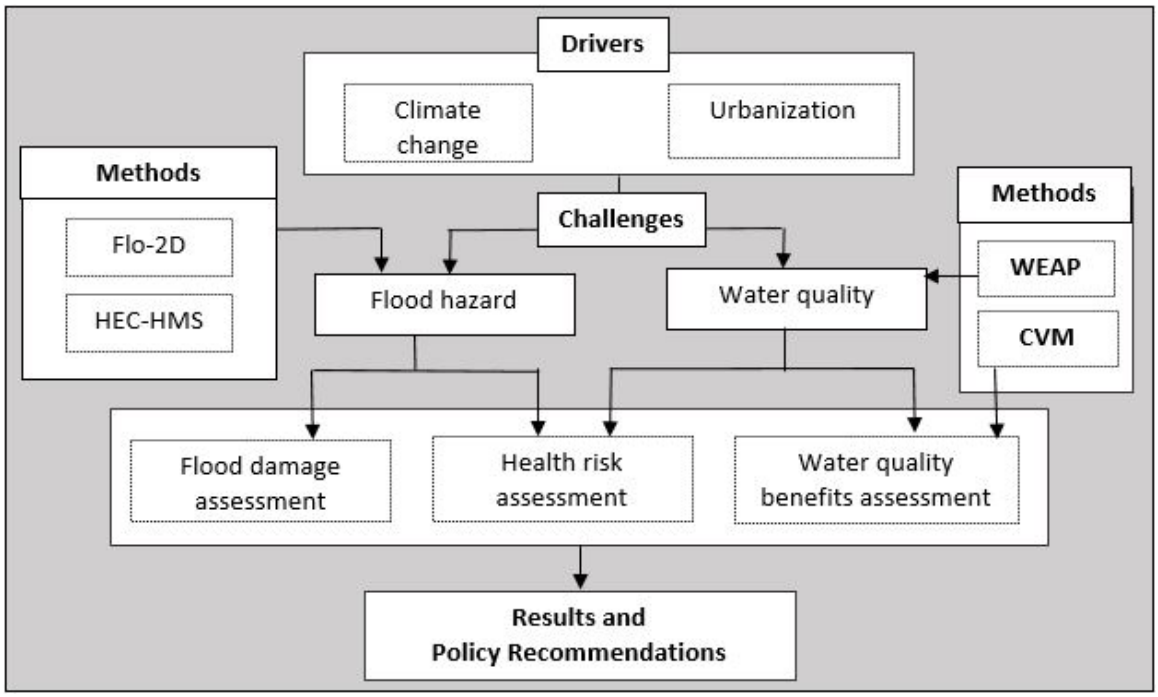

Figure 2.1 Research framework implemented in this study

The primary goal of the WUI project is to develop and apply science-based research to assess the value of sustainable water environments in urban areas with a focus on Asia. Simulation models accompanied by scenario analyses were developed to project various elements of future urban water environments (e.g., water quality, urban flooding) and to estimate the benefits of improving them. A scenario-based planning approach enables WUI experts to answer "what-if" questions by predicting and analyzing future water pollution. The analysis of water problems relies on scenarios under current conditions and possible future situations (various degrees of intervention). Predictive models make it possible to simulate future water environments by considering changes in land cover, population, climate, water infrastructure, and other factors. The research findings generated

through the interdisciplinary approach of WUI will fill an important gap in the global understanding of changes in urban water environments and contribute to improved policymaking in these key areas.

The main dimension of the interdisciplinary approach for addressing issues confronting Asian cities and, consequently, that of the research program can be outlined as follows: a) flood risk assessment and management, including an economic assessment of the physical damage caused by urban flooding; b) water quality assessment; c) flood water-related health risk assessment; and d) economic evaluation of water quality improvement (Figure 2.1). The systems analysis is the core of the research framework, which aims to integrate the outcomes of one study into another and analyze results with respect to a series of comprehensive goals and objectives. The procedure used in studies that utilize systems analysis includes research in different selected cities, technical models, and future scenarios affecting urban water infrastructure.

2.2 Flood hazard

Flood hazard can be characterized by the depth of water, flow velocity, and flood duration over the ground surface. In this study, water depth was adopted as the main factor in the flood hazard assessment. Flood hazard analysis was explored at different spatial and temporal scales considering various simulation times and data. The effects of climate and land cover changes were evaluated by carrying out a flood inundation simulation for 2030 to analyze future flood damage, and various scenarios based on the implementation of potential flood control measures were analyzed to demonstrate the effects of adaptation strategies. The master plan as well as the stakeholders of the city were consulted to determine the effectiveness of potential countermeasures while carrying out the flood hazard simulation. Computer-based modeling was utilized to assess and analyze the hazard and vulnerability as well as to facilitate the comprehension of the magnitude and frequency of flood events.

Flood hazard estimation requires a detailed understanding of flood inundation characteristics at various locations within the target area. This study assessed the likely impacts of climate, land cover change and flood control measures on flood inundation in rapidly growing cities to design strategies to achieve a sustainable urban water environment. Prior to flood hazard simulation, various input data, tools, and techniques were reviewed as well as various climate and land cover change impact studies on hydrometeorology. Additionally, the likely changes in extreme precipitation, flood discharge, and inundations were analyzed using different tools and techniques. Land cover data were largely based on Landsat imagery and their projections using Land Change Modeler for ArcGIS (Jain et al., 2010).

Various structural and nonstructural countermeasures are applied to mitigate flood events and their effects. Because urban rivers flow through densely populated areas, there is little room for widening channels or large centralized structures, which necessitates a comprehensive approach and distributed facilities for flood-risk control in urban areas. While the general climate change trends are known, predicting the degree of change between the present and a given future date is difficult. The future climate could be very different depending on the most likely global future scenario

selected, and the projections of future climate made by different GCMs are subjected to assumptions in the models related to the representation of physical processes, parameterization, model complexity, and so on. Thus, there is great uncertainty in what the future climate could be, and this is especially manifested in rainfall projections, which exhibit large differences among models. Such inconsistencies in rainfall projections make it difficult to adopt large investments in infrastructure for future water security and thus reduce the available options for response. Considering the uncertainties related to future climate change, the measures must be incremental, and the response targets must be continuously improved as the accuracy of the projections increase and new knowledge is generated. Multiple GCMs and RCPs were employed to provide a range of extreme rainfall values and thus a range of flood depths. To reduce the number of hydrologic simulations, climate scenarios were broadly classified into two categories, moderate and extreme, considering the mean values of the projected extreme rainfall events.

Due to the difficulties in meeting even the present flood control targets, it is not feasible to seek large investments for further flood controls, especially given the large degree of uncertainty associated with climate change. Therefore, basin-wide "soft" measures for flood risk reduction, known as water-sensitive urban design (WSUD), are imperative for meeting the flood control demands of the future.

Soft measures that can be readily adopted under uncertain future climate include onsite measures in the form of storage facilities that are incorporated into city planning to prolong the concentration time combined with facilities to infiltrate excess rainfall runoff from rooftops and paved areas to reduce the direct runoff volume. To address urbanization through WSUD measures, greater infiltration and preservation of lost water bodies were considered. The research investigated the stability of local water cycles to inform sustainable water management in densely populated urban areas and adopted an integrated water management approach by understanding and managing the total hydrological cycle.

There is increasing recognition that flood risk reduction, such as the reduction of other disaster risks, should be "mainstreamed" into the development process. Therefore, flood risks must be factored into various city sectoral strategies and policies, and this requires understanding the effects of potential flood hazards on various development programs, how the policies and programs in other development sectors influence the magnitude of the flood hazards, and the vulnerability of the society to the flood hazards. The most common approach has been to combine basin-scale hydrologic-hydraulic models, so a representative river basin was selected to understand the flood risk. A hydrologic model was not necessary for cities where the complete river system was well within the urban boundary.

2.3 Flood damage

In recent decades, natural disasters, including flooding, have become more common and severe. Flood hazards induce catastrophic consequences for the affected people and national economies, and the impacts can be divided into three categories: social, economic, and environmental (Mechler,

2016). In particular, climate change and unplanned urbanization in developing countries are the main drivers increasing the frequency and strength of urban flood disasters (Mishra and Herath, 2014). Local decision makers, governments, and the international community are aware of this situation and the risk of flooding to people, infrastructure, and national economies, so many strategies have been adopted in different countries and several international agreements have been ratified. The uncertainty and unpredictability of flooding are forcing local governments to pay attention to this type of natural disaster, so a better understanding of projected flood risks will be very useful to decision makers in adopting suitable flood control strategies and enhancing the efficiency of mitigation measures. Moreover, quantification of flood loss can be a significant parameter to boost the attentiveness of local decision makers in the implementation of suitable flood control measures (Kefi et al., 2018). Some approaches have been applied to estimate flood damage, which is classified as tangible or intangible and direct or indirect (Jonkman et al., 2008). Tangible damage is measured in monetary terms, while intangible economic damage cannot be measured directly. Direct damage is mainly due to the physical impacts of the hazard, but the impacts on national economies and interruptions of business can be considered indirect damage. In this work, the main objective is to estimate future tangible direct flood damage in target cities using an approach based on integrating hydrologic and economic data in a geographic information system (GIS).

2.4 Water quality

Improving the urban water environment is of great significance considering the close linkage between humans and ecosystems and biodiversity and the impacts of water scarcity on different uses such as fishing, recreation, tourism, and cultural and religious activities. Therefore, we aim to contribute to sustainable urban development by creating scientific tools to forecast the future state of urban water environments and by contributing to capacity building in the target areas.

To achieve the aforementioned goal, the strategies were divided into two parts: generating science-based evidence and providing recommendations to policy makers or stakeholders to better manage water resources in the future. To create science-based evidence, we aimed to assess water quality according to key factors under various scenarios, including population growth, urbanization, and climate change in the target cities. While building and running the numerical simulations, we engaged in active discussions with local counterparts to improve the fit of the models to the real situations and to predict the future conditions considering existing master plans for wastewater management in the year 2030.

2.5 Economic benefit of improving urban water quality

A clean water environment has important amenity values that contribute to the quality of urban life. The majority of urban water benefits represent nonconsumptive use values that include benefits derived from pleasant views and clean air as well as recreational activities and aesthetics. Damages to and the pollution of urban watercourses, rivers, canals, and wetlands cause negative externalities,

e.g., the loss of non-priced benefits, so amenity values should be systematically assessed in urban planning and measured in monetary terms. The empirical study used the contingent valuation method (CVM) to examine the benefits of a clean urban environment associated with willingness to pay (WTP). The study was designed to measure the use- and non-use values of a clean urban water environment based on two water quality standards, swimmable and fishable, and the results were used to perform a cost-benefit analysis of current and future water-related management issues and various urban planning decisions.

2.6 Floodwater-borne infectious diseases

Urban flooding and heavy rainfall are often associated with waterborne infectious diseases. Flooding causes municipal wastewater to overflow from urban sewerage, septic tanks, and latrines, all of which contain pathogenic microorganisms. Various types of microorganisms have been identified in water, and the symptoms caused by the different pathogens vary from mild and self-limited discomfort to fatal diseases, including diarrhea (many pathogens), dysentery (*Shigella* spp., *Entamoeba hystolytica*), cholera (*Vibrio cholerae*), typhoid (*Salmonella enterica* serovar Typhi), and leptospirosis (*Leptospira* spp.). Several epidemiological studies have revealed that flooding events, especially those in urbanized areas, are related to outbreaks of waterborne diseases. For example, Su et al. (2011) found a significant relation between heavy precipitation and the occurrence of leptospirosis, and Huang et al. (2016) found an increased number of gastroenteritis cases after flooding events.

To assess the health risks caused by pathogens in floodwater, numerical simulation models were developed using the quantitative microbial risk assessment (QMRA) framework. The models can quantify the health risk as the number of gastroenteritis cases following a flooding event using the outputs of the flood inundation model and the water quality model together with other input data. Norovirus was selected as a reference pathogen to represent various pathogens found in water because it is the leading cause of acute gastroenteritis worldwide with 698.8 million cases and 218,800 deaths annually (Bartsch et al., 2016), and the virus has been detected in domestic wastewater, river water, and floodwater in Southeast Asian countries (Phanuwan et al., 2006, Kuroda et al., 2015). Hypothetical scenarios were developed to simulate the exposure of residents to the pathogens by unintentional ingestion of floodwater during outdoor activities (e.g., walking and wading). Based on the model output, health risk maps were generated under different scenarios that showed the geographical distribution of gastroenteritis cases.

2.7 Low-carbon technology in wastewater facilities

2.7.1 Objectives of the low-carbon technology assessment

The low-carbon technology assessment has the following objectives:

- To forecast future GHG emissions from wastewater management systems according to the development scenarios;

- To estimate the effects of reducing GHG emissions by introducing low-carbon technologies; and
- To develop a guide for estimating GHG emissions from wastewater management systems for wide use by policy makers and practitioners.

2.7.2 Activities conducted under the assessment

The assessment is composed of the following steps, which are shown in Figure 2.2. The assessment begins from the baseline settings, such as the target city, target GHGs and target year, etc., with the collection of relevant information. After reviewing the methodologies related to GHG emissions from wastewater management, those applicable to the target cities are selected and tailored, and the scenarios assuming the introduction of low-carbon technologies are developed simultaneously. Then, GHG emission reduction is estimated for each scenario using the developed methodologies. To widely distribute the calculation method, the steps taken to calculate GHG emission reduction are summarized as a guide and combined with the calculation sheets. The steps are also described in Section 3.9.

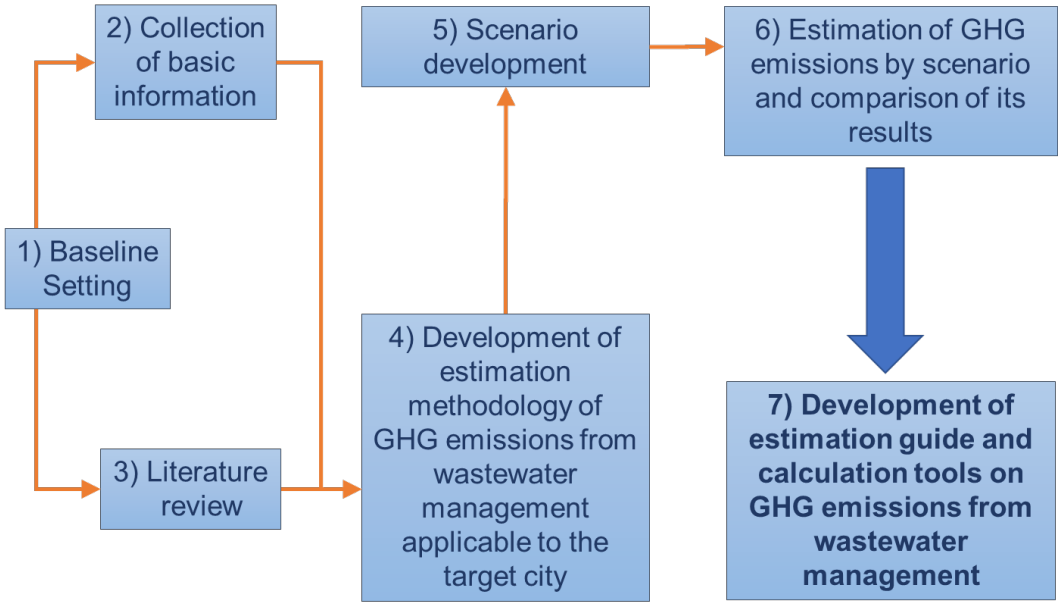

Figure 2.2. Overall workflow of the assessment

2.8 Public engagement

As an initiative under the United Nations University - Institute for the Advanced Study of Sustainability (UNU-IAS), the research of WUI is directed towards issues of great policy relevance, so WUI works closely with governments and other partners to translate UN agreements into national and local actions in study cities. In particular, WUI aims to engage with city authorities to convert project findings into policy interventions.

The policy dialogue activities target government officials, practitioners, researchers, and donor agencies in two phases. In the first phase, workshops with stakeholders are carried out to assess the policy needs and interests of governments in study cities and to identify areas of cooperation for refining model analyses and policy recommendations. In the second phase, additional workshops are held to deliver the results of case studies and policy recommendations for adoption by government counterparts. To ensure that the participants of the workshops are as broadly representative as possible, stakeholder mapping is conducted because such identification is one of the key elements of successful public engagement (OECD, 2012).

Furthermore, WUI aims to strongly emphasize capacity building activities to advance global efforts towards a more sustainable future. Indeed, WUI disseminates project outputs and conducts a number of model training workshops in collaboration with local research institutions.

Furthermore, a series of training workshops are held that target researchers and practitioners involved in developing strategies that advance sustainable water environments. The aim of these training workshops is to provide guidance and practical experience for potential model users and to enable model application and customization.

2.9 Case study locations

This project selected eight cities in six countries (Figure 2.3) as the target areas for the case studies, namely, Chennai (India), Hanoi (Vietnam), Jakarta (Indonesia), Kathmandu (Nepal), Lucknow (India), Manila (Philippines), Medan (Indonesia), and Nanjing (China). These cities are facing rapid population growth and urbanization and thus serious water-related problems such as urban flooding and/or water pollution. The geographical distribution in East, Southeast, and South Asia was also considered.

One or more rivers flowing in the cities were selected, and projection models of flood inundation and river water quality were developed using data obtained in collaboration with research institutes and agencies in the target cities. In selected cities, field analyses were also conducted to evaluate current river water quality, physical damage caused by past flooding events, and the perception and willingness of people to contribute to improving water infrastructure.

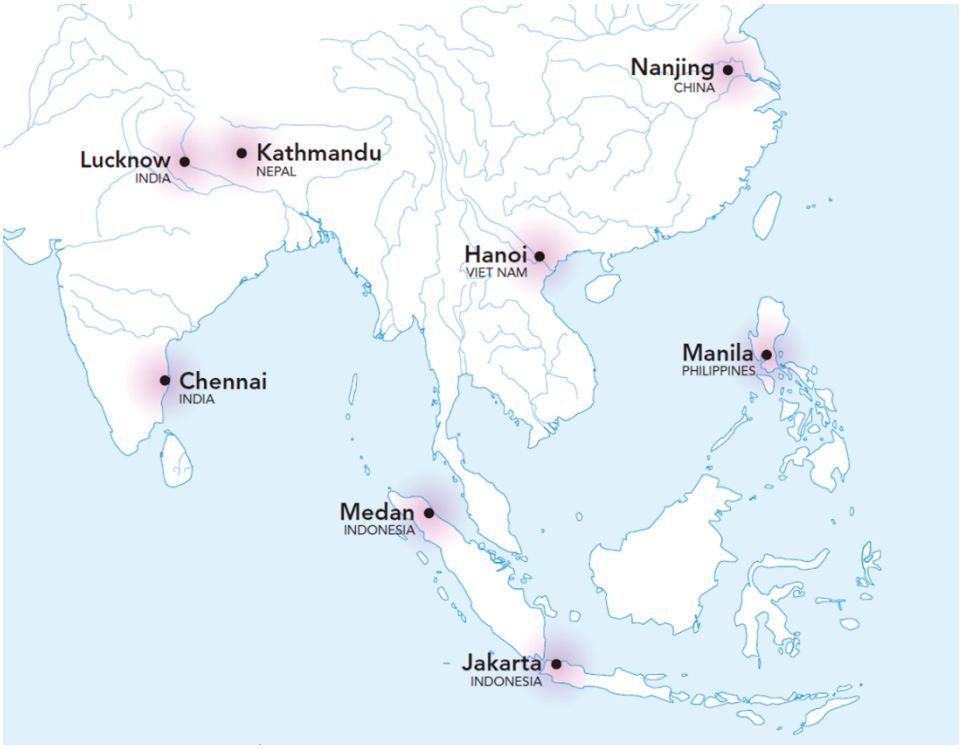

Figure 2.3. Target cities of the case studies

References

Bartsch, S.M.; Lopman, B.A.; Ozawa, S.; Hall, A.J.; Lee, B.Y. Global economic burden of norovirus gastroenteritis. *PLoS One* **2016**, 11, e0151219.

Huang, L.Y.; Wang, Y.C.; Wu, C.C.; Chen, Y.C.; Huang, Y.L. Risk of flood-related diseases of eyes, skin and gastrointestinal tract in Taiwan: A retrospective cohort study. *PLoS One* **2016**, 11, e0155166.

Jain, R.K.; Jain, K.; Ali, S.R. Modeling urban land cover growth dynamics based on Land Change Modeler (LCM) using remote sensing: A case study of Gurgaon, India. *Advances in Computational Sciences and Technology* **2017**, 10(10): 2947-2961.

Jonkman, S.N.; Bockarjova, M.; Kok, M.; Bernardini, P. Integrated hydrodynamic and economic modelling of flood damage in the Netherlands. *Ecol. Econ.* **2008**, 66: 77–90.

Kefi, M.; Mishra, B.K.; Kumar, P.; Masago, Y.; Fukushi, K. Assessment of tangible direct flood damage using a spatial analysis approach under the effects of climate change: Case study in an urban watershed in Hanoi, Vietnam. *ISPRS Int. J. Geo-Inf.* **2018**, 7, 29.

Kuroda, K.; Nakada, N.; Hanamoto, S.; Inaba, M.; Katayama, H.; Do, A.T.; Nga, T.T.V.; Oguma, K.; Hayashi, T.; Takizawa, S. Pepper mild mottle virus as an indicator and a tracer of fecal pollution in water environments: Comparative evaluation with wastewater-tracer pharmaceuticals in Hanoi, Vietnam. *Sci. Total Environ.* **2015**, 506–507: 287–298.

Mark, O.; Jørgensen, C.; Hammond, M.; Khan, D.; Tjener, R.; Erichsen, A.; Helwigh, B. A new methodology for modelling of health risk from urban flooding exemplified by cholera—Case Dhaka, Bangladesh. *J. Flood Risk Manag*. 2018, 11: S28-S42.

Mechler, R. Reviewing estimates of the economic efficiency of disaster risk management: Opportunities and limitations of using risk-based cost-benefit analysis. *Nat. Hazards* **2016**, 81: 2121–2147.

Mishra, B.K.; Herath, S. Assessment of future floods in the Bagmati River basin of Nepal using bias-corrected daily GCM precipitation data. *J. Hydrol. Eng*. **2015**, 20(8): 05014027.

OECD. *Planning Guide for Public Engagement and Outreach in Nano Technology*; OECD: Paris, France, 2012. Available at https://www.oecd.org/sti/biotech/49961768.pdf [Accessed 15 Jan. 2018].

Phanuwan, C.; Takizawa, S.; Oguma, K.; Katayama, H.; Yunika, A.; Ohgaki, S. Monitoring of human enteric viruses and coliform bacteria in waters after urban flood in Jakarta, Indonesia. *Water Sci. Technol*. **2006**, 54, 203–210.

Su, H.P.; Chan, T.C.; Chang, C.C. Typhoon-related leptospirosis and melioidosis, Taiwan, 2009. *Emerg. Infect. Dis*. **2011**, 17: 1322–1324.

3 Methodology

3.1 Precipitation change assessment

To evaluate the effects of climate change, the variation in monthly precipitation is considered in this study. Regarding future precipitation, statistically downscaled and bias-corrected (using regression analysis) GCM output at the local level is used for consistent impact valuation. Downscaled output has a temporal resolution of 24 hours and a spatial resolution of 120 km and is thus aptly suited to the observed daily precipitation data. Three different GCMs, namely, MIROC5, HadGEM2-ES and MRI-CGCM3, are considered in this work because of their widespread use and high temporal resolution compared to other climate models. On the other hand, two RCPs, 4.5 (normal emission scenario) and 8.5 (extreme emission scenario), were used that assume that global annual GHG emissions (measured in CO_2-equivalents) will continue to rise throughout the 21st century (IPCC, 2014). Here, GCM data from both past and future in 20-year periods, depending on data availability, are used for the current and future (2030) climatic conditions, respectively.

This study assessed the impact of climate change at the basin scale, and the precipitation change impact assessment was performed by comparing data from observation stations and the respective grid cells. A reliable precipitation dataset for each of the GCMs and RCPs for the current and future climate was prepared using the quantile-based bias correction method. The climate change impact was assessed by comparing the monthly precipitation values and return-period precipitation estimates for 50- and 100-year periods for the current and future climate.

The precipitation change assessment was initiated with the selection of an appropriate observation rainfall gauge station, assuming no significant variation in daily rainfall across the study basin due its small size. Among the various rainfall stations distributed throughout the study area, the station with the longest series of records as well as the most central location was considered for analyzing the change in precipitation. These daily precipitation data were made available via our local counterpart, and depending on the city, precipitation data for 20 to 25 years were used for comparison. The precipitation outputs of multiple GCMs were analyzed to derive statistics, such as the extreme values for different return periods, and the mean monthly values were used for the comparative analysis.

Changes in estimated return periods are a convenient way of presenting changes in extreme precipitation for a basin. The return period values are derived through frequency analysis for each of the grids using the current and future climate precipitation datasets, and in this study, Empirical and Gumbel frequency analyses were performed for the annual maximum daily precipitation series to assess the change in extreme precipitation events.

3.2 Land cover change projection

Land cover is a relevant indicator to identify the exposure of assets to flood risk. As the target is to assess the future situation, two options for projecting land cover are explored. The first is to use

official databases provided by local organizations as in the case of the Jakarta analysis, and the second option is to generate future land cover using remote sensing techniques in a GIS environment as was done for Chennai, Hanoi, Lucknow, Manila, and Medan. This approach based on GIS and remote sensing is described in Figure 3.1. Remote sensing products are widely used to produce suitable land use and land cover (LULC) maps, and they can also provide adequate tools to assess spatial and temporal land-use changes (Akinyemi et al., 2017). In this research, two past satellite images of the study area were employed to predict future land cover (2030). Landsat images were downloaded from https://earthexplorer.usgs.gov/.

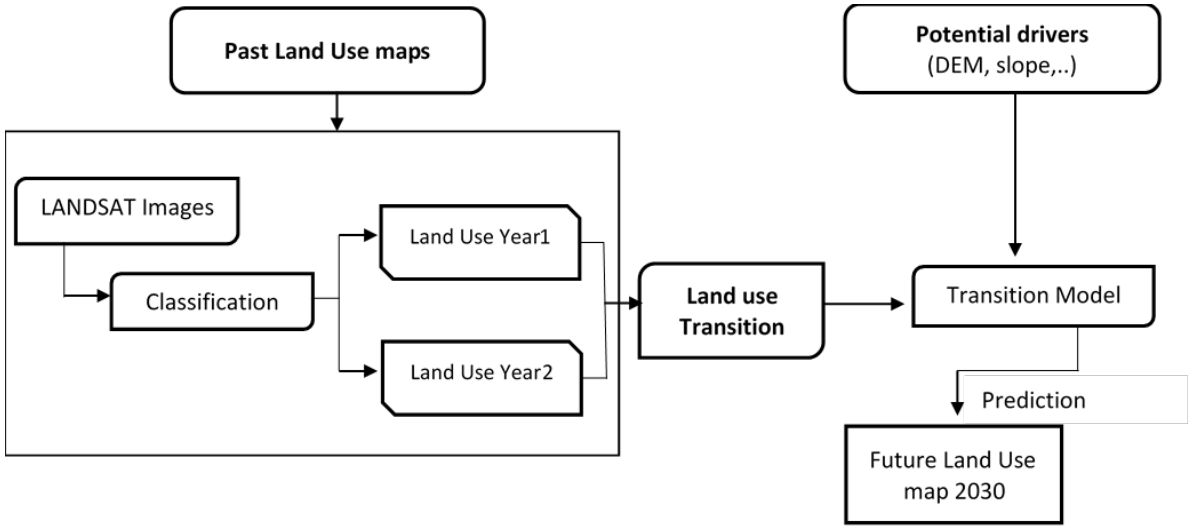

Figure 3.1. Land-use change approach. DEM: digital elevation model

Prior to image analysis, appropriate data processing, such as band compositing and clipping, was completed. Considering the main objective of this work and the resolution of the dataset, only a few classes were identified for the analysis through a supervised classification method using the maximum likelihood algorithm, land cover maps were prepared based on four (4) land cover types as indicated in Table 3.1.

Table 3.1. Land cover types

Land Cover Type	Description
Built-up Area	Residential, Commercial and Industrial areas, settlements and infrastructure
Water body	Rivers, Lakes, ponds, canals and reservoirs
Agricultural land	Cultivated areas
Green land	Gardens, grasslands, vegetated lands, mixed forests, orchards

To generate the land cover projection, Land Change Modeler for ArcGIS Software Extension 2.0, which was developed by Clark Labs of Clark University, was used to predict the land cover pattern based on the previous change trend. In this work, a Markov chain and logistic regression were applied to determine the suitable spatial configuration considering particular driving factors, of which the digital elevation model (DEM) and slope were the most important and were applied to influence proportional change.

The future land cover simulation will be useful for identifying the potential land cover change, which can be of interest for regional planning. Additionally, it will be useful for flood hazard assessment and flood damage evaluation.

3.3 Population growth estimation

For the water quality simulation in this project, we mainly considered household discharge and thus the population distribution at lower administrative divisions such as the ward, taluka or subdistricts for current and future years. The current and past population estimates in all target areas was collected from our local counterparts using census data, and while the future trends were estimated using the ratio method based on population projections by the United Nations Department of Economic and Social Affairs (UN DESA) (UN DESA, 2015), projected population data were not available from some local governments as in the case of Jakarta, Medan, Chennai, Lucknow, Kathmandu and Nanjing. However, if predicted by local government agencies such as Vietnam Water, Sanitation and Environment in the case of Hanoi and the Philippines Statistics Authority in the case of Manila, the local projections were used.

3.4 Flood inundation modeling

Flood inundation modeling consisted of hydrologic-hydraulic modeling with major inputs, including extreme rainfall values, DEM, land cover, and flood control measures (Figure 3.2). In the beginning, hydrologic modeling using HEC-HMS was carried out to generate flood hydrographs at the inlet point of the inundation study. Later, these flood hydrographs were incorporated into the FLO-2D, the two-dimensional hydraulic routing model, to generate flood inundation for the lower regions.

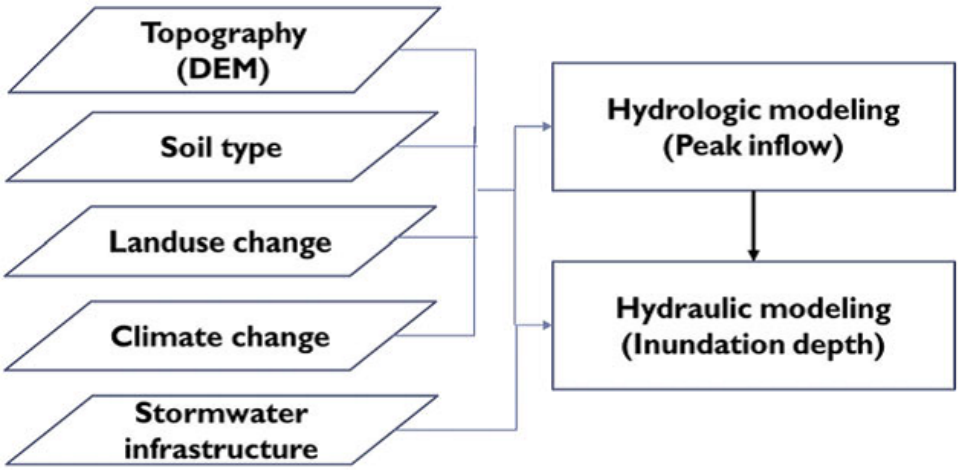

Figure 3.2. Framework for flood hydrographs and inundation modeling

Urban floods often occur at the subdaily scale, but daily rainfall values are only available as hourly data on the intensity and availability of rainfall are rare. Hence, temporal downscaling is necessary to convert daily rainfall data to sub-daily rainfall data. Synthetic rainfall distributions built in the HEC-HMS and FLO2D models enabled hourly rainfall data to be generated.

Output from various GCMs (MRI-CGCM 3, MIROC5, HadGEM) were evaluated with the observed rainfall data to obtain a better result by applying the quantile-quantile bias-correction technique. Intensity-duration-frequency (IDF) curves for the entire study urban watershed were produced to examine the present and future extreme rainfall events to identify the impact of climate change and urbanization on rainfall.

Earlier, the quantile mapping technique was applied to minimize the bias in rainfall frequency and intensity in the GCM data. This method consisted of two steps as follows: (1) truncating the GCM rainfall distribution at a threshold value, which can be derived from the inverse gamma cumulative distribution function (CDF) of the zero nonexceedance probability of the observational data, and (2) matching the CDF of the truncated GCM data series and observational data series by taking the inverse CDF of the GCM data with observational shape and scale parameters.

Design rainfall, the maximum amount of precipitation for a given duration and return period, is often required for planning different hydraulic structures. Frequency analysis is commonly used to estimate the design rainfall when there are adequate annual extreme rainfall intensity data available, and the results are commonly presented in the form of inverse distribution function (IDF) curves (Minh Nhat et.al, 2008). To build the IDF curve, a selected probability distribution is traditionally independently fitted to the observed annual extreme rainfall for various durations, but this method has certain limitations. Therefore, both empirical and Gumbel frequency distribution techniques were applied to conduct the frequency analysis.

Hydrological modeling is commonly used to estimate the hydrological response due to precipitation in a catchment, and there are different types of available models from black box models, which

require fewer basin data, to physically based models that require a large amount of basin data. The selection of the model depends on the objectives of the basin flood prediction, and in this research, hydrologic modeling was primarily performed to generate flood hydrographs at the inlet location of the inundation modeling area. The discharge from the upper region, which was used as inflow to the lower basin, was simulated using the HEC-HMS model (Feldman, 2000), which is a lumped conceptual and continuous hydrological model capable of analyzing run-off based on hourly to daily precipitation. It can be applied to simulate urban flooding and flood frequency and used in planning flood warning systems, stream restoration, and/or reservoir flooding spillway capacity (US Army Corps of Engineers, Hydrologic Engineering Center, 2010, Rafiei Emam et al., 2016).

The Watershed Modeling System (WMS) program was used to prepare the initial parameters of the HEC-HMS, which is open source software for modeling the rainfall-runoff process that was developed by the Hydrologic Engineering Center of the U.S. Army Corps of Engineers. The software includes a graphical user interface for managing and analyzing the model data. It is important to mention that the HEC-HMS is not an actual hydrological model itself but rather than software that enables the user to perform hydrological modeling based on a wide selection of common mathematical models used in hydrology, and it represents the rainfall-runoff process in a watershed in a simplified manner.

Depending on the condition of the basin being modeled and the available data, an adequate mathematical model for each of the previously defined four components of the rainfall-runoff process must be chosen. In this study, the hydrologic modeling is primarily performed to generate flood hydrographs with certain statistical return periods resulting from single design rainfall events with the same return periods.

FLO-2D, a two-dimensional flood routing model to simulate run-off was used to map the inundation areas (Haltas et al., 2016). The model is capable of numerically routing a flood hydrograph while predicting the area of inundation and simulating flood wave attenuation, and it simulates the progression of the flood hydrograph, conserving flow volume, over a system of square grid elements representing topography and flow roughness. Flood hydrographs at the inlet section, spatial information on the land uses, elevation and soil conditions, and the rainfall duration and amounts are supplied as inputs in the model to generate inundated areas as outputs. A FLO-2D project dataset requires the potential flow surface topography to be represented in a square grid format. Although grid elements of any size can be used by the model, the time step is governed by the wave celerity, so small grid elements require small time steps.

3.5 Direct flood damage

In this work, flood damage assessment is based on three main components, hazard assessment, exposure, and vulnerability, which are integrated in a GIS environment to assess direct flood damage and to identify the spatial distribution of damaged areas under current and future scenarios. The spatial analysis approach applied at the specific watersheds of the study areas required several parameters and datasets such as satellite images, topographic data, soil characteristics, property

prices, and flood damage rates, as explained in the methodology flowchart (Figure 3.3). The parameters and components applied to assess flood damage were mainly converted to raster format and georeferenced to the geographic coordinate system of the study area. In this research, current and future situations were comparatively analyzed, and through specific scenarios related to the impacts of climate and land cover change and the effect of the implementation of flood adaptation measures, levels of flood damage were estimated. In this study, ArcGIS 10.4.1 was used for data processing and analysis. These analyses can increase the awareness of policy makers and can be useful for developing effective strategies for flood risk prevention and reduction.

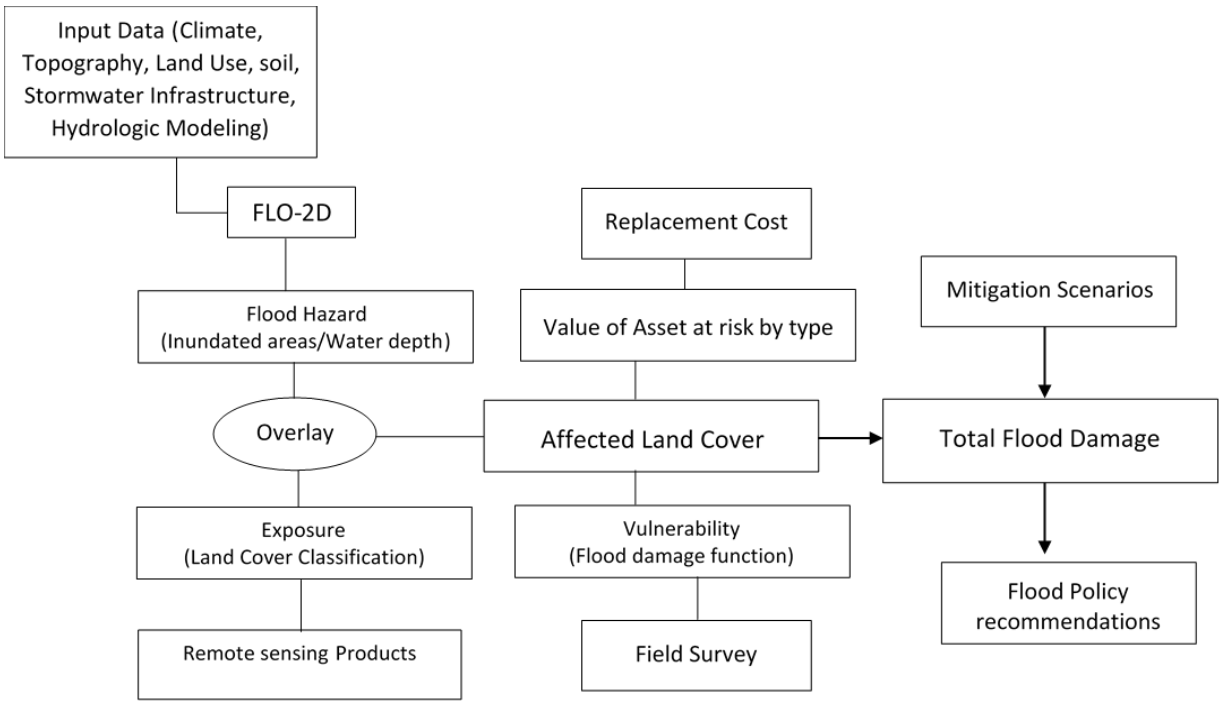

Figure 3.3. Flowchart of the modeling methodology

3.5.1 Hazard assessment

Water depth is applied as the main factor in the flood hazard assessment, and it is generated from flood simulations as described in Section 3.4.

3.5.2 Exposure

The exposure component represents the element at risk, and it is correlated to land use. As explained in Section 3.2, remote sensing products are used; two previous satellite images were classified using the supervised classification maximum likelihood algorithm with ArcGIS software and validated. Landsat sensors have a moderate spatial resolution of 30 m, at which it was quite difficult to distinguish individual houses or buildings and to establish a detailed land-use map. However, the resolution was sufficient to distinguish urban growth at a regional scale. Therefore,

four classes, namely built-up areas, water bodies, agricultural land, and green land, were identified based on the classification. To measure damage in monetary terms, data on the value of assets at risk were integrated into the analysis as the value of assets can indicate the replacement cost or depreciated/repair cost (Albano et al., 2015). In this work, however, this value was estimated based on the assumption that damaged assets must be replaced by a similar object (Messner et al., 2007). Indeed, the values of the built-up class were expressed as replacement costs of residential and nonresidential buildings, and the infrastructure damage was added to the analysis using weighting factor approaches (Jongman et al., 2012, Tu Vu et al., 2017). Consequently, it was assumed that infrastructure losses are proportionate to total residential losses.

3.5.3 Vulnerability

The indicator of vulnerability was evaluated based on the susceptibility of exposed assets to contact with water, and it is represented by a flood-depth damage function that is very useful for direct damage assessment and that can be generated by two methods. The first produces the function from the losses following flooding as was done for Hanoi, Manila, and Jakarta. Using this option, the flood-depth damage function is derived from data collected from field surveys using regression analysis. The dependent variable is the direct damage percentage, and the independent variable is flood depth. The depth of flooding is related to the damage caused, and this correlation can be a relevant way to construct the flood-depth damage function based on a past flood event. Indeed, the flood-depth damage function is an important component of direct flood estimation. In this work, the flood-depth damage was constructed as a logistic function developed using XLSTAT software.

Field surveys were conducted in the local areas of our case studies. Face-to-face interviews were conducted with local people in affected residential and nonresidential areas using specific questionnaires composed of three main parts: Part I: household characteristics; Part II: flood risk/damage; and Part III: flood risk management measures. In Part II, the questions were mainly related to past flood events, which was helpful to determine the relationship between the impacts on properties at risk and flood characteristics and to establish the flood-depth damage function, whereas Part III was associated with the perception of local people about flood risk reduction. Potential respondents were selected from the flood hazard map generated and calibrated based on past flood events, and the map was also helpful for dividing the target population into common groups/classes. During the survey, a global positioning system (GPS) unit was used to determine the exact location of the selected classes, and a population for each group was then randomly chosen and interviewed.

The second method is called the synthetic flood damage function, which was applied for Chennai and Lucknow. In this case, the function is established from detailed inventories of the types of land use and potential losses (Handmer et al., 2002). For these three case studies, the flood-depth damage function was generated from the work done by (Huizinga et al., 2017).

3.6 Water quality

To simulate water quality, we selected a numerical simulation tool that is capable of handling both hydrological and water quality components in a transdisciplinary manner. In addition to being transdisciplinary in nature, the tool had to be freely available to our target cities and not data intensive. Water Evaluation and Planning (WEAP), a decision support system tool, is widely used in the planning and management of integrated water resources; this model supports extensive environmental master planning functionalities to represent wastewater generation and treatment. Additionally, WEAP includes a catchment module for rainfall-runoff simulation, which eliminates the need to identify another hydrologic model for streamflow simulation, which is an essential input parameter for water quality modeling. The WEAP hydrology module enables the estimation of rainfall runoff and pollutant travel from a catchment to water bodies.

The WEAP model greatly supports scenario formation functionalities that consider policy alternatives for current and future conditions that are well supported by several scientific findings. The module enables the estimation of rainfall runoff and pollutant travel from a catchment to water bodies, and scenarios can be developed based on key drivers affecting water quality and quantity viz. population growth, industrial and commercial activities, land use and land cover, the capacity and status of treatment plants, climate change, and several other factors. WEAP also provides a GIS-based interface to represent wastewater generation and treatment systems, and it can simulate several conservative water quality variables (that follow exponential decay curves) and nonconservative water quality variables in addition to pollution generation and removal at different sites.

The WEAP model was used to simulate future total water demand and water quality variables for 2030, which will be useful for assessing alternative management policies for the different river basins in our target areas. Water quality modeling requires a wide range of input data including point and nonpoint pollution sources; past spatiotemporal water quality; detailed information from a master plan about wastewater treatment infrastructures both existing and planned by 2030; demographical trends; hydrometeorological information, including drainage networks; river flow-stage-width relationships; and land use/land cover. Different hydroclimatic data (daily rainfall, air temperature, relative humidity, and wind velocity) have been collected for the past 20-30 years for the different areas used to establish the model. Daily average stream flow data measured at different river gauges in our target river from the past 20 years were utilized to calibrate and validate the WEAP hydrology module simulation. Data on important water quality indicators (biochemical oxygen demand (BOD), NO_3 and *Escherichia coli*) at the spatiotemporal scale for our river of interest was used to calibrate and validate the water quality module of the WEAP software.

The WEAP model was applied for the different river basins considering different command areas with interbasin transfers. Hydrologic modeling requires the entire study area to be split into smaller catchments while accounting for confluence points and physiographic and climatic characteristics. The WEAP hydrology module computes the catchment surface pollutants generated over time by multiplying runoff volume by the concentration or intensity of different types of land use. During simulation, land use information was broadly categorized into three categories: agricultural,

forested, and built-up areas. Soil data parameters were identified using previous secondary data and literature.

Under the WEAP hydrology module, the soil moisture method was used to estimate the different hydrological parameters for this study. This method can simulate different components of the hydrologic cycle, including evapotranspiration, surface runoff, interflow, base flow, and deep percolation (Sieber and Purkey 2011). Here, each catchment is divided into two soil layers, an upper and a lower, that represent shallow-water and deep-water capacities, respectively. The upper soil layer is targeted for spatial variation in different types of land use and soil types whereas the lower soil layer is considered to represent groundwater recharge and baseflow processes, and its parameters remain the same for the entire catchment. Different hydrological components are estimated with z_1 and z_2 as the initial relative storage (%) for the upper (root zone) and lower (deep) water capacities, respectively (Equations (1)–(5)).

$$ET = Potential\ evapotranspiration * (5z_1 - 2z_2^2)/3 \quad (1)$$

$$Surface\ runoff = Precipitation\ (P) * z_1^{Runoff\ resistance\ factor} \quad (2)$$

$$Interflow = (Root\ zone\ conductivity * preferred\ flow\ direction) * z_1^2 \quad (3)$$

$$Percolation = Root\ zone\ conductivity * (1 - preferred\ flow\ direction) * z_1^2 \quad (4)$$

$$Baseflow = Deep\ conductivity * z_2^2 \quad (5)$$

The water quality module of the WEAP tool makes it possible to estimate pollution concentrations in water bodies and is based on the Streeter–Phelps model, in which two processes govern the simulated oxygen balance in a river: consumption by decaying organic matter and reaeration induced by an oxygen deficit (Sieber and Purkey, 2011). BOD removal from water is a function of water temperature, settling velocity, and water depth (Equations 6 to 9):

$$BOD_{final} = BOD_{init} \exp^{\frac{-k_{rBOD}L}{U}} \quad (6)$$

where $k_{rBOD} = k_{d20}^{1.047(t-20)} + \frac{\upsilon_s}{H}$ (7)

BOD_{init} = BOD concentration at beginning of reach (mg/L); BOD_{final} = BOD concentration at end of reach (mg/L); t = water temperature (°C); H = water depth (m); L= reach length (m); U = water velocity in the reach; v_s = settling velocity (m/s); k_r, k_d and k_a = total removal, decomposition and aeration rate constants, respectively (1/time); and kd_{20} = decomposition rate at reference temperature (20°C). The oxygen concentration in the water is a function of water temperature and BOD:

$$Oxygen\ saturation\ \ or\ \ OS = 14.54 - (0.39t) + (0.01t^2) \quad (8)$$

$$O_{final} = OS - \left(\frac{k_d}{k_a - k_r} \right) \left(\exp^{-k_r L/U} - \exp^{-k_a L/U} \right) BOD_{init} - \left[(OS - O_{initial}) \exp^{-k_a L/U} \right] \quad (9)$$

O_{final} = oxygen concentration at end of reach (mg/l), and $O_{initial}$ = oxygen concentration at beginning of reach (mg/l).

Similarly, chemical oxygen demand (COD) and nitrate are simulated considering intake by decaying organic and inorganic matter and reaeration induced by oxygen deficit.

3.6.1 Model setup

First, the vector or raster file of the administrative boundary of the study area and a map of the river of interest is imported using WEAP software. After tracing the river on the top of t manually, we create our problem domain. The whole problem domain (and its different components) is divided into several subcatchments, which are further subdivided into different subbasins, to consider the influent locations of the river and its major tributaries that are represented by their respective WEAP nodes. Other major considerations are number of demand sites (which usually depends on the lowest administrative unit of the study area for which data are available) and wastewater treatment plants to accurately represent the current situation in the study area. Here, demand sites denote defined domestic (population) and industrial centers whose attributes explain the water consumption and wastewater discharge in the river of concern. Wastewater treatment plants (WWTPs) are pollution-handling facilities with design specifications that include the total capacity and pollutant removal efficiencies. In this case, an upflow anaerobic sludge blanket (USAB) treatment and the accompanying pollutant removal efficiency is considered in the modeling. The daily volume of domestic wastewater generation is area specific and ranges from 100-180 liters per day per capita, but because of the lack of precise data available for some of the areas, the volume was fixed at 130 liters of average daily consumption per capita. Apart of this, we do need to plot river gauge stations or ground water supply. Finally, the different types of links (return flow, transmission flow, and runoff/infiltration) were used to finalize the model setup.

Scenario analysis is performed by defining a time horizon for which alternative wastewater generation and management options are explored, which is 2030 in this case. The business-as-usual condition is represented by a reference scenario under which all the existing elements are considered currently active. Consequently, the new/upgraded WWTPs (information taken from the local master plan) are modeled as scenarios representing deviations from the current conditions (reference scenario). The baseline year under the current reference scenario also varies for all study areas based on the availability of past data.

3.6.2 Model performance evaluation

Before conducting future scenario analysis, the performance of the WEAP simulation is evaluated based on a significant association between the observed and simulated hydrological and water

quality parameter values using the trial and error method. Hydrology module parameters (mainly effective precipitation and runoff/infiltration) were adjusted during simulation to reproduce the observed monthly stream flows for the period of a certain year to validate the hydrology module (Table 3.2), and the water quality simulation was validated by comparing the simulated and observed water quality parameter concentrations at some observation points. This location and time were selected based on the consistent availability of observed water quality data. The main parameters adjusted on a step-by-step basis were discharged household water quality parameter concentrations both at the observation site and the river head. Once the correlation between the observed and simulated values statistically confirmed the suitability of the model performance in this problem domain, future simulations of both water quality and hydrological parameters were initiated.

Table 3.2. Summary of parameters and steps used for calibration

Parameter	Initial Value	Step
Effective precipitation	100%	±0.5%
Runoff/infiltration ratio	50/50	±5/5
Household discharged water quality parameters concentrations both at the observation site and river head	X mg/L or CFU/100 ml	±0.5%

3.7 Economic benefit of improving urban water quality

3.7.1 Introduction

The WTP principle is the fundamental concept used to evaluate all the economic benefits associated with the assessment of water resource benefits and associated investments. These benefits are represented by the maximum monetary amount that individuals are willing to pay to attain a desired good or service instead of not having the good or service produced by the proposed investment. For standard goods/services that are offered through competitive markets, this monetary amount is usually determined by the price of the good/service plus an additional amount that an individual would be willing to pay to have the right to obtain this good/service at the market-determined price; in economics, it is generally termed the consumer surplus.

The CVM is the most frequently applied method in the valuation of environmental assets, and it represents a stated preference technique that is used by economists to assess the monetary value of nonmarket goods, such as water quality. The CVM or conjoint analysis has an advantage over other stated preference techniques because it allows us to measure both the use and nonuse values of environmental goods, and it bypasses the need to refer to market prices by explicitly asking individuals to express the monetary values they place on environmental goods, primarily through actual or hypothetical payments. The techniques for obtaining the individuals' values include personal, mail and phone questionnaires, bidding games and public referendums and workshops.

3.7.2 Sampling

If one desires to conduct CVM research in a large study area such as a city, district, or even village, there are simply too many individuals to survey. Therefore, such cases require careful selection of a subset of individuals to draw conclusions about the willingness to pay of the entire set of individuals; this is known as sampling.

There are many sampling techniques and approaches, but our goal is not to repeat the material of a standard applied statistics course. The researcher must ensure that each individual considered for the sample has the same probability of being selected. Sampling for CVM should be based on random or probability samples, so the use of nonprobability sampling techniques is not encouraged.

Sampling is an important part of a CVM study, and how carefully and reliably it is designed will affect the WTP estimates, results and conclusion of the study. Sampling is a complex topic, so it is advised that specialized sources be consulted for further information about the design and implementation of sampling strategies.

3.7.3 Questionnaire design

Each CVM study has distinctive features, so it is not possible to present specific rules for every questionnaire. In our case, however, we applied similar techniques to each study due to similar issues with water quality issues and our interest in comparing the final WTPs of each target city. However, the survey approaches differed in some cities, which will be explained in subsequent chapters. As the questionnaire is the principal tool in the CVM, its design is critically important.

First, as a courtesy, as well as a requirement in some countries, the analyst should mention that the survey is voluntary, that a respondent has the right to refuse to answer any question and that the answers are confidential and will not be released. Another requirement is to keep the questionnaire brief and as simple as possible; a respondent should be able to finish the survey in 15-20 minutes so as not to become annoyed.

Generally, the CVM survey consists of three parts: (1) an explanation of the good being valued and the hypothetical situation that the respondent has to confront/imagine, (2) the question of the respondent's willingness to pay for the environmental good, and (3) follow-up questions related to the general attitudes towards the good under consideration and the socioeconomic characteristics of the respondent. The sample survey that was used in our assessments is provided in the annex.

3.7.4 Questionnaire pretesting

All CVM questionnaires must be pretested in the field but not under the actual target conditions and locality. The objective of the pretesting is to check how a potential respondent will understand the format of the questions, the logic and coherence of the questions, and the identification of possible biases. The pretest sample size should include at least 30 respondents. After obtaining the results of the pretest survey, analysts evaluate the results and if necessary, revise the survey, delete

unnecessary questions, and add information gained from the pretest study. Thus, the improved questionnaire will be an effective tool for identifying WTP and increasing the participation of respondents.

3.7.5 Preliminary workshops

We conducted workshops in each city to identify the hypothetical water quality improvement scenario for the particular surveys. This is one of the key tasks in preparing for the CVM because in the absence of an actual market for such an environmental good, researchers must create a hypothetical market and request that respondents place a value on the proposed change in the environmental service. Such a hypothetical scenario was selected as the Surface Water Quality Improvement Program for each city, of which there were two components: (1) constructing new wastewater treatment facilities and (2) expanding the existing sewerage system. The questionnaire was translated into the most commonly spoken language in a city. As a payment vehicle, i.e., how a respondent is supposed to pay their WTP, an addition to their monthly utility payment was chosen.

City-specific approaches and WTP estimation techniques are provided separately for each city in subsequent sections.

3.8 Floodwater-borne infectious diseases

During flooding, residents in affected areas are forced to walk in the floodwater while they are outside buildings, which may result in the unintentional ingestion of floodwater that is affected by domestic wastewater overflow from sewer lines, septic tanks, and rivers, all of which contain various human pathogens. It has been reported that the concentrations of human pathogens and indicator microorganisms in floodwater were similar to those in river water in the area (Phanuwan et al., 2006). Thus, the residents face a potential health risk from infectious diseases (e.g., gastroenteritis) due to human pathogens in floodwater.

In this section, the health risk of floodwater-borne gastroenteritis was evaluated under three scenarios describing current situation, future situation without mitigation measures (business-as-usual scenario), and future status considering all measures to mitigate urban flooding and water quality deterioration (with measures scenario). The outputs from the flood inundation model and the water quality model under each scenario were used in combination with other input data (Figure 3.4).

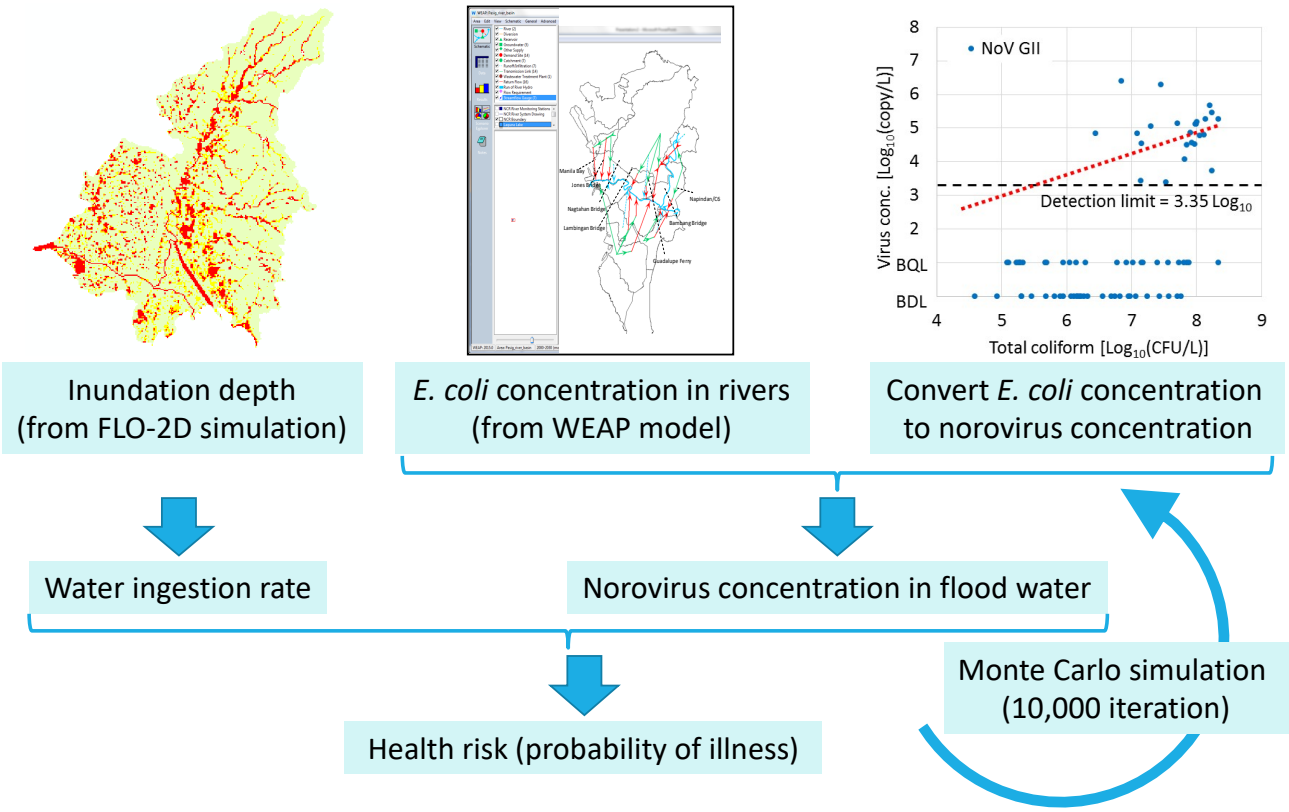

Figure 3.4. Health risk assessment framework

3.8.1 Concentration of noroviruses in floodwater

The simulated concentration of *E. coli* (output of the WEAP model) was used to develop a lognormal distribution to consider the temporal and special heterogeneity in *E. coli* concentration. The WEAP model evaluates water quality at multiple points along the target river. The parameters of the distribution, μ and **σ**, were calculated using the *E. coli* concentrations for all the monitoring points. The concentrations were converted to natural logarithms, and the arithmetic mean and standard variation of the logarithms were used as the μ and **σ** values of the lognormal distribution, respectively.

The *E. coli* concentration was then converted to the concentration of noroviruses. Concentrations of pathogenic viruses and indicator bacteria (e.g., *E. coli*) in urban river water have rarely been reported in Southeast Asia. Inaba et al. (2014) evaluated concentrations of five human viruses and fecal indicator bacteria in the Nhue River, Vietnam (n = 88 in total), and among the tested viruses, Pepper Mild Mottle Virus (PMMoV) showed the highest rate of occurrence (93%), which was much higher than that of human pathogens (e.g., Norovirus GI: 27%, Norovirus GII: 34%). PMMoV is proposed as a viral surrogate of fecal contamination in water because it is abundant in healthy human feces, sewage, and sewage-polluted water bodies compared to viral pathogens such as noroviruses (Kuroda et al., 2015), so this virus was selected as the surrogate for human viruses to analyze the correlation between fecal indicator bacteria and human viruses as well as the differences between bacterial indicators and viruses in terms of detection methods (culture methods vs molecular methods) and their stability in the water environment. The slope of the regression line

was extracted and used to indicate the relationship between *E. coli* (independent variable) and noroviruses (dependent variable) in the target river. Then, the intercept of the regression line was estimated using the observed concentrations of Norovirus GII and *E. coli* in the Nhue River.

3.8.2 Unintentional ingestion of floodwater

Residents in flooded areas are exposed to floodwater while they are outside protected buildings or shelters. The amount of floodwater ingested by residents was estimated by multiplying the proportion of time people spend outdoors and amount of water ingestion per hour using the following assumptions.

According to Diffey (2011), the mean times that people spend outdoors on weekdays and weekends were 1.43 and 2.38 hours, respectively. Since the risk assessment framework does not consider if the flood occurs on weekdays or weekends, we used the weighted average of the two values (1.70 hours/day) to represent the time that residents spend outdoors during flooding.

As for the amount of unintentional floodwater ingestion, it is reasonable to assume that it depends on the water depth. Residents who experienced the massive flooding following Typhoon Ondoy in 2009 in Manila stated that they began to swim in floodwater when the water level reached their breast. To include such a situation in the scenario, we assumed that the amount of floodwater ingested by residents in a flooded area is proportional to the water depth up to breast height (75% of the total height) and that the rate of water ingestion is the same when swimming in water higher than breast height. Schoen and Ashbolt (2010) developed a lognormal distribution ($\mu = 2.92$ and $\sigma = 1.43$) for the amount of unintentional water ingestion during swimming for one hour based on an observation dataset by Dufour et al. (2006), which was used here. Tables 3.3 summarizes the average height of people in the Philippines, Indonesia, and India; for Vietnam and China, the age-stratified average height and population size by age class were used to calculate the average height (Tables 3.4 and 3.5).

Table 3.3. Average human height in the Philippines, Indonesia, and India (unit: cm)

	Male	Female	Average
Philippines	163	151.4	157.2
Indonesia	158	147	152.5
India	164.7	151.9	158.3

Source: Food and Nutrition Research Institute, Department of Science and Technology, Philippines, 2014 (Philippines), Frankenberg and Jones, 2004 (Indonesia), Mamidi et al., 2011 (India)

Table 3.4. Age-stratified average human height in Vietnam

Age	Average height (male), cm	Population, %	Average height (female), cm	Population, %
20-24	164.44	10	153.42	9.8
24-29	164.32	9.2	153.34	9.1
30-34	163.59	8.2	152.66	8.0
35-39	163.59	7.8	154.34	7.6
40-44	163.31	7.0	153.68	7.0
45-49	163.50	6.2	153.32	6.3
50-54	162.93	4.9	153.57	5.1
55-59	162.16	3.2	152.95	3.5
60-64	161.21	2.0	151.27	2.3
65-69	160.46	1.5	149.90	1.8
> 70	158.30	3.4	146.10	4.5
Total		63.4		65.0
Weighted average	163.2		152.7	
Average height	158.0			

Source: National Institute of Nutrition, Ministry of Health, Vietnam, 2010 (height) and General Statistics Office, Ministry of Planning and Investment, Vietnam, 2011 (population)

Table 3.5. Age-stratified average height of China

Age	Average height (male), cm	Population (2015), thousands	Average height (female), cm	Population (2015), thousands
20-24	171.9	53,345.01	159.9	47,942.12
24-29	171.6	67,067.19	159.6	62,668.00
30-34	170.8	52,460.60	159.1	49,655.80
35-39	169.9	49,280.47	158.5	46,797.25
40-44	169	60,763.51	157.8	57,936.82
45-49	168.7	63,100.43	157.7	61,271.14
50-54	168.3	52,081.98	157.7	50,104.19
55-59	167.5	40,669.66	156.8	39,303.46
Total		438,768.8		415,678.8
Weighted average	169.8		158.4	
Average height	164.1			

Source: General Administration of Sport of China, 2014 (height) and United Nations Department of Economic and Social Affairs, 2017 (population)

3.8.3 Risk calculation

The cumulative probability of gastroenteritis by noroviruses in each grid was calculated by accumulating the hourly probability of infection based on the output of the flood inundation model (hourly water depth in each grid) and the water quality model. The dose-response relationship for the Norovirus GI.1 8fIIa strain without considering the effect of aggregation (Teunis et al., 2008) was used to calculate the probability of infection and the probability of illness due to a given infection. A Python-based program was developed to calculate the health risk with 10,000 iterations using the Monte Carlo approach.

The assumptions made in this assessment should be noted. The concentration of noroviruses in floodwater was assumed to be equal to that in the Ciliwung River, and the effect of dilution by rainwater was not considered because Phanuwan et al. (2006) reported that the concentrations of indicator bacteria and pathogenic viruses were higher in floodwater than in river water, which raised the possibility of additional sources of noroviruses such as resuspension of river sediment and overflow of septic tanks and sewer lines. All norovirus genomes detected using quantitative PCR were assumed to be complete and from viable viral particles.

3.9 Low-carbon technology in wastewater facilities

The low-carbon technology assessment methodologies consisted of 1) setting basic conditions for GHG estimation, 2) revising the existing GHG estimation approaches, and 3) developing GHG estimation tools. The following sections describes the approach in detail.

3.9.1 Setting Basic Conditions for GHG Estimation

To calculate GHGs, the base and target years and target GHGs were determined. First, the base and target years for GHG estimation were set as 2015 and 2030, respectively, to compare the difference in GHG emission between the two years. For the target GHGs, the following seven (7) gases of international importance were identified: CO_2, CH_4, N_2O, PFC, HFC, SF_6, and NF_3. Among them, three (3) gases, carbon dioxide (CO_2), methane (CH_4) and nitrous oxide (N_2O), were selected as the major GHGs released during the operation of wastewater management systems. CO_2 emissions arise from the combustion of fossil fuels at the WWTP while CH_4 and N_2O emissions emerge during sludge treatment by anaerobic reaction.

3.9.2 Identification of Applicable Low-Carbon Technologies

With the objective of identifying low-carbon technologies to reduce GHG emissions from the plant, the items that could produce high GHG emissions were first determined. Then, technical measures to reduce such GHG emissions were scrutinized to select some effective measures such as low-carbon technologies.

1) WWTP items relevant to High GHG Emissions

- Target Stage of the WWTP Lifecycle

To identify the period when the volume of GHG emissions from the WWTP is highest, the available data on CO_2 emissions were examined by the WWTP lifecycle stage, e.g., construction, operation, and disposal.

As illustrated in Figure 3.5, the operational stage of the main facilities is the largest source of CO_2 emission that accounts for 64% of the total. In addition, the operational stage of administration facilities and the other stages account for 19%. Consequently, the operational stage of the WWTP was selected as the target period since more than 80% of the total CO_2 emissions are produced at this stage.

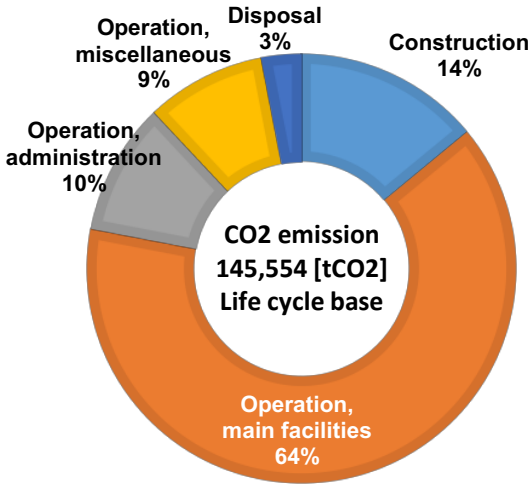

Figure 3.5. Power consumption in the WWTP lifecycle
Source: Manual global warming countermeasures in wastewater management

- Target WWTP Equipment

The power consumption, which is directly proportional to CO_2 emissions, was examined according to the WWTP equipment. The blower consumes the most power, accounting for 60% of the total power consumption of the WWTP followed by the pumps, as illustrated in Figure 3.6. Compared to the pumps, the operational duration of the blower appears to be longer to allow aerobic reaction through the aeration process, which results in higher power consumption. As a result, the blower and pumps were selected as the target pieces of equipment of the WWTP.

Based on the abovementioned identification of the target stage and equipment of the WWTP, the activities that could cause relatively high GHG emissions were designated as "Operation of blowers and pumps of the WWTP".

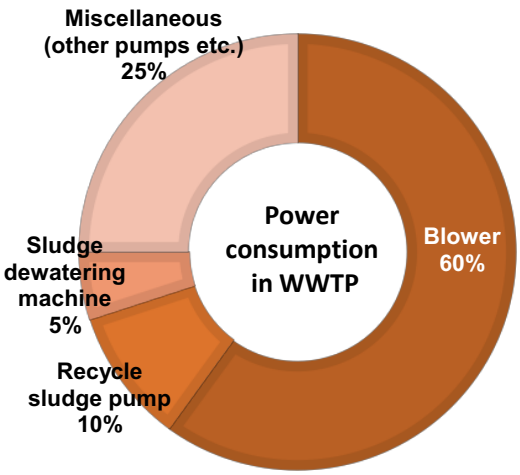

Figure 3.6. Power consumption in the WWTP lifecycle
Source: Manual global warming countermeasures in wastewater management

2) Potential Low-Carbon Technologies to be Applied

The overall structure of a WWTP is illustrated in Figure 3.7. Largely, WWTP facilities are grouped into i) wastewater treatment process facilities including the pumping station, ii) sludge treatment process facilities, and iii) others. In accordance with this classification, low-carbon technologies were identified as listed below. In addition to the energy savings due to the introduction of high-efficiency machines and the optimization of their operation, the generation of renewable energy, such as biogas and solar power systems, could be considered for implementation at the WWTP site to effectively reduce GHG emissions (Table 3.6).

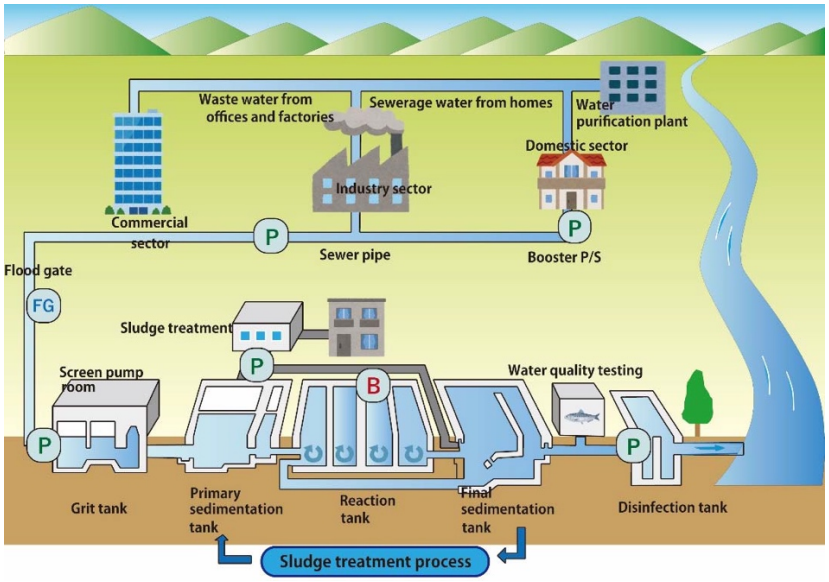

Figure 3.7. Typical WWTP in an urban area.
P, FG and B stand for "pump", "flood gate" and "blower", respectively.

Table 3.6. Target activities and descriptions of low-carbon technologies

Process	Target activities	Description
1) Water treatment process	a) Introduction of high-efficiency pumps	This methodology shall be applied to projects that aim to save energy through the introduction of high-efficiency pumps in the target cities/countries.
	b) Introduction of high-efficiency blower	This methodology shall be applied to projects that aim to save energy through the introduction of high-efficiency blowers in the target cities/countries.
	c) Optimization of pump operation in WWTP/sewerage system	This methodology shall be applied to projects that aim to streamline operation through an optimization policy, such as an integrated pump control system, SCADA system, etc., in the target waste water treatment plant.
	d) Introduction of inverter into sewerage system	This methodology shall be applied to projects that aim to save energy through the application of inverter-control systems to the pumps of the drainage and sewerage facilities in the target countries/cities.
2) Sludge treatment process	e) Introduction of high-efficiency dewatering machine	This methodology shall be applied to projects that aim to save energy through the introduction of a high-efficiency dewatering machine.
	f) Optimization of sludge operation	This methodology shall be applied to projects that aim to perform sludge collection with a lightweight sludge scraper, an optimized collection method, etc. in the target waste water treatment plant.
	g) Utilization of biogas for power generation	This methodology shall be applied to projects that aim to i) avoid the methane emissions generated from sludges at the WWTPs through the installation of methane recovery systems and ii) reduce the use of fossil fuels by the existing power plants by replacing them with biogas as a renewable energy source.
3) Others	h) Introduction of solar power system to WWTP site	This methodology shall be applied to the projects that aim to generate renewable energy through the installation of a solar photovoltaics system in the unused space of the sewerage facilities, e.g., wastewater treatment plant covering, in the target countries/cities.

3.9.3 Revision of Existing Estimation Approaches

1) Literature Review

To scrutinize the GHG estimation methodology for the WWTP, the approved calculation formulas, which have been officially endorsed by a technical agency or third-party entity in accordance with its validation process, were reviewed, such as the Clean Development Mechanism (CDM), J-VER and the Joint Crediting Mechanism (JCM). The reviewed wastewater management methodologies are listed in Table 3.7.

Of the existing methodologies, JCM is the most suitable in terms of being simple, user-friendly and conservative. Therefore, JCM was mainly used to develop methodologies for low-carbon technologies; CDM, J-VER, etc. would be considered for application in this assessment in the case of necessity.

Table 3.7. Approved GHG estimation methodologies in wastewater management

#	Methodology No.	Title	Area
Clean Development Mechanism			
1	ACM0014	Treatment of wastewater	Biogas
2	AM0020	Baseline methodology for water pumping efficiency improvements	Pump
3	AM0069	Biogenic methane use as feedstock and fuel for town gas production	Biogas
4	AM0080	Mitigation of greenhouse gases emissions with treatment of wastewater in aerobic wastewater treatment plants	Biogas
5	AM0022	Avoided Wastewater and On-site Energy Use Emissions in the Industrial Sector	Biogas
6	AM_CLA_0122	Calculation of the effluent flow from an activated sludge plant based on influent flow and sludge flow measurements	Sludge treatment
7	AM_CLA_0051	Request for clarification with regard to applying K factors and sludge	Others
8	AM_REV_0224	Mitigation of greenhouse gas emissions from treatment of industrial wastewater	Others
9	AM_REV_0201	The aim of this request for revision of an approved methodology is to allow its use to a project where the wastewater is dewatered and subsequently directed to land application	Sludge treatment
10	AM_REV_0182	Revision of ACM0006 to include biogas from anaerobic wastewater treatment	Biogas
11	AM_REV_0174	Possibility to include wastewater solids that are separated from the wastewater to prevent open lagoon clogging and	Sludge treatment

#	Methodology No.	Title	Area
		therefore have a different baseline, in a scenario 1 type anaerobic digester wastewater treatment project	
12	AM_REV_0171	Revision of ACM006 to include biogas generated by anaerobic wastewater treatment using approved and applicable methodologies for greenfield projects. Clarification on Biomass Residue definition	Biogas
13	AM_REV_0078	Request for revision to include Greenfield projects (i.e. new wastewater treatment plant deserving new plants or urban developments)	Biogas
14	AM_REV_0031	Controlled combustion of municipal solid waste (MSW) and sludge to generate energy in Shaoxing City, China (the Project activity)	Biogas
15	AMS-II.C	Demand-side energy efficiency activities for specific technologies	Pump
16	AMS-II.S.	Energy efficiency in motor systems	Pump
17	AMS-III.E.	Avoidance of methane production from decay of biomass through controlled combustion, gasification or mechanical/thermal treatment	Biogas
18	AMS-III.H.	Methane recovery in wastewater treatment	Biogas
19	AMS-III.I.	Avoidance of methane production in wastewater treatment through replacement of anaerobic systems by aerobic systems	Biogas
20	AMS-III.Y.	Methane avoidance through separation of solids from wastewater or manure treatment systems	Biogas
21	AMS-III.V.	Decrease of coke consumption in blast furnace by installing dust/sludge recycling system in steel works	Biogas
J-VER			
22	E005	Utilization of sewage sludge	Biogas
23	E030	Renewal of sewage sludge dryers	Sludge dryer
Joint Credit Mechanism			
24	VN_AM004	Anaerobic digestion of organic waste for biogas utilization within wholesale markets	Biogas

2) Joint Crediting Mechanism (JCM)

An outline under the JCM scheme, both the reference and project scenarios for the methodologies, must be developed (Figure 3.8). Below, the reference scenario is calculated as the business-as-usual emissions, which represent valid emissions generated by providing the same outputs or service level of the proposed JCM project. On the other hand, the project scenario is calculated based on monitored electricity and fuel consumption. Additionally, the reference and project emissions are defined below based on the above scenario. Reference emissions are calculated on the basis of project emissions derived from monitored fuel and electricity consumption with the following assumptions.

Reference emissions = (Energy/fuel consumption under reference scenario) × (Emission factor of energy/fuel consumed under reference scenario)

The project emissions are calculated on the basis of monitored electricity and fuel consumption.

Project emissions = (Energy/fuel consumption under project scenario) × (Emission factor of energy/fuel consumed under project scenario)

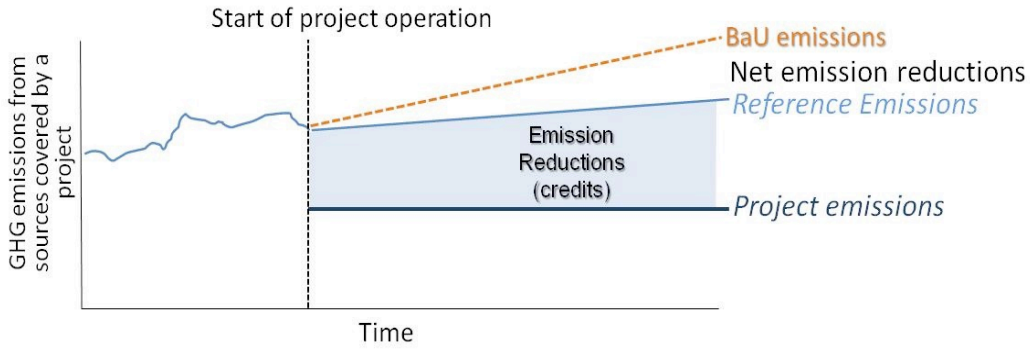

Figure 3.8. Comparison of business-as-usual emissions, reference emissions, and project emissions

3.9.4 Development of a GHG Estimation Tool

1) Scenario development

Since most of the target cities in the assessment could be equipped with a master plan and/or any other plan relevant to wastewater management, GHG emission reduction was estimated assuming that proposed low-carbon technologies would be adopted under such plans. Three (3) scenarios were developed as detailed below: a) business-as-usual, b) master plan scenario and c) low-carbon technologies scenario.

a) Business-as-usual scenario: Current wastewater management facilities shall be maintained without implementation of the master plan up to 2030.

b) Master plan scenario: The master plan or any other plans relevant to wastewater management shall be implemented up to 2030 without the introduction of low-carbon technologies.

c) Low-carbon technology scenario: Low-carbon technologies shall be introduced in the implementation of the master plan or other relevant plans up to 2030. This scenario is equal to the project scenario in the GHG estimation tool.

2) Tool Development for GHG Estimation

As described in Section 3.9.2, the following eight (8) low-carbon technologies were selected:

a) Introduction of high-efficiency pumps;

b) Introduction of a high-efficiency blower;

c) Optimization of pump operation in the WWTP/sewerage system;

d) Introduction of an inverter into the sewerage system;

e) Introduction of a high-efficiency dewatering machine;

f) Optimization of sludge operation;

g) Utilization of biogas for power generation;

h) Introduction of a solar power system to the WWTP site.

Calculation methodologies for GHG emissions were developed for each technology and described as follows.

i) Calculation of GHG emissions under the business-as-usual scenario;

ii) Calculation of GHG emissions for the master plan and low-carbon technologies scenarios.

The formulas to calculate GHG emissions were developed for each of the technologies as summarized in Table 3.8.

GHG emission reduction by introducing low-carbon technologies is calculated by the following formula:

GHG emission reduction = master plan emission – low-carbon technology emission

The abovementioned formulas are further detailed in the GHG calculation methodologies with the developed calculation sheets as shown in Annex A and Annex B, respectively.

Table 3.8. Formula for calculating GHG emission

Low-carbon technologies	Master plan emissions[*1] (tCO_2)	Low-carbon technology emissions[*2] (tCO_2)
a) Introduction of high-efficiency pumps	Power consumption of the conventional pumps[*3] (MWh) × CO_2 emission factor for the electricity consumption by the pump (tCO_2/MWh)	Power consumption of the high-efficiency pumps (MWh) × CO_2 emission factor for the electricity consumption (tCO_2/MWh)
b) Introduction of high-efficiency blower	Power consumption of the conventional blower[*3] (MWh)× CO_2 emission factor for the electricity consumption by the pump (tCO_2 / MWh)	Power consumption of the high-efficiency blower (MWh) × CO_2 emission factor for the electricity consumption (tCO_2 / MWh)
c) Optimization of pump operation in WWTP/sewerage system	Master plan emissions [tCO_2] = Total power consumption of the normal pump operation [MWh] × CO_2 emission factor for the electricity consumption [tCO_2 / MWh]	Low-carbon technology emissions [tCO_2] = Total power consumption of the pumps operated by an integrated system [MWh] × CO_2 emission factor for the electricity consumption [tCO_2 / MWh]
d) Introduction of inverter into sewerage system	Master plan emissions [tCO_2] = Power consumption of the normal pump operation [MWh] × CO_2 emission factor for the electricity consumption of the pump [tCO_2 / MWh]	Low-carbon technology emission [tCO_2] = Power consumption of the inverter-controlled pump [MWh] × CO_2 emission factor for the electricity consumption of the pump [tCO_2 / MWh]
e) Introduction of high-efficiency dewatering machine	Master plan emissions [tCO_2] = Power consumption of the conventional dewatering machine [MWh] × CO_2 emission factor for the electricity consumption of the machine [tCO_2 / MWh]	Low-carbon technology emissions [tCO_2] = Power consumption of the high-efficiency dewatering machine [MWh] × CO_2 emission factor for the electricity consumption of the machine [tCO_2 / MWh]
f) Optimization of sludge operation	Master plan emissions [tCO_2] = Total power consumption of the normal sludge collection system [MWh] × CO_2 emission factor for the electricity consumption [tCO_2 / MWh]	Low-carbon technology emissions [tCO_2] = Total power consumption of the optimized sludge collection system [MWh] × CO_2 emission factor for the electricity consumption [tCO_2 / MWh]

Low-carbon technologies	Master plan emissions*1 (tCO_2)	Low-carbon technology emissions*2 (tCO_2)
g) Utilization of biogas for power generation	Amount of electricity supplied by the grid to the area (MWh) × CO_2 emission factor for the electricity consumption (tCO_2 / MWh)	Power consumption of methane recovery and biogas power generation system (MWh) × CO_2 emission factor for the electricity consumption (tCO_2 / MWh)
h) Introduction of solar power system into WWTP site	Amount of electricity supplied by the grid to the area (MWh) × CO_2 emission factor for the electricity consumption (tCO_2 / MWh)	Power consumption of solar photovoltaics system operation (MWh) × CO_2 emission factor for the electricity consumption (tCO_2 / MWh)

Notes.

*1: Master plan emissions are GHG emissions from the operation of the existing and planned pumps proposed in the master plans in accordance with the MP scenario.

*2: Low-carbon technology emissions are GHG emissions from the operation of the existing and planned pumps proposed in the master plan with introduction of low-carbon technologies.

*3: Conventional pump/blower is a pump/blower that has a high market share in the target city/country.

References

Akinyemi, F.O. Land change in the central Albertine rift: Insights from analysis and mapping of land use-land cover change in north-western Rwanda. *Appl. Geogr.* **2017**, 87: 127–138.

Albano, R.; Mancusi, L.; Sole, A.; Adamowski, J. Collaborative strategies for sustainable EU flood risk management: FOSS and geospatial tools–Challenges and opportunities for operative risk analysis. *ISPRS Int. J. Geo-Inf.* **2015**, 4: 2704–2727.

Diffey, B. L. An overview analysis of the time people spend outdoors. *Br. J. Dermatol.* **2011**, 164: 848–854.

Dufour, A.P.; Evans, O.; Behymer, T.D.; Cantu, R. Water ingestion during swimming activities in a pool: A pilot study. *J. Water Health* **2006**, 4, 425–430.

Haltas I.; Tayfur G.; Elci S. Two-dimensional numerical modeling of flood wave propagation in an urban area due to Ürkmez dambreak, İzmir, Turkey. *Nat. Hazards* **2016**, 81(3): 2103–2119.

Handmer, J. The chimera of precision: Inherent uncertainties in disaster loss assessment. *Int. J. Mass Emerg. Disasters* **2002**, 20: 325–346.

Huizinga, J.; de Moel, H.; Szewczyk, W. *Global flood depth-damage functions. Methodology and the database with guidelines*; EUR 28552 EN. Publications Office of the European Union: Luxembourg, 2017.

Inaba, M.; Katayama, H.; Nga, T.T.V.; Furumai, H. Detection of genus Kobuvirus for evaluation as virus indicator for fecal contamination source tracking from Nhue River in Hanoi, Vietnam, In: *Southeast Asian Water Environment, Vol. 5*, Yamamoto, K.; Furumai, H.; Katayama, H.; Chiemchaisri, C.; Puetpaiboon, U.; Visvanathan, C.; Satoh, H.; Eds.; IWA Publishing: London, UK, pp. 61–66. 2014.

Intergovernmental Panel on Climate Change. *Climate Change 2014: Synthesis Report*. Core Writing Team; Pachauri, R.K., Meyer, L.A., Eds.; IPCC: Geneva, Switzerland, 2014.

Kuroda, K.; Nakada, N.; Hanamoto, S.; Inaba, M.; Katayama, H.; Do, A.T.; Nga, T.T.V.; Oguma, K.; Hayashi, T.; Takizawa, S. Pepper mild mottle virus as an indicator and a tracer of fecal pollution in water environments: Comparative evaluation with wastewater-tracer pharmaceuticals in Hanoi, Vietnam. *Sci. Total Environ.* **2015**, 506-507: 287–298.

Jongman, B.; Kreibich, H.; Barredo, J.I.; Bates, P.D.; Feyen, L.; Gericke, A.; Neal, J.; Aerts, J.C.J.H.; Ward, P.J. Comparative flood damage model assessment: Towards a European approach. *Nat. Hazards Earth Syst. Sci.* **2012**, 12: 3733–3752.

Jonkman, S.N.; Bockarjova, M.; Kok, M.; Bernardini, P. Integrated hydrodynamic and economic modelling of flood damage in the Netherlands. *Ecol. Econ.* **2008**, 66: 77–90.

Kefi, M.; Mishra, B.K.; Kumar, P.; Masago, Y.; Fukushi, K. Assessment of tangible direct flood damage using a spatial analysis approach under the effects of climate change: Case study in an urban watershed in Hanoi, Vietnam. *ISPRS Int. J. Geo-Inf.* **2018**, 7: 29.

Kelman, I.; Spence, R. An overview of flood actions on buildings. *Eng. Geol.* **2004**, 73: 297–309.

Mechler, R. Reviewing estimates of the economic efficiency of disaster risk management: Opportunities and limitations of using risk-based cost-benefit analysis. *Nat. Hazards* **2016**, 81: 2121–2147.

Messner, F.; Penning-Rowsell, E.; Green, C.; Meyer, V.; Tunstall, S.; van der Veen, A. *Evaluating flood damages: Guidance and recommendations on principles and methods*; FLOODsite Integrated Flood Risk Analysis and Management Methodologies Report T09-06-01; HR Wallingford: Oxfordshire, UK, 2007.

Le, M.N.; Tachikawa, Y.; Sayama, T.; Takara, K. Estimation of sub-hourly and hourly IDF curves using scaling properties of rainfall at gauged site in Asian Pacific Region. *Annuals of Disaster Prevention Research Institute, Kyoto University* **2008**, 51B: 63-73.

Mishra, B.K.; Herath, S. Assessment of future floods in the Bagmati River basin of Nepal using bias-corrected daily GCM precipitation data. *J. Hydrol. Eng.* **2015**, 20(8): 05014027.

Phanuwan, C.; Takizawa, S.; Oguma, K.; Katayama, H.; Yunika, A.; Ohgaki, S. Monitoring of human enteric viruses and coliform bacteria in waters after urban flood in Jakarta, Indonesia. *Water Sci. Technol.* **2006**, 54: 203–210.

Rafiei Emam A.; Mishra B.K.; Kumar P.; Masago Y.; Fukushi K. Impact assessment of climate and land-use changes on flooding behavior in the upper Ciliwung River, Jakarta, Indonesia. *Water* **2016**, 8: 559.

Schoen, M. E.; Ashbolt, N. J. Assessing pathogen risk to swimmers at non-sewage impacted recreational beaches. *Environ. Sci. Technol.* **2010**, 44: 2286–2291.

Sieber, J.; Purkey, D. *Water Evaluation And Planning (WEAP) User Guide*; Stockholm Environment Institute, U.S. Center: Somerville, MA, 2015. http://www.weap21.org/downloads/WEAP_User_Guide.pdf [Accessed on July 2nd, 2018].

Teunis, P.F.M.; Moe, C.L.; Liu, P.; Miller, S.E.; Lindesmith, L.; Baric, R.S.; Le Pendu, J.; Calderon, R. L. Norwalk virus : How infectious is it ? *J. Infect. Dis.* **2008**, 1476: 1468–1476.

Tu Vu, T.; Ranzi, R. Flood risk assessment and coping capacity of floods in central Vietnam. *J. Hydro-Environ. Res.* **2017**, 14: 44–60.

US Army Corps of Engineers, Hydrologic Engineering Center. *Hydrologic modeling system (HEC-HMS). User's manual v3.5*; US Army Corps of Engineers, Hydrologic Engineering Center (HEC): Davis, CA, 2010.

United Nations Department of Economic and Social Affairs, Population Division *World Urbanization Prospects: The 2014 Revision*; ST/ESA/SER.A/366; United Nations: New York, NY, 2015.

4 Case studies

4.1 Hanoi

4.1.1 Introduction

Hanoi, the capital of Vietnam, is located in the northwestern area of the Red River Delta. Following the expansion of the administrative boundary in 2008, the area is currently 3,359 km^2 and is divided into 12 urban and 17 rural districts, with 1 district-level town (General Statistics Office, 2017). The climate is characterized as humid subtropical, with hot summers and rainy and mild winters. In addition to the three main rivers, namely, the Red River, the Day River, and the Nhue River, there are many small rivers and canals comprising a dense water network together with many ponds and lakes. The population of Hanoi was 7,202,900 as of 2015 (General Statistics Office, 2017), and it is projected to increase to 8.2 million by 2034 (General Statistics Office and United Nations Population Fund, 2016).

The study area is the watershed of the To Lich River system, which consists of four urban rivers flowing through central Hanoi, namely, the To Lich River, the Lu River, the Set River, and the Kim Nguu River (Figure 4.1.1). Due to its geographical characteristics, Hanoi, like many other Vietnamese cities, is prone to flooding; it lies in a low and flat area, which contributes to the increased risk of floods. In addition, river water pollution is also severe (Quan et al., 2010, Dao et al., 2010) due to a lack of wastewater treatment.

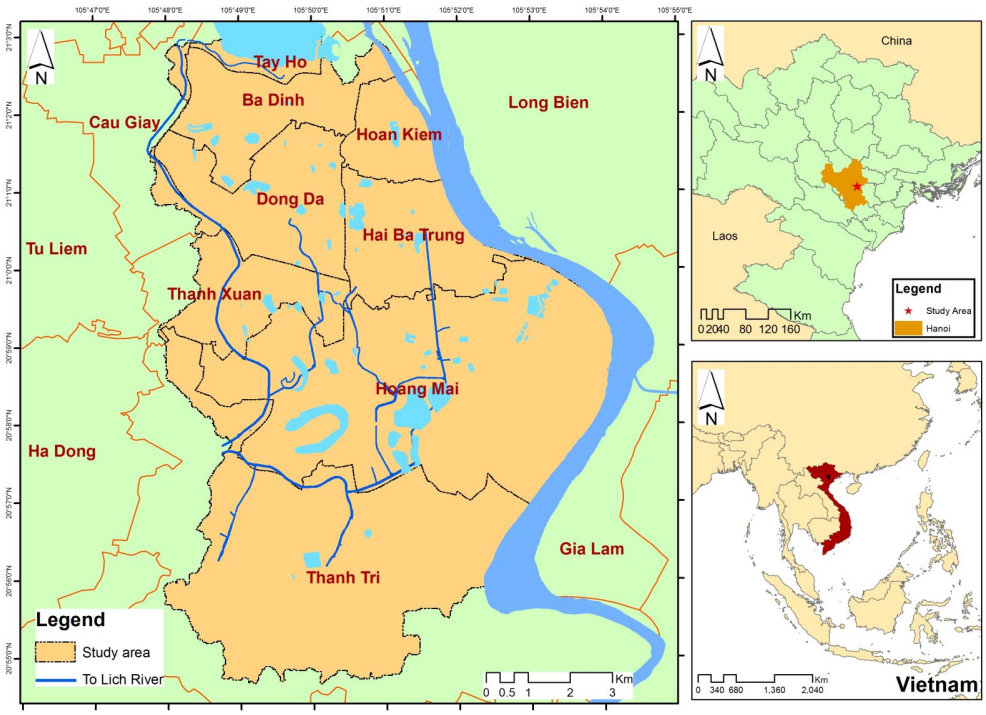

Figure 4.1.1. Study site of Hanoi

4.1.2 Methodology

4.1.2.1 Precipitation change

This study examined the impact of climate change on rainfall under different scenarios over the central area of Hanoi, Vietnam, using a baseline period of 1985 to 2004. Daily rainfall observations from the Hanoi station covering this period were collected for bias correction of the GCM outputs by comparing them with the GCM simulations using a quantile mapping technique. The GCM rainfall data, which are output from five GCMs, were derived from CMIP5, and the observational rainfall data were provided by the Vietnam Institute of Meteorology, Hydrology and Climate Change. The study constructed rainfall IDF curves for baseline and future periods, so it was necessary to exploit simulated and projected rainfall data from GCMs. To construct future IDF curves, daily rainfall data were simulated over 2020-2044 based on combinations of 3 GCMs: MRI-CGCM3, MIROC5 and HadGEM-ES. The performance of the downscaling method was evaluated, and the IDF curves were developed for comparative assessment.

To evaluate the effects of climate change on water quality, we evaluated the change in monthly average precipitation, and the GCM output was downscaled at the local level for reliable impact assessment. Based on the rate of change in the observed historical rainfall values and downscaled future precipitation data, we estimated the average rate of increase based on regression analysis. This growth rate was applied to the current rainfall values to obtain future rainfall values. Statistical downscaling followed by trend analysis, a less computationally demanding technique that enables the reduction of biases in precipitation frequency and intensity (Goyal and Ojha, 2011), was used here to obtain climate variables at the monthly scale. The MRI-CGCM3 and MIROC5 precipitation scenarios under RCPs 4.5 and 8.5 were used for the future simulation to assess the impact climate change. In this study, the GCM data were from the 1980-2004 and 2020-2044 periods (each with a 25-year length) and represent the current and future (2030) climate, respectively.

4.1.2.2 Land cover change

Land cover was established to determine the exposure of assets to flood hazards. In this case study, the land cover for 2030 was predicted through the analysis of two past land cover assessments, and the technique was based on the use of remote sensing products and LCM for ArcGIS Software Extension 2.0 considering the driving factors, as explained in Section 3.2. In this work, a Landsat 5 image from 2007 and a Landsat 8 image from 2016 were utilized as described in Table 4.1.1 to establish useful LULC maps for the current flood simulation and to predict the LULC of 2030 based on the appropriate drivers.

Table 4.1.1. Satellite images applied

No.	Path/Row	Data Set	Acquisition Data	Cloud Cover
1	127/045	Landsat 5 TM C1 Level 1	08/05/2007	7%
2	127/045	Landsat 8 OLI/TIRS C1 Level 1	01/06/2016	13%

Four LULC classes, namely, built-up areas, water bodies, agriculture land, and green land, were identified based on the supervised classification. Then, the land cover layer was overlaid with flood hazard data to identify affected areas in the GIS environment.

4.1.2.3 Population change

The future population was estimated by the ratio method using growth rate data for Hanoi city from Vietnam Water, Sanitation and Environment (VIWASE, 2015). The results are shown in Table 4.1.2.

Table 4.1.2. Future projected population growth in different catchment areas using the VIWASE projection rate

District	2015	2030	Area (km^2)
Ba Dinh	237,600	170,000	9.25
Cau Giay	242,500	147,500	12.03
Dong Da	387,800	255,000	9.96
Hoan Kiem	150,700	130,000	5.29
Hoang Mai	252,800	254,500	39.81
Tay Ho	143,300	119,800	24.01
Hai Ba Trung	311,200	200,700	10.09
Thanh Tri	211,600	355,488	62.93
Tu Liem	463,100	778,008	75.33
Thanh Xuan	244,100	135,000	9.08

4.1.2.4 Urban flooding

Hanoi, the capital of Vietnam, experiences devastating flood events (e.g., 2008 October-November flood). The city has a humid subtropical climate and flat terrain (flat terrain), which result in frequent flooding during the rainy season. The major river systems around metropolitan Hanoi are the Red, Da, Day and Nhue; the To Lich, Lu, Set and Kim Nguu Rivers passing through central Hanoi are tributaries of the Nhue River. Districts in Central Hanoi (112 km^2) were considered for the investigation of urban flood inundation.

Various reports and a master plan were reviewed to explore feasible options for flood risk management to improve the urban water environment of Hanoi. In this study of central Hanoi, there was no need to include hydrologic modeling simulations as the river systems were found to originate well within the inundation modeling area.

In line with the Hanoi drainage master plan/vision, various scenarios were analyzed, including (i) climate and land cover change considerations, (ii) climate and land cover change with lake preservation, and (iii) climate and land cover change with lake preservation and WSUD. Lake preservation and WSUD were applied as feasible countermeasures for improving flood risk management, and recent drainage management works were largely reported in 2 phases. Major activities carried out under the Phase 1 (1999-2005) drainage project included sewerage rehabilitation, pumping at 45 m^3/s and dredging to tackle a 2-year flood return period flood. Similarly, the major activities of the Phase 2 (2009-2014) included sewerage expansion, dredging of lakes/rivers, dam improvements/regulations and pumping capacity increases from 45 to 90 m^3/s to tackle the 10-year return period. The Hanoi drainage plan to 2030 and vision to 2050 state that three main drainage systems will be erected in the basin of the To Lich, Nhue and Day Rivers in addition to the construction of pumping stations, an urban irrigation network, and reservoirs with self-draining capacity. The FLO-2D model, a two-dimension channel and floodplain flood routing model, was applied to predict floodwave attenuation, floodplain inundation and spatially variable water surface elevations. The 2008 Hanoi flood event was used to calibrate the flood inundation model.

4.1.2.5 Direct flood damage

The assessment of flood damage is related to three main components, namely, hazard, exposure and vulnerability, as explained in detail in Section 3.5. As an indicator of vulnerability, the flood-depth damage function is generated from field surveys with the collaboration of the University of Economics and Business, Vietnam National University, Hanoi. A field survey was conducted at the ward level during March 2017, and interviews were conducted with local people in affected residential and nonresidential areas using specific questionnaires. Potential respondents were selected from the flood hazard map that was generated and calibrated based on the 2008 flood event, and In total 293 responses were collected from residential and nonresidential sectors from several locations, as presented in Figure 4.1.2. Flood damage in the study area was estimated under current conditions, and two scenarios related to climate change and the implementation of flood measures were also simulated as described in Section 4.1.2.4.

Figure 4.1.2. Field survey locations

4.1.2.6 Water quality

Basic information regarding the model and data requirements

As explained in Section 3.6, the WEAP model was used to simulate future water quality variables in the year 2030 to assess alternative management policies for the To Lich River basin. Apart from our main objective, the model also simulates river flow, storage, pollution generation, treatment and discharge while considering different users and environmental flows. Here, according to the master plan (Vietnam urban water supply and wastewater project, 2015), water flowing in the targeted river (To Lich) will be transported to another location, and treated water from Ho Tay WWTP will be diverted to the To Lich River.

For water quality modeling, wide range of input data was provided including household discharge and its locations and concentrations, past spatiotemporal water quality, wastewater treatment plants (Ministry of Natural Resources and Environment (MONRE)), population, historical rainfall, temperature (VIWASE), drainage networks (MONRE), river flow-stage-width relationships, river length, surface water inflows and land use/land cover (MONRE).

A WEAP model was developed for the To Lich, Set, Lu and Kim Nguu River basin for four command areas with interbasin transfers. Hydrologic modeling requires that the entire study area be split into smaller catchments with consideration of the confluence points and the physiographic and climatic characteristics (Figure 4.1.3). The hydrology module within the WEAP tool enables modeling of the catchment runoff and pollutant transport into the river; pollutant transport from a catchment accompanied by rainfall-runoff is enabled by selecting the water quality modeling option. Pollutants

that accumulate on catchment surfaces during nonrainy days reach water bodies through surface runoff, and the WEAP hydrology module computes catchment surface pollutants generated over time by multiplying the runoff volume and concentration or intensity for different types of land use.

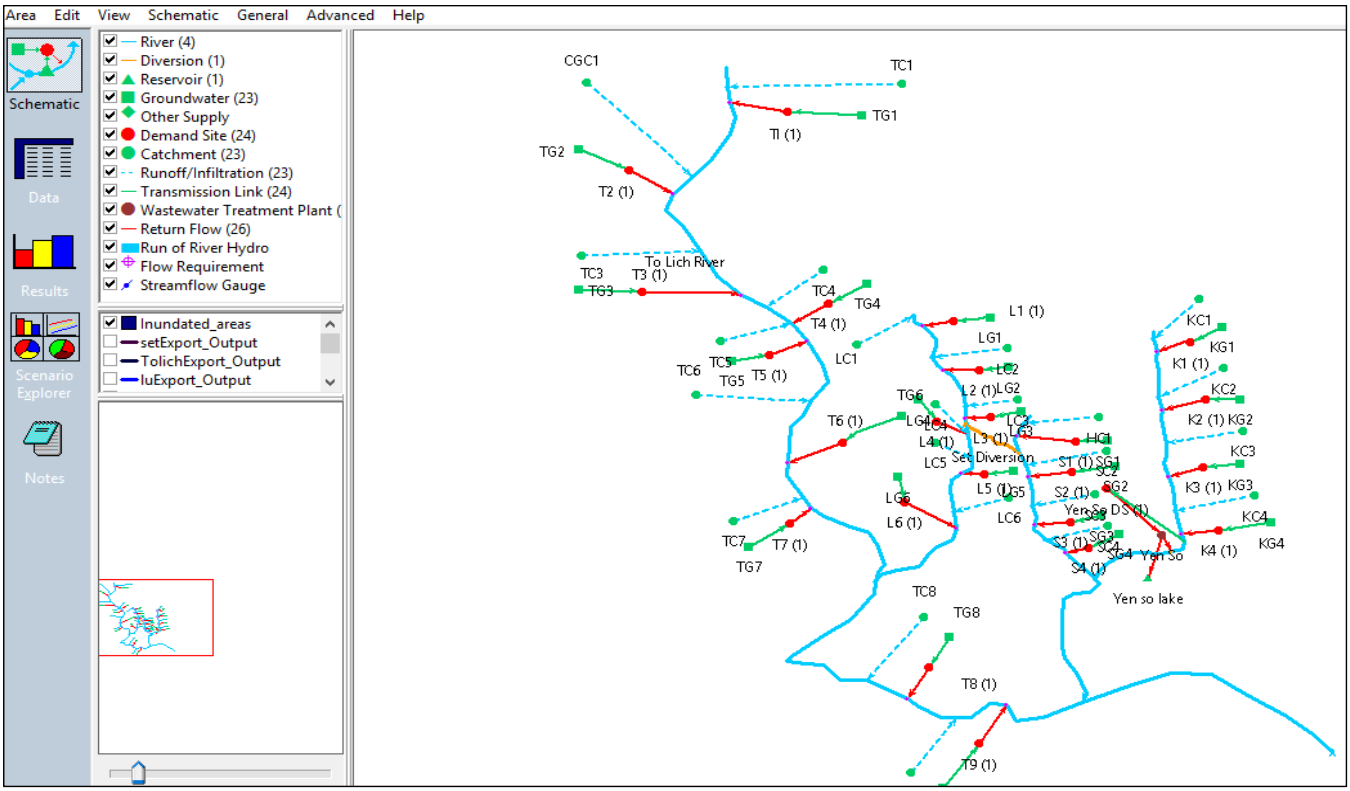

Figure 4.1.3. The network of the four rivers with subcatchments and the locations of wastewater treatment plants, water quality stations, and streamflow measurement stations

During simulation, the land use information was broadly grouped into three categories: agricultural, forest, and built-up areas. The soil data parameters were identified using previous secondary data and the literature. The population distribution results and the future trends at these four command areas were calculated by the ratio method using the VIWASE projection rate as explained in Section 4.1.2.3. Regarding future precipitation data, different GCM outputs were used after bias correction, which is explained in detail in Section 4.1.2.1.

Model setup

The entire problem domain and its different components are divided into three catchments that are further subdivided into twenty-three subbasins considering the influent locations of the major tributaries (Figure 4.1.3). Other major considerations are the twenty-four demand sites and one wastewater treatment plant representing the problem domain. Here, demand sites are meant to identify domestic (population) and industrial centers whose attributes explain water consumption

and wastewater pollution loads per capita, water supply sources and wastewater return flows; dynamic attributes are described as functions of time and include population and industrial growth. Wastewater treatment plants are pollution-handling facilities with design specifications that include total capacity and pollutant removal rates. The flow of wastewater into the To Lich, Set, Lu and Kim Nguu Rivers and the tributaries mainly travels through domestic, industrial and stormwater runoff routes. Here, a UASB-SBR type of wastewater treatment plant is considered in the modeling, and its treatment efficiency is assumed to be 94% for COD, 97% for BOD, 77% for TN and 99.69% for fecal coliform bacteria (Khan et al., 2013). Future WWTPs must employ UASB-SBR technology according to the master plan, but the types and technology of current WWTPs are not specific. Therefore, we selected this advanced technology for both current and future WWTPS for the sake of simplicity. In the absence of detailed information, the daily volume of domestic wastewater generation was estimated as 130 liters of average daily consumption per capita based on a review of the literature.

Water quality is simulated using two possible scenarios, as shown in Table 4.1.3, for the years 2015 and 2030, using 2011 as a reference year and considering population increase, land use change, wastewater generation and its treatment at wastewater treatment facilities. First, the business-as-usual scenario, under which the effects of population growth and climate change on water quality are predicted for the year 2030 using the average values of two GCMS and two RCPs and keeping the capacity of all the existing wastewater treatment plants (200 MLD) constant. Here, the small range in the simulated water quality is due to changes in the GCMs and RCPs. For the scenario with measures, only the To Lich River was considered. Here, all the water in the river will be diverted, and all the treated water from the Ho-Tay WWTP, which is located to the north, will be brought to the To Lich River.

Table 4.1.3. Summary of all the criteria considered for different future water quality simulation scenarios

Scenario	Components
Business as usual	Climate change + population growth +WWTP of 200 MLD
With measures	Climate change + population growth +treated wastewater from Ho Tay WWTP will be transferred to the To Lich River

4.1.2.7 Economic benefit of improving urban water quality

A questionnaire for the Hanoi study was designed as follows. 1) The first part requested background data/the profile of the respondent; 2) the second part was related to awareness of the current water quality situation; and 3) the main part included WTP questions (use- and nonuse), which were divided into subquestions:

1. *Are you willing to pay to improve the water quality of waterbodies in Hanoi?*
   ☐ YES ☐ NO

2. *In addition to the monthly utility bill, how much would you be willing to pay as a monthly, per-household fee for various levels of improvement in the water quality of the city's waterbodies?*

As options, we provided five cards specifying amounts ranging from VND 1,000 to 500,000 or suggested that the respondent indicate their own amount.

Some 50 respondents in Hanoi were selected for a pilot study to pretest a developed questionnaire. The objective was to determine whether the survey was logical and if the WTP questions were correctly understood by the residents. The main survey was conducted in the inner districts of Ba Dinh, Dong Da, Hai Ba Trung, and Hoan Kiem (old districts) in December 2016; a total of 550 interviews were completed.

The random stratified sampling method was used because we could not secure a list of voters from the local government, and we did not want to use a telephone book to conduct sampling for the survey because the entire area of the megacity would not have been covered. The selection techniques were based on two classes: (1) walking distance to the river, which assumes that one can reach the nearest waterbody within 30 min, and (2) the need to drive or take public transportation to the nearest waterbody. The SPSS statistical package was used for the analysis; the WTP was estimated by logit and probit models.

4.1.2.8 Floodwater-borne infectious diseases

The risk assessment model for floodwater-borne infectious gastroenteritis was developed following the methodology in Section 3.8 to evaluate the number of cases of disease caused by norovirus that occurred in the flooded area in central Hanoi. Three scenarios were developed, one to simulate the current situation (current scenario) and two to simulate the future situation as of 2030 with or without mitigation measures, namely, a with mitigation scenario and business-as-usual scenario, respectively. The results of the flood inundation model and water quality model corresponding to each scenario were used to represent the current or future situation of urban flooding and surface water quality. For the flood situation with mitigation, the result of the "Climate change + lake preservation/regulation + WSUD" scenario was used. The current and future population in each FLO-2D grid (31,361 grids in total) was calculated using the total current and future population of the city as described in Section 4.1.2.3, the area of the city, and the area of the FLO-2D grid (3,600 m^2). The area and population used in this analysis was summarized in Table 4.1.2. The total population in the study area was 2,644,700 for 2015 and 2,545,996 for 2030 (3.7% decrease).

4.1.2.9 Low-carbon technology in wastewater facilities

The amount of GHGs emitted from wastewater treatment facilities was estimated following the methodology stated in Section 3.9. Three scenarios were developed, namely, the current scenario, 2030 without low-carbon technology scenario, and 2030 with low-carbon technology scenario. The current scenario evaluates GHG emissions under the current conditions (i.e., emission from existing

facilities), and the 2030 without low-carbon technology scenario evaluates GHGs emission from the existing and planned facilities stated in the master plan (MWSS, 2016) using technologies (e.g., pumps, blowers) that are currently available in Southeast Asia. Finally, the 2030 with low-carbon technology scenario was used to evaluate GHG emissions assuming the implementation of low-carbon technologies as stated in Section 3.9.2. Based on the two scenarios for 2030, we evaluated the potential reduction in GHG emissions from wastewater facilities in the target area.

4.1.3 Results and discussion

4.1.3.1 Precipitation change

The results indicate that the mean corrected monthly rainfall and the frequency of wet days are considerably closer to the observational data than the raw rainfall estimates. The bias correction method accurately captured extreme rainfall values for all 3 GCMs. Of the 3 GCMs, rainfall intensity was found to be increasing in MRI-CGCM3 and HadGEM-ES by the end of the century and decreasing in the MIROC5 climate model. However, assuming climate change will worsen the extreme flood situation, the MRI-CGCM3 and HadGEM-ES projections were considered to simulate flood inundation. Table 4.1.4 shows a comparison of rainfall intensity for a 50-year return period at the Hanoi station for different GCM and emissions scenarios. This result was obtained by using the Gumbel distribution for the frequency analysis of the observational daily rainfall datasets from 1985 - 2004. The potential impact of climate change on extreme rainfall events were studied by analyzing rainfall IDF curves for the present and future climate of Hanoi. For the 50-year return period, rainfall intensity is projected to increase by 23% and 50% under the RCP4.5 and RCP8.5 emission scenarios, respectively. For the flood inundation simulation under future climate, the mean of the MRI-CGCM3- and HadGEM-ES-based rainfall, i.e., 414 mm, was used. The results of this study are of significant practical importance for the design, operation and maintenance of storm water management infrastructures under climate change.

Table 4.1.4. Fifty-year return period daily maximum rainfall (mm) over central Hanoi

Observation	GCM (RCP 4.5)			RCP 8.5		
	MRI	MIROC	HadGEM	MRI	MIROC	HadGEM
334.5	416.5	297.5	411.6	592.8	333.0	410.9

As for the monthly precipitation scenario, the results shown in Figure 4.1.4 clearly indicate that annual precipitation simulated from the GCM output is not much different from current, observed value. The total annual precipitation values according to observed_2015, Sim_2030_MRICGCM3_45, Sim_2030_MIROC5_45, Sim_2030_MRICGCM3_85, and Sim_2030_MIROC5_85 are 1644.5, 1637.4, 1658.9, 1647.8 and 1641.1 mm, respectively. Finally, for the water quality simulation, we used MRICGCM3 with RCP_8.5.

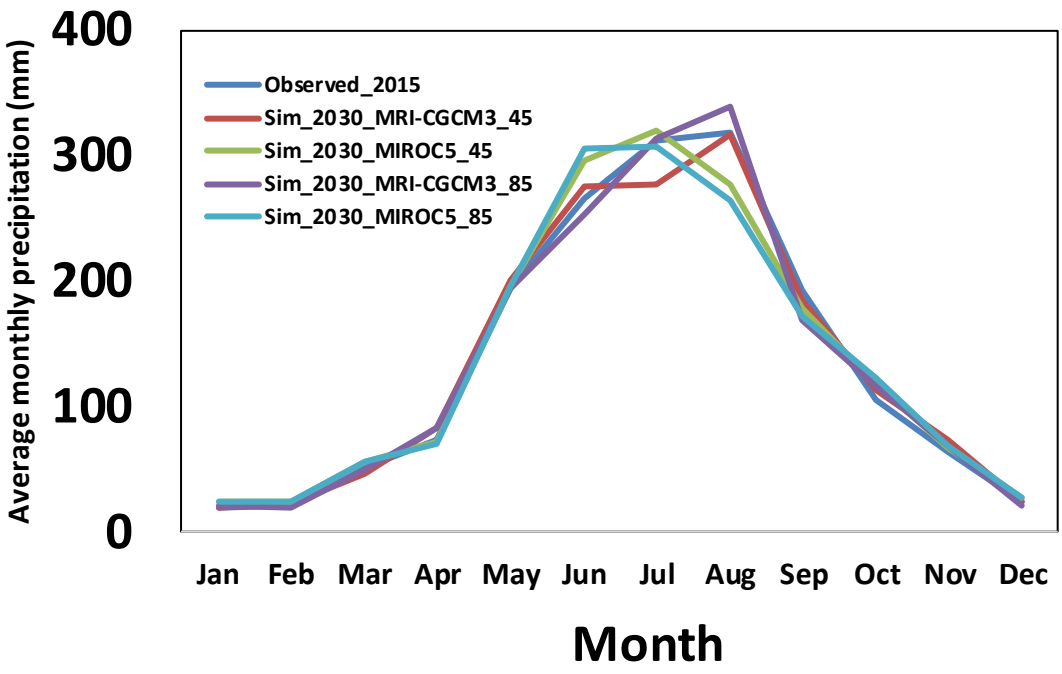

Figure 4.1.4. Graph showing the results of a comparative study of the current and future monthly rainfall at Lang station

4.1.3.2 Land cover change

The future land cover in 2030, as derived from two past satellite images, showed an 7% increase in built-up areas (Figure 4.1.5). The expansion of cities in unsuitable areas may contribute to the exposure of buildings and infrastructure to a high flood threat level. People migrate to cities seeking a better life, which results in urban sprawl along riversides or in floodplains. The comparison of urbanization in the study area under the current and future scenarios demonstrated that the urban districts, such as Ba Dinh, Dong Da, Hai Ba Trung, Hoan Kiem, Thanh Xuan, and Hoang Mai, will undergo little change, but Thanh Tri, as a rural district, will likely be more urbanized in the future (Figure 4.1.6). In fact, urbanization changes hydrological processes within watersheds, resulting in fluctuating surface infiltration characteristics (Du et al., 2012) and may consequently increase the flood risk.

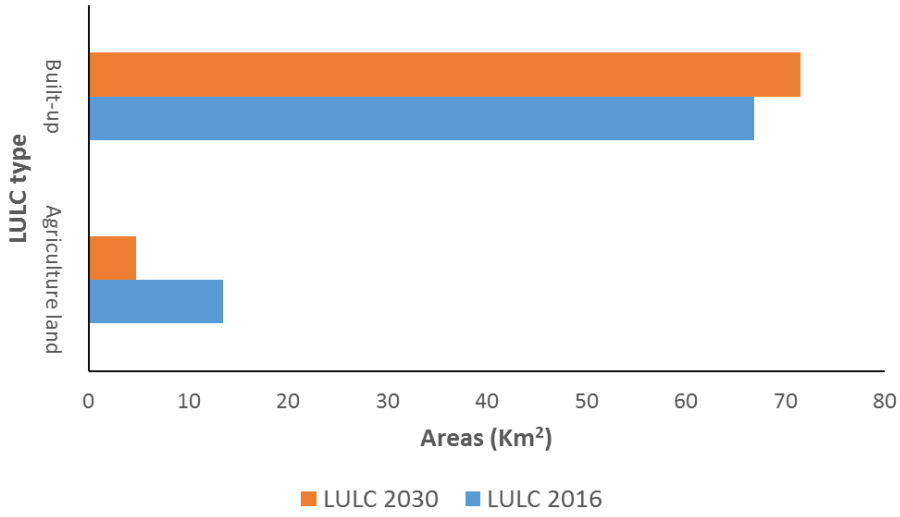

Figure 4.1.5. Land cover change in the future

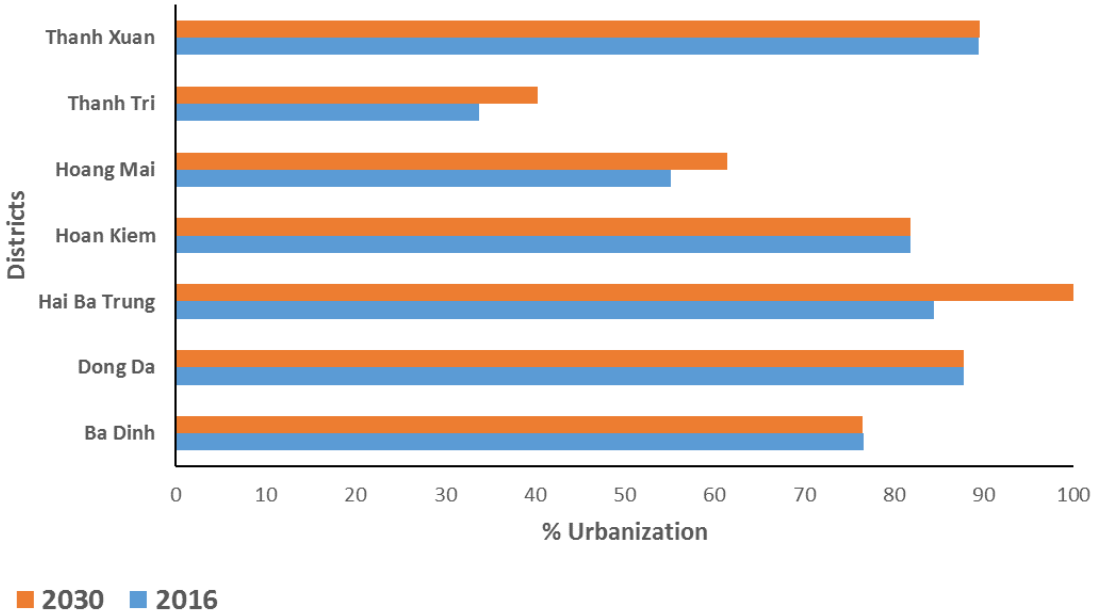

Figure 4.1.6. Urban growth by district

The spatial extent is an important factor in damage assessment (Pistrika et al., 2014). Due the low resolution of the Landsat images, the built-up class is applied as an aggregated land cover category that includes residential and nonresidential areas. Hence, our analysis is considered a meso-scale damage evaluation, which is convenient for regional analysis.

4.1.3.3 Urban flooding

Flood inundation simulations for were conducted for current and future conditions with different combinations of climate change, lake preservation and WSUD (Figure 4.1.7). The pond and lake system has been very important for agricultural development, the water supply for residents, water

regulation in floods and the rainy season, and the creation of beautiful landscapes for tourism development. However, there has been a significant loss of such water bodies and their benefits in recent years. For the future simulation, flood storage of 8 million cubic meters was assumed with the preservation/regulation of lake/ponds with an area of 4 km^2 and a depth of 2 m.

The conventional approach to urban drainage is based on removing excess water from the inundated area into receiving bodies as quickly and safely as possible through underground pipe systems. Retaining the water for infiltration or monitoring the run-off is a better alternative than constructing larger pipes, so adoption of the WSUD technique will help to reduce peak run-off flow by 15-20%. Therefore, it is important to have regulations in urban construction management. Assuming the WSUD option, a 40-mm increase in infiltration was assumed for the extreme rainfall event.

Under the climate change scenario the daily rainfall and inundation area significant increase. In 2030, an 19% increase in inundation area was projected for the 50-year return period, but the study found that lake preservation/regulation can reduce the additional inundation caused by climate change. WSUD will further decrease the flood inundation area (65%). Despite considerations of lake preservation/regulation and WSUD, the inundation area significantly increased, although much less than under the current condition. This indicates that further flood management (drainage) measures should be considered such as channel improvement, dredging, increased pumping, awareness raising, etc. The significant increase in inundation area/depth supports the consideration of flood management (drainage) systems for extreme events with longer return periods (instead of the current 10-year return period). The southwest and south areas of the city, such as Thanh Tri District, require greater attention as these areas are expected to be severely affected by flood with deeply inundated areas.

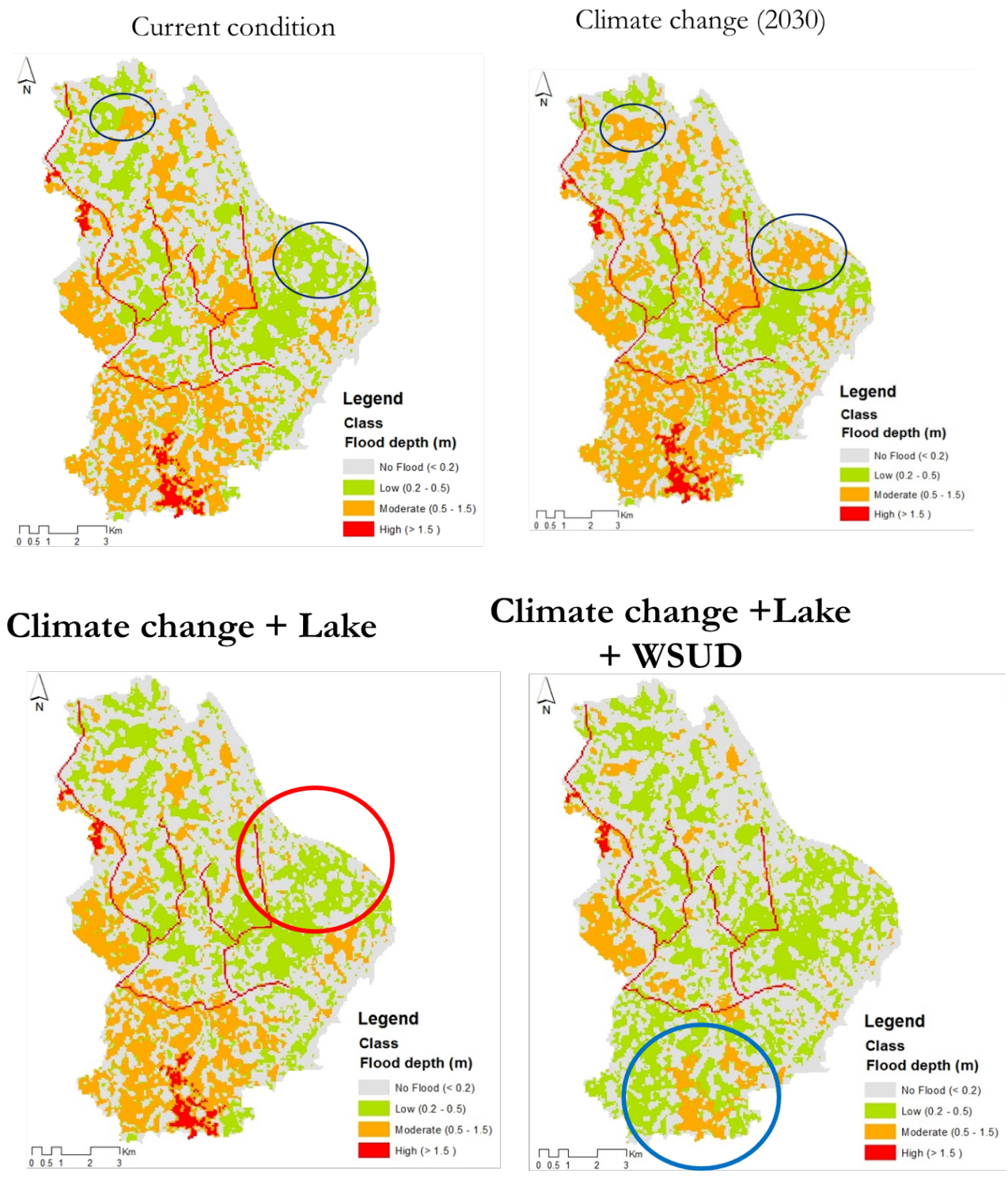

Figure 4.1.7. Comparison of flood inundation under current and future conditions

4.1.3.4 Direct flood damage

Tangible direct damage was estimated in this study, and the flood damage map was established using a combination of the hazard, exposure, and vulnerability components in a GIS with a grid size of 60 × 60 m. The calibration of the baseline results depended on the damage estimate from the Hanoi government for the 2008 flood (VCCFSC, 2008). The results indicated that the total damage

will increase with the impacts of climate change, but flood mitigation will reduce the total damage in the study area. In fact, the comparison between the current and future scenarios showed a 26% increase in the total damage with the effect of climate change, but the implementation of combined flood measures will decrease flood losses by 29%. The flood damage maps in Figure 4.1.8 illustrate that the spatial distribution of flood damage is mainly correlated with the water depth and inundated area parameters. The damage is higher in the southern areas than in the northern areas of the watershed, and the losses in the western area are more significant than in the eastern cities. Alternatively, the implementation of flood protection measures will protect the more vulnerable regions and reduce flood loss.

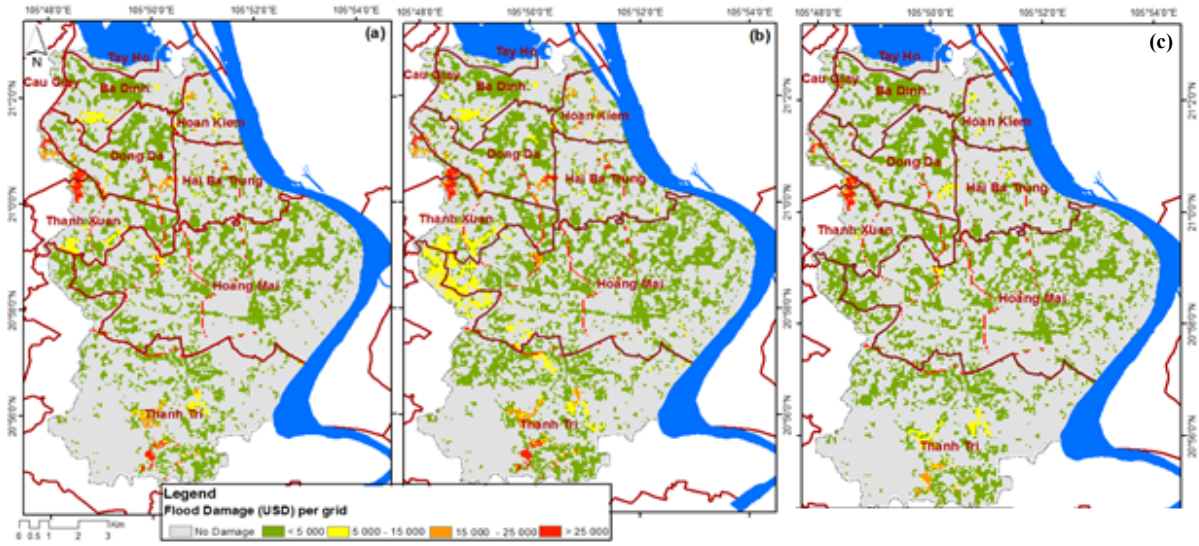

Figure 4.1.8. Flood damage map: (a) current scenario, (b) future scenario with climate change, and (c) combined measures (WSUD and Lake)

The analysis of flood damage in the main inundated district demonstrates that the damage will increase with the magnitude of the water depth, which is explained by the application of the flood-depth damage function. However, Figure 4.1.9 reveals that in the case of Thanh Tri District, the total damage is not significantly correlated with the water depth. In fact, in this rural district, the average water depth is higher, but the total damage remains low. This result can be explained by the high degree of urbanization and the property value of the assets. Indeed, floods are a type of natural disaster that affects both urban and rural areas, but the economic impacts in urban areas are more serious due to the greater value of the assets at risk (Neal et al., 2009). In addition, due to urbanization, green land will be converted to impervious lands, such as roads and buildings, which will reduce infiltration and increase runoff, so the occurrence of more severe floods is increasing (Rafiei Emam et al., 2016). Regarding water depth, the Thanh Xuan and Thanh Tri Districts are the main areas that are most vulnerable to flooding because they are located in low-lying areas. Topography plays an important role in the magnitude of flooding (Bosher and Chmutina, 2017). In addition, lake preservation and drainage improvement will contribute to reducing the damage in the inundated districts. Indeed, the combination of several measures, such as retention ponds,

permeable paving, or block storage, can be implemented to reduce the peak flow and magnitude of a flood (Ramos et al., 2017).

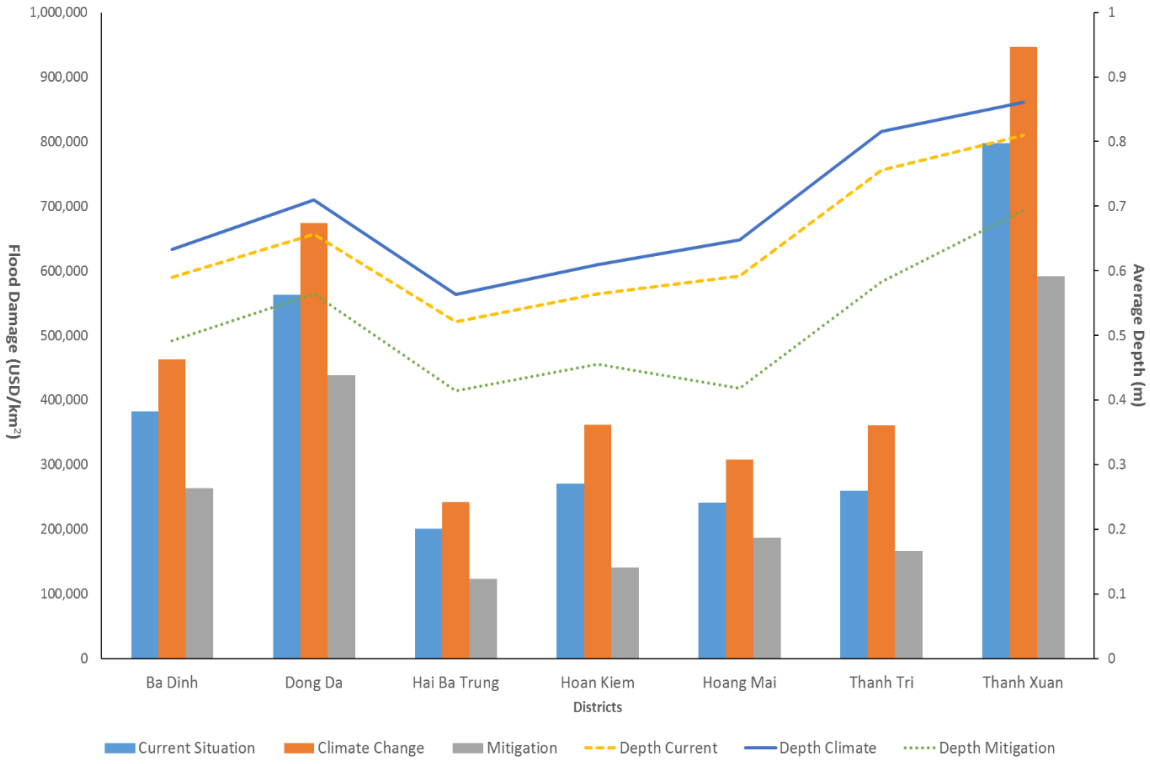

Figure 4.1.9. Flood damage by district

Climate change combined with the unplanned expansion of built-up areas increases the vulnerability of urban areas to flooding and thus economic damage. Consequently, the adoption of appropriate flood countermeasures, as presented in this study, is required. For this reason, local decision-makers should emphasize flood adaptation and mitigation measures for sustainable urban development, and several parameters, such as climate, land-use change, and topography, should be considered in the design and implementation of suitable flood management techniques. In addition, decision-makers and planners should consider hazard maps that combine physical and socioeconomic factors to establish effective and suitable urban planning strategies (Bathrellos et al., 2012).

4.1.3.5 Water quality

Future simulation and scenario analyses of Water Quality

Future simulation of river water quality using selected parameters (BOD and *E. coli*) was conducted under two different scenarios (business-as-usual and with measures) to predict conditions in 2030, and the results are shown in Figures 4.1.10, 4.1.11, and 4.1.12. The effects of both climate change and population changes are prominent in the status of water quality, which is further deteriorated in 2030 when compared to the current situation. Additionally, water quality is worse in the

downstream sampling locations of most of the rivers. According to water quality guidelines, the water in many of the locations, especially downstream, fails to qualify as Class B for use in agriculture and aquaculture (< 25 mg/L BOD). Due to climate and population changes, the water quality (expressed as BOD) will be further deteriorated by 53.1% on average in 2030 compared to the current situation. According to the master plan, all domestic wastewater currently flowing into the rivers, except for the Kim Nguu River, will be transferred to new wastewater treatment plants, and we suggest that the rivers be supplemented with treated wastewater from surrounding wastewater treatment plants or water from other sources to maintain the river flow and improve the water quality as shown under the mitigation plan scenario (85.8% reduction compared to the business-as-usual scenario).

If this masterplan succeeds by 2030, no treated wastewater will be released into the To Lich, Kim Nguu, Lu and Set Rivers, so these rivers will dry during the dry season. However, based on the with-mitigation scenario under which treated wastewater from Ho Tay WWTP (22.8 MLD) will be transferred to the To Lich river, the water quality will be much better throughout the stream. To revive all four rivers and achieve class B water quality, the local government must consider diverting some of the treated wastewater into these rivers to maintain their flow, especially during the dry season. However, the effects on flow rate remain uncertain but could be researched through regular monitoring once diversion is implemented. Furthermore, the national integrated sewerage and septage management program should be implemented on a priority basis, considering various factors such as population density and growth and global changes for both short- and long-term measures.

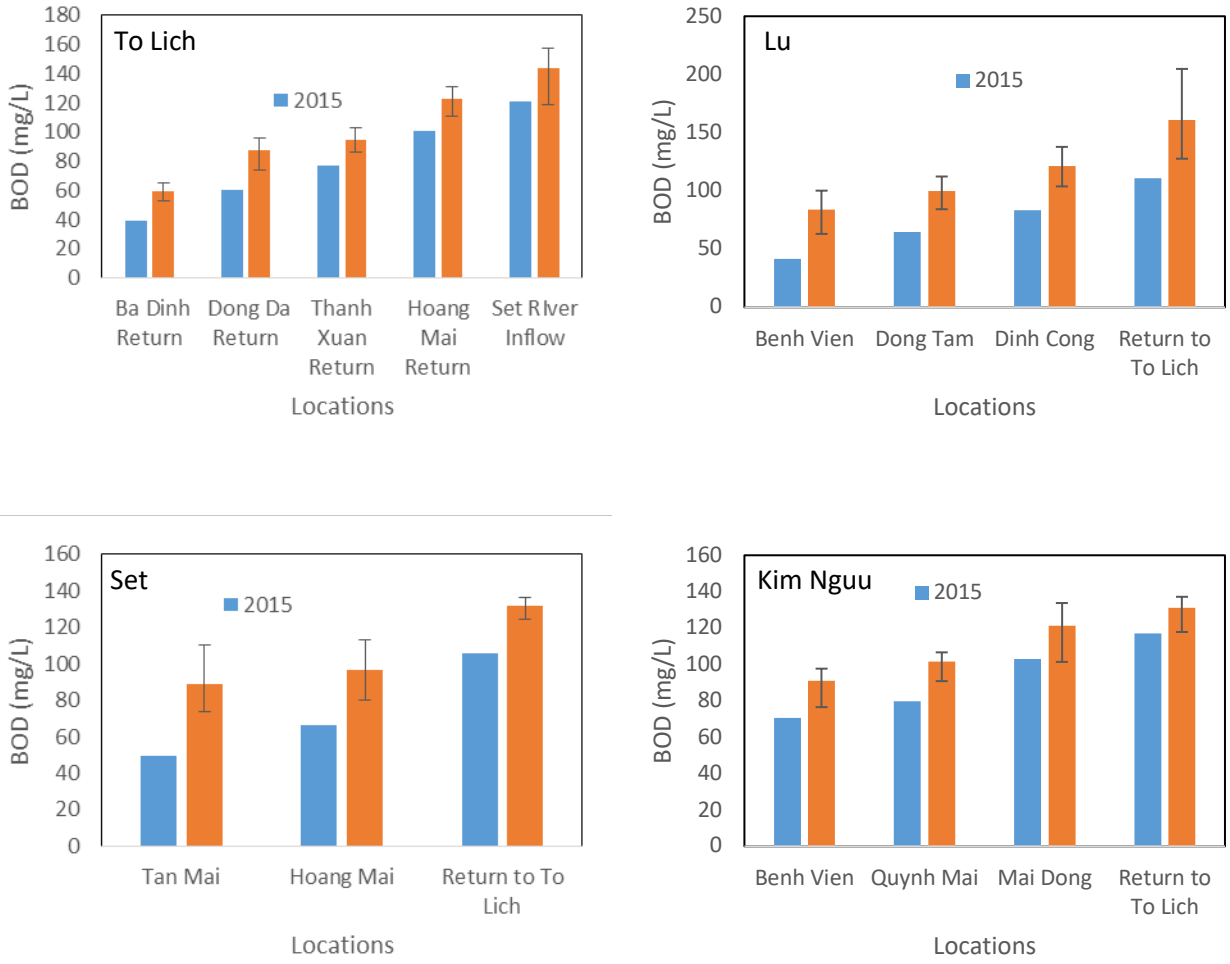

Figure 4.1.10. Simulated BOD values using the business-as-usual scenario for all four river systems

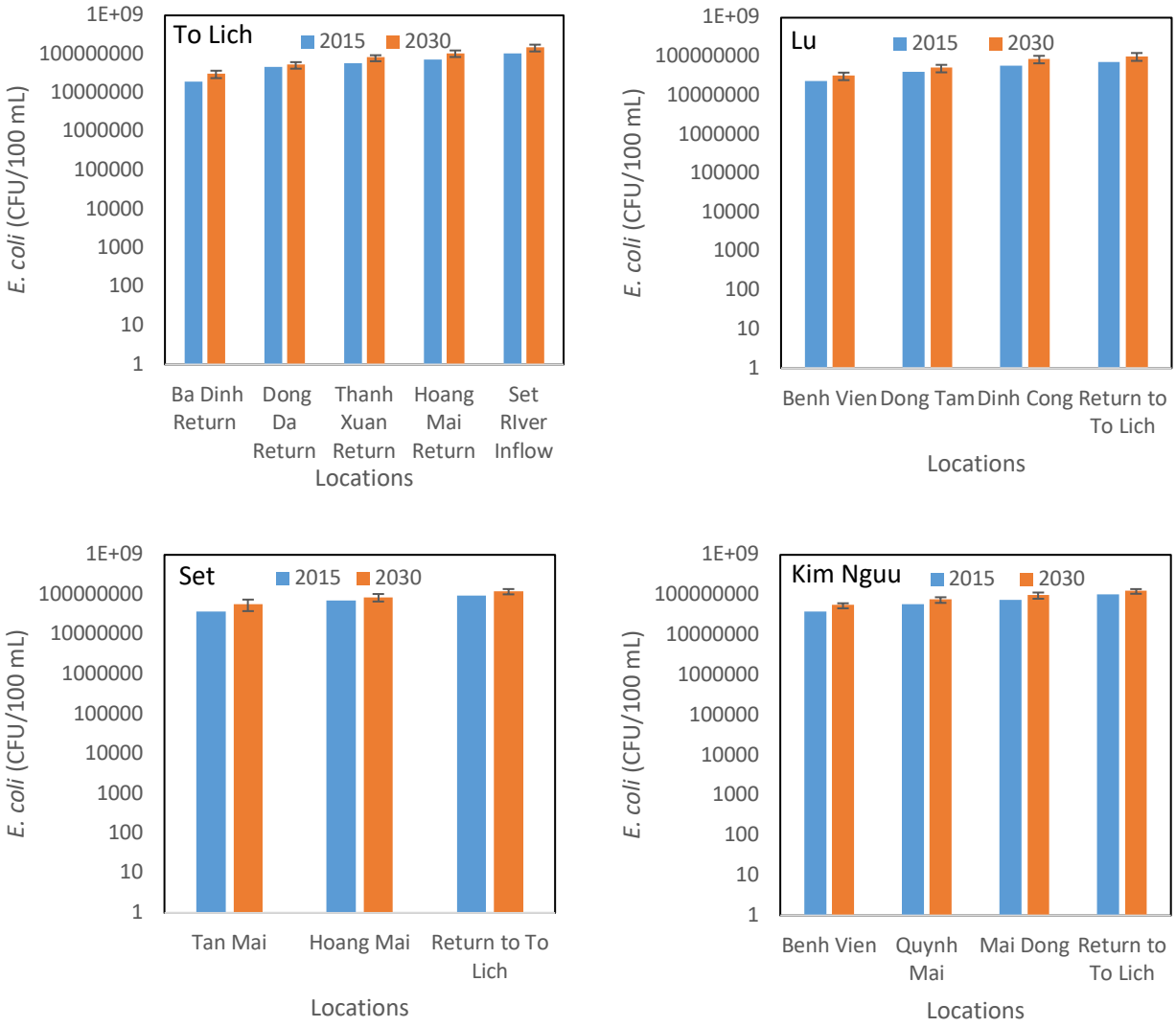

Figure 4.1.11. Simulated *E. coli* values using the business-as-usual scenario for all four river systems

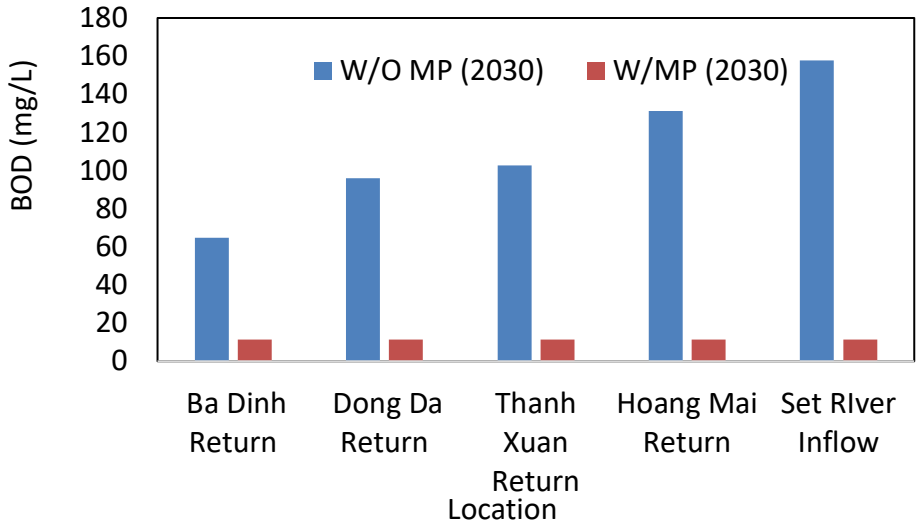

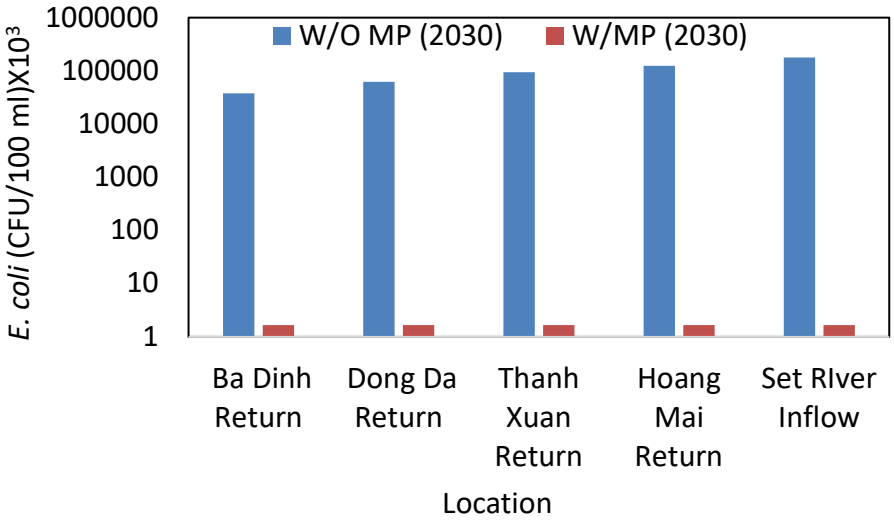

Figure 4.1.12. Simulated water quality results for BOD and *E. coli* for the scenario with measures, under which all wastewater will be diverted from the To Lich River and treated wastewater from the Ho Tay WWTP will be transferred to the To Lich River

4.1.3.6 Economic benefit of improving urban water quality

Out of 550 total questionnaires, only 414 were submitted to further analysis (75% response rate). From the sample, 91% had visited (intentionally) the city's waterbodies in the last month: 22% went regularly, 29% went a few times, and 49% went once. The majority of respondents acknowledged the problem of water pollution in the city's waterbodies; for the question of whether the water quality is sufficiently acceptable for participating in recreational activities, 55% responded not sufficiently acceptable for recreational and other activities, 38% sufficient, and 7% did not know.

Below, Figure 4.1.13 presents the socioeconomic profile of the sampled population in Hanoi City, demonstrating that the sample was representative.

The main results of the study relate to the estimation of WTP values and the calculation of the total economic value for the entire population of the city. The average use WTP for swimmable water quality was estimated as VND 15,069 (USD 0.66) per capita; the average use WTP for fishable water quality was estimated as VND 14,840 (USD 0.65) per capita; the average nonuse WTP for swimmable water quality was estimated as VND 42,922 (USD 1.88) per capita; and the average nonuse WTP for fishable water quality was estimated as VND 42,466 (USD 1.86) per capita. The main determinants of WTP were income and the educational status of the respondent. The total economic value of water quality improvements in Hanoi was estimated to be USD 87 million per year.

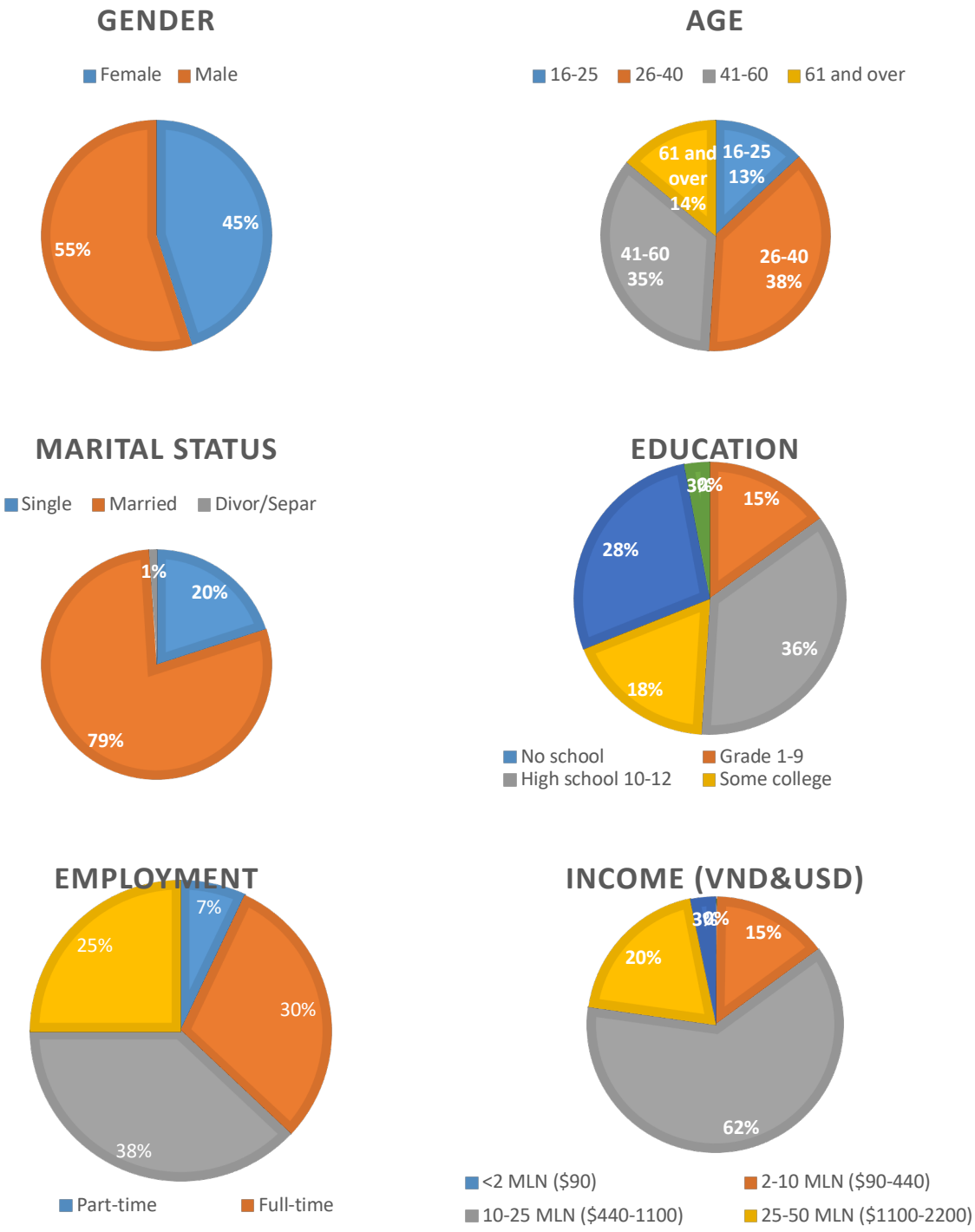

Figure 4.1.13. Socioeconomic profile of the sample (Hanoi city study)

4.1.3.7 Floodwater-borne infectious diseases

The simulated risk of floodwater-borne gastroenteritis under the three scenarios, expressed as the number of gastroenteritis cases caused by noroviruses per grid, is shown in Figure 4.1.14. The purple grids represent high-risk areas (more than 0.1 cases per grid); the orange represent medium risk (0.01 – 0.1 cases per grid); the yellow represent low risk (less than 0.01 cases per grid); and the white represent no risk (no flood areas). Under the current scenario, the risk was high in the north part of the study area (Figure 4.1.14 a)), and under the business-as-usual scenario, additional high-risk areas were observed in the west and south. However, under the with mitigation scenario, the high-risk areas were significantly reduced and confined to small areas in the north. The distribution of the high-risk areas was different from that in the flood analysis, which showed severe flooding only in the south of the study area (see Figure 4.1.7). Although the probability of disease depends on the severity of flooding (i.e., related to the maximum depth), the number of disease cases is also affected by the population in each grid; the additional high-risk areas in the north were due to the high population density.

The total number of gastroenteritis cases caused by norovirus was 902 under the current scenario, which was relatively high among the target cities and partly due to the severe flood inundation and water pollution. The number was projected to increase by 41% in 2030 if no measures were taken to reduce urban flooding and water pollution (business-as-usual scenario, 1,275 cases in total). This increase was smaller than in other cities, partly because the population in the Hanoi study area will decrease by 3.7% by 2030 while the populations of all other cities are projected to increase by 29 – 41%. Thus, the elevated risk in the future is mainly due to the change in precipitation. When the countermeasures for reducing urban flooding and water pollution were included in the analysis (with mitigation scenario), the total number of cases was reduced to 242, an 81% reduction compared to the business-as-usual scenario. Therefore, we urge stakeholders to act to reduce the risk of flood-related infectious diseases. It was indicated that implementing water management measures would also protect citizens from floodwater-borne infectious diseases.

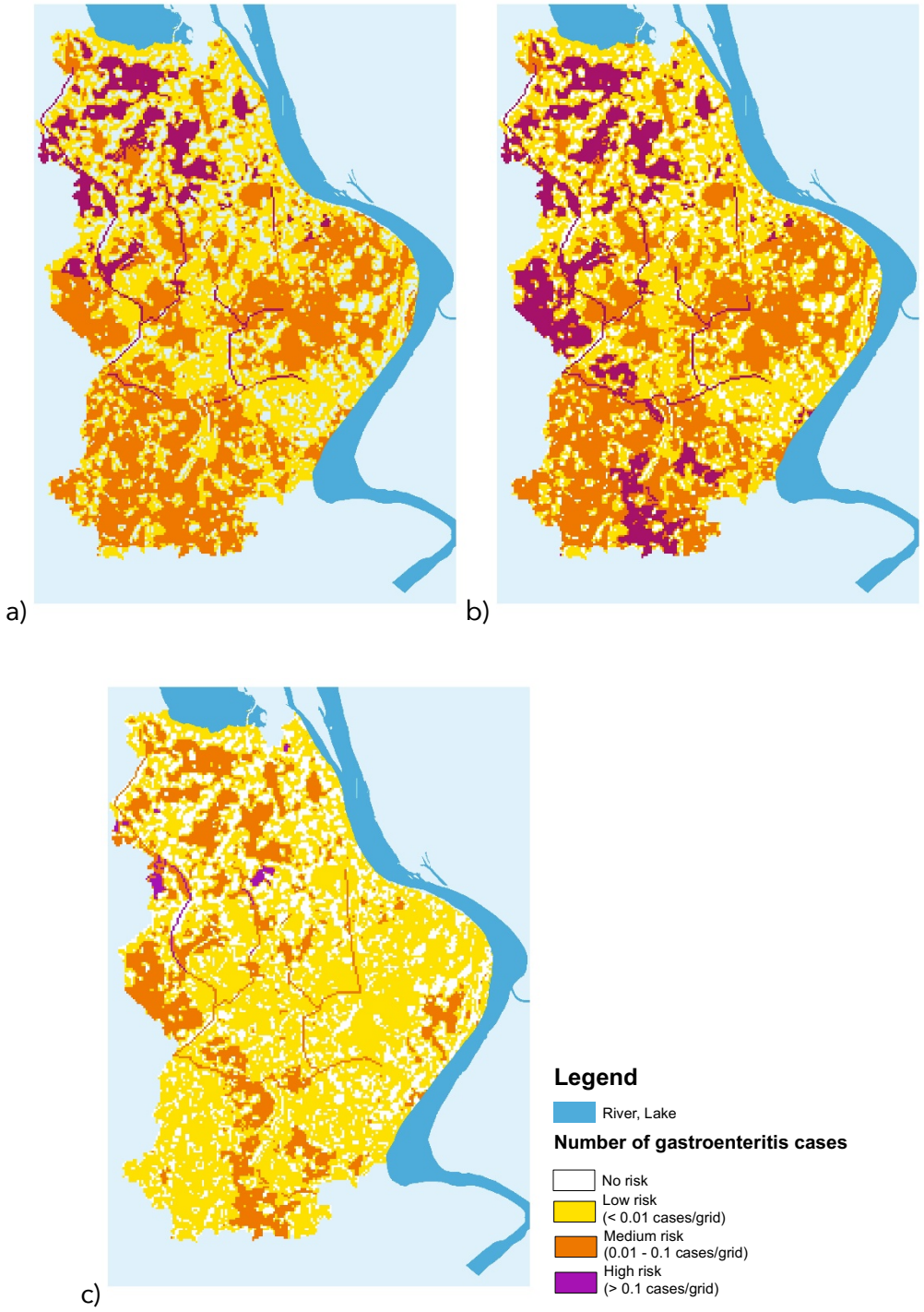

Figure 4.1.14. Simulated health risk (number of floodwater-borne gastroenteritis cases due to norovirus) for Hanoi under the a) current scenario, b) business-as-usual scenario, and c) with mitigation scenario

4.1.3.8 Low-carbon technology in wastewater facilities

1) Information Collected for Existing and Planned Wastewater Management Facilities

Existing Facilities

In the target area, there are currently four (4) WWTPs, (Truc Bach, Kim Lien, Yen So and Bay Mau) with a total capacity of 220,000 m^3/day as shown in Figure 4.1.15 and Table 4.1.5 below.

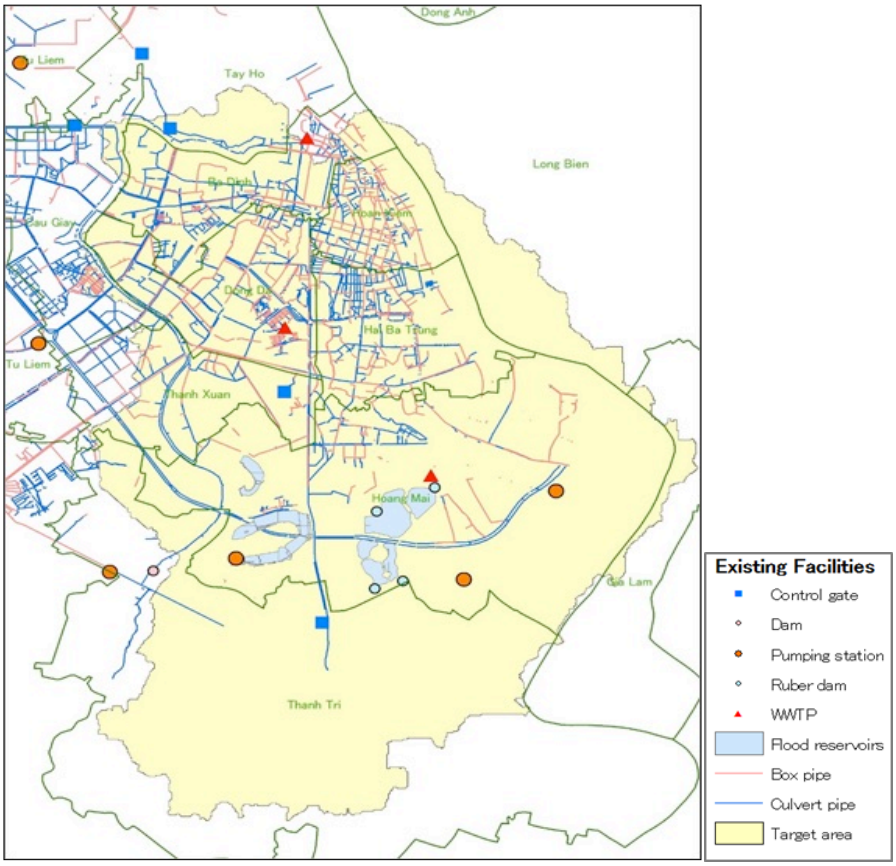

Figure 4.1.15. Existing wastewater management facilities in Hanoi city

Table 4.1.5. Existing WWTPs in the target area of Hanoi city

Name of WWTP	Capacity (m^3/day)
Truc Bach	2,300
Kim Lien	3,700
Yen So	200,000
Bay Mau	14,000
Total	220,000

Planned Facilities

The Target Area encompasses four (4) planned WWTPs with a total capacity of 441,000 m^3/day, as shown in Table 4.1.6.

Table 4.1.6. Planned WWTPs in the target area of Hanoi city

WWTP	Expected Capacity (m^3/day)	
Yen Xa	270,000	
Phu Do	84,000	
Ngu Hiep	21,000 – 34,000	(Average: 27,500)
Vinh Ninh	21,000—33,000	(Average: 27,000)
Dai Ang	21,000 – 44,000	(Average: 32,500)
Total	441,000	

2) Calculation of GHG emission reduction

Due to a lack of data, the applicability of some low-carbon technologies could not be examined. Consequently, the following four (4) technologies were scrutinized as described below: Tool 1) introduction of high-efficiency pumps, Tool 2) introduction of high-efficiency blowers, Tool 3) installation of a biogas power generation system and Tool 4) introduction of a solar power system.

Tool 1. Introduction of high-efficiency pumps

In calculating the GHG emission reduction, EC_{lp} (annual power consumption of the low-carbon technology, i.e., pumps) is generally obtained by monitoring the pumps to be installed. Since this assessment targets the planning phase, the available data, such as master plans, BAU and relevant data obtained through the field survey, were used to estimate EC_{lp}.

- Data and parameters

Table 4.1.7 summarizes the data used to calculate the GHG emission reduction using Tool 1.

- Calculation of GHG emission reduction (ER)

Based on the data collected and calculated above, the GHG emission reduction with the introduction of Tool 1 is estimated as follows:

$$ER = ME – LE = 1{,}172\ tCO_2/year$$

Table 4.1.7. Data used to calculate the GHG emission reduction using Tool 1: Introduction of high-efficiency pumps for Hanoi city.

Parameter	Value	Remarks
FE_{EL}: CO_2 emission factor	0.8154 tCO_2/MWh	Grid Emission Factors, Institute for Global Environment Strategies (https://pub.iges.or.jp/)
$\eta_{M/P}$: MP pump efficiency	53%	Nominal value of conventional pump
η_{Pj}: Low-carbon technology pump efficiency	85%	Nominal value of energy-saving pump
Size of pumps to be installed	3,500 m^3/hour of capacity with 63 kw of power consumption	Specification of the pump commonly installed in the WWTPs of the target cities
Annual treatment capacity of existing and planned pumps	198,300,000 m^3/year	-
Operation hours per year	56,657 hours/year	Annual treatment capacity of the existing and planned pump/capacity of pump to be installed = 198,300,000/3,500
EC_{lp}: Power consumption of the low-carbon technology pump per year	3,569 MWh/y (existing pumps: 1,188 MWh/y, planned pumps: 2,381 MWH/y)	EC_{lp} = Operation hours per year * power consumption of pump to be installed = 56,657* 0.063
ME: MP emissions per year	4,668 tCO_2/year (existing pumps: 1,554 tCO_2/year, planned pumps: 3,114 tCO_2/year)	ME = EC_{lp} * $\eta_{pj}/\eta_{M/P}$ * FE_{EL}= 3,569 * 0.85/0.53 * 0.8154
LE: Low-carbon technology emissions per year	3,496 tCO_2/year	LE = ME of existing pumps + ECpp of planned pumps* FE_{EL} = 1,554 + 2,381 * 0.8154

Tool 2. Introduction of High-Efficiency Blowers

As shown in the Figure on page 3, the electricity consumption of a pump is 1/6 that of the blower. This ratio was employed to calculate the GHG emissions.

On the other hand, the energy saving rate of the blower to be installed was assumed to be 10% in consideration of the general specifications of recent energy-saving blowers.

- Data and parameters

The data used to calculate the GHG emission reduction using Tool 2 are listed in Table 4.1.8 below.

Table 4.1.8. Data used to calculate the GHG emission reduction using Tool 2: Introduction of high-efficiency blowers for Hanoi city

Parameter	Value	Remarks
FE_{EL}: CO_2 emission factor	0.8154 tCO_2/MWh	Grid Emission Factors, Institute for Global Environment Strategies (https://pub.iges.or.jp/)
Rate of energy saving by the introduction of Tool 2	10%	Nominal value of energy-saving blower
Rate of power consumption by blower and pump	Power consumption of blower: power consumption of pump = 6 : 1	According to Figure 3.6
ME: MP emissions per year	28,007 tCO_2/year (existing pumps: 9,321 tCO_2/year, planned pumps: 18,686 tCO_2/year)	ME = ME of Tool 1 *6
LE: Low-carbon technology emissions per year	26,138 tCO_2/year	LE = ME of existing pumps + ME of planned pumps * (1-0.1) = 9,321 + 18,686 * 0.9

- Calculation of GHG emission reduction (ER)

Based on the data collected and calculated above, the GHG emission reduction with the introduction of Tool 2 is estimated as follows:

$$ER = ME - LE = 1{,}869\ tCO_2/year$$

Tool 3. Installation of a Biogas Power Generation System

The installation of biogas power generation would replace the current use of fossil fuel-based energy with that of renewable energy with zero emissions. Therefore, the GHG emission reduction with the introduction of this technology could be considered the same as the amount of MP emissions.

- Data and parameters

Table 4.1.9 summarizes the data used to calculate the GHG emission reduction by introducing Tool 3.

Table 4.1.9 Data used for Tool 3: Installation of a biogas power generation system for Hanoi city

Parameter	Value	Remarks
FE_{EL}: CO_2 emission factor	0.8154 tCO_2/MWh	Grid Emission Factors, Institute for Global Environment Strategies (https://pub.iges.or.jp/)
Rate of wastewater treatment volume and power generation	Wastewater treated daily (m^3/day): power generation (MWh/year) = 40,000 : 1,380	Based on the data of the Eniwa city wastewater treatment facility (http://www.city.eniwa.hokkaido.jp/www/contents/1366006820944/index.html)
Total amount of water treated daily by WWTPs in the target area	661,000 m^3/day	-
EG_{BI}: Electricity supplied by the grid to the WWTP area	26,254 MWh/year	-
EC_{BI}: Power consumption by the biogas power generation system	0 MWh/year	-
ME: MP emissions per year	21,408 tCO_2/year	$ME = EG_{BI} * FE_{EL}$
LE: Low-carbon technology emissions per year	0 tCO_2/year	$LE = EC_{BI} * FE_{EL}$

- Calculation of GHG emission reduction (ER)

Based on the data collected and calculated above, the GHG emission reduction with the introduction of Tool 3 is estimated as follows:

$$ER = ME – LE = 21,408\ tCO_2/year$$

Tool 4. Power Generation by Introducing a Solar Power System

As with the installation of biogas power generation, a solar power system represents renewable energy with zero emissions. Therefore, the GHG emission reduction could be considered the same as the amount of MP emissions.

- Data and parameters

Table 4.1.10 shows the data used to calculate the GHG emission reduction with the introduction of Tool 4.

Table 4.1.10. Data used for Tool 4: Power generation by introducing a solar power system for Hanoi city.

Parameter	Value	Remarks
FE_{EL}: CO_2 emission factor	0.8154 tCO_2/MWh	Grid Emission Factors, Institute for Global Environment Strategies (https://pub.iges.or.jp/)
Area required for power generation	20,000 m^2/MW	-
Hours of operation per day	8 hours/day	-
Days of operation per year	200 days/year	-
Rate of wastewater treatment capacity to the potential PV area in WWTP	Site area of WWTP (m^2): potential PV area (m^2) = 1 : 0.46	Based on the data acquired from the layout of Bay Mau WWTP, Hanoi, Vietnam
Total site area of WWTP	389,990 m^2	ditto
Potential PV area	179,395 m^2	Site area of WWTP * 0.46 = 389,990 * 0.46
Electricity generated	8.97 MW	Potential area/required area for power generation = 179,395/20,000 = 8.97
Daily/annual hours of operation of the solar power system	8 hours/day, 1,600 hours/year	200 days/year
EG_{PV} = Electricity supplied by grid to WWTP area (MWh/year)	14,352 MWh/year	EG_{PV} = power generated * annual operational hours of the solar panel = 8.97 * 1,600 = 14,352
EC_{BI}: Power consumption by the solar power system	0 MWh/year	-
ME: MP emissions per year	11,072 tCO_2/year	ME = EG_{PV} * FE_{EL} = 14,352 * 0.8154 = 11,702
LE: Low-carbon technology emissions per year	0 tCO_2/year	LE = EC_{PB} * FE_{EL} = 0

- Calculation of GHG emission reduction (ER)

Based on the data collected and calculated above, the GHG emission reduction with the introduction of Tool 4 is estimated below:

$$ER = ME - LE = 11{,}702\ tCO_2/year$$

Summary: GHG Emission Reduction through the Introduction of Four Tools

The total GHG emissions with the introduction of the abovementioned four (4) tools is 36,151 tCO_2/year. Figure 4.1.16 shows that the introduction of low-carbon technologies could reduce the total GHG emissions by 59.0%. Among the four (4) technologies for which GHG emission reduction was examined, a biogas power generation system is considered the most effective for GHG emission reduction, as it accounts for 59% of the total reduction.

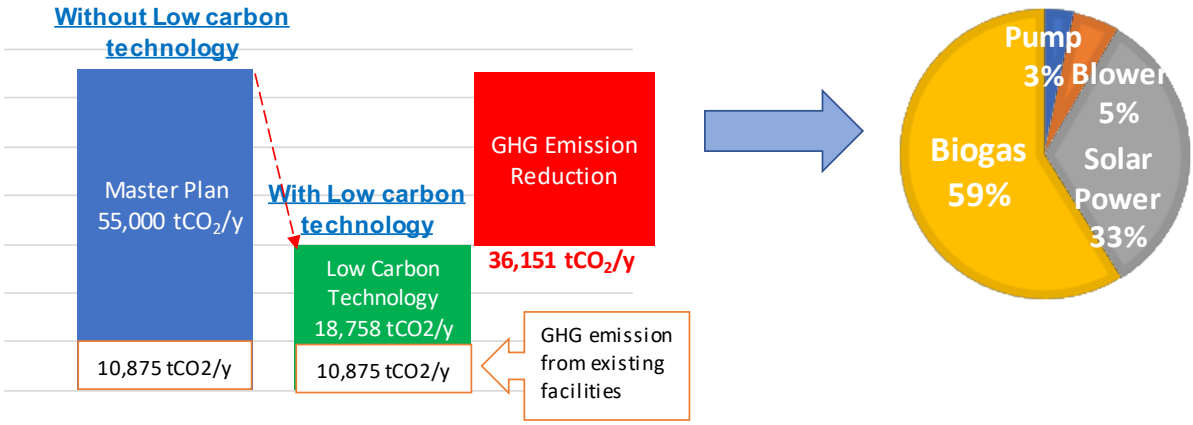

Figure 4.1.16. GHG emission reduction through the application of low-carbon technologies according to the master plan of Hanoi City

References

Bathrellos, G.D.; Gaki-Papanastassiou, K.; Skilodimou, H.D.; Papanastassiou, D.; Chousianitis, K.G. Potential suitability for urban planning and industry development using natural hazard maps and geological-geomorphological parameters. *Environ. Earth Sci.* **2012**, 66, 537–548.

Bosher, L.; Chmutina, K. *Disaster Risk Reduction for the Built Environment*; Willey Blackwell: Oxford, UK, 2017.

Dao, C.A.; Con, P.M.; Khai, N.M. Characteristic of urban wastewater in Hanoi City – nutritive value and potential risk in using for agriculture. *VNU J. Sci. Earth Sci.* **2010**, 26, 42–47.

Du, J.; Qian, L.; Rui, H.; Zuo, T.; Zheng, D.; Xu, Y.; Xu, C.Y. Assessing the effects of urbanization on annual runoff and flood events using an integrated hydrological modeling system for Qinhuai River basin, China. *J. Hydrol.* **2012**, 464–465: 127–139.

General Statistics Office, Socialist Republic of Viet Nam. *Vietnam population projection 2014 – 2049*; Vietnam News Agency Publishing House: Hanoi, Vietnam; 2016.

General Statistics Office, Socialist Republic of Viet Nam. *Statistical Yearbook of Viet Nam 2016*; Statistical Publishing House: Hanoi, Vietnam, 2017.

Goyal, M.K.; Ojha, C.S.P. Evaluation of linear regression methods as downscaling tools in temperature projections over the Pichola Lake Basin in India. *Hydrological Processes* **2011**, 25: 1453-1465.

Khan, A.A.; Gaur, R.Z.; Diamantis, V.; Lew, B.; Mehrotra, I.; Kazmi, A.A. Continuous fill intermittent decant type sequencing batch reactor application to upgrade the UASB treated sewage. *Bioprocess Biosyst Eng.* **2013** 36: 627–634.

Neal, J.C.; Bates, P.D.; Fewtrell. T.J.; Hunter, N.M.; Wilson, M.D.; Horritt, M.S. Distributed whole city water level measurements from the Carlisle 2005 urban flood event and comparison with hydraulic model simulations. *J. Hydrol.* **2009**, 368: 42–55.

Pistrika, A.; Tsakiris, G.; Nalbantis, I. Flood depth-damage functions for built environment. *Environ. Process.* **2014**, 1: 553–572.

Quan, P.V.; Furumai, H.; Kurisu, F.; Kasuga, I.; Ha, C.T.; Chieu, L.V. Water Pollution characterization by pathogenic indicators in water runoff in the downtown of Hanoi, Vietnam. *J. Water Environ. Technol.* **2010**, 8: 259–268.

Rafiei Emam, A.; Mishra, B.K.; Kumar, P.; Masago, Y.; Fukushi, K. Impact assessment of climate and land-use changes on flooding behavior in the Upper Ciliwung River, Jakarta, Indonesia. *Water* **2016**, 8: 559.

Ramos, H.M.; Perez-Sanchez, M.; Franco, A.B.; Lopez-Jimenez, P.A. Urban floods adaptation and sustainable drainage measures. *Fluids* **2017**, 2: 61.

Vietnam Central Committee for Flood and Storm Control (VCCFSC). *Damage situation caused by flood at provinces in November 2008 (Annex 2)*; Vietnam Central Committee for Flood and Storm Control: Hanoi, Vietnam; 2008.

Vietnam Urban Water Supply and Wastewater Project (VUWSW). *Masterplan for wastewater management for year 2030*. Vietnam Urban Water Supply and Wastewater Project: Hanoi, Vietnam; 2015.

4.2 Jakarta

4.2.1 Introduction

Jakarta is located on the northwest coast of Java Island at the mouth of the Ciliwung River on Jakarta Bay, which is an inlet of the Java Sea, and it is the capital and largest city as well as the economic, political and cultural center of Indonesia. Approximately 9 million people live in Jakarta itself, over an area of 660 km^2, but the population is steadily increasing due to migration from other parts of the country. Thirteen rivers intersect Jakarta Province, and the Ciliwung River catchment is the largest. Combined with the wet season rains and insufficient drainage due to clogging, these rivers make Jakarta prone to flooding, which occurs every year. Widespread flooding occurred in 1996, 2002 and 2007, inundating up to 40% of the city. Furthermore, all the rivers are heavily polluted by gray water from households and commercial buildings combined with industrial discharge, pesticide and fertilizer run-off from agricultural land, solid waste, and fecal matter from overflowing or leaking septic tanks. The rising demand for water in Jakarta Province has put pressure on water quality, but very few studies have addressed the status of water resources and strategies for their management in the near future. Therefore, this research aims to provide policy recommendations for sustainable water management in Jakarta.

The study area for this research is downstream of the Ciliwung River basin and intersects the Special Capital City District of Jakarta (DKI Jakarta), including the entire 420-km^2 area of the watershed (Figure 4.2.1). The Ciliwung River originates upstream at Tugu Puncak, Bogor Province and flows northward through the cities of Depok and Jakarta before finally terminating in Jakarta Bay. Of the 117 km of the Ciliwung River, this study focuses on a 75-km length inside Jakarta city with an elevation ranging from 5 to 350 m above mean sea level that supports 4.5 million people. The average annual rainfall is 2,683 mm, and the mean annual temperature is 29 °C. Based on the land use/land cover map, the entire area is divided into the following classes: buildings, farmland, forest, freshwater, grass, open land, paddy field, river, swamp, trees and urban. Rapid urbanization and exponential population growth in Jakarta and the surrounding area of the megacity, called Jabodetabek (Jakarta-Bogor-Depok-Tanggerang-Bekasi), have resulted in environmental deterioration, especially of water resources.

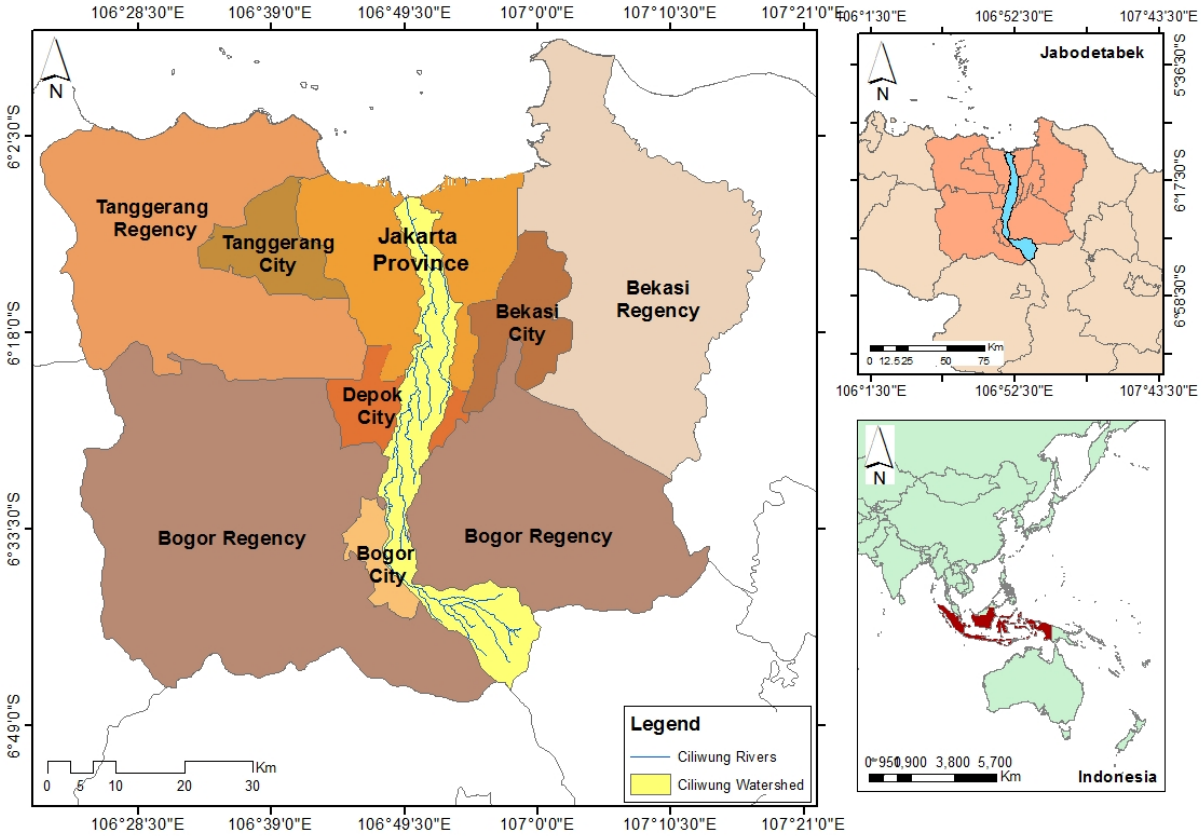

Figure 4.2.1. Location of the Ciliwung River basin

4.2.2 Methodology

4.2.2.1 Precipitation change

This study assessed the impact of climate change on precipitation at the basin scale, and the assessment was performed by comparing data from observation stations and their respective grid cells. A reliable precipitation dataset was prepared for each of the GCMs and RCPs for the current and future climate using the quantile-based bias correction method, and the climate change impact assessment was performed by comparing the monthly precipitation values and return period precipitation estimates for 50- and 100-year periods for both scenarios.

The first step in the precipitation change assessment was the selection of an appropriate rainfall gauge station, considering the variation in daily rainfall over the study basin. Among the various stations in the study area, those with the longest durations of regular recordings as well as central locations were considered for analyzing the change in precipitation, so depending on the city, precipitation data collected over 20 to 25 years were used to compare the effects on precipitation. The precipitation outputs of multiple GCMs were analyzed to derive statistics, such as extreme values for different return periods and mean monthly values.

Estimates of the change in return period are a convenient way of presenting changes in extreme precipitation for a basin. Return period values are derived by carrying out frequency analysis for

each of the grids for the current and future climate precipitation datasets, and in this study, this was performed on the annual maximum daily precipitation series to estimate the return period values. Empirical and Gumbel frequency analyses were carried out for current and future precipitation data series to assess the change in extreme precipitation events, and the means of RCP 4.5- and 8.5-based return period values were later calculated to represent moderate (average) and extreme future climates. These mean values enabled current and future flood inundation scenarios to be simulated.

To evaluate the effects of climate change on water quality, we evaluated the change in monthly average precipitation. Based on the rate of change in the observed historical rainfall values and downscaled future precipitation data, we estimated the average rate of increase based on regression analysis. This growth rate was applied to the current rainfall value to obtain future rainfall values. Statistical downscaling was followed by trend analysis, which is a less computationally demanding technique that enables bias reduction in the precipitation frequency and intensity (Goyal and Ojha, 2011), to obtain climate variables at a monthly scale. The GCM output was downscaled at the local level for reliable impact assessment (Sunyer et al. 2015), and the precipitation outputs of MRI-CGCM3 and MIROC5 were used for the future simulation to assess the impact of climate change because of their wide use and high resolution compared to other climate models. This study is based on the RCP 4.5 and 8.5 emission scenarios, which assume that global annual GHG emissions peak around 2040 and then decline (IPCC 2014). In this study, the GCM data are from the 1985-2004 and 2020-2039 periods (each with a 20-year duration), which represent the current and future (2030) climate, respectively. The results shown in Figure 4.2.2 clearly indicate that the annual precipitation simulated from the GCM output is not much different than is currently observed. The total annual precipitation values in the cases of observed_2015, Sim_2030_MRICGCM3_45, Sim_2030_MIROC5_45, Sim_2030_MRICGCM3_85, and Sim_2030_MIROC5_85 are 2679.9, 2656.9, 2622.8, 2653.6 and 2612.1 mm, respectively. Finally, for water quality simulation, we used MRICGCM3 with RCP 8.5.

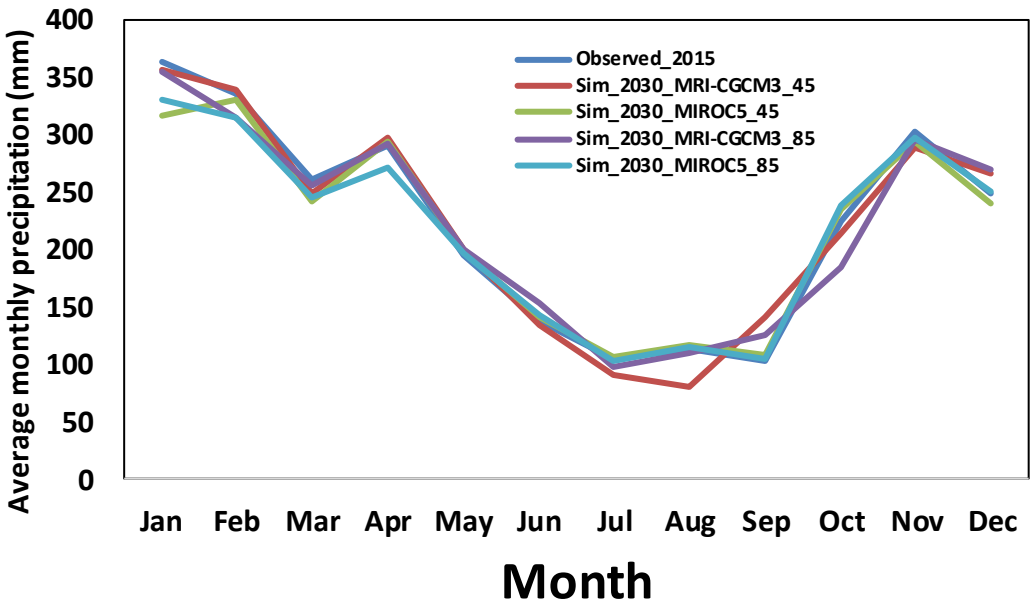

Figure 4.2.2. Current and future monthly rainfall at Depok station

4.2.2.2 Land cover change

The Greater Jakarta land cover base maps for 2009 and 2030 were provided by Lembaga Ilmu Pengetahuan Indonesia (LIPI). Initially, these land cover maps were provided in GIS format with varying class names such as buildings, farmland, forest, freshwater, grass, open land, paddy field, pond, swamp, tree, urban, and so forth. For the purpose of hydrologic and flood inundation modeling, these maps were broadly categorized into four classes, namely, agriculture, vegetation, urban, and water, considering their similarity to particular classes in the original maps, as presented in Figure 4.2.3.

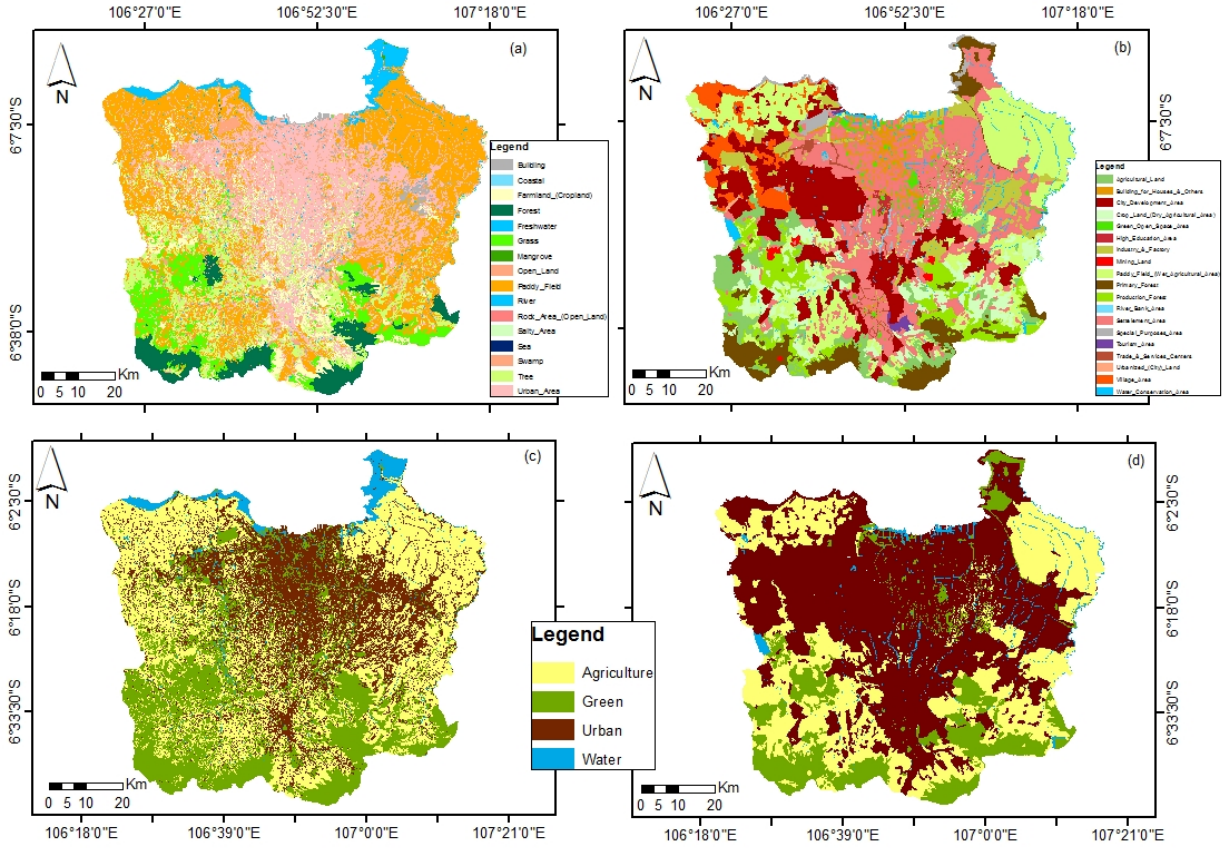

Figure 4.2.3. Comparative land use maps of Greater Jakarta, Indonesia: (a) 2009 original, (b) 2030 original, (c) 2009 derived and (d) 2030 derived (Mishra et al., 2017)

4.2.2.3 Population growth

To estimate the effect of population growth (one of our two major key drivers) on the status of water quality, the entire study area was divided into different demand sites that mainly represent the populations of different cities on both sides of the Ciliwung River within our study and that directly impact the river through the discharge of domestic sewerage water. The future population was estimated by the ratio method using projected growth rate data from UN DESA (2015). A total population of 2,302,495 was considered for the base year, i.e., 2000, in our study area, and for the future population, an annual growth rate of 1.71% was considered for the 2001 to 2030 period. Henceforth, the populations considered for the current year (2015) and the target year (2030) were 4,170,705 and 5,759,983, respectively.

4.2.2.4 Urban flooding

Prior to the urban flood inundation simulation in this study, various studies of the impact of climate and land use change on hydrometeorology were reviewed, and changes in extreme precipitation and flood discharge and inundations were found to be likely using different tools and techniques, thus providing valuable conclusions for academicians and urban planners in the field of flood-risk

management. The Ciliwung River basin of Greater Jakarta was investigated as a case study for this study due to the frequent incidences of flooding in the city that are considered one of the greatest problems currently facing the area. High flow rates in the Ciliwung River, which flows through the center of Jakarta, regularly cause extensive flooding during the rainy season (Formánek et al., 2013).

Flood inundation simulation consisted of hydrologic and hydraulic modeling. The hydrologic modeling was carried out for the upstream of the Katulampa section. By using high river flows at this section as inflows in the hydraulic (flood) model, inundation depths were determined up to the Manggarai gate. Model calibration was conducted using the February 2007 flood event, which was characterized as having an approximate return period of 50 years as well as the worst event in the last several decades, causing huge tangential and nontangential losses. Future floods (2030) were simulated for moderate (average) and extreme rainfall conditions as mentioned in the "precipitation change" section. Later, these simulated values were compared with inundation depths/extents for the current climate. Overall, we estimated and compared flood inundations for 50-year return rainfall values considering current, moderate future and extreme future conditions.

4.2.2.5 Direct flood damage

The approach used to assess flood damage in Jakarta is explained in detail in Section 3.5, but in this section, the flood depth damage function was derived from data collected through field surveys in collaboration with the Center of Environmental Research, Research and Community Services Institute, Bogor Agricultural University, Indonesia. Approximately 401 responses were collected from residential and nonresidential sectors from several locations as presented in Table 4.2.1 and Figure 4.2.4. Flood damage in the study area was estimated under current conditions, and two climate scenarios were also simulated (average and extreme climate), as described in Section 4.2.2.4.

Table 4.2.1. Field survey locations

Location	District (Kecamatan)
East Jakarta (Jakarta Timur)	Jatinegara, Kramat Jati, Matraman, Pasar Rebo
South Jakarta (Jakarta Selatan)	Jagakarsa, Pancoran, Pasar Minggu, Tebet
Depok City	Beji, Cimanggis, Pancoran Mas, Sukmajaya
Bogor Regency	Bojong Gede, Sukaraja
Bogor City	Bogor Selatan, Bogor Utara, Bogor Timur

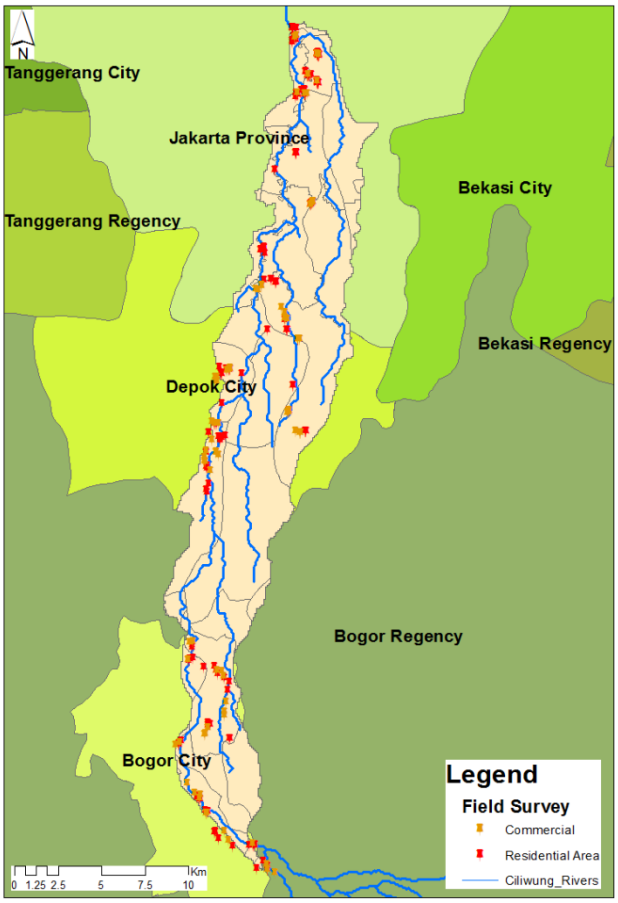

Figure 4.2.4. Field survey locations

4.2.2.6 Water quality

Basic information regarding the model and data requirements

As explained in Section 3.6, the WEAP model was used to simulate future water quality variables in the year 2030 to assess alternative management policies for the Ciliwung River basin. To model water quality, a wide range of input data was provided including household discharges, their locations and concentrations, past spatiotemporal water quality, wastewater treatment plants (Ministry of Public Works), population, historical rainfall, temperature (Indonesian Agency for Meteorology, Climatology and Geophysics), drainage networks (Department of Public Works), river flow-stage-width relationships, river length, surface water inflows and land use/land cover (LIPI).

The WEAP model was developed for the Ciliwung River basin for four command areas with interbasin transfers. Hydrologic modeling requires that the entire study area be split into smaller catchments with consideration of the confluence points and physiographic and climatic characteristics (Figure 4.2.5). The hydrology module within the WEAP tool enables the catchment runoff and pollutant transport processes into the river to be modeled, and pollutant transport from a catchment accompanied by rainfall runoff is enabled by ticking the water quality modeling option. Pollutants that accumulate on catchment surfaces during nonrainy days reach water bodies through

surface runoff, and the WEAP hydrology module computes catchment surface pollutants generated over time by multiplying the runoff volume by the concentration or intensity for different types of land use.

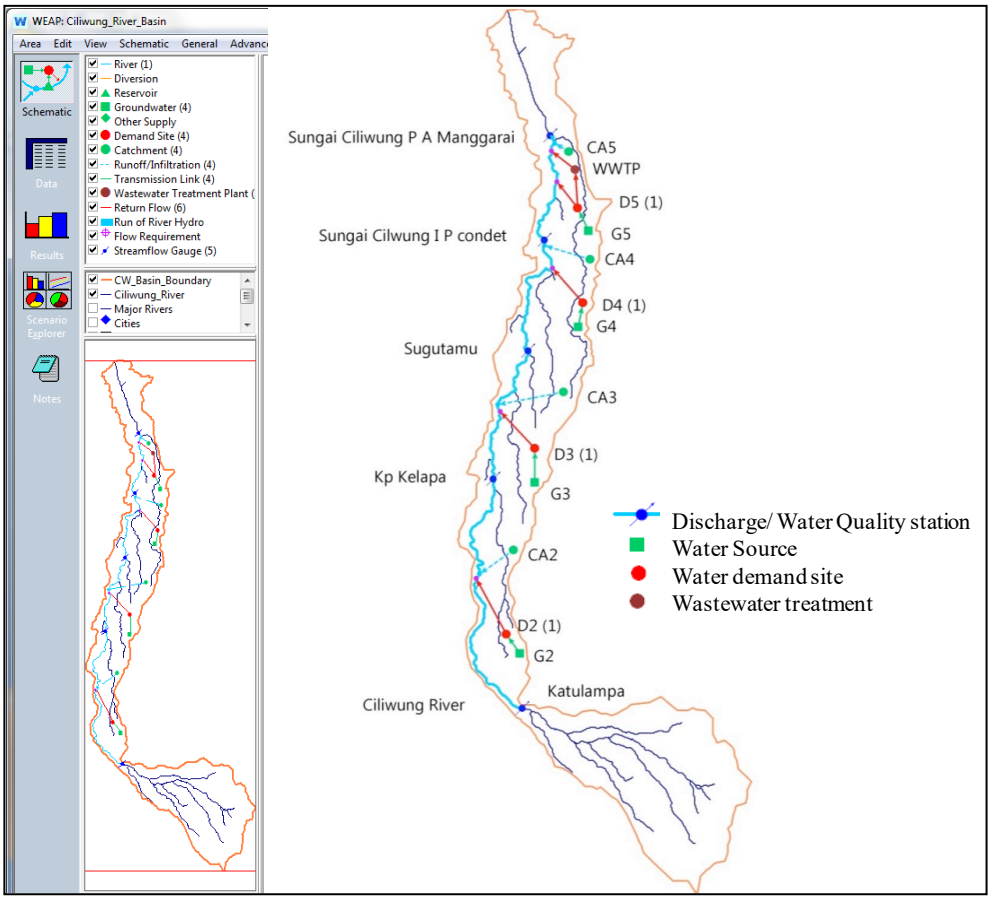

Figure 4.2.5. Schematic diagram showing the problem domain for water quality modeling in Greater Jakarta using the WEAP interface

During simulation, the land use information was broadly grouped into three categories, viz., agricultural, forest, and built-up areas. The soil data parameters were identified using previous secondary data and the literature. Daily rainfall had been collected at the Citeko meteorological station for the period from 1980 to 2016, and daily average stream flow data from 1984-2016 had been measured at five stations, namely, Katulampa, Kelapa, Sugutamu, IP Condet and Manggarai, on the Ciliwung River and were utilized to calibrate and validate the WEAP hydrology module simulation. Water quality indicator data (BOD, *E. coli* and NO_3) were also collected at four of the above five stations and used for water quality modeling (Figure 4.2.5). The resulting population distributions and their future trends at these four command areas were calculated by the ratio method using the UN DESA projection rate explained in Section 4.2.2.3. Regarding future precipitation data, different GCM outputs were used after bias correction, which is explained in detail in Section 4.2.2.1.

Model setup

The entire problem domain and its different components were divided into five catchments that were further subdivided into thirteen subbasins considering the influent locations of major tributaries (Figure 4.2.5). Other major considerations in representing the problem domain were the fourteen demand sites and one wastewater treatment plant. Here, demand sites mean domestic (population) and industrial centers defined by their attributes that explain the water consumption and wastewater pollution loads per capita, water supply source and wastewater return flow. Dynamic attributes are described as functions of time and include population size and industries.

The current master plan only mentions a planned increase in WWTP capacity but not the type of treatment plant and technology that will be implemented. However, as for other cities that we have investigated in this project, the UASB-SBR type of wastewater treatment plant was considered in the modeling, and its treatment efficiency was assumed to be 94% for COD, 97% for BOD, 77% for TN and 99.69% for fecal coliform (Khan et al. 2013). The reason for selecting UASB-SBR technology for both current and future WWTPs was to ensure homogeneity with other cities. No precise data are available regarding the total volume of wastewater production from domestic sources, so in the absence of such detailed information, the daily volume of domestic wastewater generation was estimated to be 130 liters of the average daily consumption per capita based on a literature review. Numerical simulation was conducted using different scenarios called the business-as-usual scenario and the scenario with mitigation measures. For the business-as-usual scenario, the WWTP capacity was 22 MLD (total number=1), whereas this capacity was 520 MLD for the scenario with mitigation measures, and total number of proposed additional WWTPS by 2030 was 2 (total number = 3) (Ministry of Public Works, Jakarta City, Indonesia, 2014).

The scenario analysis was conducted by defining a time horizon based on which alternative wastewater generation and management options can be explored. The business-as-usual scenario was represented by selecting all the existing elements as being currently active and observing the effect of climate change and population growth. For the scenario with measures, all the conditions were the same as under the business-as-usual scenario except that the addition of new/upgraded WWTPs (information taken from local master plan) were modeled. Detailed information on the existing (functional) and planned wastewater treatment plants in DKI Jakarta used for modeling is presented in Table 4.2.2.

Table 4.2.2. Existing (functional) and planned wastewater treatment plants in DKI Jakarta

Wastewater treatment plant	Design capacity (in MLD)			Design effluent standard (BOD mg/l)			Coverage area (% of population served)		
	2000 (Baseline)	2020	2030	2000	2020	2030	2000	2020	2030
Setiabudi	22	37	54	60	33	24	2	5	5
Wijaya Kususma and Duri Kosambi	-	264	313	-	24	20	-	35	55
Sawah Besar	-	-	337	-	-	20	-	-	85

4.2.2.7 Economic benefit of improving urban water quality

A questionnaire was designed for the Jakarta study as follows. 1) The first part asked for background data/the profile of the respondent; 2) the second part related to awareness of the current water quality situation; and 3) the pain part included WTP questions (use- and nonuse), which were divided into subquestions:

1. *Are you willing to pay to improve the water quality of Jakarta waterbodies?*

   ☐ YES ☐ NO

2. *How much would you be willing to pay as a monthly per-household fee for various levels of improvement in the water quality of the city's waterbodies in addition to your monthly utility bill?*

We provided ten cards as options that specified amounts ranging from IDR 3,000 to 100,000 or suggested that the respondent indicate their own amount.

Some 50 respondents in Jakarta were selected for a pilot study that pretested a developed questionnaire (May 7-14, 2017). The objective was to check whether the survey was logical and if the WTP questions were correctly understood by the residents. The main survey was conducted in 5 municipalities (North, South, East, West, and Central) during July 4-28, 2017; a total of 500 interviews were completed.

The random stratified sampling method was used because we could not secure a list of voters from the local government and did not want to use the telephone book to compile sampling for the survey because it did not cover the entire area of the megacity. The selection techniques were based on two classes: (1) walking distance to the river, which assumed that one can reach the nearest waterbody within 30 min, and (2) the need to drive or take public transportation to the nearest waterbody. The SPSS statistical package was used for the analysis, and the WTP was estimated by logit and probit models.

4.2.2.8 Floodwater-borne infectious diseases

The effects of urban flooding and water quality deterioration, which are affected by both climate change and urbanization (population increase and land use change), on public health were examined using the risk of infectious gastroenteritis from noroviruses in floodwater as a reference. The health risk was evaluated using the outputs of the flood inundation model (Section 4.2.2.4) and

the water quality model (Section 4.2.2.6) along with other input data such as the current and future population (Section 4.2.2.3). The risk assessment model developed in Section 3.8 was used to estimate the number of gastroenteritis cases caused by noroviruses in floodwater under current and future situations. Two scenarios were developed for the future situation: a business-as-usual scenario that did not include any flood mitigation and water quality improvement measures and a with-mitigation measures scenario that included all techniques developed for flood mitigation (Section 4.2.2.4) and water quality improvement (Section 4.2.2.6).

4.2.2.9 Low-carbon technology in wastewater facilities

The amount of GHGs emitted from wastewater treatment facilities was estimated following the methodology stated in Section 3.9. Three scenarios were developed, namely, the current scenario, 2030 without low-carbon technology scenario, and 2030 with low-carbon technology scenario. The current scenario evaluated GHG emissions under current conditions (i.e., emission from existing facilities), and the 2030 without low-carbon technology scenario evaluated GHG emissions from existing and planned facilities stated in the master plan (Ministry of Public Works, Jakarta City, Indonesia, 2014) using technologies (e.g., pumps, blowers) currently available in Southeast Asia. The 2030 with low-carbon technology scenario evaluated GHG emissions assuming the implementation of the low-carbon technologies stated in Section 3.9.2. Based on the two scenarios for 2030, we evaluated the potential reduction in the emission of GHGs from wastewater facilities in the target area.

4.2.3 Results and discussion

4.2.3.1 Precipitation change

Using bias-corrected GCM data for the 1985–2004 and 2020–2039 periods, the impacts of climate change on precipitation over the Ciliwung River basin were assessed. The quantile-based bias corrections first identified the bias pattern in the GCM precipitation data by comparing the daily observations with the corresponding GCM data, which indicated that peaks in the GCM values were significantly smaller than those in the observation values. Moreover, the GCM precipitation data had significantly more wet days than the observed data. The performance of the quantile-based correction technique was evaluated by comparing the monthly average rainy days and the daily amounts of precipitation, which indicated a similar number of rainy days and extreme rainfall magnitudes, thereby demonstrating the effectiveness of the quantile-based bias-correction technique.

Rainfall IDF curves can be used to estimate rainfall intensities for different durations and return periods, and frequency analysis using the Gumbel extreme value method enabled rainfall IDF curves to be generated and the change in extreme precipitation over the Ciliwung River watershed to be assessed for the present and future climate scenarios. In this study, the 1-day maximum precipitation for the 50- and 100-year return periods was determined for the current and future precipitation

datasets (Table 4.2.3). For all return periods and all durations, these values clearly indicate that extreme precipitation events will be more frequent and intense in the future.

Table 4.2.3. Comparison of 1-day maximum rainfall under current and future climate conditions

Return period, years	One-day maximum rainfall, mm		
	Current	Future average of three GCMs	Future extreme among three GCMs
50	207	227	330
100	228	249	365

4.2.3.2 Land cover change

The comparison of the 2009 and 2030 land cover maps of Greater Jakarta showed significant urban growth, to 88% of the area, and a drastic decrease in green areas by 46%. More details are presented in Table 4.2.4. In the Ciliwung River basin study area, the urban area will increase by 42%; moreover, the urbanization will be more significant in Bogor (regency and city), with an estimated expansion to 85% of the area.

Table 4.2.4. Land cover change over Greater Jakarta

Land cover type	LU 2009 (km^2)	LU 2030 (km^2)	Change (%)
Built-up	1,926	3,624	88
Agricultural area	2,834	2,125	-25
Green land	1,913	1,014	-46
Water bodies	252	153	-39

4.2.3.3 Urban flooding

The FLO-2D inundation modeling was applied between Katulampa and Manggarai of the Ciliwung River basin. The model parameters were calibrated by comparing the observations with the simulated flood characteristics from the February 2007 flood event and then adjusted by comparing the observed and simulated inundation depths at multiple locations. The roughness coefficient was adjusted to fit the simulation results to the observations by applying a "trial and error" procedure, and a range of coefficient values were applied for different land use classes. Finally, a value of 0.06 for agriculture, 0.1 for green, 0.02 for urban, and 0.01 for water were allocated for the Manning roughness parameter. The simulation time for the inundation modeling was 72 h, which accounted for the modeled 1-day maximum precipitation of the 50- and 100-year return period floods, and the output time step was 1 h. According to Table 4.2.5, the simulated and observed results (surveyed data of Formánek et al., 2013) were consistent at different locations. Additionally, the model performance was tested by comparing the observed and FLO-2D estimated flood discharge at the Ratu Jaya hydrometeorological section of the river.

Table 4.2.5. Comparison of observed and simulated inundation values at different locations

Location	Inundation depth (m)	
	Observed	Simulated
Pengadegan	1.6 – 3.0	0.03 – 4.0
Pejaten Timur	0 – 1.8	0.03 – 2.2
Bale Kambang	1.8	1.9

The simulated inundation model output was processed using the FLO-2D Mapper to determine the maximum flow depths. Figure 4.2.6 shows the flood extents and depths simulated under the current and future climate and land use scenarios, and those under the future conditions were significantly higher than under the current condition (Figure 4.2.7). These findings clearly emphasize the need for further flood adaptation and mitigation measures for sustainable urban development.

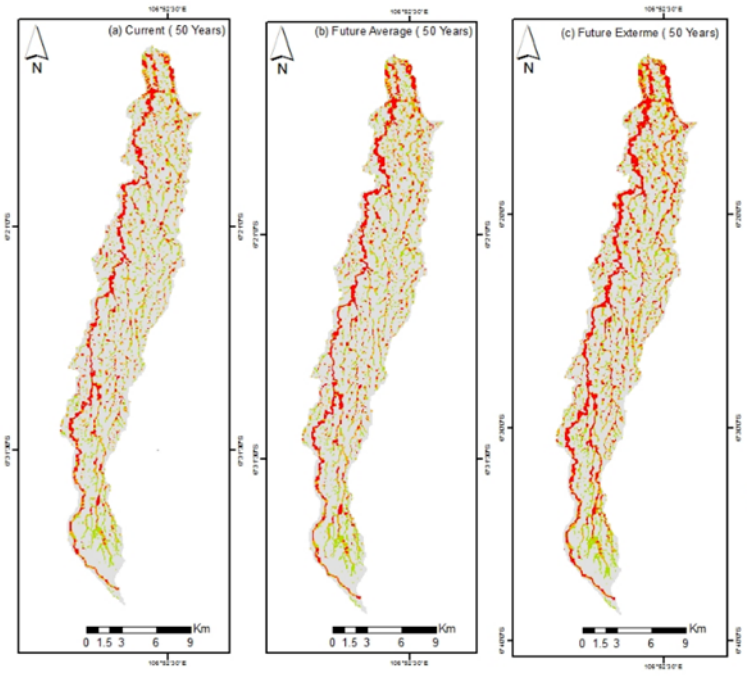

Figure 4.2.6. Comparison of flood inundations under current and future conditions

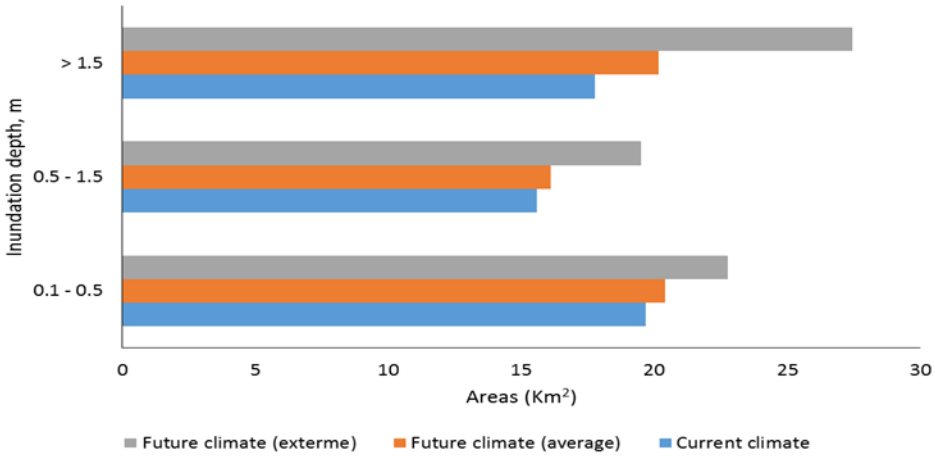

Figure 4.2.7. Change in flood extents for different depth zones for 50-year return periods

4.2.3.4 Direct flood damage

Tangible direct damage was estimated for the Ciliwung River basin, Jakarta, and the flood damage map was established using a combination of the hazard, exposure and vulnerability components in a GIS with a grid size of 90 x 90 m. However, the calibration of the baseline results depended on the damage estimate from the Jakarta government for the 2007 flood. Regarding the flood damage, an increase flood damage of 83% and 153% was observed for 2030 under the average and extreme climate change scenarios, respectively. Figure 4.2.8 highlights the results of the comparison of the flood damage maps by scenario. Due to rapid urbanization and climate change, flood loss is expected to be greater, so the magnitude of climate change can raise the risk of flooding for local people and buildings as indicated in Figure 4.2.8.

For the current situation, damage is very important in Jakarta Province (East and South Jakarta), but in the future, vulnerability will increase in all regions except Bogor (regency and city), which is expected to be more affected. In fact, flood depth will rise in this area, and the urbanization will be significant, accounting for 85% of the area as indicated in Figure 4.2.9.

These findings clearly emphasize the need for further flood adaptations and mitigation measures for sustainable urban development. Moreover, the detection of flood prone areas will enable planners to adopt appropriate urban planning and flood risk reduction strategies, such as in Bogor where suitable urban resilience strategies should be adopted to avoid the risk of and reduce exposure to flooding. Moreover, the prediction of future flooding situations will be useful for planning and designing structural and nonstructural adaptation measures; the implementation of blue-green infrastructure can help minimize the effects of floods as well as protect the environment.

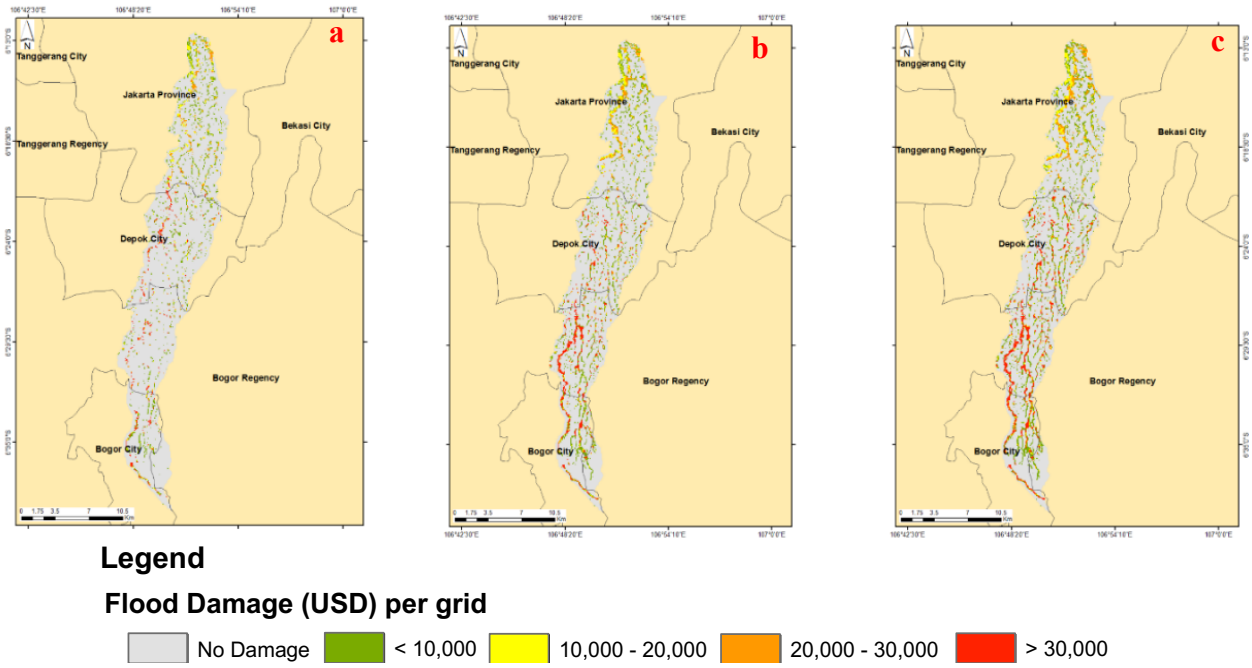

Figure 4.2.8. Flood damage map. (a) Current situation, (b) scenario 1: average climate change, and (c) scenario 2: extreme climate change

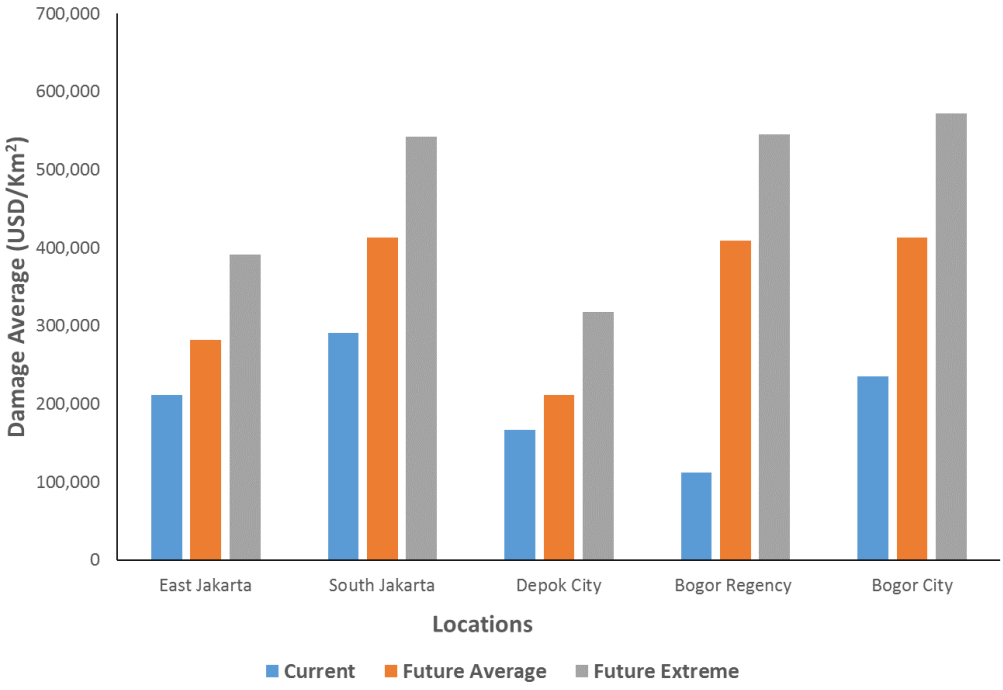

Figure 4.2.9. Flood damage assessment by region

4.2.3.5 Water quality

Model performance evaluation

Before conducting the future scenario analysis, the performance of the WEAP simulation was validated with observed and simulated hydrological and water quality parameter values. To validate the hydrology module, the parameters (mainly effective precipitation and runoff/infiltration) were adjusted using the trial and error method during the simulation to reproduce the observed monthly stream flows for the period of the years 2011 to 2014 (Table 4.2.6). The final best-fit parameters for both entities were 97% and 50/50, respectively. Figure 4.2.10(a) compares monthly simulated and observed stream flows at Kp Kelapa (average value for the 2000-2007 period), showing that they largely match for most months with a correlation coefficient (R^2) ≅ 0.80, a root-mean-square error ≅ 0.25, and an average error of 8%. In contrast, the water quality simulation was validated by comparing simulated and observed BOD concentrations during the dry and wet seasons of 2004 at Kp Kelapa location. The selection of this location and time, i.e., the year 2004, was based on the consistent availability of observed water quality data, and the results showed a strong relation between the two datasets (Figure 4.3.10(b)) (with an error of 11%), confirming the suitability of the model performance within this problem domain.

Table 4.2.6. Summary of parameters and steps used for calibration

Parameter	Initial value	Step
Effective precipitation	100%	±0.5%
Runoff/infiltration ratio	50/50	±5/5

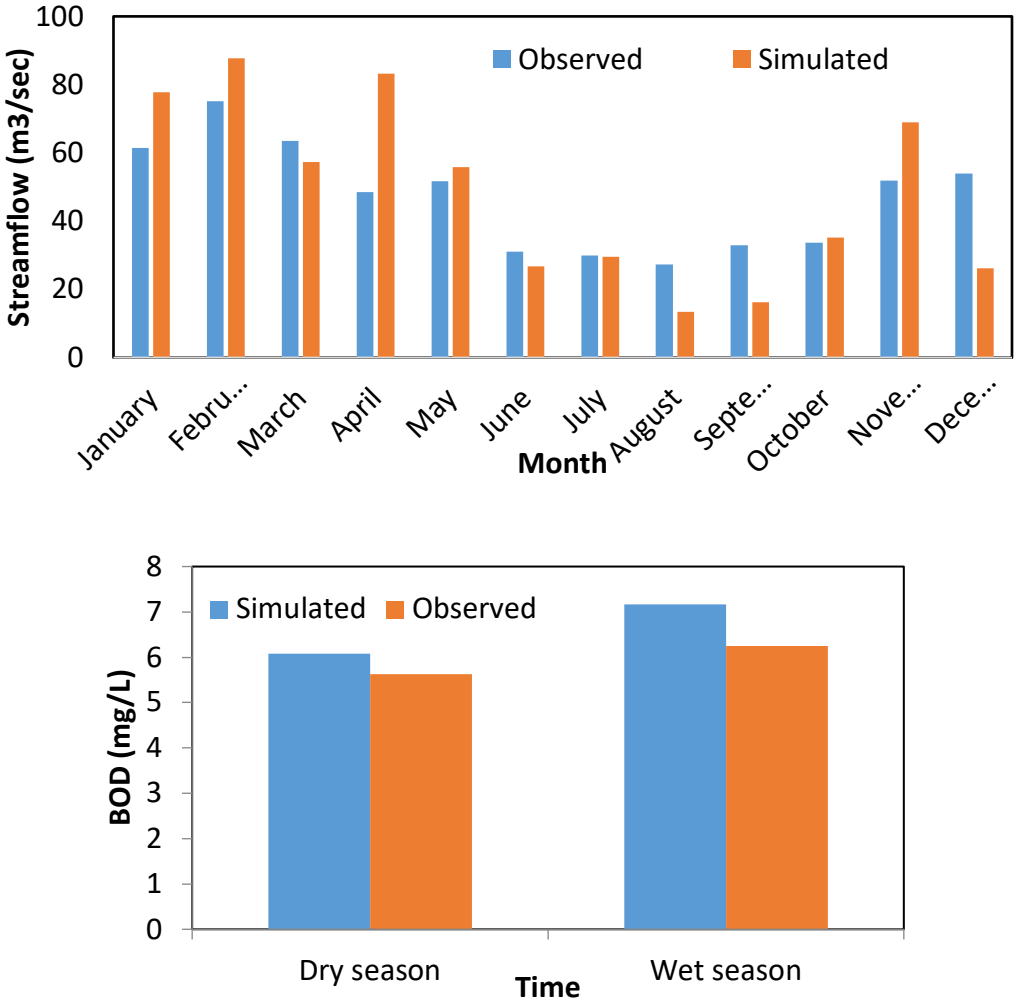

Figure 4.2.10. Validation of the model output by comparing simulated and observed (a) average monthly river discharge for the 2000-2007 period; (b) BOD values for the year 2004 at Kp Kelapa

Future water quality simulation and scenario analyses

The simulation of future water quality using selected parameters (BOD, NO_3, and *E. coli*) was conducted under two different scenarios as stated above in the section on model setup (Table 4.2.7). Spatio-temporal simulation and prediction of water quality parameters was conducted for 2015 and 2030 using 2000 as a reference or base year.

Table 4.2.7. Summary of all the criteria considered for different future water quality simulation scenarios

Scenario	Components
Business as usual	Climate change + population growth +WWTP of 22 MLD
With measures	Climate change + population growth +WWTP of 520 MLD

The results for the water quality parameters simulated using these two scenarios are shown in Figure 4.2.11. Under the business-as-usual scenario considering the currently existing wastewater treatment plant (capacity of 22 MLD and coverage of a mere 4% of the total population in the study area), the current status of the water quality throughout the river is very poor compared with local class 2 guidelines, and it is even worse in the case of downstream locations because of the cumulative effect of waste disposal and the excessive amount of untreated waste coming from upstream. The effects of both climate and population changes are prominent in determining the status of water quality, which will deteriorate further by 2030 relative to the current situation. However, based on the scenario with measures, in which all the locally generated wastewater will be collected and treated by the WWTP with a capacity of 520 MLD, the water quality status will be much better throughout the river, which is an encouraging sign. However, quality is still a matter of concern, especially in the downstream area. Based on the relationship between the wastewater collection rate and the quality of the river water, it is clear that water quality can be improved to some extent just through the horizontal growth of WWTP capacity (BOD concentration decreases from 20 mg/L to 10 mg/L with an increase collection rate from 4% to 100% as shown in Figure 4.2.11).

Explaining water quality more precisely, a high concentration of nitrate indicates the influence of untreated sewerage input. In general, most of the water samples are safe for the aquatic system in terms of NO_3, except at the PA Manggarai location, but with climate change, water quality will also deteriorate at the other locations. The BOD value currently varies from 7.65 to 11.35 mg/L, which clearly indicates that all the water samples are moderately to extremely polluted relative to the value required for the fishable category, which is described as class III in the national water quality standards (Indonesia), i.e., 6 mg/L. The *E. coli* value, a commonly used biological indicator of water quality status, also exhibits no significant improvement in the future, which might be due to the unavailability of data such as the rate of chlorination. The above result suggests that current management policies and the near-future water resources management plan are not sufficient to maintain the pollution level within the desirable limit and calls for transdisciplinary research into more holistic approaches for sustainable management.

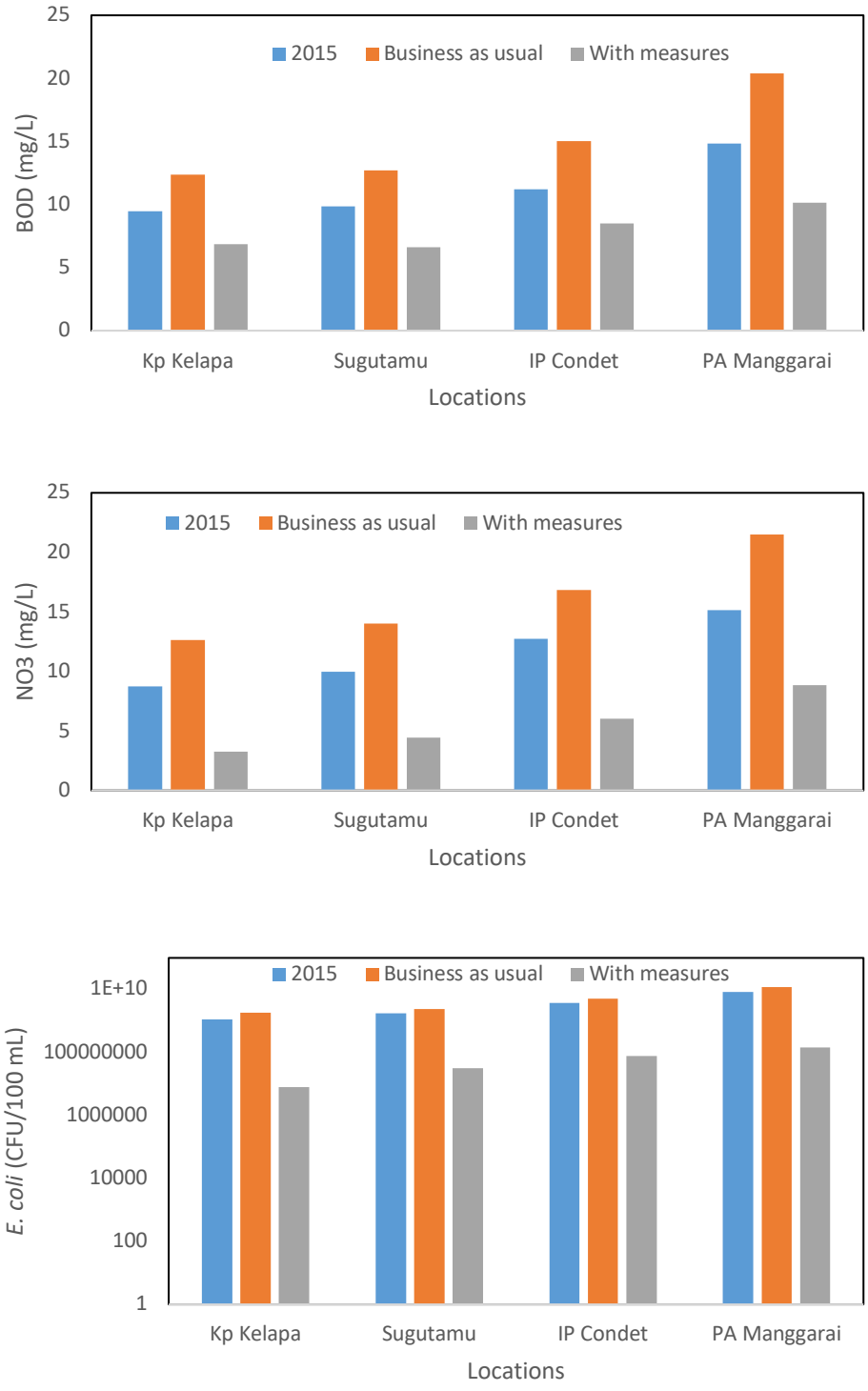

Figure 4.2.11. The simulation results for different water quality parameters, (a) BOD, (b) NO_3, and (c) *E. coli*, for four different locations in the Ciliwung River using three different scenarios

4.2.3.6 Economic benefit of improving urban water quality

Compared with other studied cities, Jakarta exhibited the lowest response rate; of a total of 500 questionnaires, only 236 were submitted for further analysis (47% response rate). Among the sampled respondents, 87% visited (intentionally) the city's waterbodies in the last month, of which 31% went regularly, 46% went a few times, 19% went once, and 4% provided no answer. Basically, the majority of respondents acknowledged the problem of water pollution in the city's waterbodies, and in answer to the question of whether the water quality is sufficiently acceptable for participating in recreational activities, they responded definitely no – 39%, probably no - 48% probably yes – 4%, definitely yes – 6%, and no answer – 3%.

Figure 4.2.12 below provides the socioeconomic profile of the sample in Jakarta City. As can be seen from the figure, the sample is representative.

The main results of the study relate to the estimation of WTP values and the calculation of the total economic value for the entire population of the city. The average use WTP for swimmable water quality was estimated to be 23,415 IDR (USD 1.70) per capita; the average use WTP for fishable water quality was estimated to be 14,876 IDR (USD 1.08) per capita; the average nonuse WTP for swimmable water quality was estimated to be 24,105 IDR (USD 1.75) per capita; and the average nonuse WTP for fishable water quality was estimated to be 16,253 IDR (USD 1.18) per capita. The main determinants of WTP were the income and educational status of a respondent. The total economic value of water quality improvements in Jakarta was estimated to be USD 89 million per year.

Clearly, benefits will not be sufficient to cover the costs of water quality improvements (the major health, water, tourism and other welfare costs associated with poor sanitation were estimated to be more than USD 6 billion in 2005 or more than 2 percent of the GDP, World Bank), so the government should develop mixed public/private, public/public sector solutions, microfinancing, and rebate systems as well as attract external funding sources for investment, service delivery, and operation and maintenance. Furthermore, massive campaigns are needed to develop the public's sense of responsibility and belonging so that the communities as a whole are willing to participate in measures to improve water quality. Partnerships are needed with four key actors that can bridge environmental communications between the government and the public: the mass media, civil society organizations, the legislature, and religious organizations. In combination with the ongoing and sustainable economic development of Indonesian economy, these measures could ensure an increase in the willingness of people to pay for improved water quality in their waterbodies as well as better and more secure life for themselves and their children.

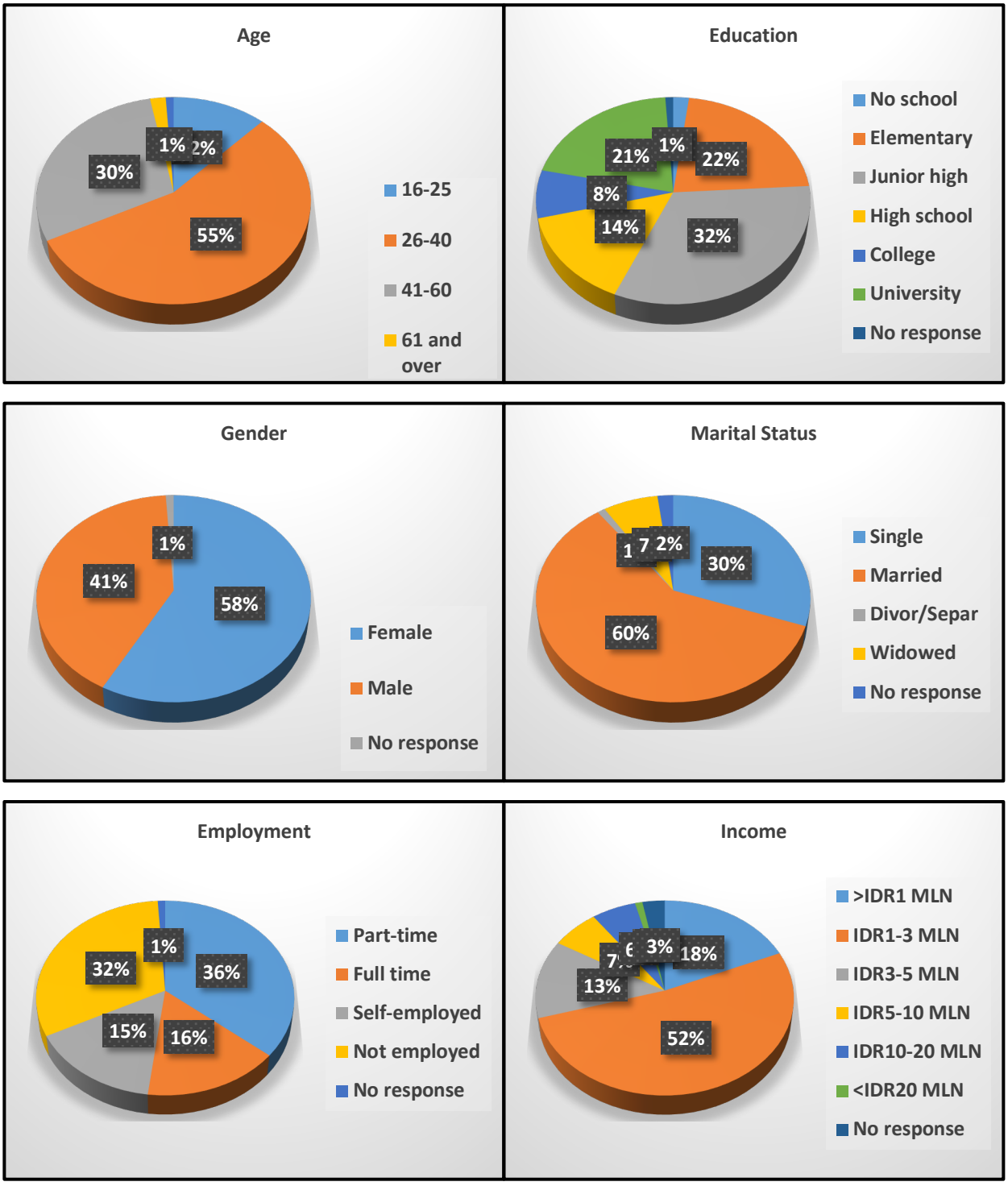

Figure 4.2.12. Socioeconomic profile of the sample (Jakarta city study)

4.2.3.7 Floodwater-borne infectious diseases

The health risk assessment model simulated the number of infectious gastroenteritis cases among residents in flooded areas using the results of both the flood and water quality simulation models. The projected number of gastroenteritis cases was 972 under the current scenario, 1,956 for the business-as-usual scenario, and 40 for the mitigation scenario; the simulation results clearly show that the number of cases of gastroenteritis will substantially increase in the near future due to the combination of increased flooding severity (9% increase in flooded areas (>50 cm)), greater deterioration of the quality of river water (31% increase in *E. coli* concentrations), and increased population (31%). Because these factors each affect the health risk independently, the total increase in health risk was greater than that of each of the input parameters. Figure 4.2.13 shows the distribution of gastroenteritis cases in flooded areas under current and future scenarios; high-risk areas (red areas in Figure 4.2.13) are clustered in populated regions, and where severe inundation is expected, in the northern part of the city. These results warrant immediate measures to prevent infectious diseases following flooding events in addition to those aimed at preventing direct harm (e.g., drowning) to residents.

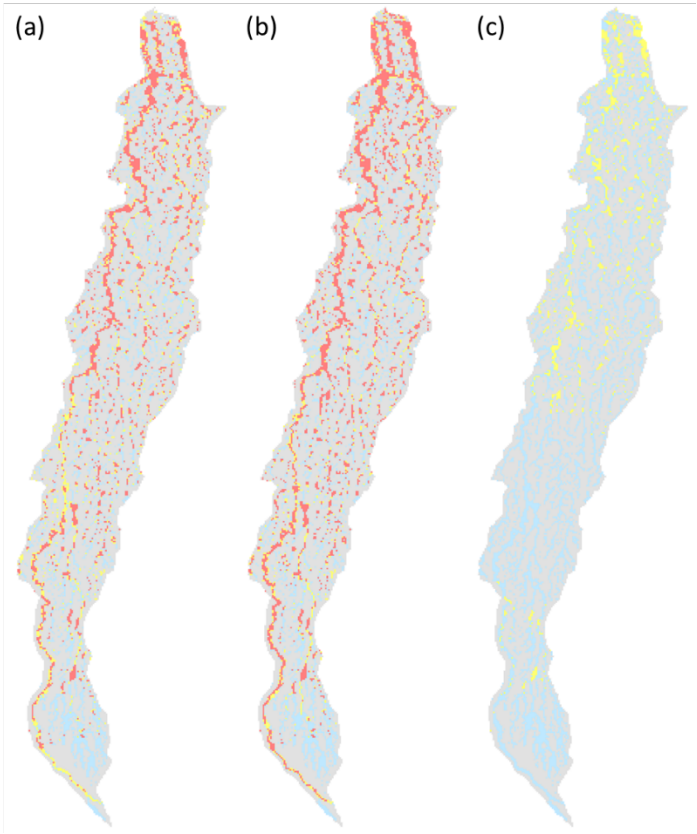

Figure 4.2.13. Geological distribution of gastroenteritis cases due to noroviruses in Jakarta

4.2.4 Low-carbon technology in wastewater facilities

Information Collected for Existing and Planned Wastewater Management Facilities

Existing Facilities

Since the coverage of the sewerage system in Jakarta is approximately 2%, the target area includes only one (1) WWTP, Setiabudi WWTP, which functions in both wastewater treatment and flood control and has a capacity of 18,031.68 m^3/day. The WWTP is composed of two ponds, the West Pond and East Pond, with aeration and manual/mechanical screens, the details of which are outlined in Table 4.2.8.

Table 4.2.8. Specifications of Setiabudi WWTP (JICA, 2012)

Physical condition		West Pond	East Pond	Total
Surface area		26,100 m^2	17,400 m^2	43,500 m^2
Water level	in high condition	4.5 m	4.7 m	-
	in low condition	1.5 m	1.5 m	-
Pond depth (effective)		3.00 m	3.20 m	
Elevation at the pond bottom		-0.5 m	-0.5 m	-
Pond capacity (effective volume)		78,300 m^3	55,680 m^3	133,980 m^3
Treatment process		Aerated lagoon	Aerated lagoon	-
Treatment capacity		13,523.76 m^3/day	4,507.92 m^3/day	18,031.68 m^3/day
Present quantity of influent		9,720 m^3/day	3,240 m^3/day	12,960 m^3/day
Retention time	Based on treatment capacity	4.3 days	5.5 days	4.7 days
	Based on present quantity	8.1 days	17 days	10.3 days
Inlet	Wastewater	3	2	5
	Drainage	6	2	8
Screen (mechanical)		2 (0)	2 (2)	4 (2)
Aerator unit		4	3	7
Effluent pump		5 x 1.10 m^3/s	3 x 1.10 m^3/s	-

Planned Facilities

DKI Jakarta is divided into fifteen (15) sewerage zones from Zone 0 to Zone 14. Except for Zone 0 where Setiabudi WWTP is located, there are currently no WWTPs in other zones, which instead depend on on-site treatment systems such as septic tanks.

Sewerage zones and the WWTP introduction plan up to 2050, as declared by Governor Regulation No.41 as of 2016, are shown in Figure 4.2.14. Accordingly, every sewerage zone will be equipped with a WWTP by 2030 as detailed in Table 4.2.9.

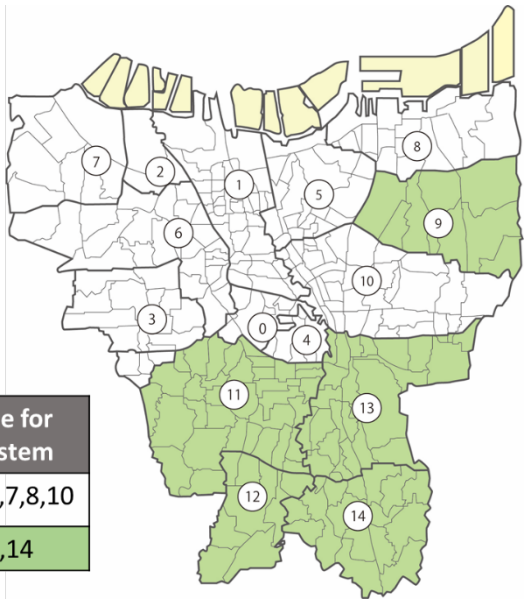

Phase of Implementation	Target Zone for Off-site system
2015-2022	1,2,3,4,5,6,7,8,10
2023-2030	9,11,12,13,14

Figure 4.2.14. Target sewerage zones under Governor Regulation No. 41 of 2016.
This figure was compiled using information gained through interviews with the JICA Expert from the Ministry of Land, Infrastructure and Transportation dispatched by the Government of Indonesia.

Table 4.2.9. Planned WWTP Capacity by Sewerage Zone of DKI Jakarta (JICA, 2012)

Sewerage zone	Capacity of planned WWTP (m^3/d)	Site area (m^2)
Zone 1	264,000	4,901
Zone 6	313,000	5,874
Zones 2-5, 7-14 (12 zones)	2,059,000	52,629
Total	2,636,000	63,404

2) Calculation of GHG emissions reduction

As with Hanoi city, the following four (4) technologies were examined as described below: Tool 1) introduction of high-efficiency pumps, Tool 2) introduction of high-efficiency blowers, Tool 3) installation of biogas power generation system and Tool 4) introduction of solar power system.

Tool 1. Energy saving by introducing high-efficiency pumps in wastewater treatment plants

In calculating the reduction in GHG emissions, EC_{lp} (annual power consumption of the low-carbon technology pump) is generally obtained by monitoring the pumps to be installed. Since this

assessment targets the planning phase, the available data, such as master plans, BAU and relevant data obtained through field surveys, were used to estimate EC_{lp}.

- Data and parameters

Table 4.2.10 summarizes the data necessary to calculate GHG emissions reduction using Tool 1.

Table 4.2.10. Data used for Tool 1: Energy saved by introducing high-efficiency pumps for Jakarta City

Parameter	Value	Remarks
FE_{EL}: CO_2 emission factor	0.8903 tCO_2/MWh	Grid Emission Factors, Institute for Global Environment Strategies (https://pub.iges.or.jp/)
ηM/P: MP pump efficiency	53%	Nominal value of conventional pump
ηPj: Low-carbon technology pump efficiency	85%	Nominal value of energy-saving pump
Size of pumps to be installed	3,500 m^3/hour of capacity with 63 kw of power consumption	Specification of the pump commonly installed in the WWTPs of the target cities
Hours of operation per year	227,488 hours/year	Annual treatment capacity of the existing and planned pump/capacity of pump to be installed = 796,209,600 / 3,500
EC_{lp}: Annual power consumption of the low-carbon technology pump	14,332 MWh/year (existing pumps: 97 MWh/year, planned pumps: 14,234 MWh/year)	ECpp = Hours of operation per year * power consumption of pump to be installed = 227,488 * 0.063
ME: MP emissions per year	20,463 tCO_2/year (existing pumps: 139 tCO_2/year, planned pumps: 20,324 tCO_2/year)	ME = ECpp * **η**M/P/**η**pj * FE_{EL}= 14,332 * 0.85 / 0.53 * 0.8903
LE: Low-carbon technology emissions per year	12,812 tCO_2/year	LE = ME of existing pumps + ECpp of planned pumps* FE_{EL} = 139 + 14,234 * 0.8903 = 12,812

- Calculation of GHG emissions reduction (ER)

Based on the data collected and calculated above, the reduction in the amount of GHG emissions due to the introduction of Tool 1 was estimated as follows.

$$ER = ME - LE = 7{,}652\ tCO_2/year$$

Tool 2. Energy Saving by Introducing High-Efficiency Blowers

As shown in Figure 3.6, the consumption of electricity by the pumps is 1/6 that of the blower. This ratio was considered in calculating GHG emissions. On the other hand, the energy saving rate of the blower to be installed was assumed to be 10% based on the general specifications of recent types of energy-saving blowers.

- Data and parameters

Table 4.2.11 summarizes the data used to calculate the GHG emissions reduction using Tool 2.

Table 4.2.11. Data used for Tool 2: Energy saving by introducing high-efficiency blowers for Jakarta city

Parameter	Value	Remarks
FE_{EL}: CO_2 emission factor	0.8903 tCO_2 / MWh	Grid Emission Factors, Institute for Global Environment Strategies (https://pub.iges.or.jp/)
Rate of Energy Saving by introducing Tool 2	10%	Nominal value of energy-saving blower
Rate of power consumption of blower and pump	Power consumption of blower : Power consumption of pump = 6 : 1	According to Figure 3.6
ME: MP emissions per year	122,781 tCO_2/year (existing pumps: 834 tCO_2/year, planned pumps: 121,947 tCO_2/year)	ME = ME of Tool 1 *6
LE: Low-carbon technology emissions per year	110,586 tCO_2/year	LE = ME of existing pumps + ME of planned pumps* (1 - 0.1) = 834 + 121,947 * 0.9

- Calculation of GHG emissions reduction (ER)

Based on the data collected and calculated above, the reduction in the amount of GHG emissions due to the introduction of Tool 2 was estimated as follows.

$$ER = ME - LE = 12{,}195\ tCO_2/year$$

Tool 3. Installation of a Biogas Power Generation System

The installation of biogas power generation represents replacing the use of fossil fuel-based energy with renewable energy with zero emissions. Therefore, the reduction in the amount of GHG emissions due to the introduction of this technology could be considered the same as the amount of MP emission. The details of this calculation are shown below.

- Data and parameters

Table 4.2.12 summarizes the data used to calculate the GHG emissions reduction using Tool 3.

Table 4.2.12. Data used for Tool 3: Installation of a biogas power generation system for Jakarta city

Parameter	Value	Remarks
FE_{EL}: CO_2 emission factor	0.8903 tCO_2/MWh	-
Rate of volume of wastewater treatment and power generation	Daily treated wastewater (m^3/day) : Power generation (MWh/year) = 40,000 : 1,380	Based on data from the Eniwa city wastewater treatment facility (http://www.city.eniwa.hokkaido.jp/www/contents/1366006820944/index.html)
Total amount of water treated by WWTPs daily in the target area	2,654,032 m^3/day	
EGBI: Electricity supplied by the grid to the WWTP area	92,321 MWh/year	
ECBI: Power consumption by the biogas power generation system	0 MWh/year	
ME: MP emissions per year	82,194 tCO_2/year	ME = ECBI * FE_{EL}
LE: Low-carbon technology emissions per year	0 tCO_2/year	PE = ECPB * FE_{EL}

- Calculation of GHG emissions reduction (ER)

Based on the data collected and calculated above, the reduction in the amount of GHG emissions due to the introduction of Tool 3 was estimated as follows.

$$ER = ME - LE = 82{,}194\ tCO_2/year$$

Tool 4. Power Generation by Introducing a Solar Power System

Like the installation of biogas power generation, a solar power system generates renewable energy with zero emissions, so its amount of GHG emissions reduction is equivalent to that of MP emission.

- Data and parameters

Table 4.2.13 summarizes the data used to calculate the GHG emissions reduction using Tool 4.

- Calculation of GHG emissions reduction (ER)

Based on the data collected and calculated above, the reduction in the amount of GHG emissions due to the introduction of Tool 4 is estimated as follows.

$$ER = ME - LE = 2{,}426\ tCO_2/year$$

Table 4.2.13. Data used for Tool 4: Power generation by introducing a solar power system for Jakarta city

Parameter	Value	Remarks
FE_{EL}: CO_2 emission factor	0.8903 tCO_2/MWh	Grid Emission Factors, Institute for Global Environment Strategies (https://pub.iges.or.jp/)
Area required for power generation	20,000 m^2/MW	
Hours of operation per day	8 hours/day	
Days of operation per year	200 days/year	
Ratio of wastewater treatment capacity to the potential PV area in the WWTP	Site area of WWTP (m^2) : potential PV area (m^2) = 1 : 0.46	Based on the data acquired from the layout of Bay Mau, Hanoi, Viet Nam
Total site area of WWTP (m^2)	74,043 m^2	Based on the data acquired from the layout of Bay Mau, except for the planned WWTPs for which data are available.
Potential PV area (m^2)	34,060 m^2	Total site area of WWTP * 0.46 = 74,043* 0.46
Electricity generated (MW)	1.7 MW	Potential area/required area for power generation = 34,060/20,000 = 1.7
Hours of operation of the solar power system	8 hours/day, 1,600 hours/year	200 days/year
EGPV = Electricity supplied by the grid to the WWTP area (MWh/year)	2,725 MWh/year	EGPV = power generated * annual operational hours of the solar panels = 1.7 * 1,600
ECPB = Power consumption by the solar power system	0 MWh/year	
ME: MP emissions per year	2,426 tCO_2/year	ME = EGPV * FE_{EL} = 2,725 * 0.8903 = 2,426
LE: Low-carbon technology emissions per year	0 tCO_2/year	LE = ECPB * FE_{EL} = 0

GHG Emissions Reduction by Introducing the Four Tools

In total, the GHG emissions after the introduction of the abovementioned four (4) tools is 104,466 tCO_2/year, which accounts for 46% of MP emission (Figure 4.2.15). Among the proposed technologies, the biogas power generation system is considered the most effective strategy for reducing GHG emissions as it accounts for 79% of the total.

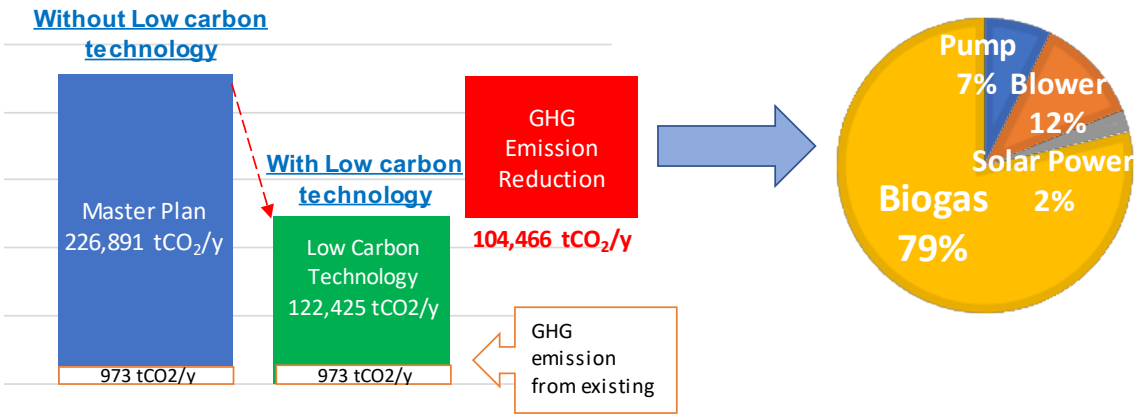

Figure 4.2.15. GHG emissions reduction due to the application of low-carbon technologies in the Jakarta master plan

References

Formánek, A.; Silasari, R.; Syahril, M.; Kusum, B.; Kardhana, H. Two-dimensional model of Ciliwung River flood in DKI Jakarta for development of the regional flood index map. *J. Eng. Technol. Sci.* **2013**, 45(3): 307-325.

Goyal, M.K.; Ojha, C.S.P.; Evaluation of linear regression methods as downscaling tools in temperature projections over the Pichola Lake Basin in India. *Hydrological Processes* **2011**, 25: 1453-1465.

Intergovernmental Panel on Climate Change. *Climate Change 2014: Synthesis Report*. Core Writing Team; Pachauri, R.K., Meyer, L.A., Eds.; IPCC: Geneva, Switzerland, 2014.

Japan International Cooperation Agency. *The project for capacity development of wastewater sector through reviewing the wastewater management master plan in DKI Jakarta in the Republic of Indonesia, Final Report*; 2012. http://open_jicareport.jica.go.jp/pdf/12078622_01.pdf [Accessed on 18th October, 2018]

Mishra, B.K.; Rafiei-Emam, A.; Masago, Y.; Kumar, P.; Regmi, R.K.; Fukushi, K. Assessment of future flood inundations under climate and land use change scenarios in the Ciliwung River Basin, Jakarta. *J. Flood Risk Manag.* **2018**, 11(S2): S1105-S1115.

Sunyer, M.A.; Hundecha, Y.; Lawrence, D.; Madsen, H.; Willems, P.; Martinkova, M.; Vormoor, K.; Bürger, G.; Hanel, M.; Kriaučiūnienė, J.; Loukas, A.; Osuch, M.; Yücel, I. Inter-comparison of statistical downscaling methods for projection of extreme precipitation in Europe, *Hydrol. Earth Syst. Sci*. 2015, 19: 1827-1847.

United Nations Department of Economic and Social Affairs, Population Division *World Urbanization Prospects: The 2014 Revision*; ST/ESA/SER.A/366, United Nations: New York, NY, 2015.

4.3 Manila

4.3.1 Introduction

The Philippines is composed of 5 main types of administrative units, namely, regions, provinces, cities, municipalities and barangays (or villages), with the region as the highest level and the barangay as the lowest. In total, there are currently 18 regions, 81 provinces, 145 cities, 1489 municipalities and 42,036 barangays (Philippine Statistics Authority (PSA), 2016). The population of the country is continually increasing; as reported by the 2015 census, the total population had reached 100,979,303, and the National Capital Region (NCR), usually named Metro Manila, is the most populated region with 12,877,253 inhabitants and a population density of 20,785 people per square kilometer (PSA, 2015a). The Philippines is actually one of the most rapidly urbanizing Asian countries; the level of urbanization was 45.3% in 2010 (PSA, 2010). Moreover, it is estimated that 102 million people (more than 65% of the total population of the country) will reside in cities by 2050 (World Bank Group, 2017). Urbanization can be considered the main driver of economic growth through increased productivity, consumption, job opportunities and poverty reduction, but unmanaged development can lead to congestion, slums, disparity and environmental pollution. In Metro Manila, water pollution is a predominant environmental problem; due to inappropriate urban expansion and inadequate wastewater treatment facilities, a huge amount of wastewater is produced, causing the deterioration of surface water resources. In fact, only 10% of the 7,000 tons of solid waste generated daily is recycled or composted, while the remaining waste is deposed into nearby water bodies (World Bank Group, 2017). Moreover, the proliferation of informal settlements along rivers and water bodies may increase water quality degradation, and it constricts the drainage system of Metro Manila, which exacerbates flooding during heavy rains. Like many megacities in Asian countries, Metro Manila is located in a flood-prone area. Many floods have occurred in the region, but tropical storm Ondoy, which hit the island of Luzon in September 2009, caused the most devastating flood. The typhoon affected 4.75 million people and totally or partially damaged 155,659 houses (National Disaster Coordinating Council, 2009). Due to its location and landscape geography, Metro Manila is considered one of the largest floodplains in the Philippines.

The target city, Metro Manila, is located between Manila Bay and Laguna de Bay at 14°40' N latitude and 121°03' E longitude (Figure 4.3.1); the total area is 636 km^2. The climate is characterized by relatively high temperatures and abundant rainfall. The temperature ranges from 21°C to 39°C, and the annual average precipitation is 2,400 mm. The city is located within one main catchment, the Marikina River basin, which consists of the Marikina, Pasig, San Juan and Tullahan Rivers, which serve as the main outlets for the network of tributaries in the basin (Lagmay et al., 2017).

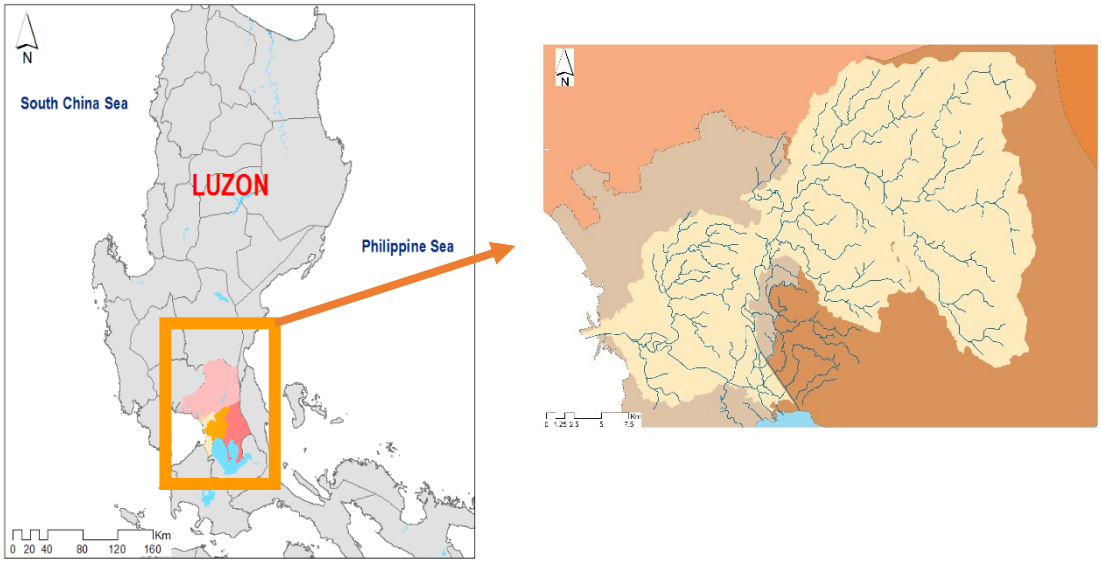

Figure 4.3.1. Location of the study area

4.3.2 Methodology

4.3.2.1 Precipitation change

Precipitation is used to determine the effect of climate change on flooding and water quality. To assess flooding, precipitation change was determined by extracting the daily climate projections of 2 GCMs, MRI-CGCM3 and MIROC5, for the RCP 4.5 and RCP 8.5 emission scenarios, as mentioned in Section 3.1. The historical precipitation outputs of these 2 GCMs were compared with observation data from the Science Garden station to identify the pattern of bias in the GCM data. The observed precipitation data were provided by the Meteorological Organization and Water Affairs Office of Metro Manila (Philippine Atmospheric, Geophysical and Astronomical Service Administration (PAGASA), 2011), and data from the 25-year period from 1980 to 2004 were compared to identify the bias pattern. Later, the quantile bias correction technique was applied to the GCM output for current and future climate projections. In this study, future climate was represented by precipitation projections for the 2020-2044 period, and Gumbel frequency analysis was applied to estimate extreme rainfall for 50- and 100-year return periods. Finally, these return period values were compared to understand the changes in the extreme rainfall pattern and their impact on flood inundation.

To evaluate the effect of climate change on water quality, we evaluated the change in monthly average precipitation. Based on the rate of change in the observed historical rainfall values and the downscaled future precipitation data, we estimated the average rate of increase based on regression analysis. This growth rate was applied to current rainfall values to obtain future rainfall values. Statistical downscaling was followed by trend analysis, a less computationally demanding technique that enables the reduction of biases in the precipitation frequency and intensity (Goyal and Ojha, 2011), to generate climate variables at a monthly scale.

4.3.2.2 Land cover change

To generate the future land cover map of the study area for 2030, two past Landsat satellite images were classified using a supervised classification maximum likelihood algorithm with ArcGIS software and validated. Land Change Modeler for ArcGIS was used to project the land cover pattern based on the previous change trend, and in this case study, Landsat 7 data from 2002 and Landsat 8 data from 2014 were employed to estimate the land cover in 2030, as indicated in Table 4.3.1. Level 1 Landsat images were downloaded from the USGS website (https://earthexplorer.usgs.gov/), and prior to image analysis, appropriate data processing was performed, such as band compositing and clipping considering the study area. Landsat sensors have a moderate spatial resolution (30 m), at which it was difficult to differentiate individual buildings or houses and to establish a detailed land cover map. However, the imagery is sufficiently clear to distinguish urban growth to determine regional coverage. Therefore, 4 classes, namely, built-up, water bodies, forest, and green land were identified based on the supervised classification.

Table 4.3.1. Satellite images applied

No.	Path/Row	Data Set	Acquisition Date	Scene Cloud Cover
1	116/050	Landsat 7 ETM C1 Level 1	03/04/2002	1%
2	116/050	Landsat 8 OLI/TIRS C1 Level 1	07/02/2014	3.06%

4.3.2.3 Population growth

To estimate the effect of population growth (one of the two key drivers examined in this study) on the status of water quality, the entire study area was divided into different demand sites that mainly represent the populations of different cities on both side of the Pasig-Marikina-San Juan River within our study area and that direct impact the river through the discharge of their domestic sewerage water. The future population was estimated by the ratio method using projected growth rate data for the NCR from PSA. A total population of 7,851,660 was considered for the base year, i.e., 2011, in our study area, and for the future population projection, annual growth rates of 1.76% and 1.73% were considered for the 2011 to 2015 and 2016 to 2030 periods, respectively. Henceforth, the population sizes considered for the current year (2015) and the target year (2030) were 8,420,018 and 10,893,734, respectively.

4.3.2.4 Urban flooding

Flooding occurs frequently in Manila during the rainy season, causing huge losses. Recent floods in 2004, 2008, 2009 and 2012 resulted in extensive inundation and considerable damage, such as human deaths, evacuations, and infrastructure breakdowns. Therefore, flood assessment is very important for reducing tangential and nontangential losses from frequent floods, and in this study, urban flood assessment was performed by coupling hydrologic-hydraulic modeling in the Pasig-

Marikina-San Juan River basin, particularly for Metro Manila (NCR). Alternative scenarios were explored and applied for the assessment of future floods including (i) climate change, (ii) climate change with a small dam (47 MCM), and (iii) climate change with a large dam (75 MCM); these countermeasures were considered in line with the Metro Manila Flood Management Plan/Vision. The target area was the Pasig-Marikina-San Juan River basin, which covers a total area of 735 km^2. Metro Manila is located in the downstream of the basin and is bounded by Manila Bay in the west and Laguna de Bay in the southeast. The headwaters of the Marikina River are in the Sierra Madre Mountains in the eastern part of Metro Manila and end in the Pasig River as indicated in Figure 4.3.2. During heavy storms, water from the Marikina River is diverted toward Laguna de Bay through the Manggahan Floodway. Typhoon Ondoy in August 2009 was used to build the hydrologic-hydraulic models.

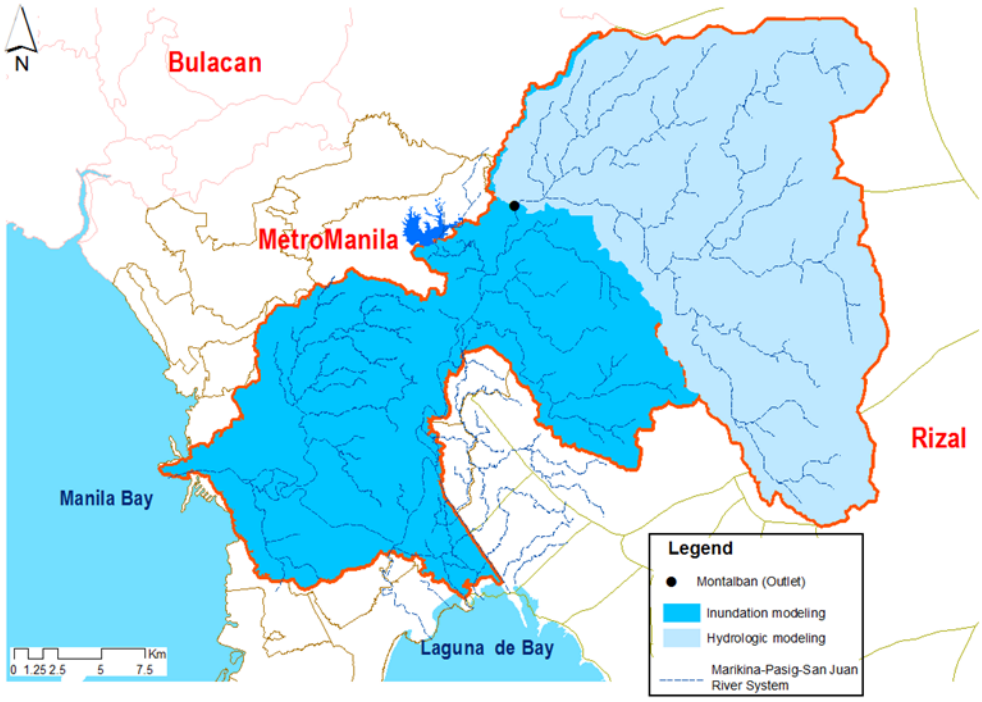

Figure 4.3.2. Flood map of the study area (401 km^2 hydrologic modeling area and 334 km^2-inundation modeling area)

The 2009 flood event was characterized as having an approximate return period of 100 years as well as being the worst event in the last several decades, causing huge tangible and nontangible losses. The FLO-2D model was used to simulate flood inundation. Hydrologic modeling was performed to generate flood hydrographs at the inlet (beginning location: Montalban) of the inundation modeling area, and HEC-HMS was used to simulate hourly inflow to the lower basin. To set up the inundation model, several types of data such as DEM, land cover, soil, and diversion channel information as well as daily meteorological (e.g., daily rainfall) and river discharge data. A soil map from the Food

and Agriculture Organization of the United Nations (FAO) soil database, a DEM map with a 1-meter resolution from Light Detection and Ranging (LiDAR) and a land cover map (30-m resolution) based on Landsat imagery were used.

4.3.2.5 Direct flood damage

A spatial analytical approach was applied to assess the future urban flood damage in the watershed of the Pasig-Marikina-San Juan River system. Specific parameters and datasets were used and integrated in GIS to determine the situation in 2030 as explained in detail in Section 3.5. Flood hazard, exposure and vulnerability are the main components of flood damage assessment. Flood hazard and exposure are described in Sections 3.4 and 3.5, respectively, and vulnerability is linked to the flood depth-damage function, which was established through the relationship between the consequences for the property at risk and the characteristics of a flood, such as depth. This function is used to predict direct or physical damage from flooding (Romali et al., 2015, Smith, 1994). To construct a flood depth-damage function based on a past flood event, field surveys were conducted at the barangay level during February - March 2017, particularly with local residents in affected areas. The surveys were focused on the relationship between the consequences for at-risk property and flood characteristics. In total, three hundred ninety-eight (398) responses were collected in the Pasig-Marikina-San Juan watershed. The locations of the surveys in each study area are presented in Table 4.3.2. Then, the flood damage in the study area under current conditions and two scenarios were also simulated in relation to climate change and the implementation of flood mitigation measures as described in Section 4.3.2.4.

Table 4.3.2 Survey locations

No	Location	District / City	Respondents
1	Metro Manila	City of Manila	85
2		Makati	27
3		Marikina	49
4		Pasig	62
5		San Juan	45
6	Rizal	Cainta	29
7		Taytay	101

4.3.2.6 Water quality

As explained in Section 3.6, the WEAP model was used to simulate future total water demand and water quality variables in 2030, which will be useful for assessing alternative management policies for the Pasig-Marikina-San Juan River basin. Water quality modeling requires a wide range of input data including point and nonpoint pollution sources; past spatiotemporal water quality; detailed

information about wastewater treatment infrastructures, both currently existing and planned by 2030 according to the master plan (Department of Environment and Natural Resources (DENR), 2016); demographical trends; hydrometeorological information (PAGASA); drainage network information (Metropolitan Waterworks and Sewerage System (MWSS)); river flow-stage-width relationships; and land-use/land-cover data (National Water Resource Board).

Daily rainfall data have been collected at Science Garden meteorological station for the period spanning 1980 to 2013 and were used for model set up. Daily average stream flow data from 2011-2014, which were measured at seven stations (Napindan, Bambang Bridge, Guadalupe Ferry, Lambingan Bridge, Nagtahan Bridge, Jones Bridge and Manila Bay at the Pasig River), were utilized to calibrate and validate the WEAP hydrology module simulation. Observed water quality data (BOD, NO_3 and *E. coli*) were also collected at seven different locations along the Pasig River for the years 2011-2014 (MWSS, 2016) and used for water quality modeling.

The WEAP model was developed for the Pasig-Marikina-San Juan River basin, which has seven catchment areas with interbasin transfers. Hydrologic modeling required that the entire study area to be split into smaller catchments with consideration of the confluence points or influent locations of major tributaries as well as physiographic characteristics. The WEAP hydrology module computes the catchment surface pollutants generated over time by multiplying runoff volume by the concentration or intensity of different types of land cover. During the simulation, land cover information was broadly categorized into three areas, namely, agricultural, forested, and built-up. Soil data parameters were identified using previous secondary data and the literature (Clemente et al., 2001).

The resulting population distributions and their future trends at these four command areas were calculated by the ratio method using the PSA projection rate, as explained in Section 4.3.2.3. Regarding the future precipitation data, a different GCM output was used after bias correction, which is explained in detail in Section 4.3.2.1.

Model setup

The entire problem domain and its different components (Figure 4.3.3) were divided into seven catchments that were further subdivided into thirteen subbasins to consider the influent locations of major tributaries, and other major considerations to accurately represent the current situation of the study area were fourteen demand sites and one wastewater treatment plant. Here, demand sites denote domestic (population-level) explanations of water consumption and wastewater discharge in the Pasig-Marikina River, and WWTPs are pollution-handling facilities with design specifications that include the total capacity and pollutant removal efficiencies. Here, the UASB-SBR type of wastewater treatment plant was considered in the modeling, and its treatment efficiency was assumed to be 94% for COD, 97% for BOD, 77% for TN and 99.69% for fecal coliform (Khan et al., 2013). The reason for selecting UASB-SBR technology for both the current and future WWTPs was that future facilities have been specified to employ UASB-SBR technology (MWSS, DENR and World Bank, 2014), but the type and technology of current WWTPs have not been precisely

documented. Thus, for the sake of simplicity, we considered this technology for both current and future WWTPs. No precise data are available regarding the total volume of wastewater produced, so in the absence of such detailed information, the daily volume of generated domestic wastewater was estimated as 130 liters of average daily consumption per capita based on a literature review. Once model set up was completed, validation was performed using the simulated water quality result for the current situation, i.e., 2015 in this case. Thereafter, numerical simulation was conducted using different scenarios termed the business-as-usual scenario and the scenario with mitigation measures. For the business-as-usual scenario, the WWTP capacity was 42.5 MLD (total number = 6). However, for the scenario with mitigation measures, it was 612 MLD, and the total number of proposed additional WWTPs by 2030 was 11 (MWSS, 2016)

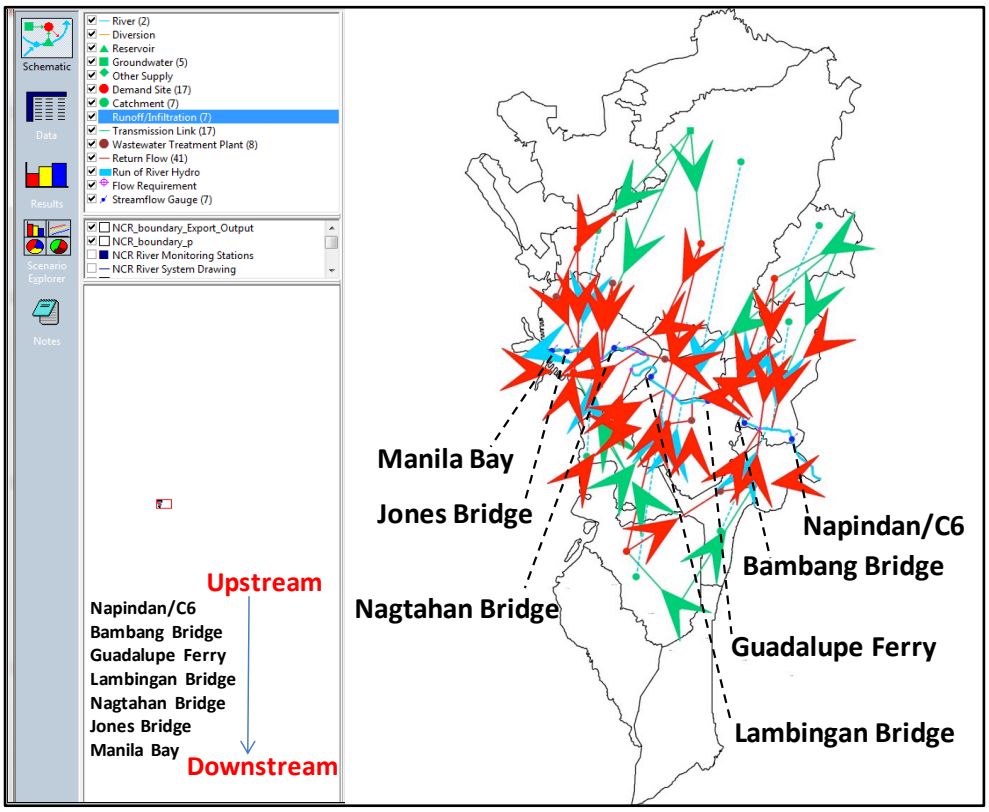

Figure 4.3.3. Schematic diagram showing the study area for water quality modeling in Metro Manila using the WEAP interface

4.3.2.7 Economic benefit of improving urban water quality

A survey-based methodology was created built on eliciting willingness-to-pay for good water quality in the waterbodies of Metro Manila. As no actual market exists for such an environmental good, the researchers needed to create a hypothetical market, and respondents were requested to reveal the value they would place on the proposed change in the environmental service. After several workshops with stakeholders in Metro Manila and meetings with government agencies in charge of the water quality issues in the city, a hypothetical water quality improvement scenario was identified.

The study examined valuation by respondents of a proposed Surface Water Quality Improvement Program in Metro Manila that consisted of two components: (1) building new wastewater treatment plants and (2) expanding the existing sewerage system. The questionnaire was translated into Tagalog, the most commonly spoken language in the megacity. The survey questionnaire was designed in three separate parts. The first part consisted of questions of awareness and behavior related to the current quality of waterbodies, causes of water pollution, visits to waterbodies, the purposes of those visits, and the effects of current water quality on human health and livelihoods. The second part presented the CVM scenario and the WTP question; the following open-ended WTP question was chosen: How much would you be willing to pay as a monthly fee per household in addition to your monthly utility bill to have water quality acceptable for swimming/fishing (keeping in mind that the existing water quality is defined as poor)? The final part revealed the socioeconomic data of the respondent and their household. The developed questionnaire was pretested before starting the main survey; 240 respondents in two cities, Quezon and Manila, were chosen for this exercise. The objective of the task was to check whether the questionnaire was logical and consistent and if the WTP questions were correctly understood. The main survey involved a total of 840 personal interviews that were conducted in August 2016 in Metro Manila. We could not secure a list of voters from the local government and did not want to use the telephone book to compile sampling for the survey as it did not cover the entire area of the megacity. Facing this challenge, random sampling based on the distance of the household to the nearest waterbody was chosen, and there were two classifications: 1) walking distance to the river, which assumes that one can reach the Pasig River within 30 minutes, and 2) the need to drive or take public transportation to enjoy the river. The SAS statistical package was used for the analysis. The possible effect of socioeconomic variables on WTP was analyzed by linear regression and Tobit models. Theoretically, the Tobit (censored regression) model would be better suited for analyzing the data as the OLS estimates could be biased (because the range of the dependent variables was limited, WTP≥0). Model estimation is usually undertaken by maximum likelihood techniques (Maddala, 1983; Kennedy, 1992).

4.3.2.8 Floodwater-borne infectious diseases

The risk assessment model for floodwater-borne infectious gastroenteritis was developed following the methodology in Section 3.8 to evaluate the number of cases of gastroenteritis caused by noroviruses in the flooded area in Manila. Three scenarios were developed, one to simulate the current situation (current scenario) and two to simulate the future situation by 2030 with or without mitigation measures, namely, the with-mitigation scenario and the business-as-usual scenario, respectively. The results of the flood inundation model and the water quality model corresponding to each scenario were used to represent the current or future urban flooding and surface water quality situations, respectively. The current and future population in each FLO-2D grid (33,447 grids in total) was calculated using the current and future population of the city as described in Section 4.3.2.3, the area of the city, and the area of the FLO-2D grid (10,000 m^2). The areas and populations

used in this analysis are summarized in Table 4.3.3; the total population in the study area was 6,605,791 for 2015 and 8,526,150 for 2030 (29% increase).

Table 4.3.3. Area and population of the cities within the target area

City	Region / province	Area [ha]	2015 population	2030 population
Kalookan City	NCR	5,580	1,583,978	1,766,981
Makati City	NCR	2,157	582,602	649,912
Malabon	NCR	1,571	365,525	407,756
Mandaluyong	NCR	929	386,276	430,904
Manila	NCR	2,498	1,780,148	1,985,815
Marikina	NCR	2,152	450,741	502,817
Pasay City	NCR	1,397	416,522	464,644
Pasig City	NCR	4,846	755,300	842,563
Quezon City	NCR	17,171	2,936,116	3,275,337
San Juan	NCR	595	122,180	136,296
Taguig	NCR	4,521	804,915	897,910
Antipolo City	Rizal	30,610	776,386	1,013,698
Cainta	Rizal	4,299	322,128	420,591
Rodriguez	Rizal	17,265	369,222	482,080
San Mateo	Rizal	5,509	252,527	329,715
Taytay	Rizal	3,880	319,104	416,642

Data sources

Area: Philippine Standard Geographic Code (http://nap.psa.gov.ph/activestats/psgc/)

2015 population: Based on the 2015 Population Census (http://psa.gov.ph/population-and-housing/title/Population)

2030 population: Highlights of the 2010 Census-Based Population Projections (https://psa.gov.ph/content/highlights-2010-census-based-population-projections)

4.3.2.9 Low-carbon technology in wastewater facilities

The amount of GHGs emitted from wastewater treatment facilities was estimated following the methodology stated in Section 3.9, and three scenarios were developed, namely, the current scenario, the 2030 without low-carbon technology scenario, and the 2030 with low-carbon technology scenario. The current scenario evaluated GHGs emission based on the current situation (i.e., emissions from existing facilities). The 2030 without low-carbon technology scenario evaluated GHG emissions from existing and planned facilities stated in the master plan (MWSS, 2016) using technologies (e.g., pumps, blowers) currently available in Southeast Asia, and the 2030 with low-carbon technology scenario evaluated GHG emissions assuming the implementation of the low-carbon technologies stated in Section 3.9. Based on the two scenarios for 2030, we evaluated the potential reduction in GHG emissions from wastewater facilities in the target area.

4.3.3 Results and discussion

4.3.3.1 Precipitation change

Daily maximum rainfall was estimated and compared for different return periods to understand the changes in extreme precipitation events under different climate change scenarios. Table 4.3.4 provides the daily maximum rainfall values for 50- and 100-yr return periods for different GCMs and emission scenarios; extreme precipitation events will be more frequent and intense in the future for all return periods and all durations. The climate change projections revealed a 25% and 40% increase in the 100-yr daily maximum precipitation for moderate and extreme conditions, respectively. Moderate and extreme conditions were established by averaging the projected return period values for the RCP 4.5 and RCP 8.5 emission scenarios, respectively.

Table 4.3.4. Comparison of precipitation extremes over Metro Manila

Return period (years)	Current	RCP 45		RCP 85	
		MRI	MIROC	MRI	MIROC
50	322.0	370.1	375.1	402.4	451.0
100	360.8	411.6	425.9	449.6	516.5

The results shown in Figure 4.3.4 clearly indicate that the annual precipitation simulated from the GCM output was not much different than currently observed. The observed total annual precipitation values for the year 2015 and the simulated results using different GCM and RCPs, i.e., MRICGCM3_45, MIROC5_45, MRICGCM3_85, and MIROC5_85, were 2,803.1, 2,806.8, 2,568.1, 2,773.6 and 2,649.2 mm, respectively. This clearly indicates that neither the monthly trend or the total annual rainfall is fluctuating significantly (within ±10%), but our goal is to show whether this small fluctuation has some effect on the future water quality status. To estimate the effect of precipitation alone on water quality, we fixed the other parameters, such as population growth, as constants and then used the simulated precipitation value as an input for the future water quality simulation starting from the year 2016, i.e., immediately following 2015. Finally, we used MRICGCM3 with RCP_8.5 for the water quality simulation.

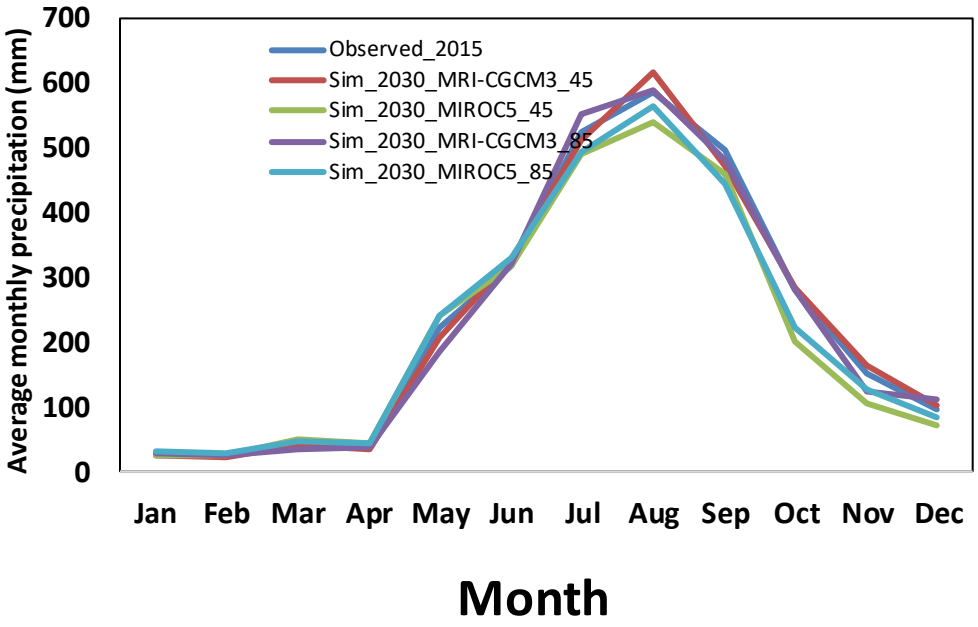

Figure 4.3.4. Graph comparing the current and future monthly rainfall as collected at the Science Garden meteorological station

4.3.3.2 Land cover change

The future land cover of 2030 as derived from two past satellites images showed an approximately 10% increase in built-up land (Figure 4.3.5). The main change was detected in northern part of the watershed in some cities of Rizal province, such as Rodriguez; the urbanization of this region will be significant in the future, as observed in Figure 4.3.6. The dynamic economic growth in Metro Manila can lead to rapid urbanization with both negative and positive consequences; indeed, megacities can provide significant employment, business, educational and cultural opportunities. For this reason, urban demographic growth will be high due to migration from rural areas; in fact, rural populations migrate to improve livelihoods and benefit from better services in urban areas (UN-HABITAT and ESCAP, 2010). However, due to a lack of appropriate infrastructure and adequate housing systems, a large number of informal settlements and slums have developed in areas that are not suitable for building such as along large rivers or in floodplains, which can increase the vulnerability of people and infrastructure in urban areas.

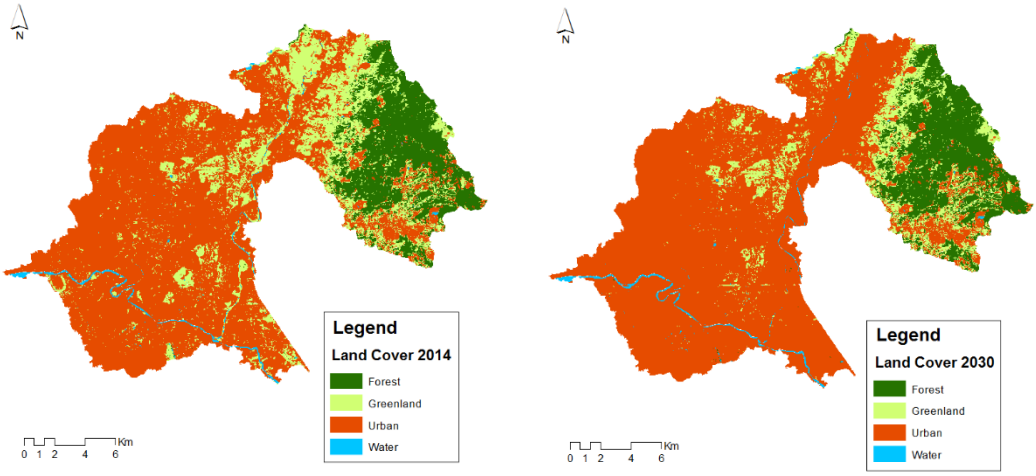

Figure 4.3.5 Land cover change map

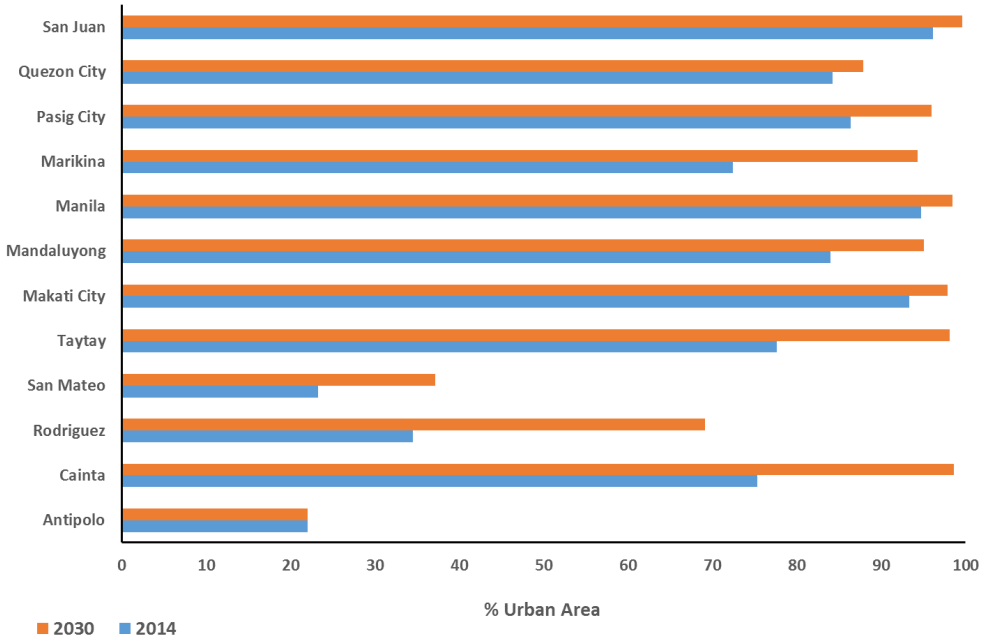

Figure 4.3.6 Land cover change by city

4.3.3.3 Urban flooding

Hydrologic simulation enabled the peak discharge generated from the upper catchment region to be estimated. Figure 4.3.7 provides a comparison of the peak discharge under current and future conditions considering climate change and flood storage, and it is obvious that climate change will greatly increase flood discharge from the upper catchment. A storage of 75 MCM in the upper region was found to be largely effective in reducing peak discharge, and this will enable a significant reduction in flood inundation. The effect of the projected climate change (moderate) in 2030 could increase peak discharge at Montalban by 30%, i.e., from 4,000 m^3/s to 5,300 m^3/s, for the 100-yr return period. Table 4.3.5 provides the extent of flood inundation under different conditions. At the

NCR boundary, the flood depth is high in the upper Marikina River, while the inundated surface area and depth of flow is decreased in the lower Marikina River due to the Manggahan Floodway. Although the Manggahan Floodway diverts the flood water toward Laguna de Bay, it is important to note that some areas alongside the Pasig River still become submerged, and the main part of Manila city has also suffered from flooding. Usually, when the water level exceeds 1.5 meters, people are subject to increased danger due to the destruction of buildings.

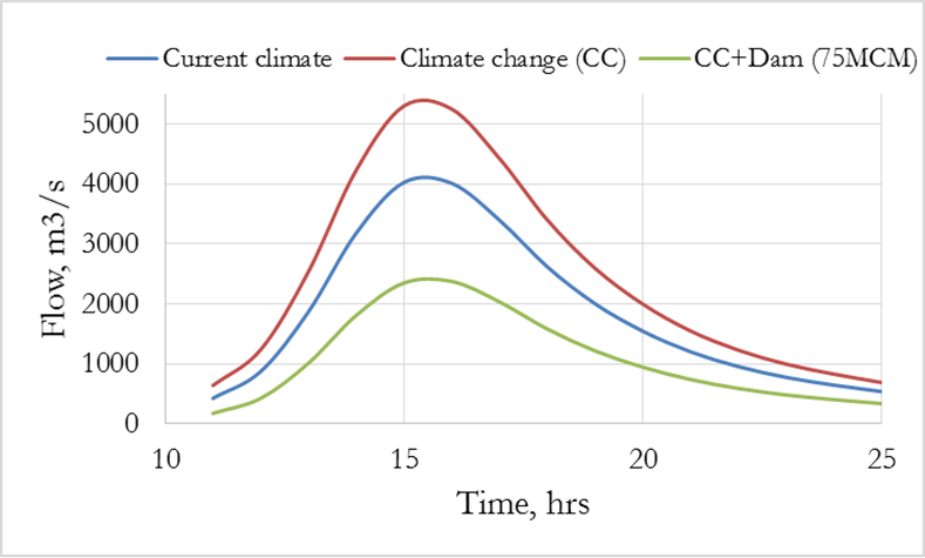

Figure 4.3.7. Comparison of hourly simulated flow at Montalban under current and future conditions

Table 4.3.5. Extent of flood inundations under current and future conditions

Flood hazard (>1.5 m)	Current	CC (extreme)	CC (extreme) + measures	CC (moderate)	CC (moderate) + measures
Inundation area (km^2)	39.12	83.41	33.28	76.07	20.8
% Change		113%	-15%	94%	-47%

Increasing flood inundation in the future underscores the need to improve flood management systems as part of the sustainable development of urban water environments. This study found that combinations of countermeasures (e.g., dams) can reduce additional inundation caused by climate change. Simulations incorporating such combinations found that dams can be highly effective in decreasing flood inundation by approximately 50%, and pumping flood water could be a better alternative in reducing inundation of low-lying regions. Inundation simulations revealed that improving river systems, controlling floods in the upstream of the Marikina River and diverting excess water from the river could protect the vulnerable area of Metro Manila city. Watershed

management as a whole, and infrastructure improvements in particular, are crucial for reducing the flood risks to Metro Manila.

4.3.3.4 Direct flood damage

In this work, flood risk was analyzed for the Pasig-Marikina-San Juan River basin. Flood damage was evaluated at the grid cell-scale of 100 x 100 m, and maps were generated and classified in GIS environment based on the impact of flood depth on losses, as illustrated in Figure 4.3.8. Significant increases in loss will occur due to the impact of future global changes, and the results showed that damage may increase by 212%. However, the simulated flood adaptations and mitigation measures revealed that the flood losses could be reduced by 35% compared to the current situation.

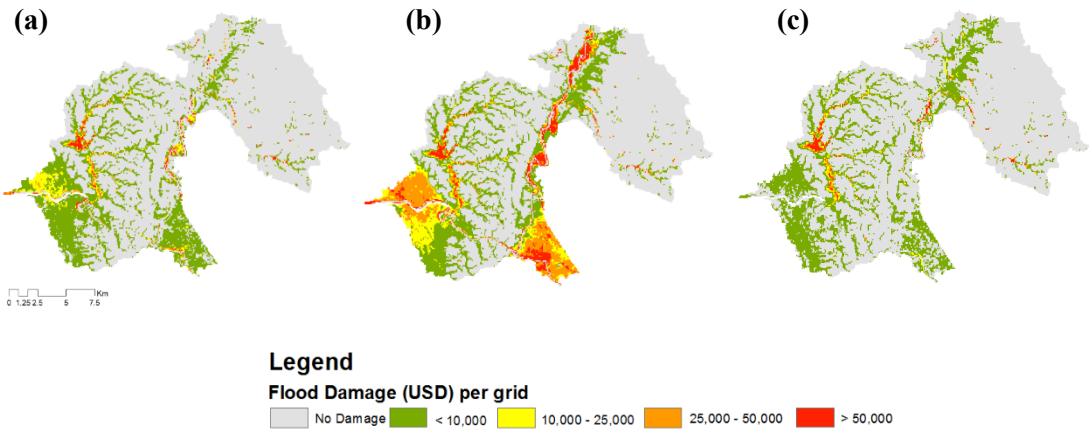

Figure 4.3.8. Spatial distribution of flood damage (Pasig-Marikina-San Juan). (a) The current situation without the effect of climate change, (b) business-as-usual scenario, and (c) with-mitigation scenario.

Flood damage mapping showed that Manila, Pasig, Taytay, and Cainta as well as some parts of Rodriguez and San Mateo are the most susceptible cities in the study area. Moreover, the damages were attributed to the magnitude of the hazard (water depth), the level of exposure (assets located in threatened areas) and vulnerability parameters. In fact, as highlighted in Figure 4.3.9, flood damage in some cities, such as Cainta or Manila, is correlated with the level of water depth, but in other cities, such as San Mateo and Rodriguez, urbanization can be a relevant factor in the growth of flood risk with or without mitigation. Due to urbanization, permeable soil will be replaced by impervious surfaces such as roads and buildings that will reduce infiltration and increase runoff. Consequently, more severe floods are occurring more frequently (Rafiei Emam et al., 2016). Finally, some cities located along the river are more susceptible to flooding, so flood damage is more important in areas such as Marikina and San Juan.

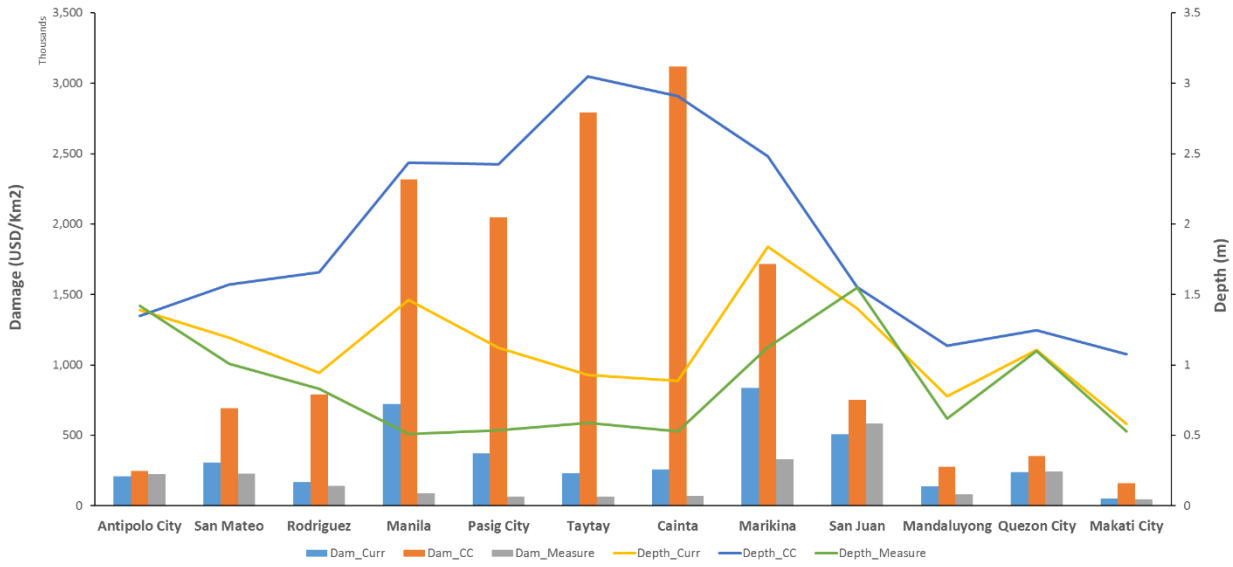

Figure 4.3.9. Flood damage by city

Climate change combined with the unplanned expansion of built-up areas can increase the vulnerability of urban areas to flooding and, therefore, the economic damage, so the adopting appropriate flood countermeasures is required, as presented in this study. For this reason, local decision makers should emphasize flood adaptation and mitigation measures for sustainable urban development, and several parameters, such as climate and land use change, should be considered in the design and implementation of these strategies.

4.3.3.5 Water quality

Model performance evaluation

Before the future scenario analysis was conducted, the performance of the WEAP simulation was validated using observed and simulated values of hydrological and water quality parameters. In the case of the hydrology module validation, the parameters (mainly effective precipitation and runoff/infiltration) were adjusted using the trial and error method during the simulation to reproduce the observed monthly stream flows for the 2011 to 2014 period (Table 4.3.6), and the final best-fit values for the two parameters were 96.5% and 55/45, respectively. Figure 4.3.10 (a) compares the monthly simulated and observed stream flows at Jones Bridge and shows that they largely match for most months with a correlation coefficient (R^2) ≅ 0.80, a root-mean-square error (RMSE) ≅ 0.25, and an average error of 7%. In contrast, the water quality simulation was validated by comparing simulated and observed BOD concentration at the Jones Bridge location; the selection of this location and time, i.e., the year 2011, was made based on the consistent availability of observed water quality data. The results revealed a strong relation between these two parameters (Figure 4.3.10 (b)) (with an error of 8%), confirming the suitability of the model performance in this problem domain.

Table 4.3.6. Summary of parameters and steps used for calibration

Parameter	Initial Value	Step
Effective precipitation	100%	±0.5%
Runoff/infiltration ratio	50/50	±5/5

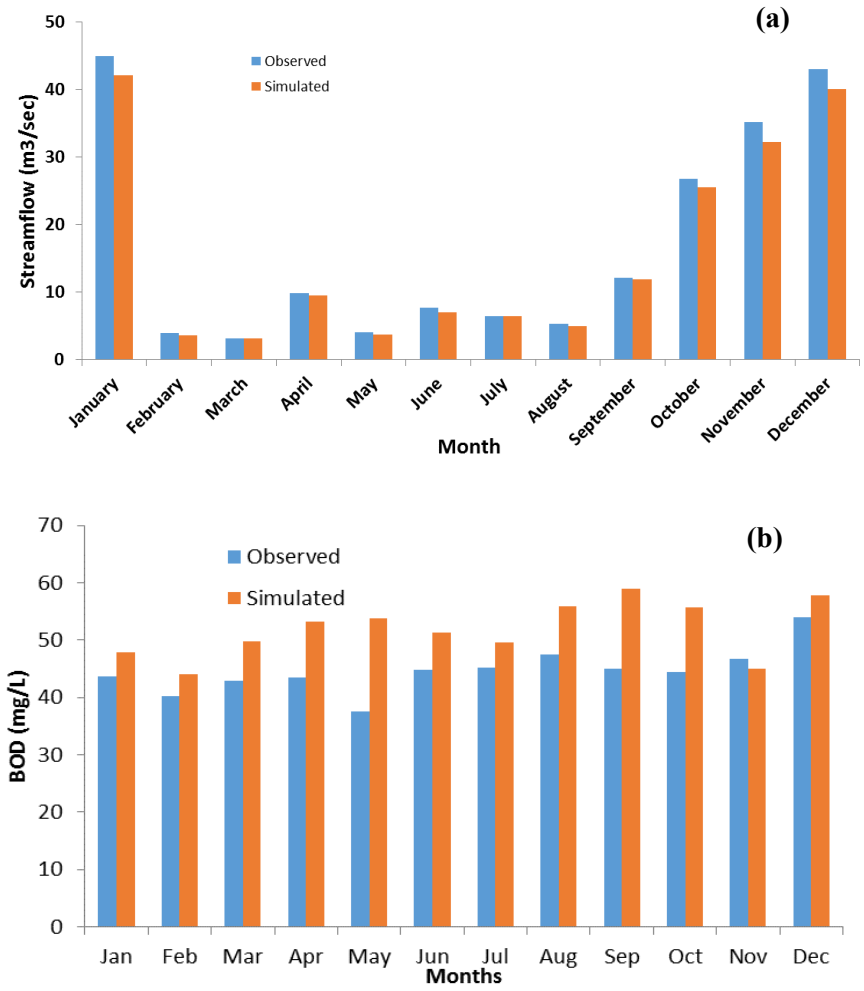

Figure 4.3.10. Validation of the model output by comparing simulated and observed (a) average monthly river discharge for the 2011-2014 period and (b) BOD values for 2011 at Jones Bridge

Scenario analyses

Future simulations of selected water quality parameters and total water demand were performed for the years 2015 and 2030, considering a business-as-usual scenario and scenarios involving possible countermeasures to predict the future water quality environment.

For water quality, the simulation was conducted using two possible scenarios, as shown in Table 4.3.7, for the years 2015 and 2030 using 2011 as reference year and considering population increase and land use change as well as wastewater generation and its treatment at wastewater treatment facilities. Once the model was calibrated, water quality parameters were simulated at the monthly scale for the year 2015, i.e., the current situation. Here, all existing WWTPs were considered along

with projected rainfall, and once the simulated values of the water quality parameters were compared with the observed values at each spatiotemporal scale, we found significant correlations (statistically supported by different R^2 and RMSE values) between these observed and simulated results. First, under the business-as-usual scenario, the effects of population growth and climate change on water quality were observed using the average values of two GCMs and two RCPs while keeping the capacity of all the existing wastewater treatment plants (42.5 MLD) constant until the year 2030. Here, small bars show the ranges of the simulated water quality values because of the change in the GCMs and RCPs. For the scenario with measures, all conditions were kept the same as for the first simulation except the wastewater plant capacity and collection rate were increased, as shown in Table 4.3.7.

Table 4.3.7. Summary of all criteria considered for the different future water quality simulation scenarios

Scenario	Components
Business as usual	Climate change + population growth +WWTP of 42.5 MLD
With measures	Climate change + population growth +WWTP of 612 MLD (100% collection rate)

The simulated water quality results using three parameters (namely, BOD, NO_3, and *E. coli*) under the business-as-usual and with-measures scenarios are shown in Figures 4.3.11 and 4.3.12, respectively. Based on the water quality parameters, a general trend of deteriorating water quality from upstream to downstream was found because of the cumulative addition of anthropogenic inputs. Additionally, when comparing the current water quality situation of the Pasig River with the desirable Class C water quality standard given by DENR, i.e., Fishable Class (i.e., BOD < 7 mg/L, NO_3^- 7 mg/L), most of the sampling locations were found to not be suitable in many sectors. More precisely, most water samples were safe in terms of NO_3 except those taken from the Manila Bay and Jones Bridge locations. The BOD value varied from 30 to 146 mg/L, clearly indicating that all of the water samples were moderately to extremely polluted; the reference BOD value required for the fishable category, i.e., Class C, according to national water quality standards (Philippines) is 7 mg/L. In the business-as-usual scenario, the concentrations of water quality parameters became even worse compared to the current condition, and this can be attributed to changes in weather conditions (with relatively higher rainfall during the rainy period and less rainfall during dry periods) coupled with additional amounts of wastewater generated by the increased population and rapid urbanization.

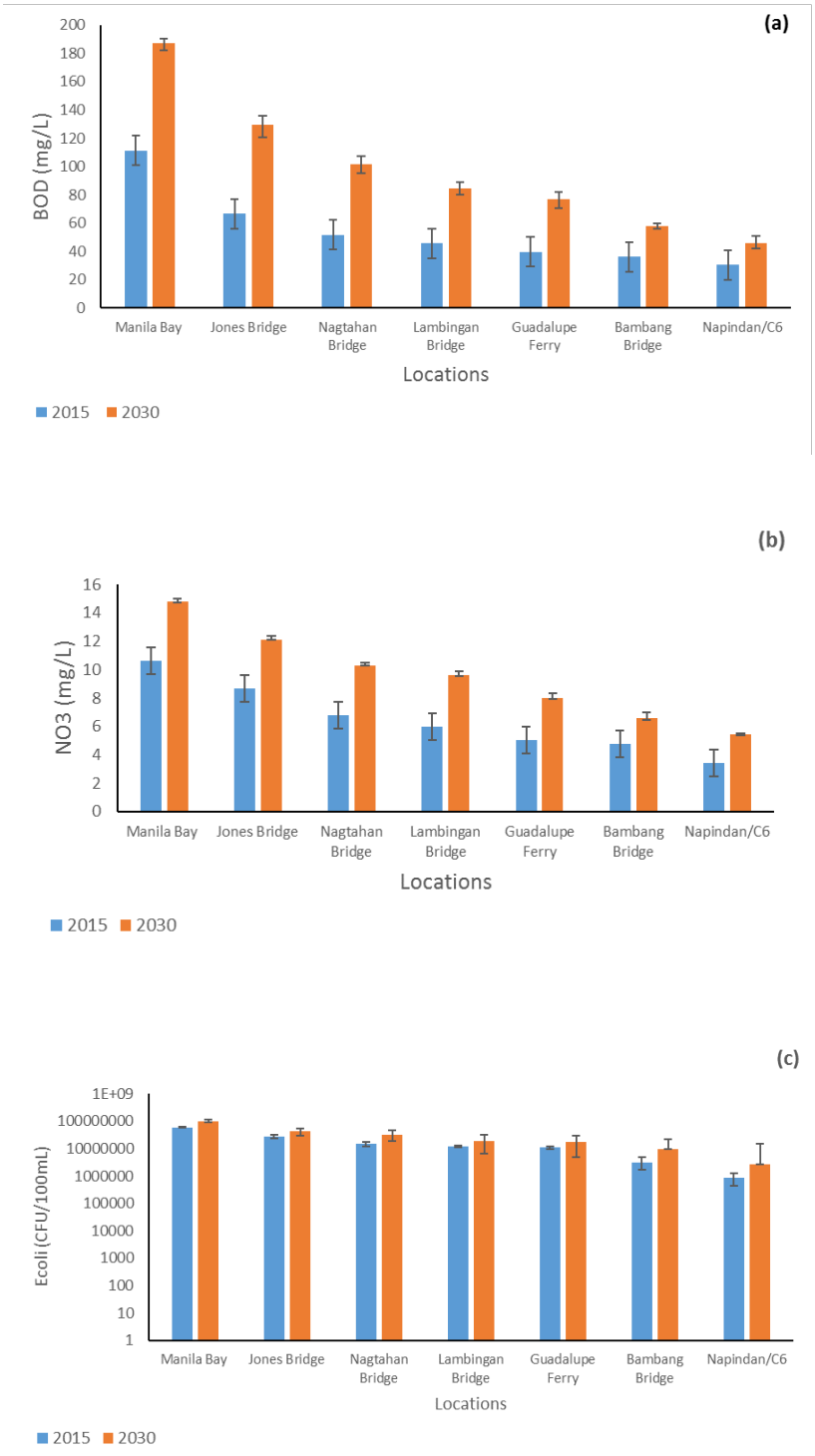

Figure 4.3.11. Simulated water quality: (a) BOD, (b) NO3, and (c) *E. coli* considering population growth, average climate change and a WWTP with a capacity of 42.5 MLD (without a master plan)

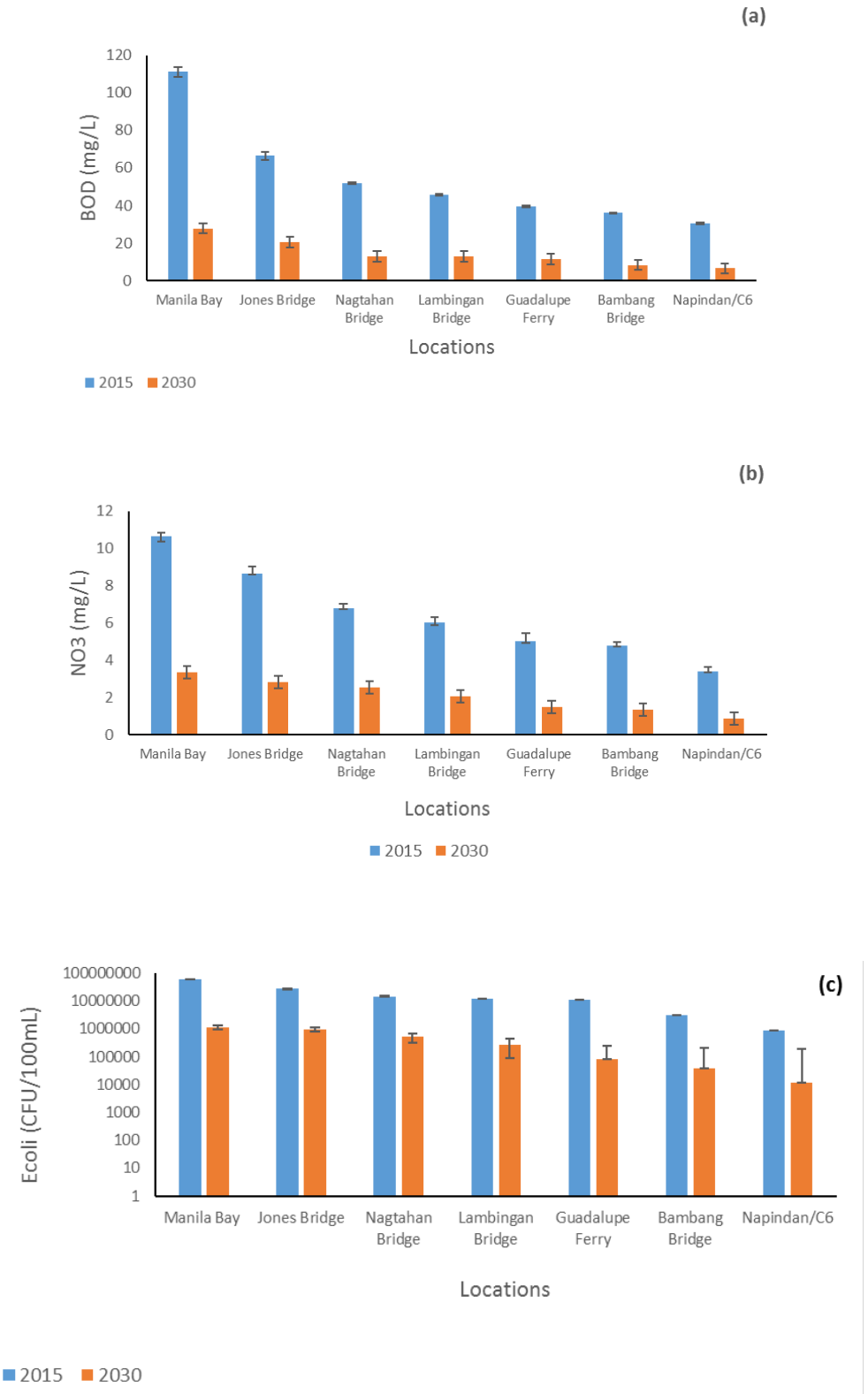

Figure 4.3.12. Simulated water quality: (a) BOD, (b) NO_3, and (c) *E. coli* considering population growth, average climate change and a WWTP with a capacity of 612 MLD (with a master plan)

The results from the scenario with measures revealed the water quality of the river system under the implementation of the current existing master plan for wastewater treatment, and it was clearly indicated that enhancing the capacity of the wastewater treatment facility by 612 MLD will improve water quality by many folds, which is encouraging. After the implementation, the average removal efficiencies achieved for BOD, NO_3 and *E. coli* would be 85%, 78% and 98%, respectively. However, considering the DENR water quality standards, many of the locations, especially those along the downstream, will not comply with Class C (fishable). Higher concentrations of nitrate indicate the influence of untreated sewerage input.

4.3.3.6 Economic benefit of improving urban water quality

There is clear interest in improving the quality of the surface water in the waterbodies of Manila according to those who placed monetary value on the service; 71% of the respondents indicated a willingness to support the proposed Surface Water Quality Improvement Program in Metro Manila. Among the 29% of the participants who voted against the proposed action plan, the most common answers were "Do not want to place monetary value" and "Objected to way question was presented"; these were considered protest (zero) answers in addition to the true WTP = 0 and thus excluded from further analysis. A maximum threshold of 5% of the income level was selected to accept the stated WTP.

The majority of the survey participants (84%) had visited or seen the rivers/lakes/canals in the city in the preceding month. Among these respondents, 45% went regularly; 34% went a few times; 6% went once; and 15% preferred not to answer this question. The majority of respondents (86%) answered that the water quality of the city's waterbodies is not sufficiently acceptable for recreational activities; 12% stated otherwise (that the water quality is sufficient); and 2% did not know whether or not the water quality was sufficient.

The socioeconomic data of respondents are given in Figure 4.3.13, and as seen from the graphs, the socioeconomic backgrounds of the respondents were representative. The employment status indicated that most of the survey participants were occupied with a full-time job (29%) or self-employed (28%). Only 9% were unemployed, and 17% were nonworking students. Most of the individuals interviewed were educated people; only 1% of respondents had not attended any form of school.

Male respondents composed the majority in our survey (51%) followed by female (43%) and unspecified (6%) participants. Middle-aged people dominated the survey (40%) while 36% were represented by the younger generation (below 25 years old), and only 5% were elderly people (61 and over). More than half of all respondents were married; one-third were single; and only 6% were divorced or separated.

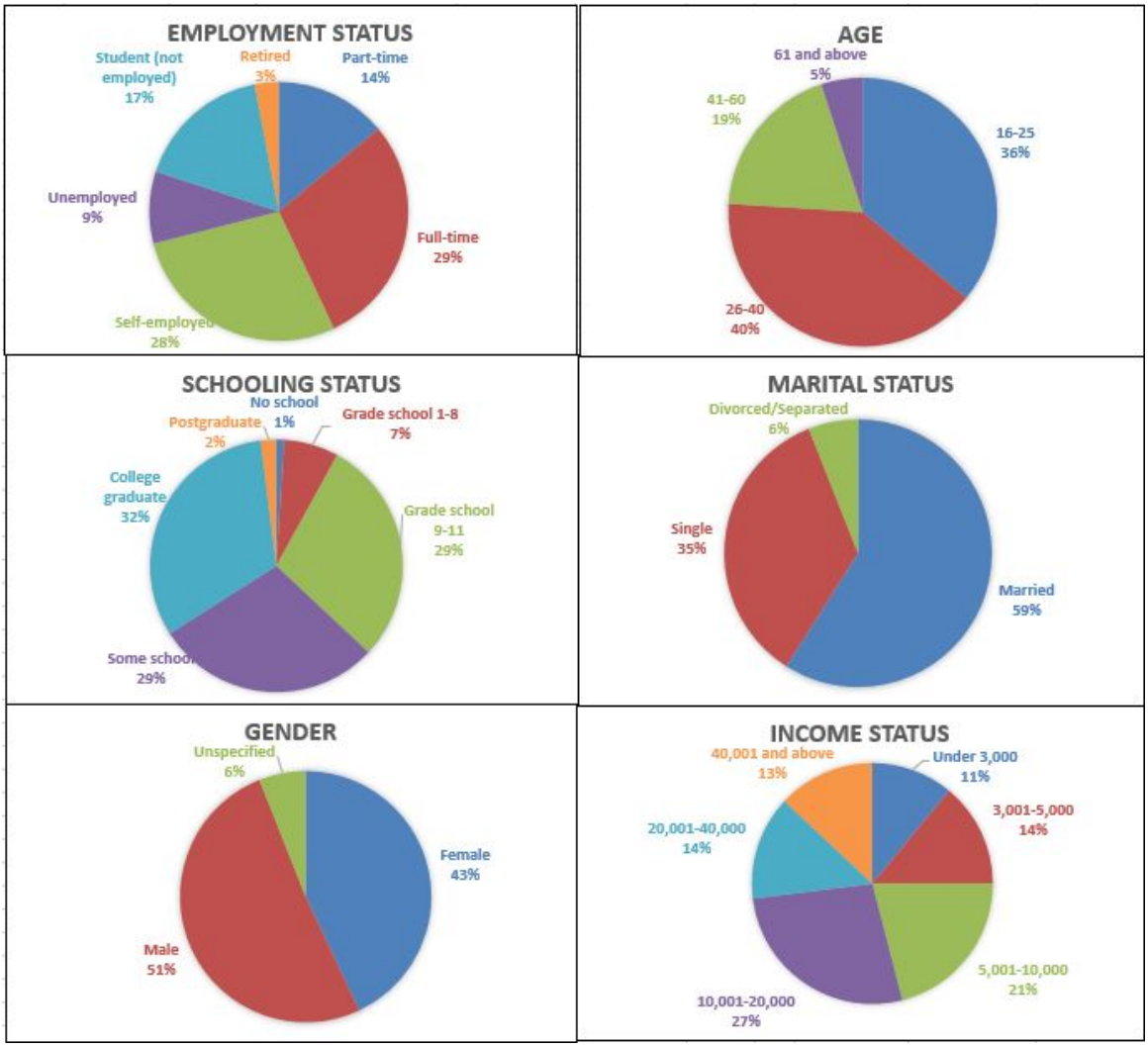

Figure 4.3.13. Socioeconomic profile of the sample (Metro Manila city study)

The willingness-to-pay for swimmable water quality (which is a higher water quality) ranged between zero and PHP 1,200 (USD 25.52) per person per month, with the average rate for implementing the proposed program being equal to PHP 10,298 (USD 12.18). The WTP for fishable water quality was between zero and PHP 1,000 (USD 21.27) per month with an average of PHP 10287 (USD 21.17). The estimated mean per capita nonuse WTP for swimmable water quality was equal to PHP 191.64 (USD 3.67) and to PHP 150.38 (USD 2.88) for fishable water quality. It should be mentioned that the questionnaire clearly stated that the payment vehicle for the use WTP would be a monthly amount added to the existing utility bill while the nonuse WTP would be charged only once; this explains why the nonuse WTP was higher than the use WTP.

The total benefits for Metro Manila can be estimated from the average WTPs for two water quality categories (PHP 102.44 and PHP 102.39). The total population of Metro Manila aged 15-60 was 7.685 million in 2011 (PSA, 2011), which implies that the value of the potential total benefits received from improved water quality under a given scenario may be within the limits of PHP 9,443 billion to PHP 9,447 billion (USD 190 million) per year.

4.3.3.7 Floodwater-borne infectious diseases

The simulated risk of floodwater-borne gastroenteritis under the three scenarios, expressed as the number of gastroenteritis cases caused by noroviruses per grid, is shown in Figure 4.3.14. The purple grids represent high-risk areas (more than 0.1 cases per grid); the orange represent medium risk (0.01 – 0.1 cases per grid); the yellow represent low risk (less than 0.01 cases per grid); and the white represent no risk (areas with no flooding). Under the current scenario, the risk was high in the downstream of the Pasig River and the San Juan River located in the southwest of the study area. In the business-as-usual scenario, additional high-risk areas were observed along the Marikina River (middle of the study area), but in the with-mitigation scenario, there were no grids with more than 0.1 cases of gastroenteritis by noroviruses. However, the high-risk areas differed from those in the flood analysis. Although the probability of causing disease depends on the severity of flooding (i.e., related to the maximum depth), the number of disease cases is also affected by the population in each grid, so the high-risk areas were clustered where severe flooding was expected and where the population density was high. The total number of cases of gastroenteritis caused by noroviruses was 1,007 under the current scenario, which was the highest among the target cities. This was partly due to the high population in the Manila target area (6,605,791 in total) but also because of the severe flood inundation and water pollution. The number was projected to increase by 151% by 2030 if no measures were taken to reduce urban flooding and water pollution (business-as-usual scenario, 2,528 cases in total), which clearly demonstrated that population growth and the change in precipitation significantly increased the risk of flood-related infectious gastroenteritis. Thus, we urge stakeholders to act to reduce the risk of flood-related infectious diseases. When the countermeasures for reducing urban flooding and water pollution were included in the analysis, the total cases were reduced substantially to 23, a 99% decline compared to the business-as-usual scenario. This indicated that taking measures on water management would also protect citizens from floodwater-borne infectious diseases.

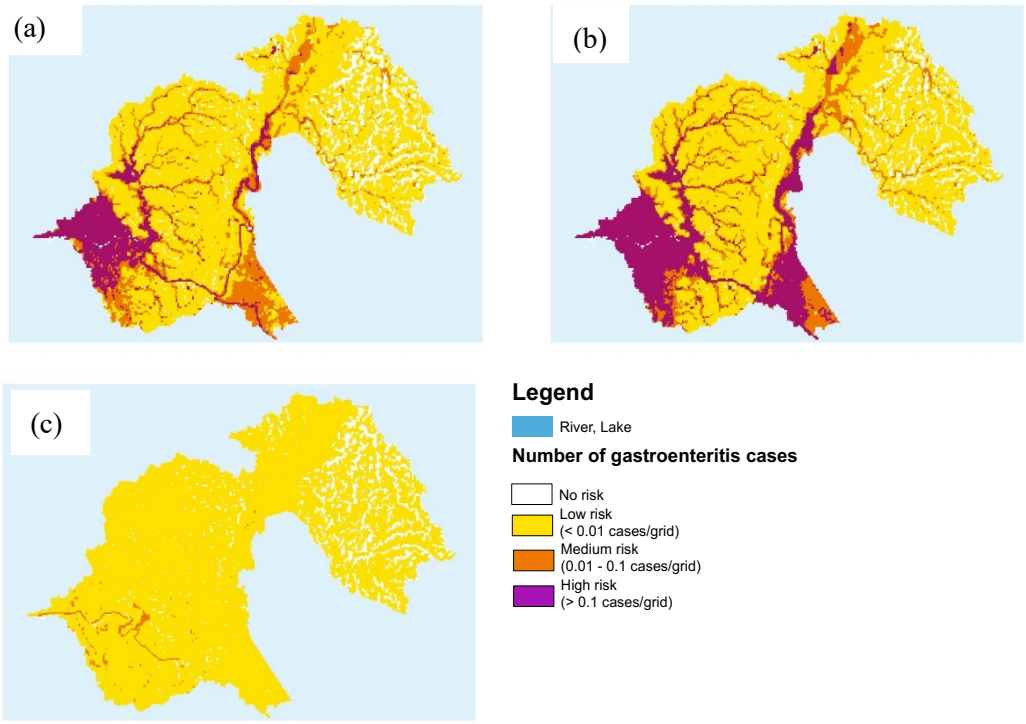

Figure 4.3.14. Simulated health risk (number of gastroenteritis cases due to noroviruses in floodwater) for Manila under a) the current scenario, b) the business-as-usual scenario, and c) the with-mitigation scenario.

4.3.3.8 Low-carbon technology in wastewater facilities

Information collected for existing and planned wastewater management facilities

Figure 4.3.15 shows the location of existing and planned WWTPs in the target area, and their capacities and site areas are summarized in Tables 4.3.8 and 4.3.9, respectively.

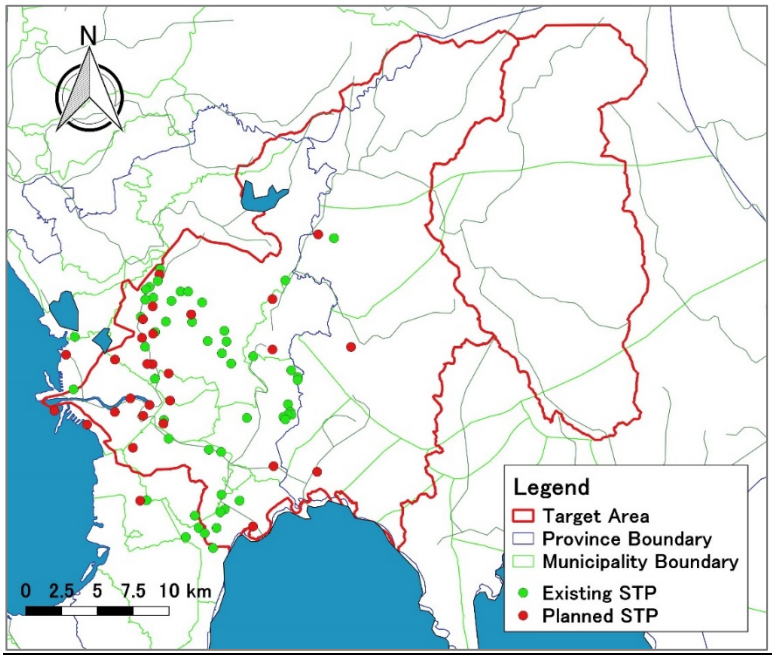

Figure 4.3.15. Location of existing and planned sewage treatment plants in the target area in Manila

Table 4.3.8. Capacity of the existing WWTPs in the target area in Manila

WWTP	Capacity of existing WWTP (m^3/d)	Site area (m^2)
Tondo	432,000	254,880
Makati South	40,000	23,600
Dagat dagatan	26,000	15,340
Others (41 WWTPs in total)	100,070	59,041
Total	598,070	352,861

Table 4.3.9. Capacity of the planned WWTPs in the target area in Manila

WWTP	Capacity of planned WWTP (m^3/d)	Site Area (m^2)
Ilugin (Pasig North and South)	120,000	70,800
Marikina North	100,000	59,000
Taguig North	75,000	44,250
Others (32 WWTPs & 2 SpTPs in total)	623,030	367,588
Total	918,030	541,638

Calculation of GHG emissions reduction

Since some of the low-carbon technologies could not be applied to estimate GHG emissions due to a lack of data, four technologies were examined as described below: Tool 1) introduction of high-efficiency pumps, Tool 2) introduction of high-efficiency blowers, Tool 3) installation of a biogas power generation system, and Tool 4) introduction of a solar power system.

Tool 1. Energy saving by introducing high-efficiency pumps in wastewater treatment plants

In calculating the reduction in GHG emissions, EC_{lp} (annual power consumption of the low-carbon technology pump) is generally obtained by monitoring the pumps to be installed, but since this assessment targets the planning phase, available data, such as the low-carbon instruments stated in the master plans or those available on the market, were used to estimate EC_{lp}. Additionally, the general specifications of the projected pumps, which are commonly installed in the WWTPs of the target cities, were employed to calculate their power consumption.

- Data and parameters

Table 4.3.10 summarizes the data necessary for calculating the reduction in GHG emissions using Tool 1.

- Calculation of GHG emissions reduction (ER)

Based on the data collected and calculated above, the amount of GHG emissions reduction due to the introduction of Tool 1 is estimated as follows.

$$ER = ME - LE = 1{,}805\ tCO_2/year$$

Table 4.3.10. Data used for energy saving by introducing high-efficiency pumps (Tool 1) for Manila city

Parameter	Value	Remarks
FE_{EL}: CO_2 emission factor	0.6032 tCO_2/MWh	Grid Emission Factors, Institute for Global Environment Strategies (https://pub.iges.or.jp/)
$\eta_{M/P}$: MP pump efficiency	53%	Nominal value of conventional pump
η_{Pj}: Low-carbon technology pump efficiency	85%	Nominal value of energy-saving pump
Size of pumps to be installed	3,500 m^3/hour of capacity with 63 kw of power consumption	-
Hours of operation per year	129,951 hours/year	Annual treatment capacity of the existing and planned pump/capacity of pump to be installed = 454,830,000/3,500
EC_{lp}: Power consumption of the low-carbon technology pump per year	8,187 MWh/y (existing pumps: 3,230 MWh/y, planned pumps: 4,957 MWH/y)	EC_{lp} = Hours of operation per year * power consumption of pump to be installed = 129,951* 0.063
ME: MP emissions per year	7,920 tCO_2/year (existing pumps: 3,124 tCO_2/year, planned pumps: 4,796 tCO_2/year)	ME = ECpp * $\eta_{pj}/\eta_{M/P}$ * FE_{EL}= 8,187 * 0.85/0.53 * 0.6032
LE: Low-carbon technology emissions per year	6,115 tCO_2/year	LE = ME of existing pumps + ECpp of planned pumps* FE_{EL} = 3,124 + 4,957 * 0.6032

Tool 2. Energy Saving by Introducing High-Efficiency Blowers

As shown in Figure 3.6, the consumption of electricity by a pump is 1/6 that of a blower, and this ratio was applied to calculate GHG emissions. However, the energy saving rate of the blower to be installed was assumed to be 10% considering the general specifications recent types of energy-saving blowers.

- Data and parameters

The data used to calculate the reduction in GHG emissions using Tool 2 are listed in Table 4.3.11.

Table 4.3.11. Data used for energy saving by introducing high-efficiency blowers (Tool 2) for Manila

Parameter	Value	Remarks
FE_{EL}: CO_2 emission factor	0.6032 tCO_2/MWh	Grid Emission Factors, Institute for Global Environment Strategies (https://pub.iges.or.jp/)
Rate of energy saving by introducing Tool 2	10%	Nominal value of energy-saving blower
Rate of power consumption of blower and pump	Power consumption of blower : Power consumption of pump = 6 : 1	According to Figure 3.6
ME: MP emissions per year	47,520 tCO_2/year (existing pumps: 18,746 tCO_2/year, planned pumps: 28,774 tCO_2/year)	ME = ME of Tool 1 *6
LE: Low-carbon technology emissions per year	44,643 tCO_2/year	LE = ME of existing pumps + ME of planned pumps * (1-0.1) = 18,746 + 28,774 * 0.9

- Calculation of GHG emissions reduction (ER)

Based on the data collected and calculated above, the amount of GHG emissions reduction due to the introduction of Tool 2 is estimated as follows.

$$ER = ME - LE = 2{,}877\ tCO_2/year$$

Tool 3. Installation of a Biogas Power Generation System

A biogas power generation system replaces the use of fossil fuel-based energy with renewable energy with zero emissions. Therefore, the reduction in the amount of GHG emissions due to the introduction of this technology could be considered to be equal to the amount of MP emissions. The detailed calculation is shown below.

- *Data and parameters*

Table 4.3.12 summarizes the data necessary to calculate the reduction in GHG emissions due to Tool 3.

Table 4.3.12. Data used for the installation of a biogas power generation system (Tool 3) for Manila

Parameter	Value	Remarks
FE_{EL}: CO_2 emission factor	0.6032 tCO_2/MWh	Grid Emission Factors, Institute for Global Environment Strategies (https://pub.iges.or.jp/)
Rate of volume of wastewater treatment and power generation	Daily treated wastewater (m^3/day): Power generation (MWh/year) = 40,000 : 1,380	Based on data from the Eniwa city wastewater treatment facility (http://www.city.eniwa.hokkaido.jp/www/contents/1366006820944/index.html)
Total amount of water treated daily by WWTPs in the target area	1,516,100 m^3/day	-
EG_{BI}: Electricity supplied by the grid to the WWTP area	52,306 MWh/year	-
EC_{BI}: Power consumption of the biogas plants	0 MWh/year	-
ME: MP emissions per year	31,551 tCO_2/year	$ME = EG_{BI} * FE_{EL}$
LE: Low-carbon technology emissions per year	0 tCO_2/year	$LE = EC_{BI} * FE_{EL}$

- *Calculation of GHG emissions reduction (ER)*

Based on the data collected and calculated above, the amount of GHG emissions reduction due to the introduction of Tool 3 is estimated as follows.

$$ER = ME - LE = 31{,}551\ tCO_2/year$$

Tool 4. Power Generation by Introducing a Solar Power System to Wastewater Treatment Plants

Like the installation of biogas power generation, a solar power system represents renewable energy with zero emissions, so the reduction in the amount of GHG emissions is equal to the MP emissions.

- Data and parameters

Table 4.3.13 shows the data used to calculate the GHG emissions reduction due to Tool 4.

Table 4.3.13. Data used for power generation by introducing a solar power system (Tool 4) for Manila

Parameter	Value	Remarks
FE_{EL}: CO_2 emission factor	0.6032 tCO_2/MWh	Grid Emission Factors, Institute for Global Environment Strategies (https://pub.iges.or.jp/)
Area required for power generation	20,000 m^2/MW	-
Hours of operation per day	8 hours/day	-
Days of operation per year	200 days/year	-
Ratio of the wastewater treatment capacity to the potential PV area in WWTP	Daily treated wastewater (m^3/day): Power generation (MWh/year) = 40,000 : 1,380	Based on the data acquired from the layout of Bay Mau WWTP, Hanoi, Vietnam
Total site area of WWTP	894,499 m^2	Same as above
Potential PV area	411,470 m^2	Site area of WWTP * 0.46 = 894,999 * 0.46
Electricity generated	20.57 MW	Potential area/required area for power generation = 411,470/20,000
Daily/annual hours of operation of the solar power system	8 hours/day, 1,600 hours/year	200 days/year
EG_{PV} = Electricity supplied by the grid to the WWTP are (MWh/year)	32,918 MWh/year	EG_{PV} = electricity generated * annual operational hour of the solar panel = 20.57 * 1,600
EC_{BI} : Power consumption by the solar power system	0 MWh/year	-
ME: MP emissions per year	19,856 tCO_2/year	ME = EG_{PV} * FE_{EL} = 32,918 * 0.6032
LE: Low-carbon technology emissions per year	0 tCO_2/year	-

- *Calculation of GHG emissions reduction (ER)*

Based on the data collected and calculated above, the reduction in the amount of GHG emissions due to the introduction of Tool 4 is estimated as follows.

$$ER = ME - LE = 19{,}856\ tCO_2/year$$

Emission Reduction by Introducing the Four Tools

In total, GHG emissions after the introduction of the abovementioned four (4) tools is 56,089 tCO_2/year, as shown in Figure 4.3.16. The findings indicate that the introduction of low-carbon technologies could reduce GHG emissions by 52.5%. Among the proposed technologies, the biogas power generation system is considered the most effective strategy for reducing GHG emissions as it accounts for 56% of the total.

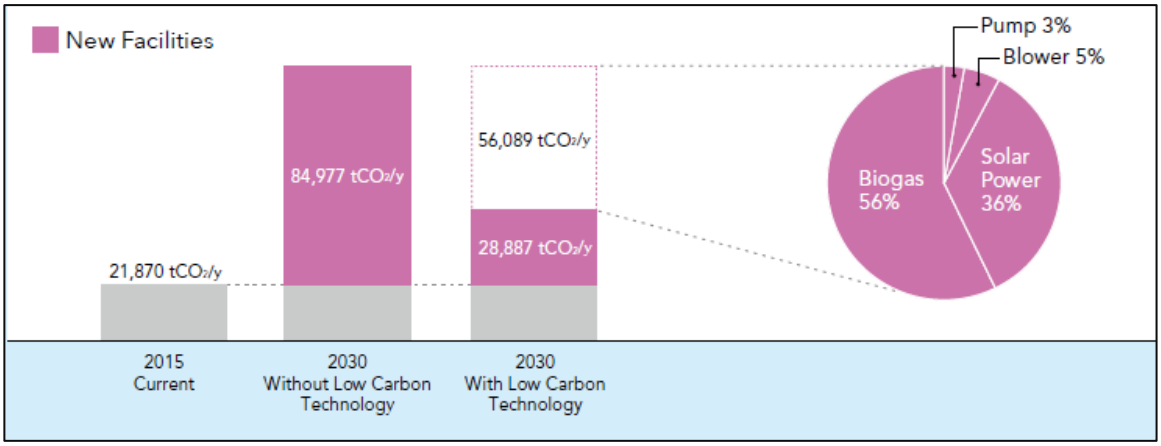

Figure 4.3.16. GHG emissions reduction through the application of low-carbon technologies, according to the master plan of Manila city

References

Clemente R.; Guillermo S.; Tabios Q.; Ramon P.; Abracosa C.; David C.; Inocencio A.B. *Groundwater Supply in Metro Manila: Distribution, environmental and economic assessment*; Discussion Paper Series No. 2001-06; Philippine Institute for Development Studies: Manila, Philippines; 2001.

Department of Environment and Natural Resources (DENR), *Updated sewerage and septage master plan. Vision for master plan for the year 2032 for Metro Manila*. Department of Environment and Natural Resources: Manila, Philippines; 2016.

Department of Environment and Natural Resources (DENR), Metropolitan Waterworks and Sewerage System (MWSS), and World Bank. *Updated Sewerage and Sanitation Master Plan for the Metropolitan Waterworks and Sewerage System*; Metropolitan Waterworks and Sewerage System: Quezon, Philippines; 2014.

Elshamy, M.E.; Seierstad, I.A.; Sorteberg, A. Impacts of climate change on Blue Nile flows using bias-corrected GCM scenarios. *Hydrol. Earth Syst. Sci*. **2009**, 13: 551–565.

Goyal, M.K.; Ojha, C.S.P.; Evaluation of linear regression methods as downscaling tools in temperature projections over the Pichola Lake Basin in India. *Hydrological Processes* **2011**, 25: 1453-1465.

Khan A.A.; Gaur R.Z.; DiamantisV.; Lew. B; Mehrotra, I; Kazmi A.A. Continuous fill intermittent decant type sequencing batch reactor application to upgrade the UASB treated sewage. *Bioprocess Biosyst. Eng.* 2013, 36: 627–634.

Kennedy, P. A. *Guide to Econometrics*, 3rd ed.; the MIT Press: Cambridge, MA; 1992.

Lagmay A.M.; Mendoza J.; Cipriano.F.; Delmendo P.A.; Lacsamana M.N.; Moises M.A.; Pellejera, N., III; Punay K.N.; Sabio G.; Santos L.; Serrano J.; Taniza H.J.; Tingin N.E. Street floods in Metro Manila and possible solutions. *J. Environ. Sci.* **2017**, 59: 39-47.

Maddala, G.S. *Limited-dependent and qualitative variables in Econometrics*; Cambridge University Press: Cambridge, UK; 1983.

Metropolitan Waterworks and Sewerage System (MWSS). *Updated sewerage and sanitation master plan for the metropolitan waterworks and sewerage system*; Berkman International Inc.; Tetra Tech, Inc.: Manila, Philippines; 2016.

National Disaster Coordinating Council, Republic of the Philippines. *Final report on Tropical Storm "Ondoy" {Ketsana} (Glide No. TC-2009-000205-PHL) and Typhoon "Pepeng" {Parma} (Glide No. TC2009-000214-PHL) (September 24-27 and September 30-October 10, 2009)*; 2009. http://www.ndrrmc.gov.ph/attachments/article/1543/Update_Final_Report_TS_Ondoy_and_Pepeng_24-27SEP2009and30SEP-20OCT2009.pdf

Philippine Atmospheric, Geophysical and Astronomical Services Administration (PAGASA). *Climatological Normals: Rainfall Normal Values (mm) 1981-2010*; 2011. http://pagasa.dost.gov.ph/index.php/climate/climatological-normals [Accessed in December 2014].

Philippine Statistics Authority (PSA). *2010 Census of Population and Housing Philippines*; 2011. https://psa.gov.ph/sites/default/files/attachments/hsd/article/Table%201_2.pdf [Accessed on 18th October, 2018]

Philippine Statistics Authority (PSA). *Philippine Yearbook. Demography*; Philippine Statistics Authority: Quezon City, Philippines, 2011.

Philippine Statistics Authority (PSA). *2015 Census of Population*; Republic of the Philippines; 2015.

Philippine Statistics Authority (PSA). *Provincial summary 2016*; Philippine Statistics Authority: Quezon City, Philippines. http://nap.psa.gov.ph/activestats/psgc/SUMWEBPROV-SEPT2016-CODED-HUC-FINAL.pdf

Rafiei Emam, A.; Mishra, B.K.; Kumar, P.; Masago, Y.; Fukushi, K. Impact assessment of climate and land-use changes on flooding behavior in the Upper Ciliwung River, Jakarta, Indonesia. *Water* **2016**, 8: 559.

Romali N.S.; Sulaiman M.A.K.; Yusop Z.; Ismail Z. Flood damage assessment: A review of flood stage–damage function curve. In *ISFRAM 2014: Proceedings of the International Symposium on Flood Research and Management*; Abu Bakar S., Tahir W., Wahid M., Mohd Nasir S., Hassan R., Eds.; Springer: Singapore; 2015.

Smith D.I. Flood damage estimation – A review of urban stage-damage curves and loss functions. *Water SA* **1994**, 20: 231 – 238.

United Nations Human Settlements Program (UN-Habitat); United Nations Economic and Social Commission for Asia and the Pacific (ESCAP). *The State of Asian Cities 2010/11*. United Nations Human Settlements Program (UN-Habitat): Nairobi, Kenya; 2010.

World Bank Group. *Philippines Urbanization Review, Fostering Competitive, Sustainable and Inclusive Cities, Full report, 2017*; World Bank Group: Washington DC, USA; 2017.

4.4 Chennai

4.4.1 Introduction

Chennai is the capital of the state of Tamil Nadu, which is located on the Coromandel Coast of the Bay of Bengal, and it is one of the largest cultural, economic and educational centers in South India. According to the 2011 Indian census, Chennai has a population of 7,088,000 in an area of 426 km^2, so it is the fifth largest city in India. Furthermore, the Chennai Metropolitan Area is one of the largest city economies in the country.

Chennai is located on the southeastern coast of India in the northeastern part of Tamil Nadu on the flat Eastern Coastal Plains. Its average elevation is 6.7 meters, and its highest point is 60 m. Two major rivers flow through the city, namely, the Cooum River through the center and the Adyar River to the south (Figure 4.4.1), and a third river called Kortalaiyar flows through the northern part of the city before draining into the Bay of Bengal at Ennore. The estuary of this river is heavily polluted with effluents released by the industries in the region, while the Adyar and especially the Cooum Rivers are heavily polluted with effluents and waste from domestic and commercial sources. Additionally, these river systems facing flooding issues almost every year. The Adyar River in south Chennai flows for 15 km in the city and 9 km in the metropolitan area. It enters Chennai at Nandambakkam, and in its journey to the sea, it transforms into a wide lagoon, the Adyar estuary, with many islands and large, sludge-filled backwaters. Chennai features a tropical wet and dry climate, and for most of the year, the weather is hot and humid. The hottest time is late May and early June, with maximum temperatures of 38–42 °C; the coolest part of the year is January, with minimum temperatures of 18–20 °C. The average annual rainfall is 1,400 mm, and the city receives most of its seasonal rainfall from the northeast monsoon winds from mid-September to mid-December. Recently, floods have hit Chennai city due to heavy rainfall in its environs; the Adyar (748 km^2) and Cooum Rivers (1,266 km^2) caused floods in Chennai due to high rainfall intensity.

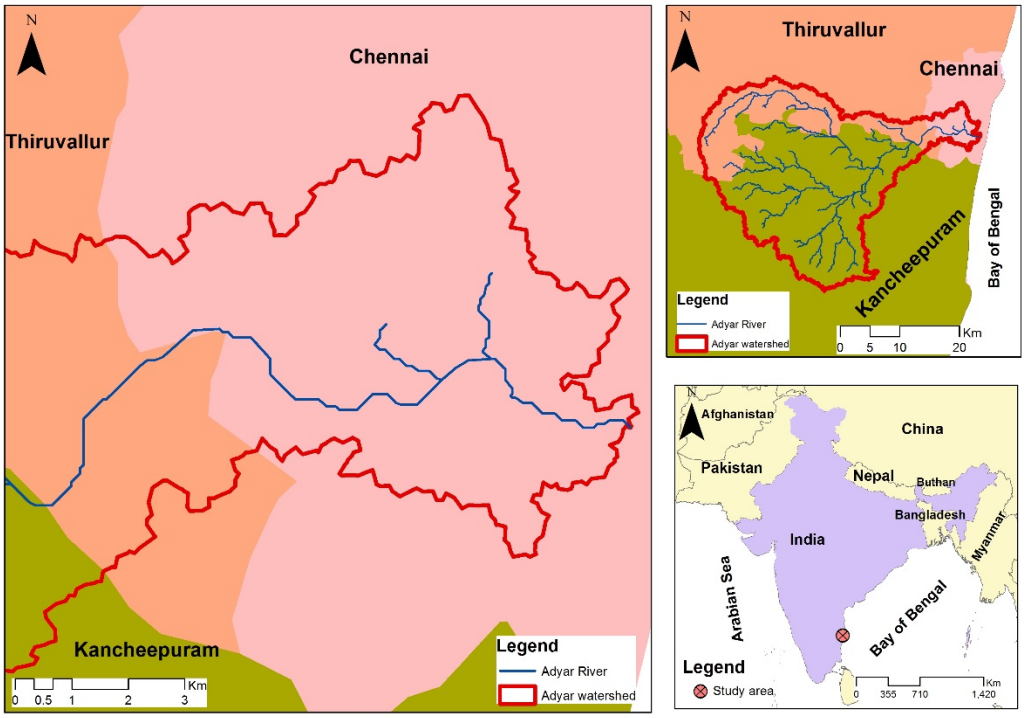

Figure 4.4.1. Map showing the course of the flow of the Adyar River passing across the south-central part of Chennai city

4.4.2 Methodology

4.4.2.1 Precipitation change

Chennai is characterized by a tropical wet and dry climate; the city receives most of its seasonal rainfall from the northeast monsoon winds from mid-September to mid-December. However, cyclones in the Bay of Bengal sometimes hit the city; the highest recorded annual rainfall was 2,570 mm in 2005. The northeast and southwest monsoons control the climate of the city. Historical rainfall was analyzed with an emphasis on flood and river pollution using 20 years of daily and monthly precipitation data (1985-2004) to understand the potential impacts of climate change, which is essential for informing both adaptation strategies and actions to avoid dangerous effects. This study involved a comprehensive assessment of the possible effects of climate change over the study area by using MRI-CGCM3 and MIROC5 GCMs with RCP 4.5 and RCP 8.5 emission scenarios. The future climate corresponded to the 2020-2039 period, and the rainfall analyses were concentrated over the Adyar River basin. Observation rainfall data from Chembarabakkam were compared with GCM outputs to ensure that the model could generate realistic values with respect to the present-day climatology of Chennai, and the model was further evaluated to quantify biases. The quantile mapping bias correction technique was applied to correct biases in the GCM rainfall projections, and Gumbel rainfall frequency analysis was applied to the bias-corrected rainfall data to estimate the daily maximum rainfall values for different current return periods.

To evaluate the effects of climate change on water quality, we evaluated the change in monthly average precipitation, and based on the rate of change in the observed historical rainfall values and downscaled future precipitation data, we estimated the average rate of increase through regression analysis. This growth rate was applied to current rainfall values to obtain future rainfall values. Statistical downscaling was followed by trend analysis, which is a less computationally demanding technique that enables bias reduction in the precipitation frequency and intensity (Goyal and Ojha, 2011), to calculate climate variables at the monthly scale.

4.4.2.2 Land cover change

Land cover maps were developed for Adyar River basin by using remote sensing products to identify the land cover categories and establish maps. Two Level 1 Landsat images were downloaded from the USGS website (https://earthexplorer.usgs.gov/) and utilized for the classification as indicated in Table 4.4.1. Land Change Modeler for ArcGIS was used to generate land cover for 2030 based on the past classification. In this work, land cover in 2005 and 2014 was used to predict land cover in 2030, and the maps were categorized by supervised classification, which is based on assigning pixel signatures to the determined classes. Due to the spatial resolution (30 m) of the Landsat images, it was quite difficult to establish a detailed LULC, so 4 classes were assigned, namely, built-up areas, water bodies, forest and green land.

Table 4.4.1. Satellite images applied

No.	Path/Row	Data Set	Acquisition Date	Scene Cloud Cover
1	142/051	Landsat 7 ETM+ C1 Level 1	16/09/2005	6%
2	142/051	Landsat 8 OLI/TIRS C1 Level 1	09/09/2014	4.88%

4.4.2.3 Population growth

To estimate the effect of population growth (one of our two key drivers) on water quality status, the entire study area was divided into different demand sites that mainly represent the populations of different cities on both sides of the Adyar River within our study area and that directly impact the river through the discharge of domestic sewerage water. The future population was estimated by the ratio method using projected growth rate data from UN DESA (2015). A total population of 5,196,533 was considered for the base year, i.e., 2013, in our study area, and for the future population projection, annual growth rates of 2.45% and 2.31% were considered for the 2012 to 2014 and 2015 to 2030 periods, respectively. Henceforth, the populations considered for the current year (2015) and target year (2030) were 5,446,829 and 7,672,113, respectively.

4.4.2.4 Flood inundation

Flooding occurs frequently in Chennai during the rainy season, causing enormous losses. Floods in 1976, 1985, 2005, and 2015 resulted in extensive inundation and induced considerable damage,

such as human deaths, evacuations, and infrastructure breakdowns. The recent flood in 2015 was triggered due to unprecedented rainfall in the catchment from 01 to 02 Dec 2015 that caused great inundation in Chennai city and its surroundings. Three major rivers flow through the city, namely, the Coum River through the center, the Adyar River to the south and the Kortalaiyar River through the northern part of the city, before draining into the Bay of Bengal. The waterways of the Chennai metropolitan region are not perennial and only receive flood discharge during the monsoon season; the rest of the year, they act as carriers of wastewater from sewage treatment plants and other sources. However, Chennai also has a geographical disadvantage; it is flat with many areas at sea level, which makes drainage challenging even under normal circumstances. When Chennai floods, there simply are not enough unobstructed channels into which the water can overflow. In this study, the issue of flooding was investigated with a focus on the Adyar River basin as it causes most of the flooding that is due to high rainfall intensity (Figure 4.4.2). Moderate and extreme climate change scenarios were assessed relative to the current conditions, and these future conditions were established by averaging the return period values of RCP 4.5 and RCP 8.5 estimates, respectively. Additionally, scenario analyses were carried out for channel improvement and water storage and diversion in line with the master plan of the Chennai Metropolitan Development Authority, Tamil Nadu, India (Chennai Metropolitan Development Authority, 2008). Because river discharges combine with urban floods (flooding due to high rainfall intensity within the city) to inundate the city, hydrological and hydraulic modeling were carried out to quantify flood discharges and inundation over the study area.

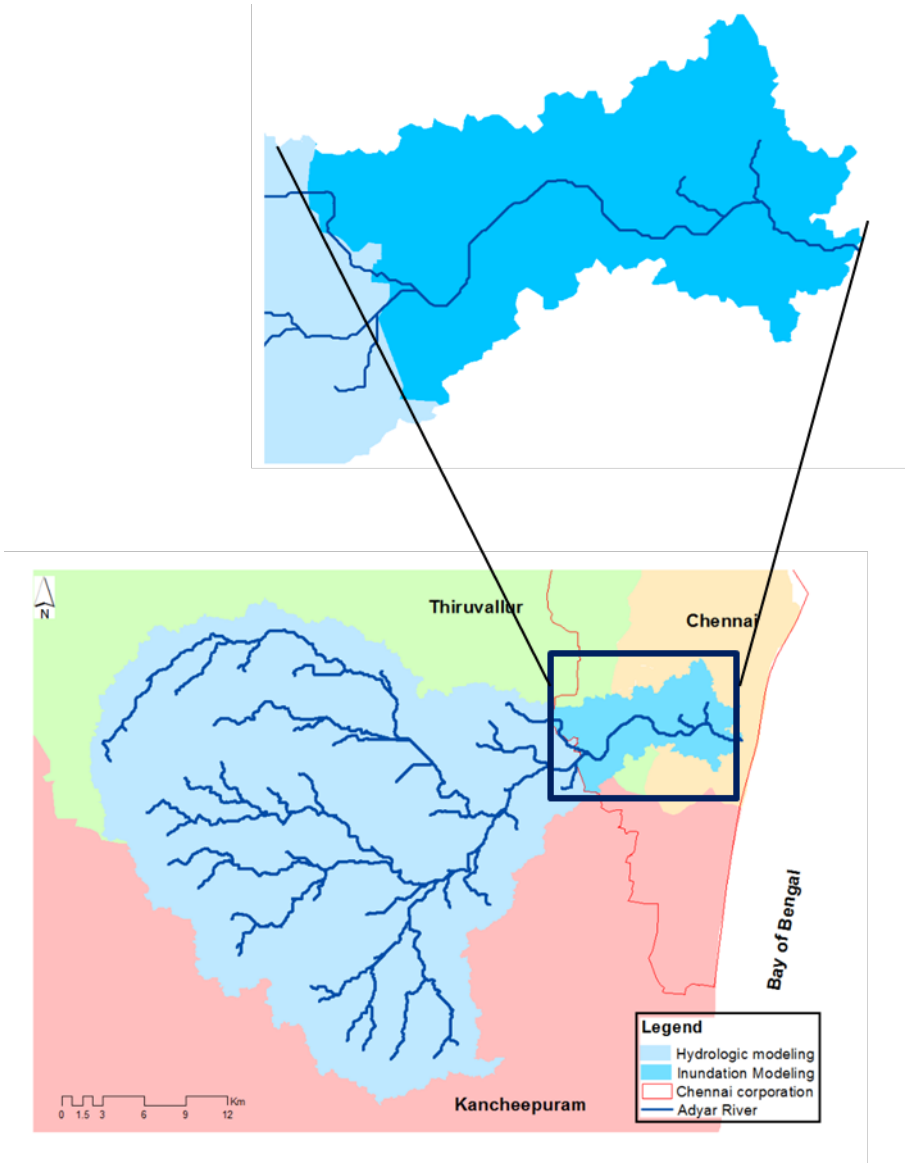

Figure 4.4.2. Adyar River basin, Chennai (total area: 871 km^2; inundation modeling: 65 km^2)

HEC-HMS hydrological modeling was performed to compute the peak discharge generated over the upper catchment region. Flood hydrographs were generated beginning at the Chennai Corporation boundary because the flood inundation was investigated over the Adyar basin within the corporation. Precise rainfall and discharge data for the catchment from the field to quantify the runoff and inundation during the flood event, which were needed to set up the hydrologic-hydraulic models, were largely lacking, so secondary and satellite-based reports were used to calibrate and validate the model. Flood inundation simulations were performed using a high-resolution (30 m derived from original 5 m-resolution data) processed Digital Surface Model, and river cross-section information was prepared from various reviews and reports. Longitudinal profiles and other topographic parameters were derived from the digital elevation data, while land cover information was largely based on Landsat images with a spatial resolution of 30 m. FAO soil data were used to derive textural information. Several countermeasures were tested that were in line with the second

master plan for the Chennai Metropolitan Area 2026 (Chennai Metropolitan Development Authority, 2008), which mentions some potential strategies such as the installation of two new tanks just above the Chembarambakkam tank to capture 1,570 million ft^3 of flood water, flood banks along the river, and pumps as well as flood diversions (10,000-15,000 Cusecs) from the Adyar River into the Covelong Valley, extension of the coverage of the drainage system, and updated design standards (to accommodate higher return periods).

4.4.2.5 Direct flood damage

To determine the tangible, direct flood damage, three main components were integrated in a GIS environment, namely, hazard, exposure and vulnerability. Flood damage was estimated for an urban portion of the Adyar watershed; more details about the approach and dataset are described in Section 3.5. For the flood damage analysis for Chennai, the flood damage depth function was based on research developed by (Huizinga et al., 2017), and the flood damage in the study area was then simulated for the current condition and two future scenarios. The simulations were conducted considering climate change and the implementation of flood control measures as explained in Section 3.4.

4.4.2.6 Water quality

Basic information regarding the model and data requirements

As explained in Section 3.6, the WEAP model was used to simulate future water quality variables in the year 2030 to assess alternative management policies for the Adyar River basin. For water quality modeling, a wide range of input data was available including point and nonpoint pollution sources, their locations and concentrations, past spatiotemporal water quality, wastewater treatment plants (Central Groundwater Board), population, historical rainfall, evaporation, temperature (Indian Metrological Department), drainage networks, river flow-stage-width relationships, river length, groundwater, surface water inflows and land use/land cover (State Water Board).

The WEAP model was developed for the Adyar River basin for four command areas with interbasin transfers. Hydrologic modeling requires that the entire study area be split into smaller catchments with consideration of the confluence points and physiographic and climatic characteristics (Figure 4.4.3). The hydrology module within the WEAP tool enables the catchment runoff and pollutant transport processes into the river to be modeled, and pollutant transport from a catchment accompanied by rainfall-runoff is enabled by ticking the water quality modeling option. Pollutants that accumulate on catchment surfaces during non-rainy days reach water bodies through surface runoff, and the WEAP hydrology module computes the catchment surface pollutants generated over time by multiplying the runoff volume by the concentration or intensity for different types of land use.

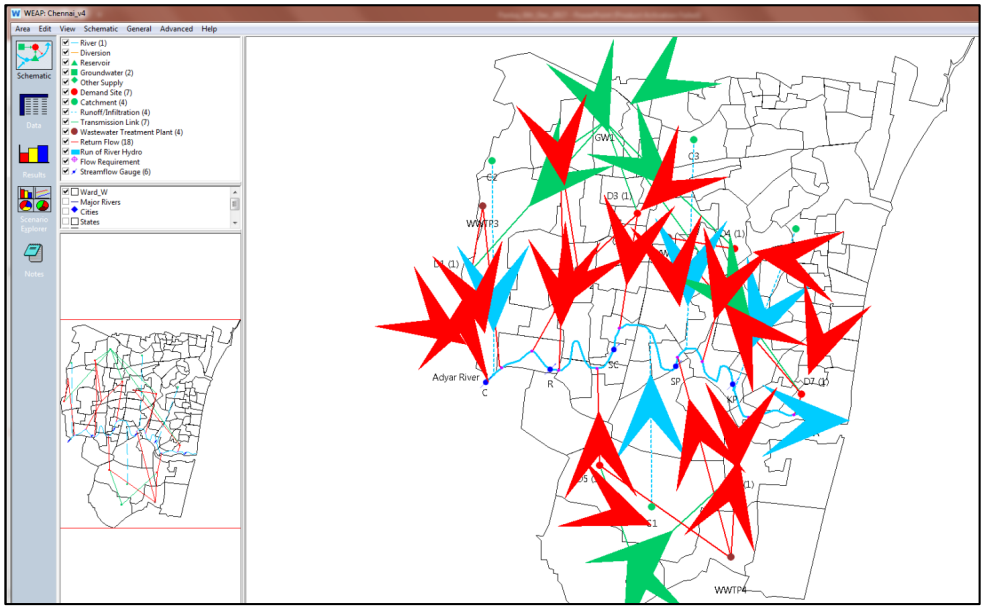

Figure 4.4.3. Schematic diagram showing the problem domain for water quality modeling in Lucknow using the WEAP interface

Daily rainfall was collected at Chembarambakkam meteorological station for the period from 1980 to 2016, and daily average stream flow data for 2011-2016 were measured at six stations, namely, Adyar, Kottupuram, Saidapet, Sanjay Colony, Ramapuram and Chembarambakkam, and then collected from the Indian Meteorological Department. These data were utilized to calibrate and validate the WEAP hydrology module simulation. Data for the water quality indicators of BOD and total coliform bacteria (which was later assumed to be equivalent to *E. coli* abundance) were also collected by Professor S. Mohan, IIT Madras, at Kottupuram, Saidapet, Sanjay Colony and Ramapuram for the years 2011-2015 and then used for water quality modeling.

The resulting population distributions and their future trends at these four command areas were calculated by the ratio method using the UN DESA projection rate, as explained in Section 4.2.2.3. Regarding the future precipitation data, different GCM outputs were used after bias correction, which is explained in detail in Section 4.2.2.1.

Model setup

The WEAP model was developed for the Adyar River basin for four catchment areas with interbasin transfers. To facilitate the hydrologic modeling, the above four catchment areas were split into six subcatchments with consideration of the confluence points and physiographic and climatic characteristics (Figure 4.4.3), and other major considerations in representing the problem domain were the seven demand sites and one wastewater treatment plant. These demand sites mainly represented the populations of different cities lying on both sides of the Adyar River within our study area that also directly impact the river through the discharge of domestic sewerage water. These dynamic attributes are described as functions of time and include population, and wastewater

treatment plants are pollution-handling facilities with design specifications that include total capacity and pollutant removal rates. The flow of wastewater into the Adyar River and its tributaries is mainly through domestic, industrial and stormwater runoff routes. Here, the UASB-SBR type of wastewater treatment plant was considered the default treatment technology in the modeling, and its treatment efficiency was assumed to be 94% for COD, 97% for BOD, 77% for TN and 99.69% for fecal coliform (Khan et al., 2013). No precise data were available regarding the total volume of wastewater production from domestic sources, so in the absence of such detailed information, the daily volume of generated domestic wastewater was estimated as 180 liters of average daily consumption per capita based on a literature review. Once model set up was completed, validation was performed using the simulated water quality result for the current situation, i.e., 2015 in this case. Thereafter, numerical simulation was conducted using different scenarios termed the business-as-usual scenario and the scenario with mitigation measures. For the business-as-usual scenario, the WWTP capacity was 180 MLD (total number = 4), whereas this capacity was 886 MLD for the scenario with mitigation measures, and the total number of proposed additional WWTPs by 2030 was 14 (total number = 18). Information on each object can be easily retrieved by clicking the corresponding graphical element, and the baseline year under the current reference scenario was 2013 in this study.

4.4.2.7 Economic benefit of improving urban water quality

The actual survey was preceded by the collection of background data and information and an extensive literature review in Tokyo in winter 2017 to better understand the situation before the field visit, and after a series of discussions, the following CVM scenario was chosen: the Surface Water Quality Improvement Program in the city of Chennai. The Program consists of two components, building a new wastewater treatment plant and expanding the city's existing sewerage system, and an additional amount on the current water bill was selected as a payment vehicle. The final stage of survey design was extensive pretesting of the developed questionnaire, and total of 55 face-to-face interviews were completed in the city of Chennai in February 2017. This time, in addition to the main issue of understanding the questions, we focused on the WTP question, the clarity of the proposed scenario and the rest of the questions. After the questionnaire had been modified and the final version was completed, the main survey of 450 respondents was conducted in March-April 2017.

Residents were given two water quality options: swimmable and fishable and they have to reveal their use and nonuse valuation related to this water quality standards.

A questionnaire was designed for the Chennai study that was similar to that of the Jakarta and Hanoi case studies. 1) The first part asked for background data/the profile of the respondent profile; 2) the second part related to awareness of the current water quality situation; and 3) the main part included WTP questions (use- and nonuse), which were divided into subquestions:

1. *Are you willing to pay to improve the water quality of Chennai waterbodies?*

   ☐ YES ☐ NO

2. *How much would you be willing to pay as a monthly, per-household fee for various levels of improvement in the water quality of the waterbodies of the city in addition to your monthly utility bill?*

We provided ten cards as for scenario with mitigation measures that specified amounts ranging from Rs 10 to 1,000 or suggested that the respondent indicate their own amount.

The random stratified sampling method was used because we could not secure a list of voters from the local government and did not want to use the telephone book to compile sampling for the survey because it did not cover the entire area of the city. The selection techniques were based on two classes: (1) walking distance to the river, which assumed that one can reach the nearest waterbody within 30 min, and (2) the need to drive or take public transportation to the nearest waterbody. The SPSS statistical package was used for the analysis, and the WTP was estimated by logit and probit models.

4.4.2.8 Floodwater-borne infectious diseases

Following the methodology in Section 3.8, the risk assessment model for floodwater-borne infectious gastroenteritis was developed to evaluate the number of cases of gastroenteritis caused by noroviruses occurred in the flooded area in Chennai. Three scenarios were developed, one to simulate the current situation (current scenario) and two to simulate the future situation by 2030 with or without mitigation measures, namely, the with-mitigation scenario and the business-as-usual scenario, respectively. The results of the flood inundation and water quality models corresponding to each scenario were used to represent the current or future urban flooding and surface water quality situations. The current and future population in each FLO-2D grid (25,388 grids in total) was calculated using the current and future population of the city as described in Section 4.4.2.3, the area of the city, and the area of the FLO-2D grid (2,500 m^2). The total population in the study area was 1,173,244 for 2015 and 1,652,572 for 2030 (41% increase).

4.4.3 Results and discussion

4.4.3.1 Precipitation change

Because the 2015 flood was considered to be a 100-year event, a return period of 100 years was used for the comparative analysis and then for the hydrologic-hydraulic analysis in this study. A comparison of the daily maximum rainfall of different return periods revealed a general increase under future climate conditions over the current climate, and the climate change projections revealed an increase of 10% and 16% in the 100-yr daily maximum precipitation for moderate and extreme conditions, respectively. This represented a significant increase that could lead to an increase in flood events.

The comparative results for the monthly precipitation pattern shown in Figure 4.4.4, and they clearly indicate that the annual precipitation simulated from the GCM output was not much different from what is currently observed. The observed total annual precipitation values for 2015 and the

simulated results using different GCMs and RCPs, i.e., MRICGCM3_45, MIROC5_45, MRICGCM3_85, and MIROC5_85, were 1652.6, 1669.8, 1715.5, 1676.3 and 1678.4 mm, respectively. To estimate the effects of precipitation on water quality alone, we fixed the other parameters, such as population growth, as constants and then used the simulated precipitation value as an input for the future water quality simulation starting from the year 2016, i.e., immediately following 2015. Finally, we used MRICGCM3 with RCP_8.5 for the water quality simulation.

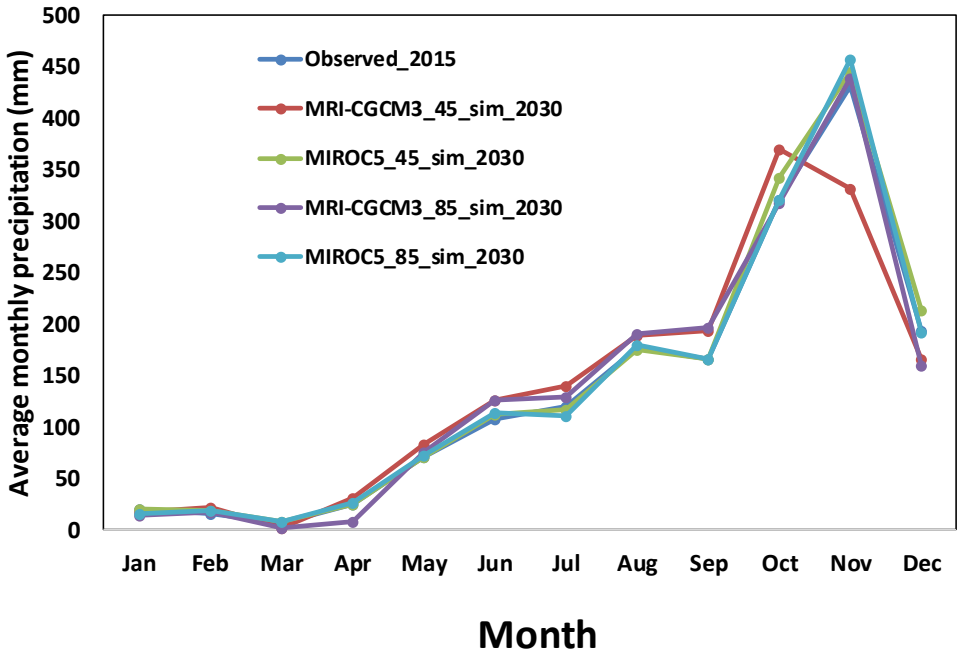

Figure 4.4.4. Graph comparing the current and future monthly rainfall collected at IIT Madras station

4.4.3.2 Land cover change

The classified land cover of the Adyar watershed for 2014 and 2030 is presented in Figure 4.4.5, and the results showed a decline in green land classes, whereas the built-up area increased. The comparison between the two periods indicated an expansion of built-up area during the period from 2014 to 2030 to approximately 40% of the total watershed. However, considering the inundation modeling area as identified in Section 4.4.2.4, the urban growth will be more significant, 46% (Figure 4.4.6). Green land will be replaced by settlement, and the changes were mainly detected in some portions of the Kancheepuram and Thiruvallur Districts. Indeed, it was estimated that built-up areas will increase by 184%, 60% and 32% in some parts of Kancheepuram, Thiruvallur and Chennai, respectively. Increased urban area can be due to economic enhancement that causes people to move from rural to urban areas. The main challenge for the local government will be to provide basic services to avoid the risk of expanding slums and informal settlements in inappropriate locations.

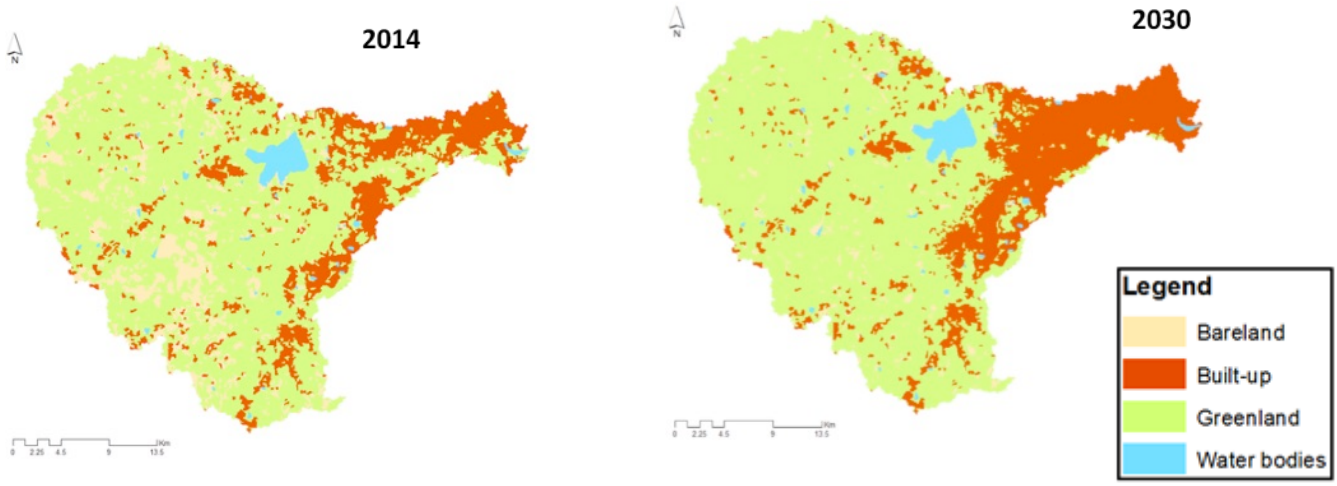

Figure 4.4.5. Land cover change map for the watershed

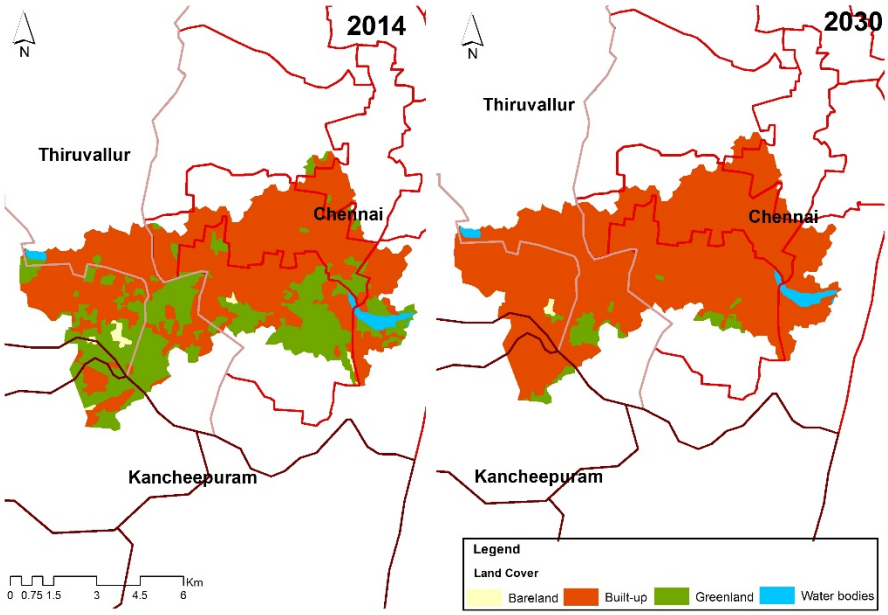

Figure 4.4.6. Land cover change map for the inundation modeling

4.4.3.3 Flood inundation

The computed peak floods at the final outlets of the Adyar River were found to be significantly larger under climate change. Figures 4.4.7 and 4.4.8 provide a comparison of peak discharges at the outlet near the Bay of Bengal, and the effect of the projected climate change (moderate) in 2030 could increase peak discharge by 15% for the 100-yr return period. Flood hydrographs at the Chennai metropolitan boundary location were used to simulate the flood inundation in the core city area, and Table 4.4.2 provides a comparison of flood inundation under different conditions: climate

change and with countermeasures. Increased flood inundation in the future revealed the need to improve flood management systems for the sustainable development of urban water environments, and structural flood control measures such as river flow capacity improvement, walls, and improved upstream diversion/storage were shown to effectively reduce flood inundation. Although the structural measures can greatly affect flood control, these interventions might require a long time for completion as well as a huge investment. Thus, to urgently realize flood mitigation, it is important to promote nonstructural measures (runoff control measures) such as the installation of rainwater storage and infiltration facilities, pond conservation and rehabilitation (*in situ*), and others. A bare earth elevation model was used to approximate the ground level inundation scenario without considering urban infrastructure, so the simulation results are approximate and can provide an overall picture of the flooding scenario.

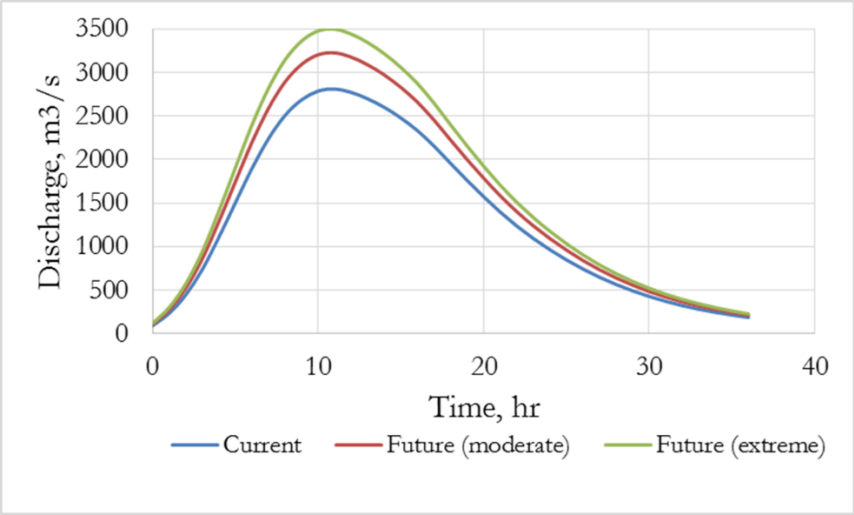

Figure 4.4.7. Comparison of peak flooding near Adyar outlet (Bay of Bengal)

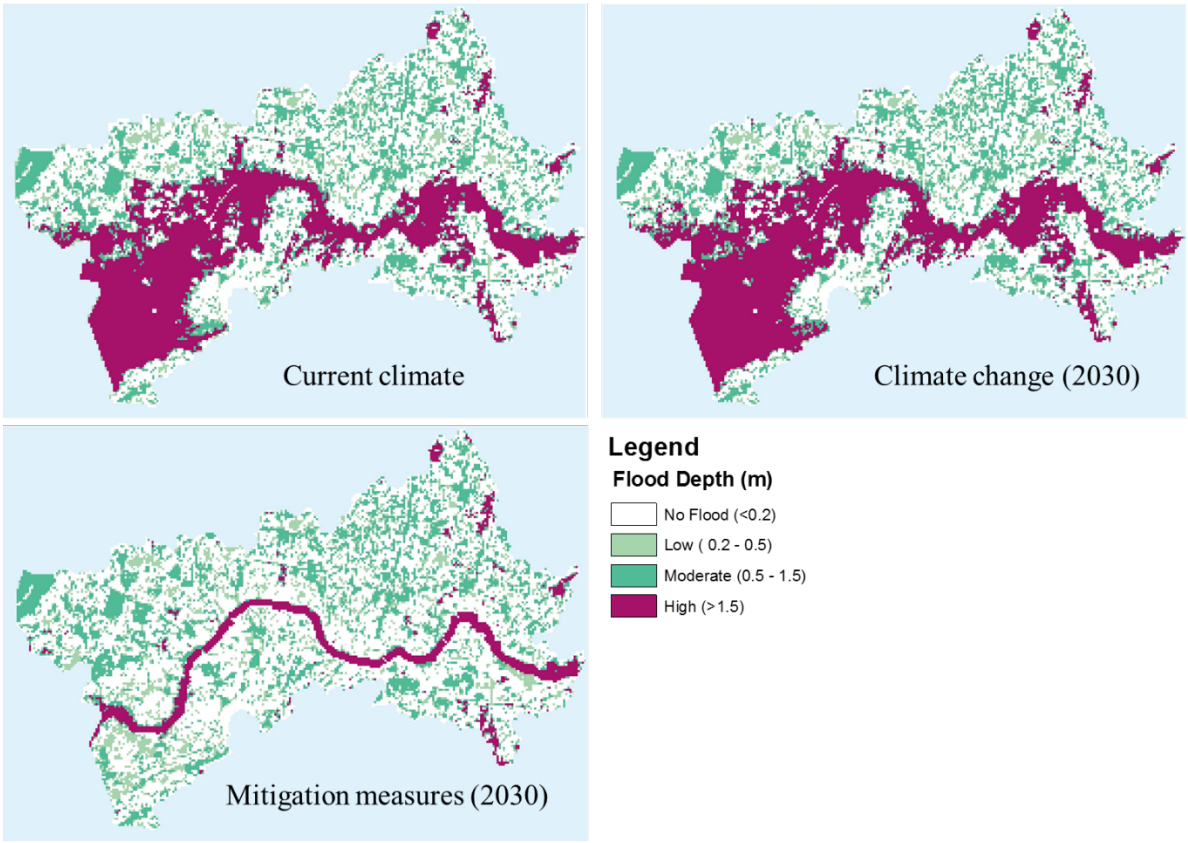

Figure 4.4.8. Spatial distribution of flood hazards
for current, climate change and mitigation conditions

Table 4.4.2. Comparison of flood inundation

Flood hazard (m)	Current	Future			
		Climate change	Channel improvement	Channel improvement + storage	Channel improvement + storage + diversion
Low (0.2-0.5 m)	5.6	5.3	7.6	8	8.4
Medium (0.5-1.5 m)	12.2	12.3	14.7	14.5	14
High (>1.5 m)	18.5	20	6.3	4.9	4.3

4.4.3.4 Direct flood damage

In this work, the flood risk was assessed for the urban portion of the Adyar River basin, so flood damage was evaluated at the 100 x 100-m grid cell scale. Maps were generated and classified, and three scenarios were assessed: case 1: current situation without climate change; case 2: future assessment with the impact of climate change; and case 3: future flood damage with mitigation. The comparison of the three scenarios revealed that there will be a significant increase in loss due to the impact of climate and land cover changes as presented in Figure 4.4.9. By comparing flood damage under current and future situations, it was found that flood loss will increase by 75% in the situation without mitigation, but damage may decrease by 75% with the implementation of flood measures.

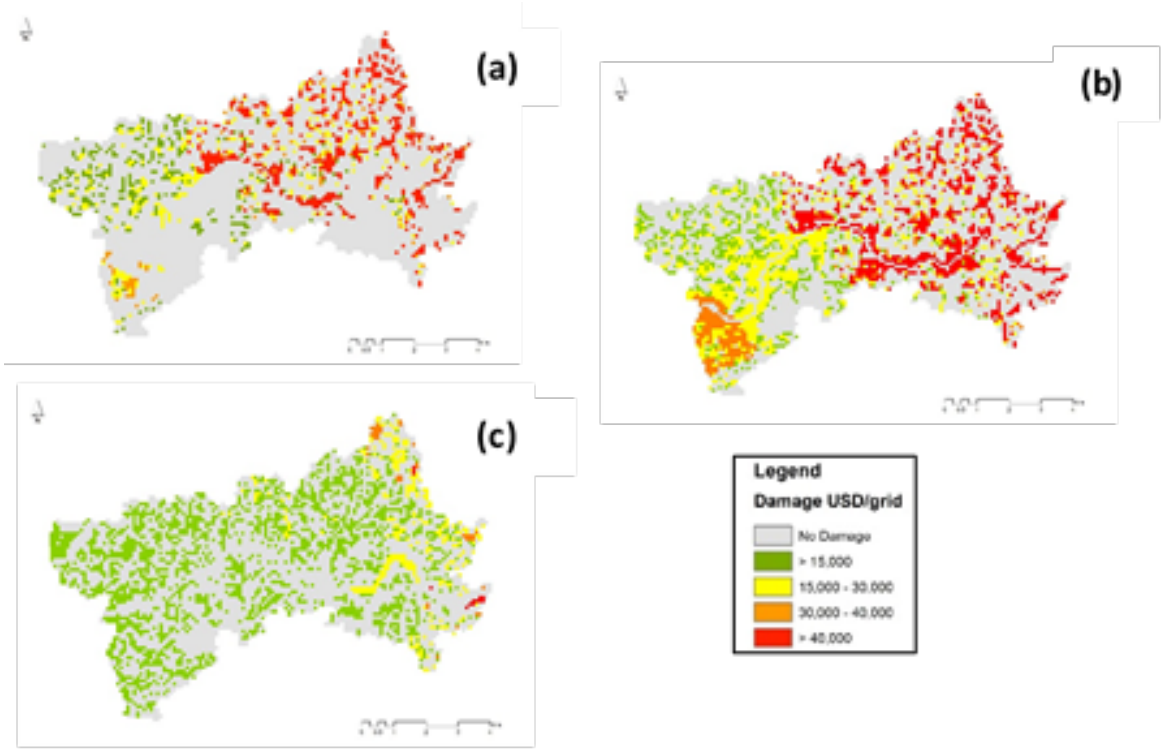

Figure 4.4.9. Spatial distribution of flood damage: (a) current situation without the effect of climate change, (b) future situation with the effect of climate change, and (c) mitigation scenario

The evaluation of flood damage in the inundated areas showed that the damage will particularly increase with water depth, and urbanization will have negative repercussions characterized by increased flood damage in some areas. Figure 4.4.10 illustrates that flood damage in Chennai is greater than in Kancheepuram and Thiruvallur, and this is may be due to the value of the property assets. However, in the case of Kancheepuram, flood damage will considerably increase with the effect of climate and land use changes. In fact, urbanization will increase by 184% in the inundated area in this district. The adaptation measures will reduce the flood depth and, consequently, the flood loss in three districts.

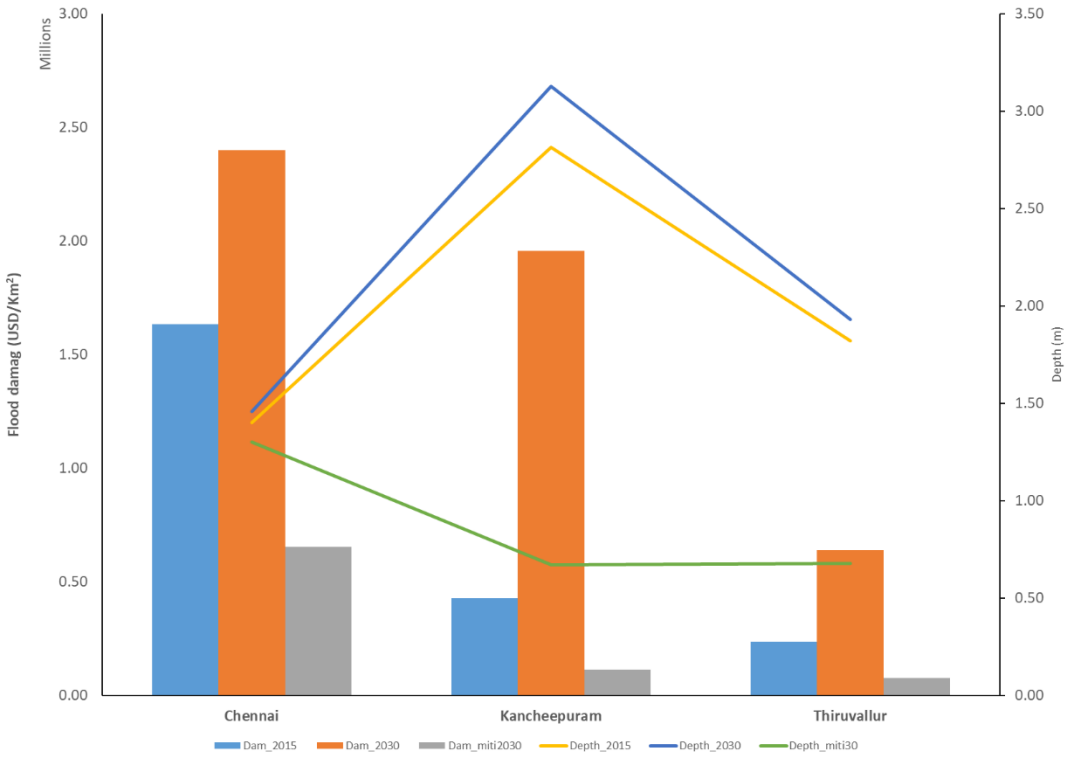

Figure 4.4.10. Flood damage by district

4.4.3.5 Water quality

Model performance evaluation

Before conducting the future scenario analysis, the performance of the WEAP simulation was validated with observed and simulated values of hydrological and water quality parameters. In the case of the hydrology module validation, the parameters (mainly effective precipitation and runoff/infiltration) were adjusted using the trial and error method during simulation to reproduce the observed monthly stream flows for the 2011 to 2015 period (Table 4.4.3), and the final best-fit values for the two parameters were 95% and 50/50, respectively. Figure 4.4.11 (a) compares the monthly simulated and observed stream flows at Sanjay Colony (average value for the 2013-2015 period) and shows that they largely match for most months with a correlation coefficient (R^2) ≅ 0.80, a root-mean-square error (RSME) ≅ 0.25, and an average error of 12%. The three months were selected for validation due to a lack of water in the river at other times of the year, especially during dry period. In contrast, the water quality simulation was validated by comparing the yearly average simulated and observed BOD concentrations for the year 2015 at different locations from upstream to downstream. These locations and time, i.e., the year 2015, were selected based on the consistent availability of the observed water quality data. The results showed a strong relationship between these two datasets (Figure 4.4.11 (b)) (with an error of 11%), confirming the suitability of the model performance in this problem domain.

Table 4.4.3. Summary of parameters and steps used for calibration

Parameter	Initial Value	Step
Effective precipitation	100%	±0.5%
Runoff/infiltration ratio	50/50	±5/5

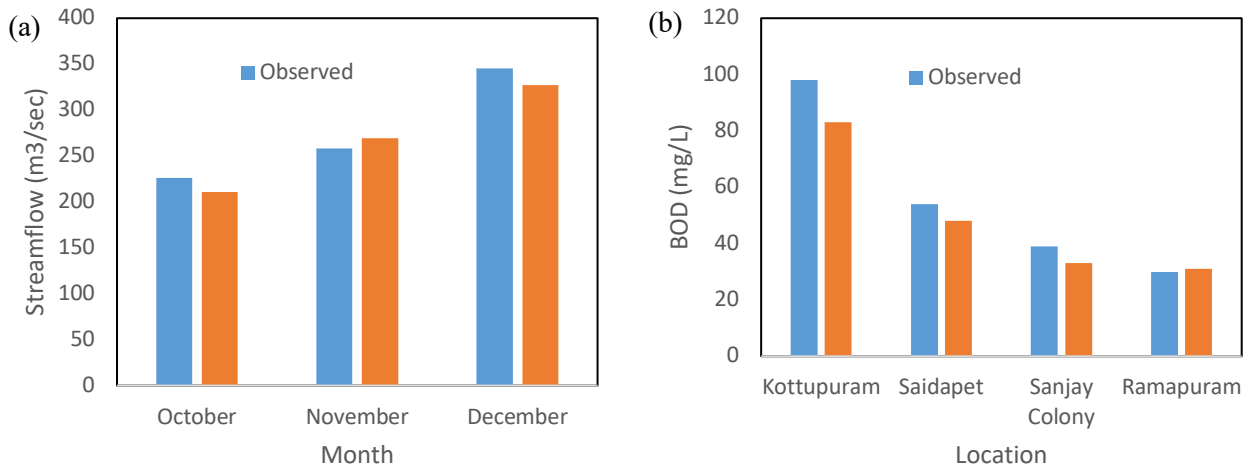

Figure 4.4.11. Validation of the model output by comparing simulated and observed data: (a) average monthly river discharge for the 2013-2015 period at Sanjay Colony and (b) average BOD values for different locations for the year 2015

Scenario analyses

For water quality, the simulation was performed using two possible scenarios, as shown in Table 4.4.4, for the years 2015 and 2030 using 2013 as reference year and considering population increase and land use change as well as wastewater generation and its treatment at wastewater treatment facilities. Once the model was calibrated, the water quality parameters were simulated at the monthly scale for the year 2015, i.e., the current situation. Here, all existing WWTPs were considered along with projected rainfall, and once the simulated values of the water quality parameters were compared with the observed values at each spatiotemporal scale, we found significant correlations (statistically supported by different R^2 and RMSE values) between these observed and simulated results. First, under the business-as-usual scenario, the effects of population growth and climate change on water quality were observed using the average values of two GCMs and two RCPs and keeping the capacity of all the existing wastewater treatment plants (180 MLD) constant until the year 2030. Here, small bars show the ranges of the simulated water quality values because of the change in GCMs and RCPs. For the scenario with measures, all conditions were kept the same as for the first simulation except the wastewater plant capacity and collection rate were increased as shown in Table 4.4.4.

Table 4.4.4. Summary of all the criteria considered for the different future water quality simulation scenarios

Scenario	Components
Business as usual	Climate change + population growth +WWTP of 180 MLD
With measures	Climate change + population growth +WWTP of 886 MLD (100% collection rate)

The simulation results for the water quality parameters (BOD and *E. coli*) using these two scenarios are shown in Figures 4.4.12 and 4.4.13. With the current wastewater treatment plant (a capacity of 180 MLD and coverage of merely 25% of the total population in the study area), the current water quality status throughout the river is very poor compared with the local guideline for class 2 water, i.e., the swimmable category (BOD < 5 mg/L and *E. coli* < 1,000 CFU/100 mL, Tamil Nadu Pollution Control Board, 2017), and it is even worse in downstream locations because of the cumulative effect of waste disposal and an excess of untreated waste coming from upstream. Both climate and population changes have prominent effects on water quality status, which will deteriorate further by 2030 when compared to the current situation (business-as-usual scenario). However, based on the scenario with measures, in which all locally generated wastewater will be collected and treated by the WWTP with a capacity of 886 MLD, the water quality will be much improved throughout the stream, which is encouraging. However, quality is still a matter of concern especially in the downstream area.

Explaining water quality more precisely, a high concentration of nitrate indicates untreated sewerage input, and with the climate change scenario, water quality will deteriorate at the other locations as well. The BOD value varied from 21 to 74 mg/L, which clearly indicates that all the water samples were moderately to extremely polluted relative to the BOD value required for a safe aquatic system, i.e., 3 mg/L (Tamil Nadu Pollution Control Board, 2017). The *E. coli* value, a commonly used biological indicator of water quality, also exhibited no significant improvement in the future, possibility because of a lack of available data such as the chlorination rate. The above result suggests that current management policies and near-future water resources management plans are not sufficient to maintain pollution within the desirable limit, and it calls for transdisciplinary research into more holistic approaches for sustainable management.

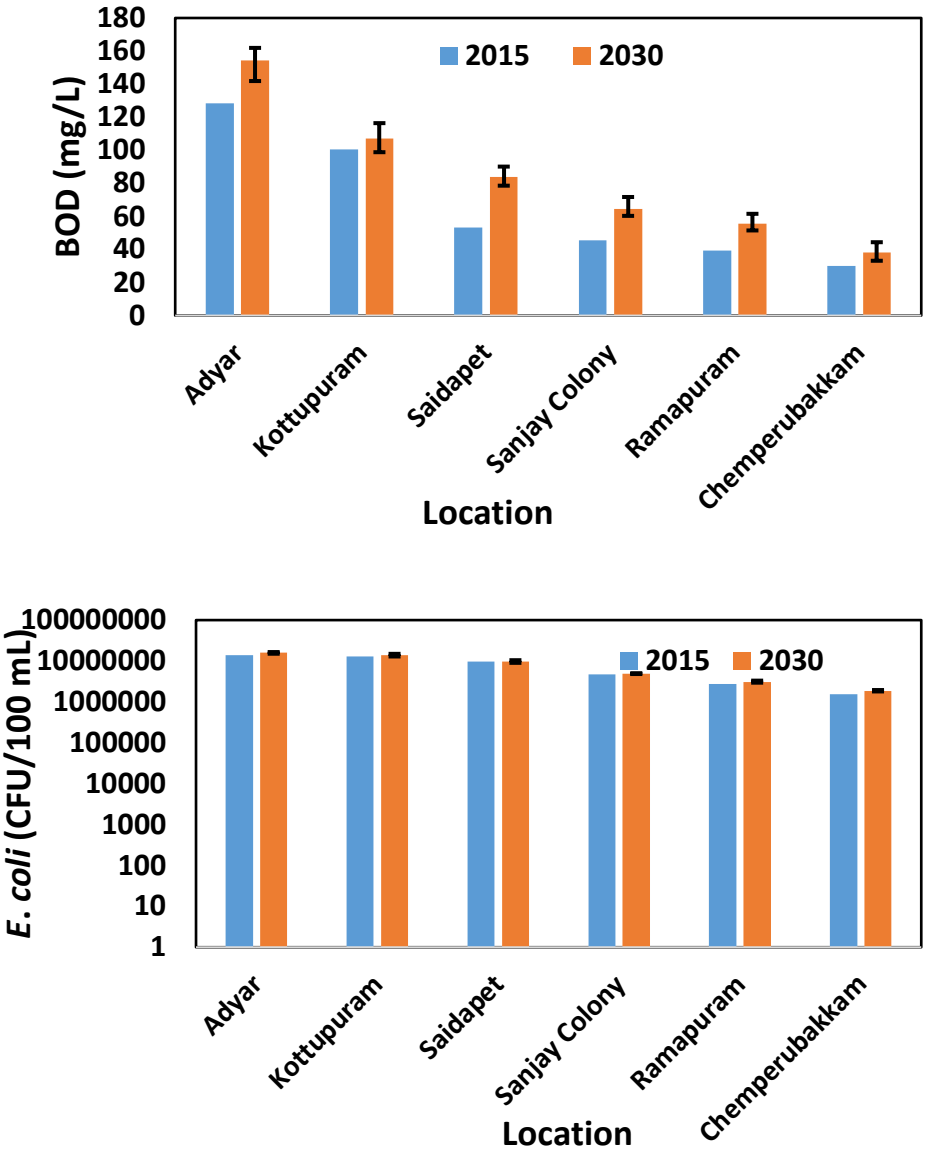

Figure 4.4.12. Simulated water quality results considering population growth, average climate change and a WWTP with a capacity of 42.5 MLD (business-as-usual scenario)

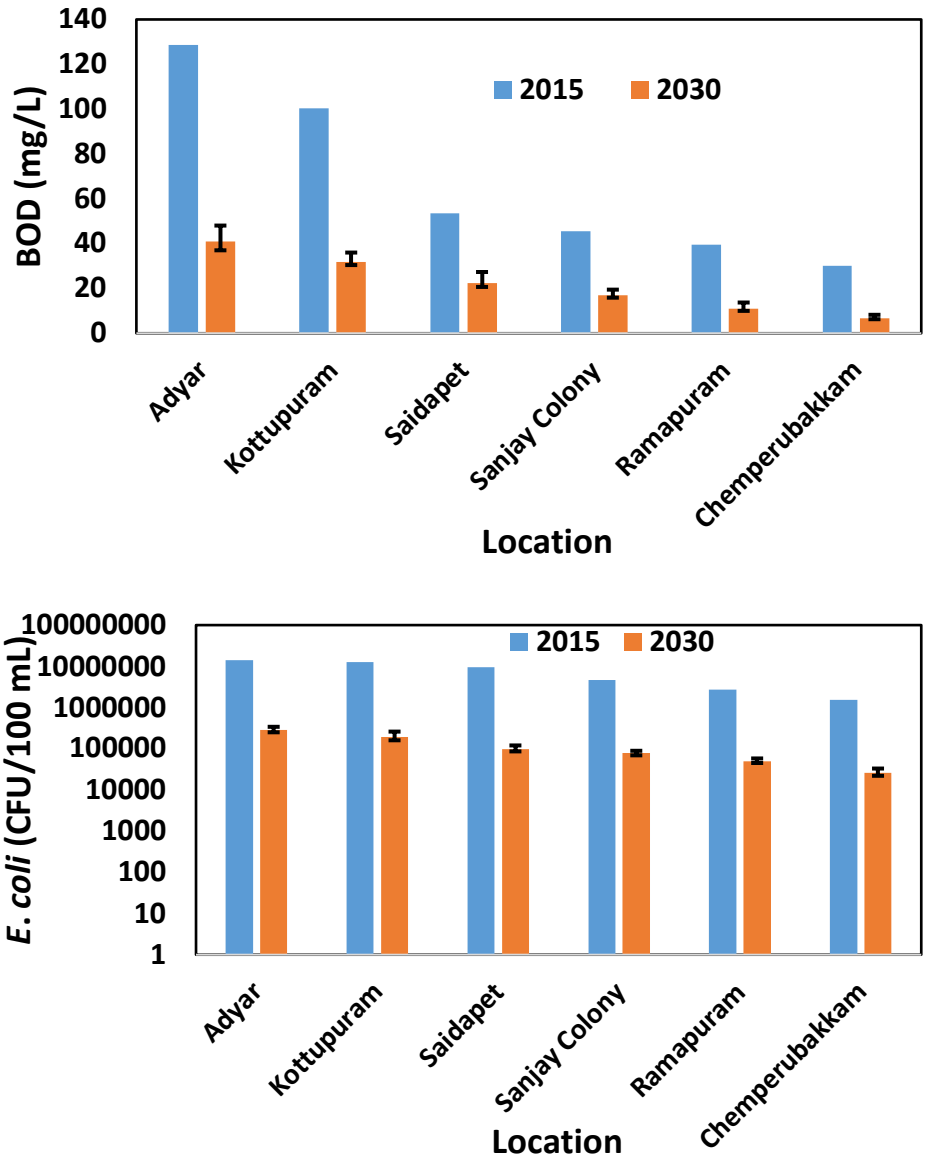

Figure 4.4.13. Simulated water quality results considering population growth, average climate change and a WWTP with a capacity of 886 MLD (scenario with measures)

4.4.3.6 Economic benefit of improving urban water quality

There is clear interest in improving the surface water quality in Chennai waterbodies according to those who placed a monetary value on the service; 56% of the respondents indicated a willingness to support the proposed Surface Water Quality Improvement Program in the city of Chennai.

The vast majority of the survey participants (74%) had visited or seen the rivers/lakes/canals of the city in the preceding month. Among the respondents, 33% went regularly; 31% went a few times, 17% went once, and 19% preferred not to answer this question. The majority of respondents (80%) answered that the water quality of the city's waterbodies is not sufficiently acceptable for

recreational activities; 7% stated otherwise (that water quality is sufficient); and 13% did not know whether or not the water quality was sufficient.

The socioeconomic data of the respondents revealed the following: 1) Gender – male 46%, female 17%, not disclosed 37%; 2) Marital status – single 24%, married 37%, not disclosed 39%; 3) Employment status – part-time 2%, full-time 41%, self-employed 6%, unemployed 19%, not disclosed 32%; 4) Education status – primary 2%, secondary 9%, undergraduate 17%, postgraduate 35%, not disclosed 37%; 5) Age – average 37, median 31; 6) Income – Average Rs 80,000 / month, median Rs 30,000 / month.

The main results of the study relate to the estimation of WTP values, and the total economic value was calculated for the entire population of the city. The average use WTP for swimmable water quality was estimated to be Rs 37.71 (USD 0.58) per capita; the average use WTP for fishable water quality was estimated to be Rs 33.81 (USD 0.52) per capita; the average nonuse WTP for swimmable water quality was estimated to be Rs 163.85 (USD 2.52) per capita; and the average nonuse WTP for fishable water quality was estimated to be Rs143.69 (USD 2.21) per capita. As in previous case studies, the main determinants of WTP were the income and educational status of a respondent. The total economic value of water quality improvements in Chennai was estimated to be USD 64 million per year.

4.4.3.7 Floodwater-borne infectious diseases

The simulated risk of floodwater-borne gastroenteritis under the three scenarios, expressed as the number of gastroenteritis cases caused by noroviruses per grid, is shown in Figure 4.4.14. The purple grids represent high-risk areas (more than 0.1 cases per grid); the orange represent medium risk (0.01 – 0.1 cases per grid); the yellow represent low risk (less than 0.01 cases per grid); and the white represent no risk (areas with no flooding). Under the current scenario, the risk was relatively high along the lower Adyar River flowing through the study area from west to east and on the north side of the river. High-risk areas (more than 0.1 cases per grid) were sporadically observed on the north side of the Adyar River, and the middle-risk area in the southwest was the Chennai International Airport, which is located on low and flat terrain and thus vulnerable to flooding. The high-risk areas were different from those in the flood analysis: those on the north side of the Adyar River, as shown in Figure 4.4.14, were not present in the flood inundation map (Figure 4.4.8). This is because the number of disease cases is affected by the population in each grid in addition to the severity of flooding (i.e., related to the maximum depth), so the high-risk areas were clustered where severe flooding was expected and where the population density was high. In the business-as-usual scenario, an additional high-risk area was observed along the Adyar River because of increased flooding severity, but in the with-mitigation scenario, there were no grids with more than 0.01 cases of gastroenteritis by noroviruses (purple and orange areas).

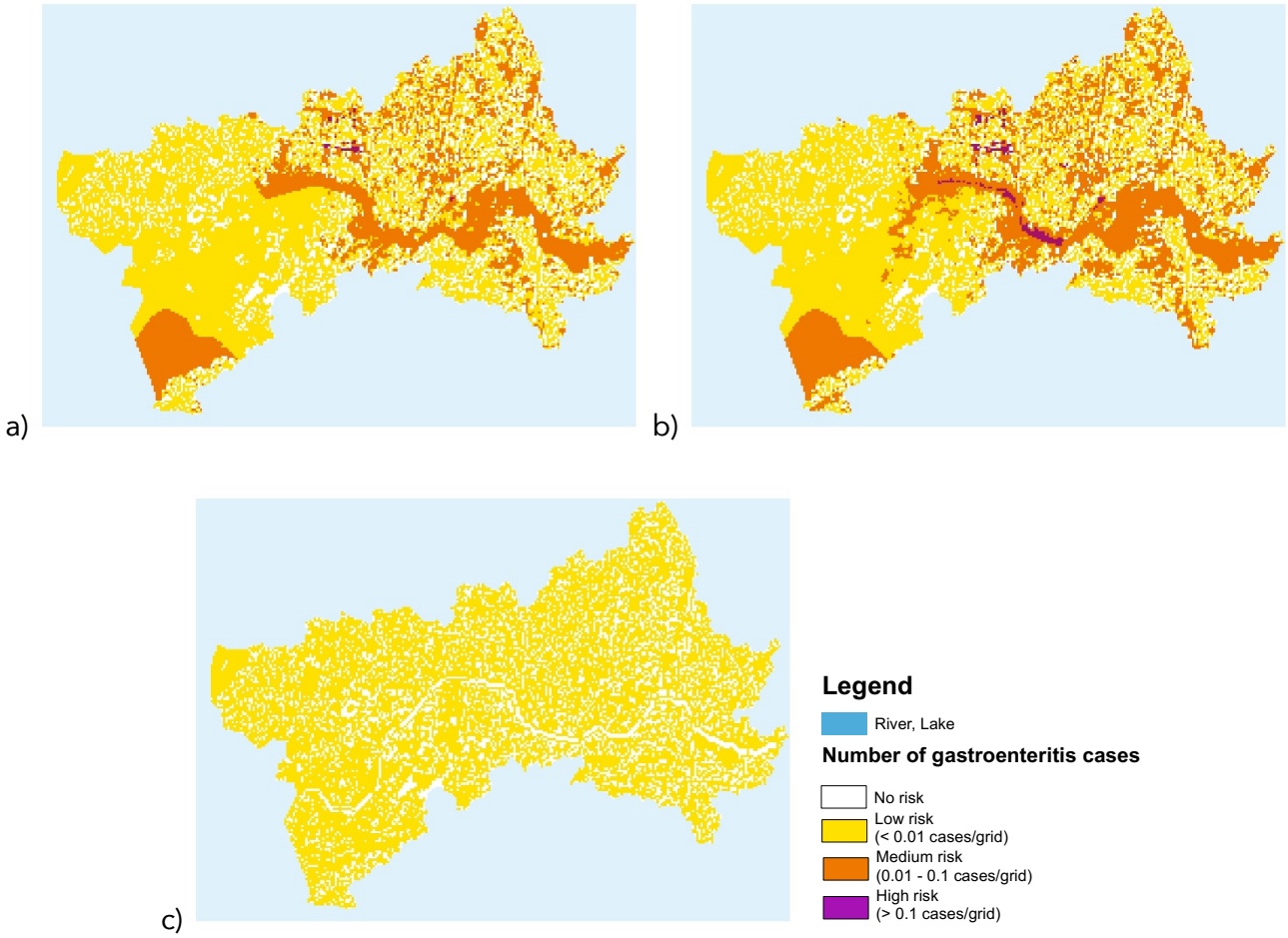

Figure 4.4.14. Simulated health risk (number of cases of gastroenteritis due to floodwater-borne noroviruses) for Chennai under the a) current scenario, b) business-as-usual scenario, and c) with-mitigation scenario

The total number of cases of gastroenteritis caused by noroviruses was 183 under the current scenario, and the number was projected to increase by 60% by 2030 if no measures were taken to reduce urban flooding and water pollution (business-as-usual scenario, 293 cases in total). This result clearly demonstrates that population growth and the change in precipitation significantly increased the risk of flood-related infectious gastroenteritis. It is recommended that stakeholders in the water management sector consider the health aspects of damages, including infectious diseases caused by urban flooding, and act to reduce the risk. When the countermeasures for reducing urban flooding and water pollution were included in the analysis, the total number of cases substantially declined to 2.2, a 99% reduction compared to the business-as-usual scenario. It was indicated that implementing water management measures would also protect citizens from floodwater-borne infectious diseases.

References

Chennai Metropolitan Development Authority. *Second master plan for Chennai metropolitan area, 2026: Vision, strategies and action plans*; Chennai Metropolitan Development Authority, Government of Tamilnadu, India; 2008.

Huizinga, J.; de Moel, H.; Szewczyk, W. *Global flood depth-damage functions. Methodology and the database with guidelines*; EUR 28552 EN; Publications office of the European Union, Luxembourg; 2017.

Khan A.A.; Gaur R.Z.; Diamantis V.; Lew B.; Mehrotra I.; Kazmi A.A.; Continuous fill intermittent decant type sequencing batch reactor application to upgrade the UASB treated sewage. *Bioprocess Biosyst. Eng*. **2013**, 36: 627–634.

Tamil Nadu Pollution Control Board. TNPCB & you. A ready reckoner for entrepreneurs; 2017. http://www.tnpcb.gov.in/pdf/tnpcb_you2013.pdf [Accessed on 18th October, 2018]

United Nations Department of Economic and Social Affairs, Population Division *World Urbanization Prospects: The 2014 Revision*; ST/ESA/SER.A/366; United Nations: New York, NY, 2015.

4.5 Lucknow

4.5.1 Introduction

Lucknow is the capital of Uttar Pradesh, India, and it is located of the central Gangetic Plain between 26°30′ and 27°10′ north latitude and 80°30′and 81°13′ east longitude (Figure 4.5.1). The city has a humid subtropical climate with a cool dry winter from December to February and a hot summer from April to June; the temperature extremes vary from 48.9°C in the summer to 1.67°C in the winter. The city receives 900 mm of rainfall annually, mostly from the southwest monsoon between July and September. The elevation of the city varies from 100 to 130 m above mean sea level and generally slopes to the east.

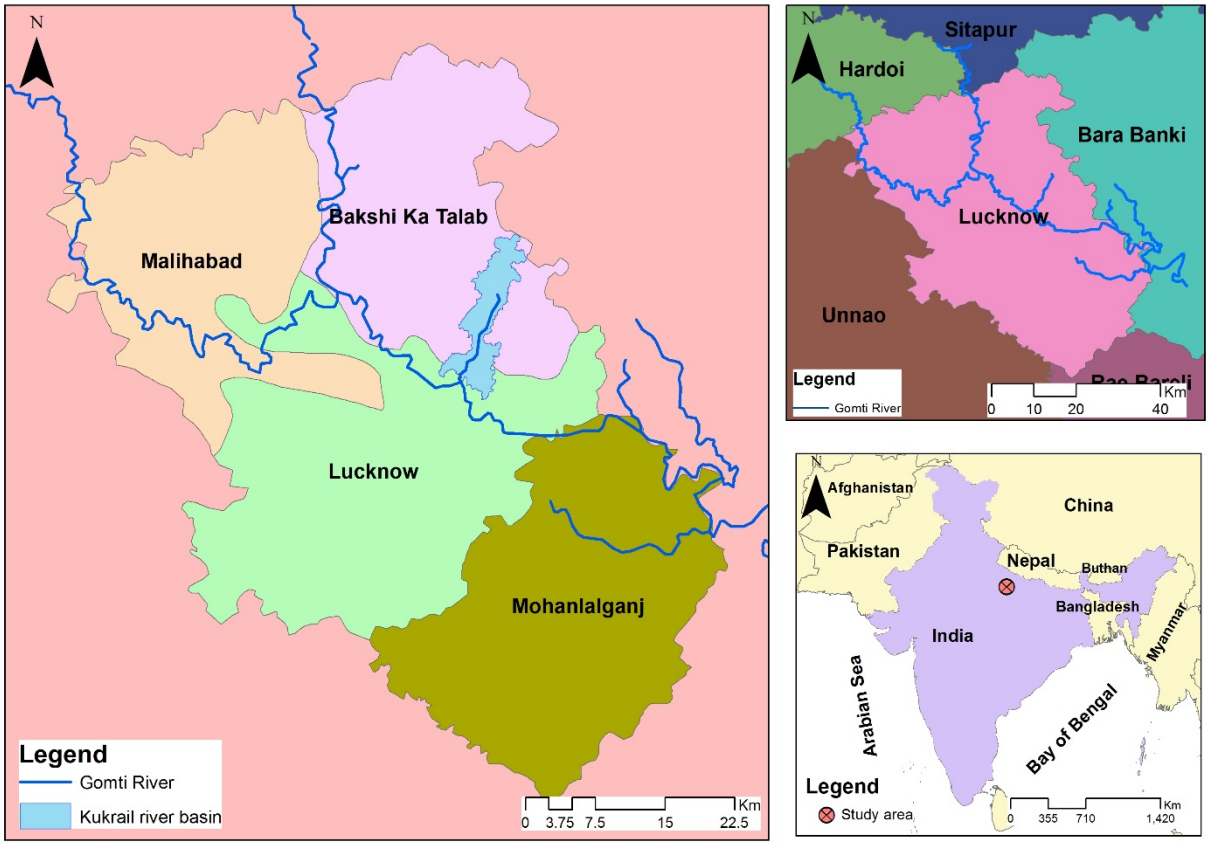

Figure 4.5.1: Map of the study area

Lucknow is one of the fastest growing cities in the country with a projected population of 4.7 million in 2031 from 2.8 million in 2011 (Lucknow Development Authority, 2016), and rapid unplanned urbanization has created many problems as it places enormous pressure on the land, water, housing, transportation, health, education, etc. This rising population has a major impact on the natural resources of the area, especially water quality and quantity. Fresh water is the most important natural resource for life, but overexploitation and unjustified water use have led to water quality deterioration.

Lucknow is bisected by a number of streams. The Gomti, the major river, flows through the center of the city from the northwest to the southeast, and it is one of the major sources of the public water supply in the city along with groundwater. As the river passes through the city, the flow becomes almost negligible, and dissolved oxygen diminishes. Sewage generation and the proper treatment and disposal of this waste is the primary problem in the city; a poorly drained sewerage system and a lack of treatment capacity and sewage treatment units has resulted in severe degradation of the quality of the river water. The sources of pollution in the Gomti River originate from gray water coming from households and commercial buildings combined with discharges from industries as well as pesticide and fertilizer run-off from agricultural land adjoining the city. Rapid urbanization is also contributing to an understated threat known as stormwater runoff; increasing runoff is inversely related to infiltration, i.e., the greater the runoff, the lower the ability of soil to hold water.

A lack of proper stormwater management facilities has led to urban flooding, and the severe flooding in Lucknow city during the monsoon period is believed to originate from insufficient drainage capacity and blockage of the drainage system due to huge volumes of garbage and polyethylene bags. A number of drains have dried up or been encroached upon by city dwellers, so the current situation for the drains is critical. They are silted or choked by garbage, so during the monsoon, the rain water overflows from drains and the surrounding areas flood. Adequate management of the drainage system is essential to ensure the natural and smooth flow of rain water, so there is a need to develop an integrated drainage management plan.

In these contexts, the current conditions and future scenarios of urban flooding and river pollution as well as their implications for human health and property damage were investigated to explore alternative measures for enhancing the urban water environment.

4.5.2 Methodology

4.5.2.1 Precipitation change

The precipitation change assessment was focused on deviations in daily maximum and monthly rainfall values, and it was initiated by screening daily rainfall observation data over the Lucknow region. A meteorological station with the geographical coordinates 26.75N, 80.75E inside Lucknow city was considered for the change assessment. Precipitation data with a baseline period of 1985-2004 were collected to represent current climate conditions, and climate projections for the 2020-2039 period of 2 GCMs, MRI-CGCM3 and MIROC5, with RCP 4.5 and RCP 8.5 emission scenarios were extracted to assess the impacts of climate change on the urban water environment. The quantile-mapping technique (a statistical bias-correction method) was applied to remove biases in the GCM precipitation outputs, and Gumbel rainfall frequency analysis of the bias-corrected data was carried out to estimate extreme rainfall values for different return periods. In this study, the 100-year daily maximum rainfall value was used to analyze flood impact, and average and maximum return period values, representing moderate and extreme climate conditions, respectively, were estimated using the mean and maximum of 4 values (combinations of MRI-CGCM3 and MRIOC5 and RCP 4.5 and RCP 8.5).

To evaluate the effect of climate change on water quality, the change in monthly average precipitation was analyzed, and a comparison of the 2015 and 2030 mean monthly precipitation values indicated little difference in the future annual precipitation compared to the current situation (Figure 4.5.2). The values for total annual precipitation in the case of observed_2015, Sim_2030_MRICGCM3_45, Sim_2030_MIROC5_45, Sim_2030_MRICGCM3_85, and Sim_2030_MIROC5_85 were 844.8, 883.1, 802.0, 831.8 and 822.1 mm, respectively.

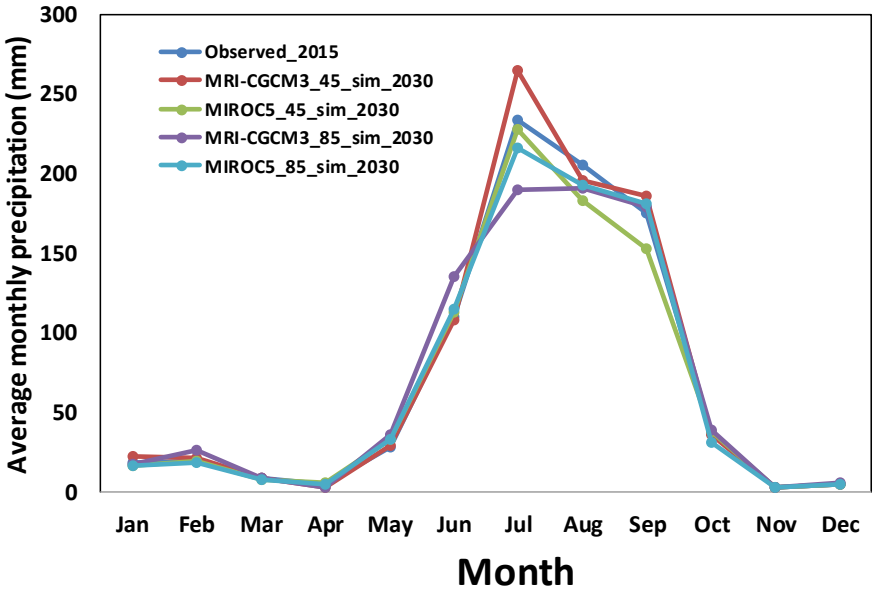

Figure 4.5.2. Comparison of current (2015) and future (2030) monthly precipitation over Lucknow city

4.5.2.2 Land cover change

Land cover maps were established for the Kukrail River basin to analyze and represent the flood risk in the city. Remote sensing products from the National Remote Sensing Center (Indian Space Research Organization) were applied for the analysis as presented in Table 4.5.1, and Land Change Modeler in IDRISI Selva 17.0 was used to assess and project the future land cover change in the study area. This approach was based on the employment of two past land cover maps and driver factors; LULC maps for 2007 and 2017 in combination with drivers such as slope or distance from specific places were used as inputs for the simulation. The model was run with a multilayer perceptron neural network, and maps of the transition potential between LULC maps were obtained that enabled the 2030 LULC map to be predicted.

Table 4.5.1. Satellite images applied

No.	Data Set	Acquisition Date
1	Linear Imaging Self-Scanning System III (LISS III)	2007
2	High-Resolution Linear Imaging Self-Scanning System IV (LISS –IV)	2017

4.5.2.3 Population growth

To estimate the effect of population growth (one of the key drivers examined in this study) on water quality status, the entire study area was divided into different demand sites that mainly represent the population of different cities on both sides of the Gomti River within study area. The future population was estimated by the ratio method using the UN DESA (2015) projection rate. A total population of 45, 89,838 was estimated for the base year (2011), and for the future population projection, the annual growth rate was considered to be 2.42, 2.24, 2.26 and 2.16% during the periods of 2011-2015, 2016-2020, 2021-2025, and 2025-2030, respectively. Accordingly, the populations for the current (2015) and target years (2030) were estimated to be 5,050,525 and 7,020,597, respectively.

4.5.2.4 Urban flooding

In general, Lucknow city does not face large-scale inundation events, but there are local pockets of water logging every year. Urban flooding in Lucknow during the rainy season causes traffic disruptions and other small-scale damages, so flood simulation under a scenario of change is required for various risk and damage assessments for the affected population. With encroachment caused by rapid urbanization, Lucknow City has already lost 46 percent of its water bodies, and urban floods are now a constant reminder of a lack of proper planning, which not only has negative environmental impacts but affects the socioeconomic dynamics of urban dwellers.

Of the 28 major drainages that enter the Gomti River (the main river), Kukrail Nala, with a basin area of 61.6 square kilometers, is an important tributary that passes through Lucknow (Figure 4.5.3). Due to its geographical characteristics, Kukrail Nala basin is expected to contain high downstream water volumes, but unplanned land use, an increase in impervious area and changing rainfall patterns have led to regular waterlogging in this area.

Figure 4.5.3. Location of Kukrail Nala basin in Lucknow city

Flood hazard was simulated for three scenarios: (i) the current condition, (ii) the future with moderate climate change condition, and (iii) the future with extreme climate change condition. In this study, moderate and extreme climate change conditions were established by averaging the return period values of the RCP4.5 and RCP8.5 emission scenarios for the MRI-CGCM3 and MIROC5 GCMs, and flood inundation was simulated using the FLO-2D model. Model calibration was based on the peak discharge value at the outlet (meeting point of the Kukrail and Gomti Rivers), and the hydrologic and hydraulic model was set up using peak discharge corresponding to the 100-yr return period at the Kukrail outlet near the Gomti River (Ahmad, 2013). The study involved an HEC-HMS model to project the change in peak discharge and runoff volumes in response to certain adaptation strategies such as stormwater infiltration practices. The model alters the runoff curve number of certain highly impervious grid cells to be semi-pervious through the linear reservoir method, which facilitates the attenuation of excess rainfall and conserves mass by routing infiltrated precipitation.

4.5.2.5 Direct flood damage

Direct flood damage was evaluated for the Kukrail River basin; the hazard, exposure and vulnerability components were estimated and integrated in a GIS environment to determine the

flood loss as explained in Section 3.5. As an indicator of vulnerability, a flood damage depth function based on the research of (Huizinga et al., 2017) was established and applied for this assessment, the flood damage in the study area was then evaluated for the current and future situations.

4.5.2.6 Water quality

As explained in Section 3.6, the WEAP model was used to simulate future water quality variables in the year 2030 to assess alternative management policies in the Gomti River basin. The model is also capable of simulating river flow, storage, pollution generation, treatment and discharge while also considering different users and environmental flows.

For the water quality modeling, a wide range of input data was provided including point and nonpoint pollution sources, their locations and concentrations, past spatiotemporal water quality, wastewater treatment plants (Central Groundwater Board), population, historical rainfall, evaporation, temperature (Indian Metrological Department), drainage networks (Department of Public Works), river flow-stage-width relationships, river length, groundwater, surface water inflows and land use/land cover (State Water Board).

The WEAP model was developed for the Gomti River basin for four command areas with interbasin transfers. Hydrologic modeling required that the entire study area be split into smaller catchments with consideration of the confluence points and physiographic and climatic characteristics (Figure 4.5.4). During simulation, the land use information was broadly categorized into three areas, viz., agricultural, forest, and built-up, and the soil data parameters were identified using secondary data and the literature. Daily rainfall was collected at the IMD Meteorological Station for the period from 1980 to 2016, and daily average stream flow data for 2011-2016 were measured at five stations, namely, Bharwara, River Weir, Pipraghat, Kuriyaghat, Manjhighat and Near Moosa Bird Sanctuary, and collected from the Indian Meteorological Department. These data were utilized to calibrate and validate the WEAP hydrology module simulation. Data for the water quality indicators of BOD and total coliform bacteria (which was later assumed to be equivalent to *E. coli* abundance) were also collected at the above five stations and used for water quality modeling (Figure 4.5.4).

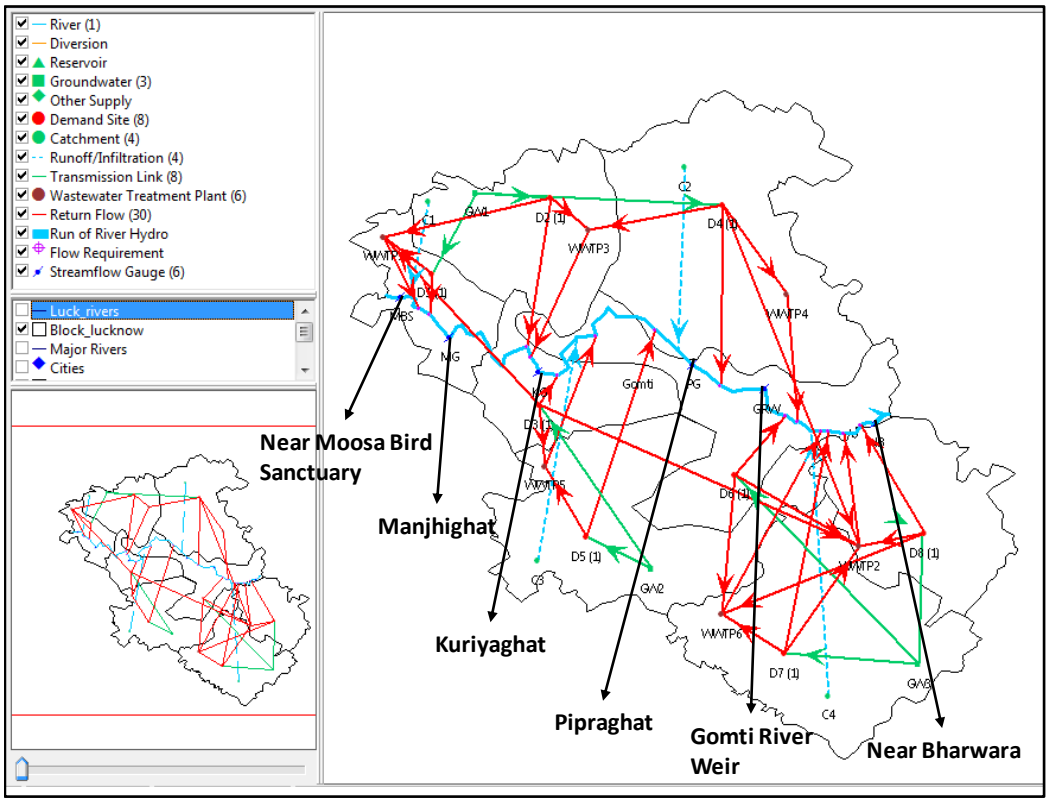

Figure 4.5.4. Schematic diagram showing the problem domain for water quality modeling in Lucknow using the WEAP interface

Model setup

The entire problem domain and its different components were divided into four catchments considering the influent locations of major tributaries (Figure 4.5.4), and other major considerations in representing the problem domain included the eight demand sites and one wastewater treatment plant. Here, demand sites are meant to identify domestic (population) and industrial centers whose attributes explain water consumption and wastewater pollution loads per capita, water supply sources and wastewater return flow. These dynamic attributes are described as functions of time and include the population and industries, and WWTPs are pollution-handling facilities with design specifications that include total capacity and pollutant removal rates. The flow of wastewater into the Gomti River and its tributaries is mainly through domestic, industrial and stormwater runoff routes. Here, the UASB-SBR type of wastewater treatment plant is considered in the modeling, and its treatment efficiency is assumed to be 94% for COD, 97% for BOD, 77% for TN and 99.69% for fecal coliform (Khan et al., 2013). No precise data are available regarding the total volume of wastewater production from different sources, so in the absence of such detailed information, the daily volume of domestic wastewater generation was estimated as 130 liters of average daily consumption per capita based on a literature.

The scenario analysis was conducted by defining a time horizon based on which alternative wastewater generation and management options were explored. The business-as-usual condition was represented by a scenario in which all the currently active existing elements were selected to

remain active to the year 2030 along with the effect of climate change and population growth. Consequently, the new/upgraded WWTPs (information taken from the local master plan) were modeled as the scenario with measures (Table 4.5.2). Under the business-as-usual scenario, only two WWTPs were operational with a combined coverage area of a mere 19% of the total population. To model future conditions using the scenario with measures, all nine WWTPs were enabled by defining their respective start-up years. Information on each object can be easily retrieved by clicking the corresponding graphical element, and the baseline year under the current reference scenario in this study was 2013.

Table 4.5.2. Summary of all the criteria considered for different future water quality simulation scenarios

Scenario	Components
Business as usual	Climate change + population growth +WWTP of 145 MLD
With measures	Climate change + population growth +WWTP of 1119 MLD (100% collection rate)

4.5.2.7 Floodwater-borne infectious diseases

The risk assessment model for floodwater-borne infectious gastroenteritis was developed following the methodology in Section 3.8 to evaluate the number of cases of gastroenteritis caused by noroviruses in the flooded area in Lucknow. Three scenarios were developed, one to simulate the current situation (current scenario) and two to simulate the future situation as of 2030 with or without mitigation measures, namely, the with-mitigation scenario and the business-as-usual scenario, respectively. The results of the flood inundation model and water quality model corresponding to each scenario were used to represent the current or future urban flooding and surface water quality situations. Since mitigation measures to reduce flood risk were not considered in the flood risk analysis as described in Section 4.5.2.4, the flood simulation result under the business-as-usual scenario was also used in the health risk assessment under the with-mitigation scenario. The current and future population in each FLO-2D grid (21,312 grids in total) was calculated using the current and future population of the city as described in Section 4.5.2.3, the area of the city, and the area of the FLO-2D grid (2,500 m^2). The total population in the study area was 69,992 for 2015 and 97,294 for 2030 (39% increase).

4.5.3 Results and discussion

4.5.3.1 Precipitation change

Table 4.5.3 provides the daily maximum rainfall values for the 50- and 100-year return periods for moderate (average) and extreme climate change conditions. Comparing the annual maximum precipitation data over 20 years (1985-2004 and 2020-2039), extreme precipitation events were found to be significantly larger in the future for all return periods and all durations. The climate change projections revealed 30% and 50% increases in the 100-yr daily maximum precipitation for

moderate and extreme conditions, respectively. Such increases in the daily rainfall could result in more flooding in the city.

To evaluate the effect of climate change on water quality, we evaluated the change in the monthly average precipitation, and a comparison of the values in Figure 4.5.5 clearly indicates that annual precipitation simulated from the GCM output is little different than that observed currently. The total annual precipitation values in the case of observed_2015, Sim_2030_MRICGCM3_45, Sim_2030_MIROC5_45, Sim_2030_MRICGCM3_85, and Sim_2030_MIROC5_85 were 844.8, 883.1, 802.0, 831.8 and 822.1 mm, respectively. to estimate the effect of precipitation alone on water quality, we fixed the other parameters, such as population growth, as constants and then used the simulated precipitation value as an input for the future water quality simulation starting from year 2016, i.e., immediately following the year 2015. Finally, we used MRICGCM3 with RCP_8.5 for the water quality simulation.

Table 4.5.3. Daily maximum rainfall for current and future climate

Return period, years	Current climate	Future climate	
		Average	Extreme
50	195	258	300
100	217	290	336

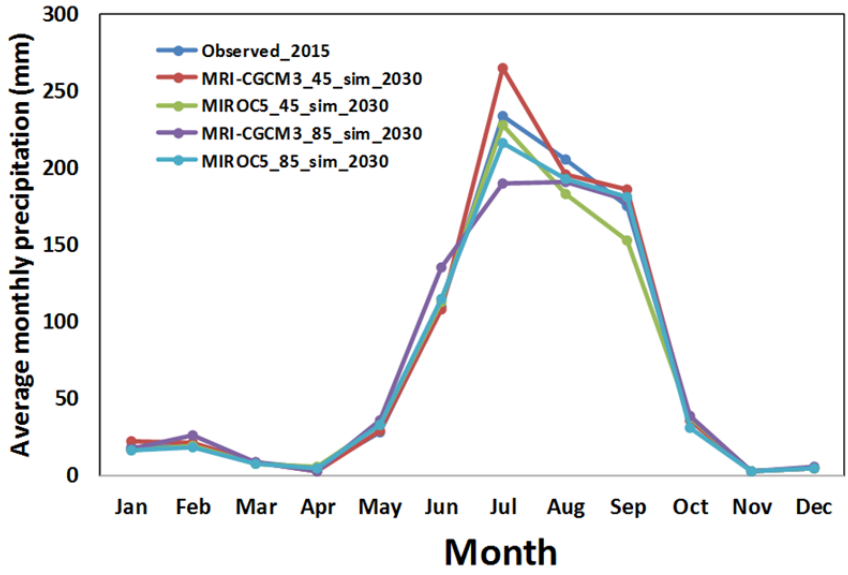

Figure 4.5.5. Comparison of current and future monthly rainfall at the IMD Dept. station

4.5.3.2 Land cover change

Figure 4.5.6 shows the classification of the current and future LULC maps, the comparison of which revealed an expansion of built-up areas accounting for 22% of the city. Urbanization is considered a driving factor of the magnitude of flooding, so the local government should adopt suitable strategies for urban planning.

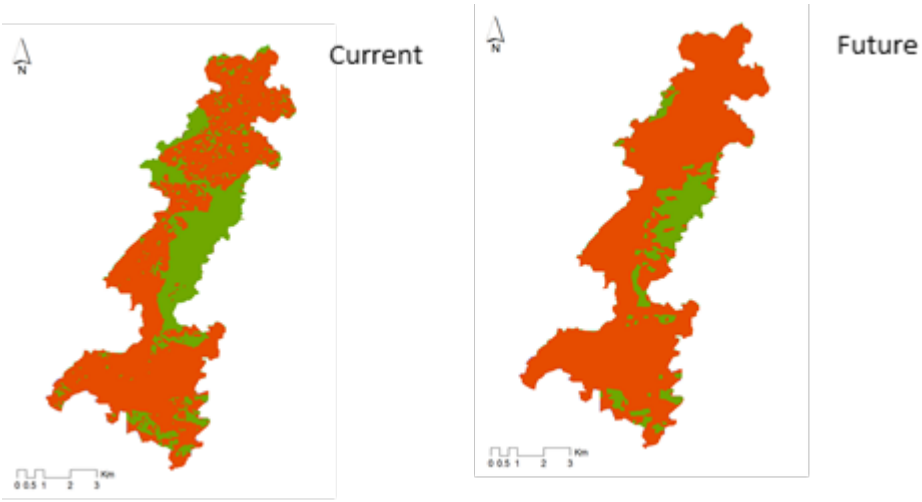

Figure 4.5.6 Land cover change map of the Kukrail watershed

4.5.3.3 Urban flooding

Figure 4.5.7 provides a spatial comparison of flood inundation over the Kukrail River basin for current and future climate conditions. In 2030, the effect of the projected climate change (moderate) can increase the area subjected to urban flooding by 20% for the 100-yr return period, and increasing future urban flood inundation reveals the need to improve flood management systems for the sustainable development of urban water environments. When analyzing the results for 50- and 100-year return periods, it was found that the peak discharge volume at the outlet of the Kukrail River may increase by 10% to 75% depending on the emission scenario. A significant reduction in peak discharge and runoff volumes was observed by attenuating the excess precipitation through source control infiltration measures. The key findings of the runoff modeling in the Kukrail River basin include a clear trend of increasing peak discharge and runoff volumes from the current to best-case to extreme-case scenarios and a gradual decrease with the use of infiltration facilities. The excess runoff can be managed onsite by implementing stormwater infiltration measures that can reduce the intensity of peak discharges under favorable conditions but only to a certain limit in extreme cases. Moreover, Lucknow is experiencing a trend of decreasing groundwater in aquifers due to overexploitation of water resources, so the prime target areas to install the infiltration system should help the rainwater permeate deeper to also increase the water levels of the aquifer. It should also be noted that infiltration facilities are more effective for short-term planning, so they may or may not generate positive results with extreme climate change. Therefore, the planners and policymakers in Lucknow should consider the role of onsite stormwater infiltration facilities and include them in the future master plan.

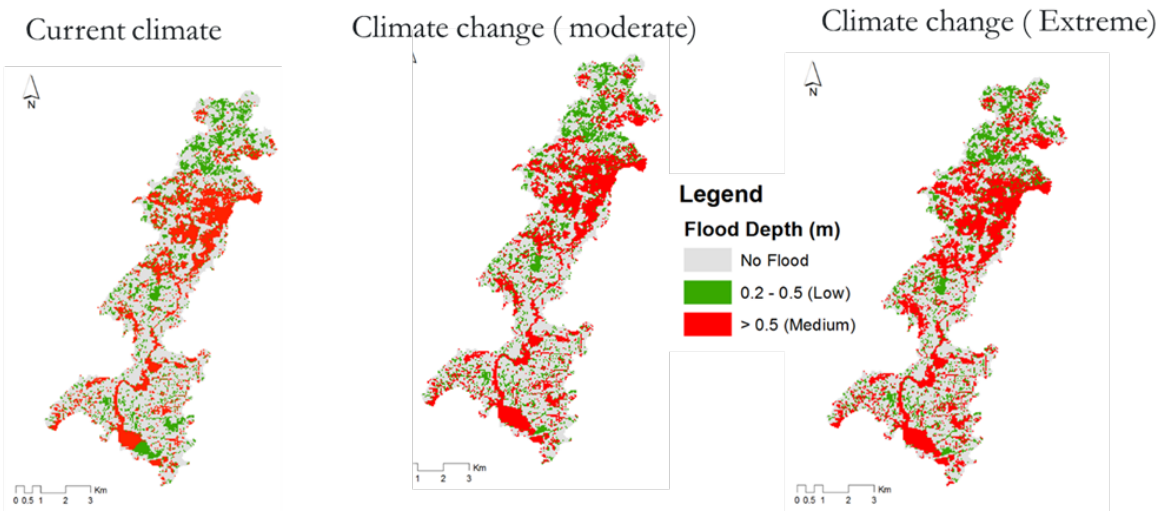

Figure 4.5.7. Comparison of flood inundation over the Kukrail River basin, Lucknow

4.5.3.4 Direct flood damage

The flood damage was evaluated in the Kukrail River basin in Lucknow, and the analysis emphasized some portions of two districts, namely, Lucknow and Bakshi Ka Talab. The spatial distribution of flood loss demonstrated that damage will be significant in the future, as exhibited in Figure 4.5.8. Compared to the current situation, it was estimated that flood damage will increase by 56%.

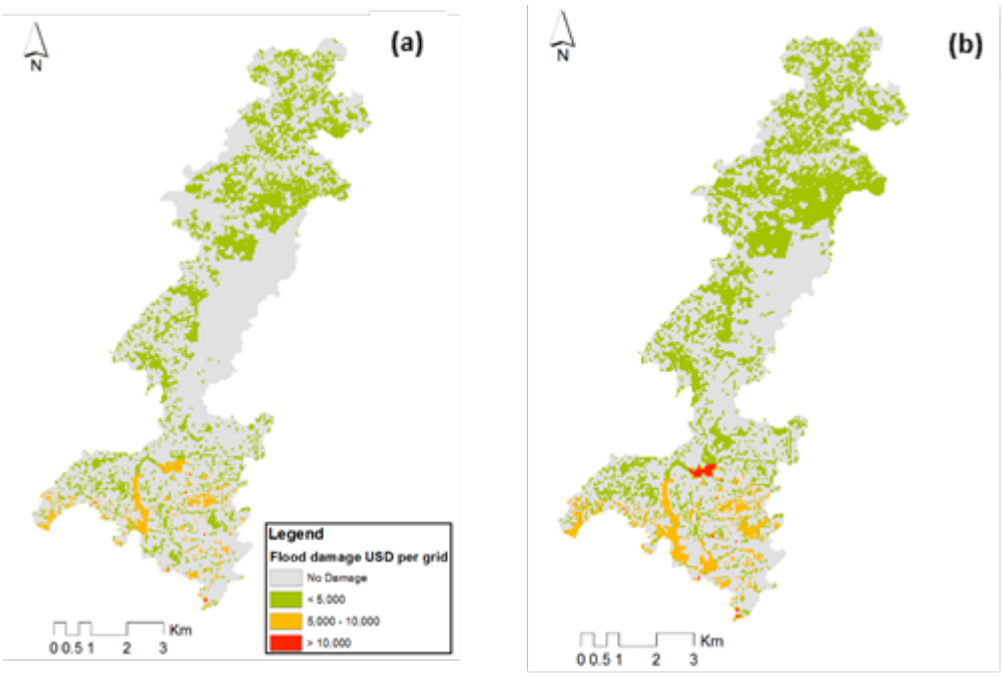

Figure 4.5.8. Spatial distribution of flood damage: (a) current situation without the effect of climate change and (b) future situation with the effect of climate change

The results by district indicated that the extent of flood damage is not only correlated with water depth but with the exposure of assets to flooding. Figure 4.5.9 shows that damage will particularly increase with the level of water depth, but the comparison of the LULC in the two cities indicated that the expansion of built-up areas will be 28% and 7% in Bakshi Ka Talab and Lucknow, respectively. Indeed, urbanization leads to an increase in the vulnerability of built-up areas to flood hazard. The quantification of future flood loss will make local decision makers aware of the risk of flooding and convince them to adopt suitable strategies for flood risk reduction at local and regional scales. Moreover, the identification of high-risk areas can be useful for prioritizing mitigation strategies and enable planners to implement efficient urban planning policies.

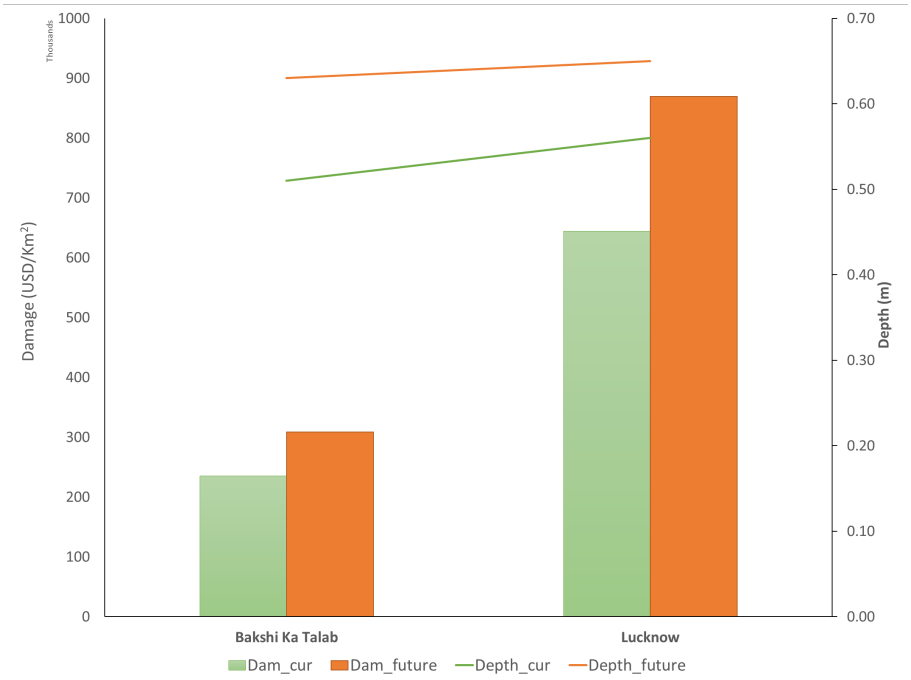

Figure 4.5.9. Flood damage by city

4.5.3.5 Water quality

Model performance evaluation

Before the future scenario analysis was conducted, the performance of the WEAP simulation was validated with observed and simulated hydrological and water quality parameter values. In the case of hydrology module validation, the parameters (mainly effective precipitation and runoff/infiltration) were adjusted using the trial and error method during simulation to reproduce the observed monthly stream flows for the 2013 to 2015 period (Table 4.5.4), and the final best-fit values for both parameters were 93% and 60/40, respectively. Figure 4.5.10 (a) compares the monthly simulated and observed stream flows at Pipraghat (average value for 2012-2014) and shows that they largely match for most months with a correlation coefficient (R^2) ≅ 0.80, a root-mean-square error (RSME) ≅ 0.25, and an average error of 10%. The three months were selected for

validation because there is no water available in the river at other times of the year, especially during the dry period. In contrast, the water quality simulation was validated by comparing the yearly average simulated and observed BOD concentrations for the year 2014 at different locations from upstream to downstream. These locations and time, i.e., the year 2014, were selected based on the consistent availability of observed water quality data. The results indicated a strong relationship between these two datasets (Figure 4.5.10 (b)) (with an error of 12%), confirming the suitability of the model performance in this problem domain.

Table 4.5.4. Summary of parameters and steps used for calibration

Parameter	Initial Value	Step
Effective precipitation	100%	±0.5%
Runoff/infiltration ratio	50/50	±5/5

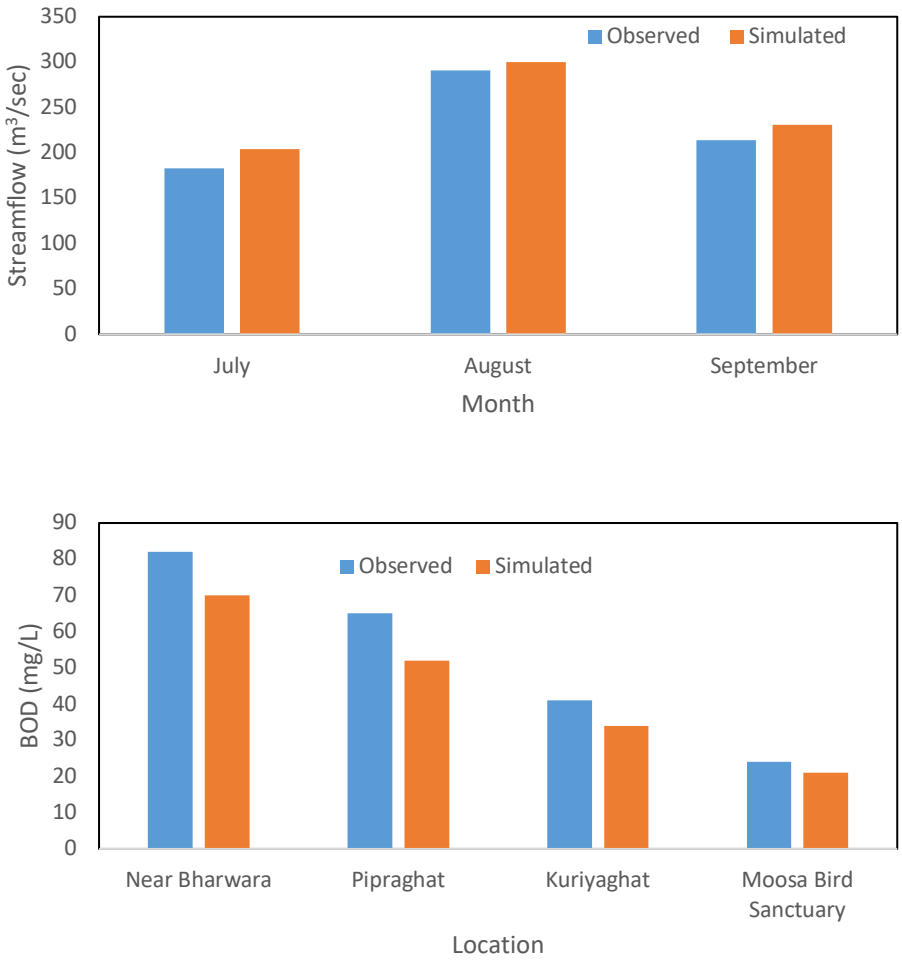

Figure 4.5.10. Validation of the model output by comparing simulated and observed (a) average monthly river discharge for the 2012-2014 period at Pipraghat and (b) average BOD values for different locations for the year 2014

Future Water Quality simulation and scenario analyses

Water quality was simulated using two possible scenarios, as shown in Table 4.5.5, for the years 2015 and 2030 using 2011 as a reference year and considering population increase and land use change as well as wastewater generation and its treatment at wastewater treatment facilities. First, under the business-as-usual scenario, the effects of population growth and climate change on water quality were observed using the average values of two GCMs and two RCPs while keeping the capacity of all the existing wastewater treatment plants (145 MLD) constant to the year 2030. Here, small bars show the ranges of the simulated water quality values because of change in the GCMs and RCPs. For the scenario with measures, all conditions were kept the same as in the first simulation except the wastewater plant capacity and collection rate were increased as shown in Table 4.5.2.

Table 4.5.5. Summary of all the criteria considered for different future water quality simulation scenarios

Scenario	Components
Business as usual	Climate change + population growth +WWTP of 145 MLD
With measures	Climate change + population growth +WWTP of 1119 MLD (100% collection rate)

Future simulation of water quality using selected parameters (BOD, and *E. coli*) was conducted under two different scenarios, namely, the business-as-usual scenario and the scenario with measures by the year 2030, and the results are shown in Figure 4.5.11. With the current wastewater treatment plant (capacity of 145 MLD and coverage of a mere 19% of the total population in the study area), the current water quality status throughout the river is very poor compared with the local guidelines for class 2 water, and it is even worse in the case of the downstream locations of the river because of the cumulative effect of waste disposal and an excess of untreated waste coming from upstream. Both climate and population changes have prominent effects on water quality, which will deteriorate further by 2030 when compared to the business-as-usual scenario. However, based on the scenario with measures, in which all the locally generated wastewater will be collected and treated by a WWTP with a capacity of 1,119 MLD, the water quality status will be much better throughout the stream, which is an encouraging sign. However, quality is still a matter of concern, especially in the downstream area. From the relationship between the wastewater collection rate and the quality of river water, it is clear that water quality can be improved to some extent just through the horizontal growth of WWTP capacity with an increase in the collection rate from 4% to 100%, as shown in Figure 4.5.12.

Explaining water quality more precisely, a high concentration of nitrate indicates the influence of untreated sewerage input, and with the climate change scenario, water quality will deteriorate at the other locations as well. The BOD value varied from 21 to 74 mg/L, which clearly indicates that all the water samples were moderately to extremely polluted relative to the BOD value required for a safe aquatic system, i.e., 3 mg/L (UPPCB 2017). The *E. coli* value, a commonly used biological indicator of water quality status, also exhibited no significant improvement in the future, possibly because of a lack of available data such as the chlorination rate. The above result suggests that current management policies and near-future water resources management plans are not sufficient to maintain pollution within the desirable limit, and it calls for transdisciplinary research into more holistic approaches for sustainable management.

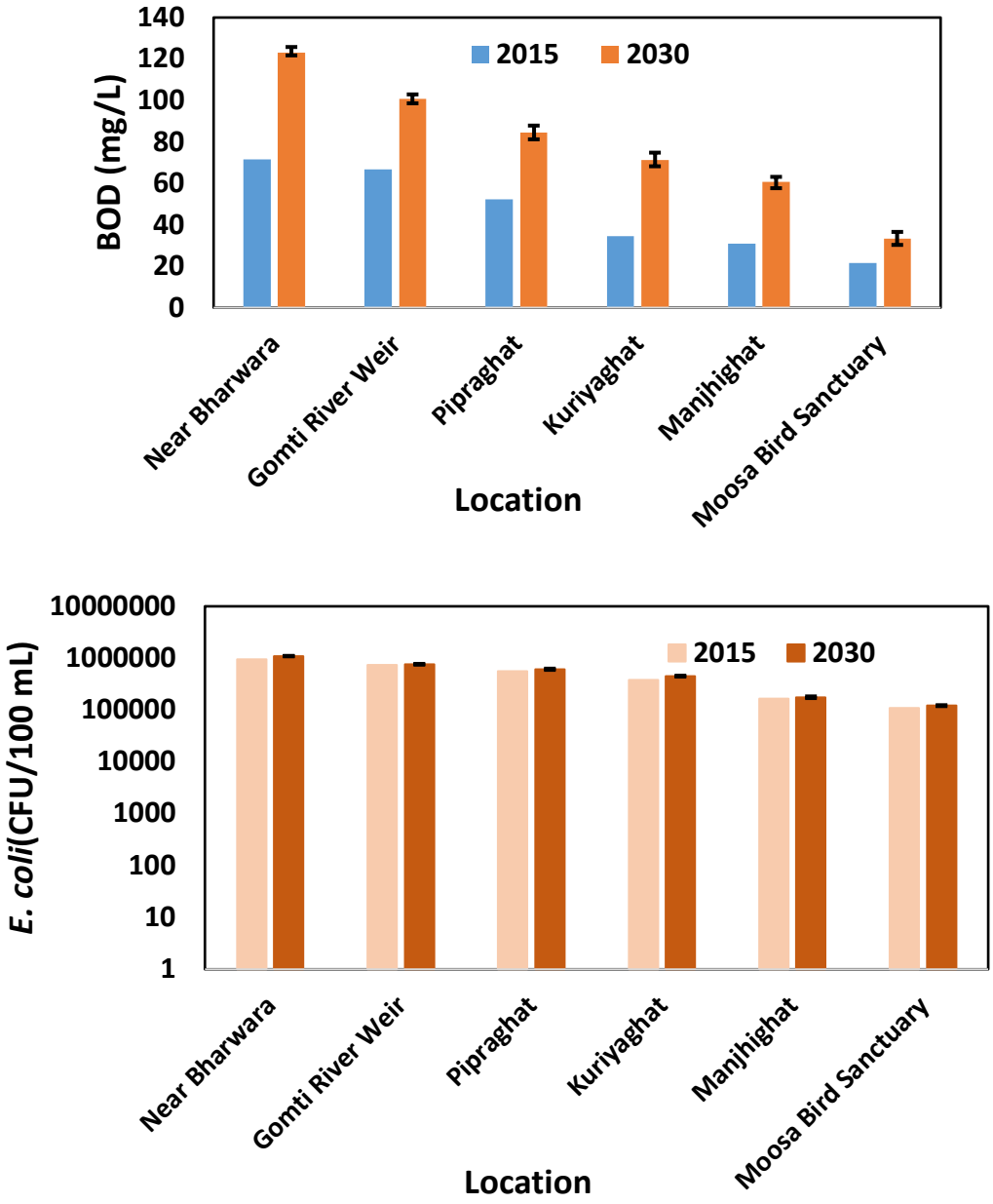

Figure 4.5.11. Simulated water quality results considering population growth, average climate change and a WWTP with a capacity of 145 MLD (business-as-usual scenario)

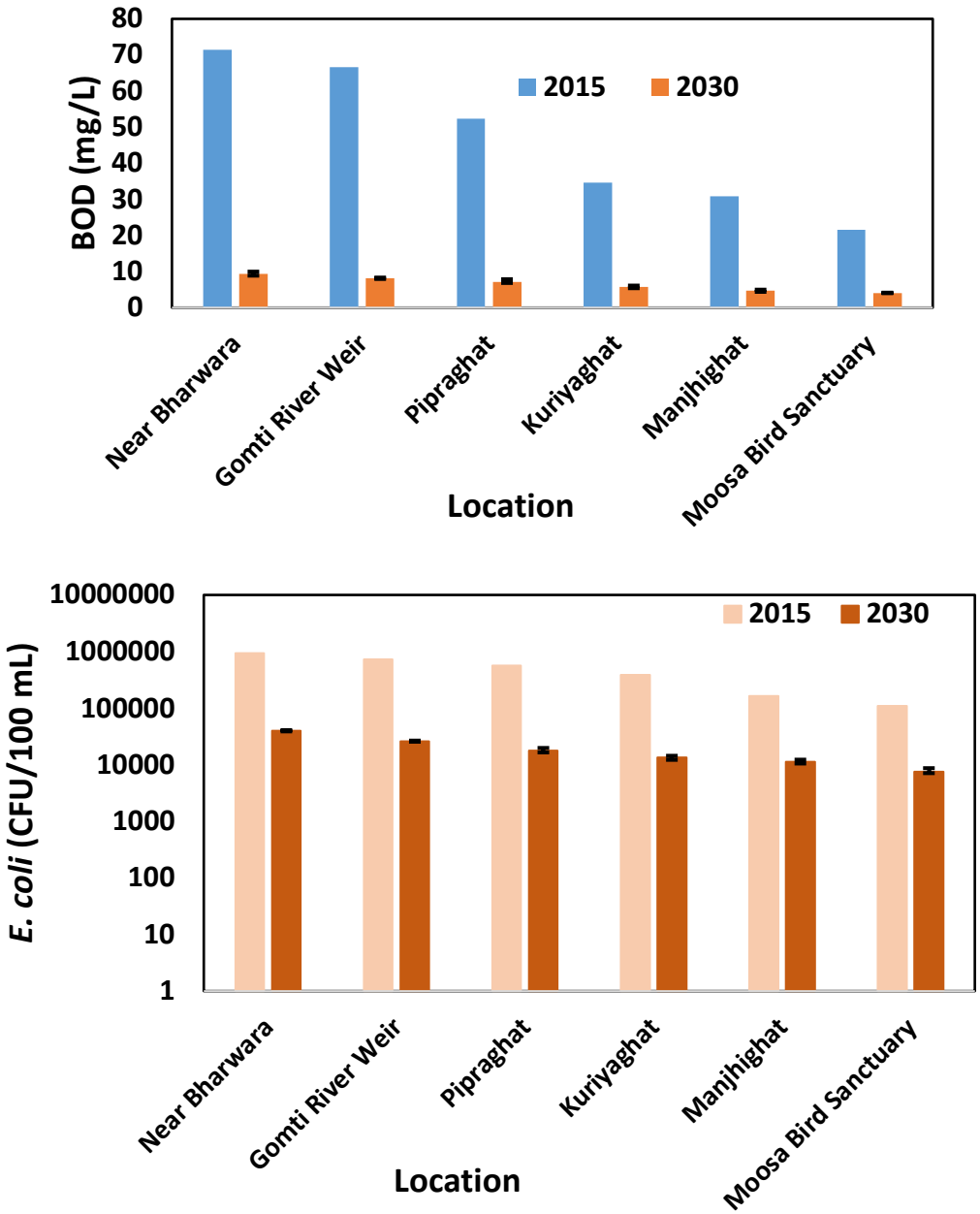

Figure 4.5.12. Simulated water quality results considering population growth, average climate change and a WWTP with a capacity of 1119 MLD (with measures)

Conclusion and policy recommendations

As expanding the wastewater treatment infrastructure to connect each household is being planned in most cities in Uttar Pradesh, this kind of simulation can be applied to other areas/cities to improve the urban water environment. Even after implementing the master plan, water quality continued to deviate from the desired quality standard, but this may be explained by a lack of consideration of factors such as climate change and differences between the water quality of river headwaters (BOD = -4 mg/L) and desirable, class B water quality (BOD < 3 mg/L). Therefore, the national integrated sewerage and septage management program should be implemented on a priority basis, considering various factors such as population density and growth and global changes for both short- and long-term measures. A lack of monetary resources has resulted in the weak implementation of government projects, so the government has not been able to provide enough wastewater facilities to treat the enormous discharges coming from domestic, industrial and solid wastes; the majority of these wastes are directly discharged into the river. Economic growth policies should be consistent with the protection, preservation and revival of the quality of the water resources in India.

4.5.3.6 Floodwater-borne infectious diseases

The simulated risk of floodwater-borne gastroenteritis under the three scenarios, expressed as the number of gastroenteritis cases caused by noroviruses per grid, is shown in Figure 4.5.13. The yellow grids represent low-risk areas (less than 0.01 cases per grid) and the white represent no risk (areas with no flooding). The estimated risk was low compared to other cities, and no high-risk (more than 0.1 cases per grid) or medium risk (0.01 – 0.1 cases per grid) grids were observed. This was because the simulated flood situation was relatively mild (see Figure 4.5.7), and the population in the study area was low under all scenarios (average population per grid was 3.3 for 2015 and 4.6 for 2030. However, it is still noteworthy that the risk was projected to increase significantly (by 125%) in the business-as-usual scenario compared to the current situation. Thus, it is recommended that stakeholders in the water management sector consider the health aspects of damages, including infectious diseases caused by urban flooding.

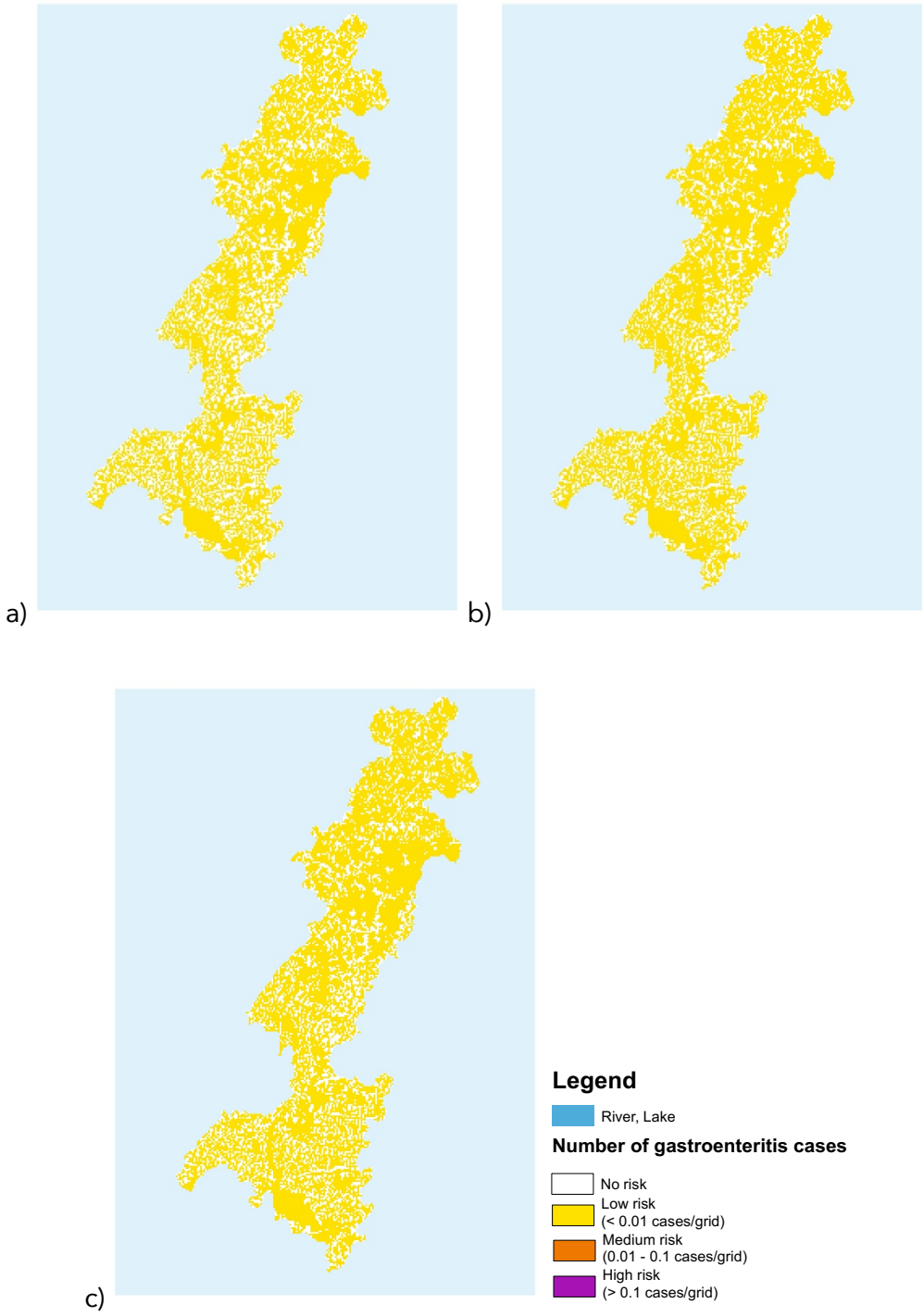

Figure 4.5.13. Simulated health risk (number of cases of gastroenteritis due to floodwater-borne noroviruses) for Lucknow under the a) current scenario, b) business-as-usual scenario, and c) with-mitigation scenario.

References

Ahmad, Z. *Hydrological study for Gomti River front development*; Project No.: CED/6134/12-13; Lucknow Development Authority: Uttar Pradesh, India; 2013.

Huizinga, J.; de Moel, H.; Szewczyk, W. *Global flood depth-damage functions. Methodology and the database with guidelines*; EUR 28552 EN; Publications office of the European Union, Luxembourg; 2017.

Khan A.A.; Gaur R.Z.; Diamantis V.; Lew B.; Mehrotra I.; Kazmi A.A.; Continuous fill intermittent decant type sequencing batch reactor application to upgrade the UASB treated sewage. *Bioprocess Biosyst. Eng*. **2013**, 36: 627–634.

Lucknow Development Authority. *Lucknow Master Plan 2031*; Lucknow Development Authority: Uttar Pradesh, India; 2016.

United Nations Department of Economic and Social Affairs, Population Division *World Urbanization Prospects: The 2014 Revision*; ST/ESA/SER.A/366, United Nations: New York, NY, 2015.

4.6 Medan

4.6.1 Introduction

Medan is the capital city of North Sumatra Province, and it is located at 3°35' N latitude and 98°40' E Longitude (Figure 4.6.1). The city is divided into 21 districts; the total population is 2,191,140; and the total area is 265 km^2. The climate is classified as equatorial and characterized by heavy and frequent rainfall; the annual rainfall is 2,263 mm, and the temperature ranges from 24°C to 32°C. There are 3 river systems in Medan city, namely, the Belawan, Deli and Percut watersheds. The Deli River is considered the most dangerous river in terms of causing flooding. In the analysis, flood risk was determined for the upper catchment area of the Deli watershed, which covers a portion of Medan city and the Deli Serdang regency, and the water quality assessment was based on the condition of the Deli River.

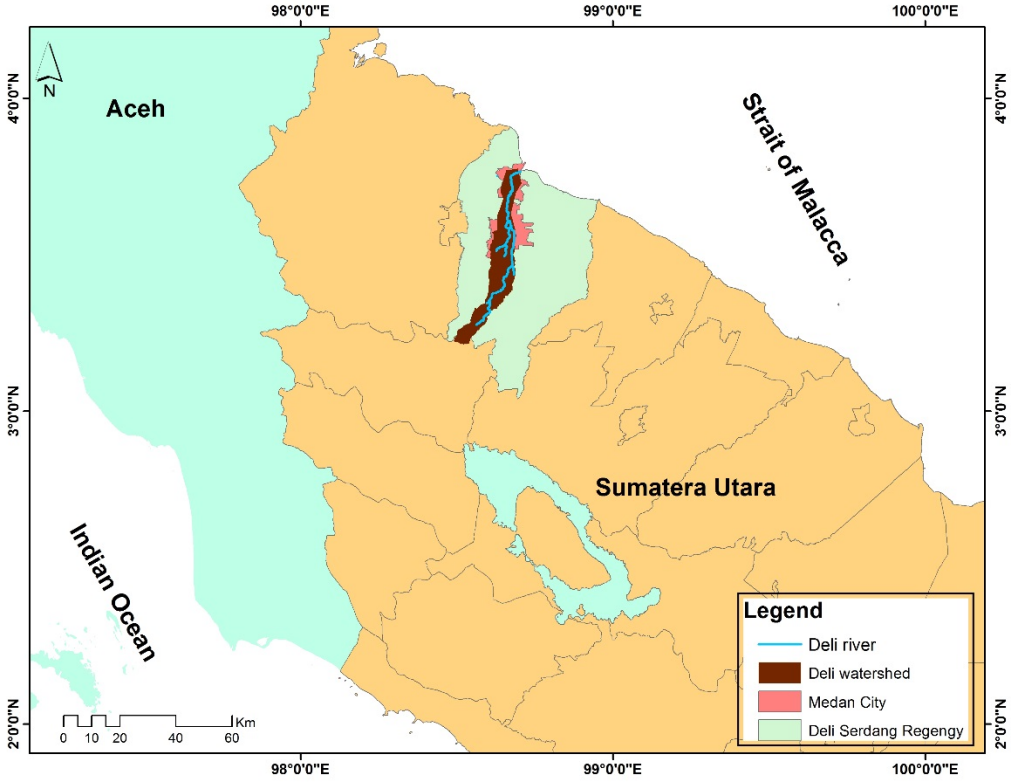

Figure 4.6.1. Location of the Deli watershed

4.6.2 Methodology

4.6.2.1 Precipitation change

In this study, precipitation was a relevant indicator for determining the effect of climate change on flooding and water quality.

For the flood analysis, the change in precipitation was determined with an emphasis on the daily maximum and mean monthly rainfall. Data were collected from three rain-gauge stations: Tutungan in the upstream, Sampali in the center of watershed, and Belawan in the downstream. The assessment of precipitation change over the study area was initiated by screening the daily rainfall

data from Sampali station, which was selected due to its location and availability of a long record (1980-2015) of rainfall data, but only rainfall data from the 1980-2004 period were considered for the precipitation change assessment. The change in daily maximum rainfall for different return periods and the mean monthly rainfall were used to compare flood inundation and river pollution conditions. Daily rainfall outputs of 3 GCMs: MRI-CGCM3, MIROC5 and HadGEM2-ES were extracted to assess future climate conditions, and out of these 3 GCMs, the MRI-CGCM3 precipitation outputs were found to be suitable considering the rainfall characteristics of the observation data. The future climate was characterized by MRI-CGCM3 rainfall data for the 2020-2044 period. The quantile mapping technique was applied to correct biases in the GCM output. Finally, empirical frequency analysis was applied to estimate the daily maximum rainfall (Figures 4.6.2, 4.6.3, and 4.6.4).

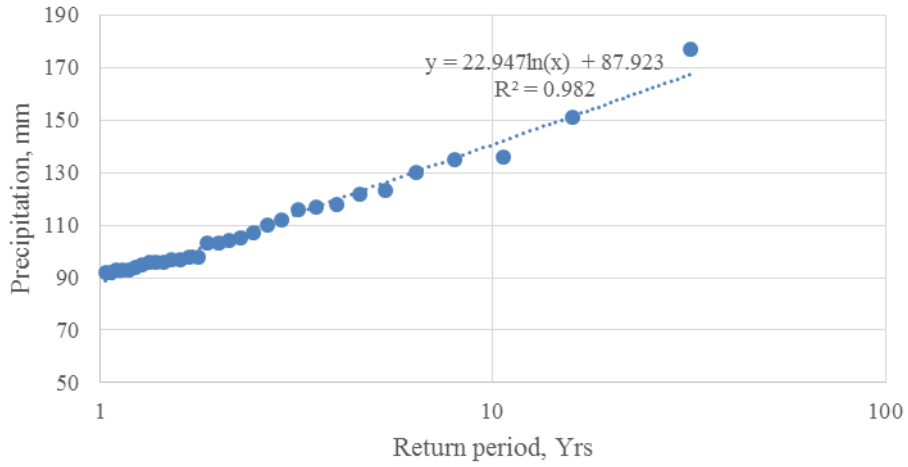

Figure 4.6.2. Empirical rainfall frequency analysis for the current climate

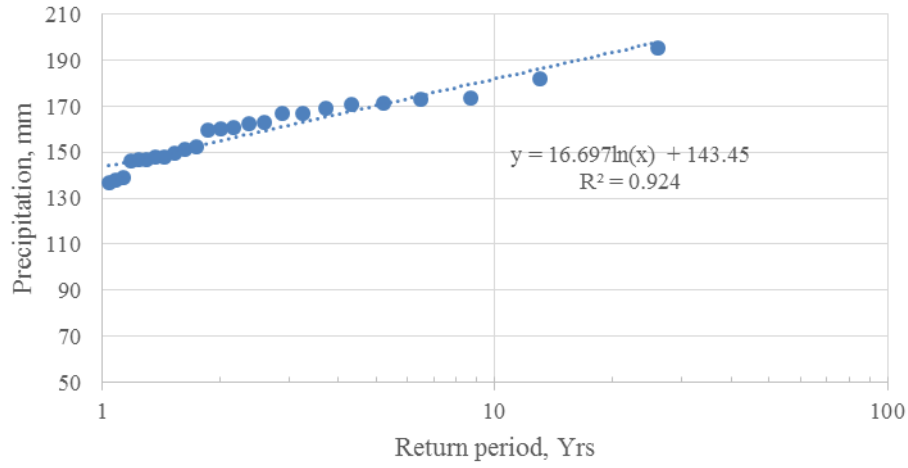

Figure 4.6.3. Empirical rainfall frequency analysis for the future climate (MRI-CGCM3 RCP 4.5)

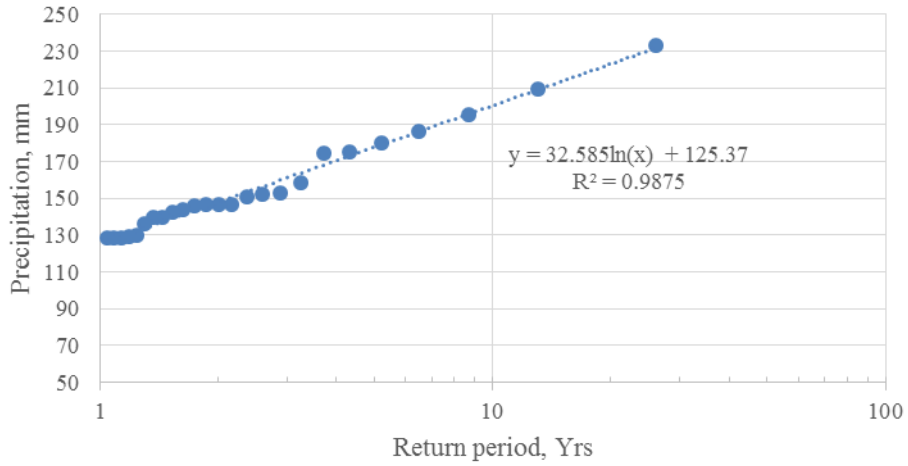

Figure 4.6.4. Empirical rainfall frequency analysis for the future climate (MRI-CGCM3 RCP 8.5)

To evaluate the effect of climate change on water quality, we evaluated the change in the monthly average precipitation. The GCM output was downscaled at the local level for reliable impact assessment (Sunyer et al., 2015). Statistical downscaling was followed by trend analysis, which is a less computationally demanding technique that enables bias reduction in the precipitation frequency and intensity (Elshamy et al., 2009), to obtain climate variables at the monthly scale. MRI-CGCM3 and MIROC5 precipitation outputs were used for the future simulation to assess the impact of climate change because of their wide use and high temporal resolution compared to other climate models. This study was based on the RCP 4.5 and 8.5 emission scenarios, which assume that global annual GHG emissions (measured in CO_2-equivalents) will peak around 2040 and then decline (IPCC 2014). In this study, the GCM data are from the 1985-2004 and 2020-2039 periods (each with a 20-year duration) and represent the current and future (2030) climate, respectively. The results shown in Figure 4.6.5 clearly indicate that the annual precipitation simulated from the GCM output differs little from the current observed data. The values for total annual precipitation in the case of observed_2015, Sim_2030_MRICGCM3_45, Sim_2030_MIROC5_45, Sim_2030_MRICGCM3_85, and Sim_2030_MIROC5_85 were 2061.6, 2139.1, 2187.1, 2114.7 and 2156.9 mm, respectively. To estimate the effect of precipitation alone on water quality, we fixed the other parameters, such as population growth, as constants and the used the simulated precipitation value as an input for the future water quality simulation starting from year 2016, i.e., immediately following 2015. Finally, we used MRICGCM3 with RCP_8.5 for the water quality simulation.

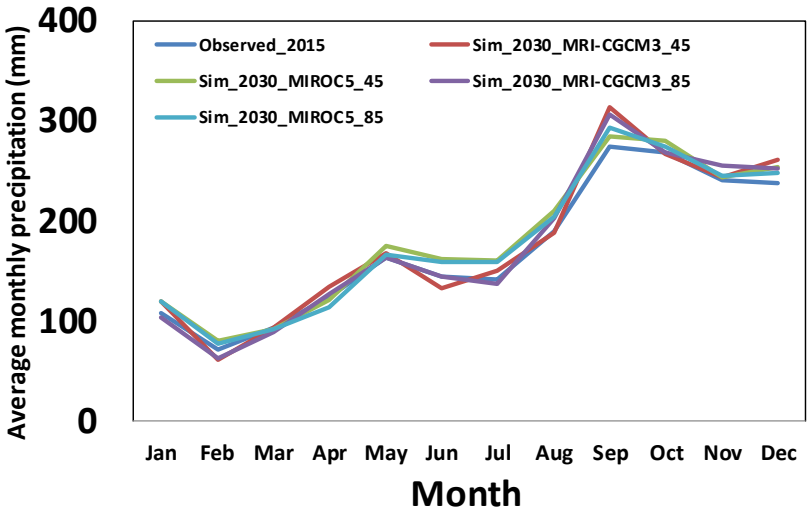

Figure 4.6.5. Graph comparing the current and future monthly rainfall

4.6.2.2 Land cover change

To predict the future land cover map of the study area for 2030, two past land cover maps were established and used for the analysis. To prepare the land cover maps for the Deli watershed, four Landsat satellite images were applied as presented in Table 4.6.1; in fact, the watershed covers two different scenes located in various Paths/Rows. For this reason, appropriate processing was required prior to image analysis and classification. The first step was to merge the two Landsat images into a single raster using the ArcGis Mosaic Dataset and then band compositing, clipping and supervised classification were performed to obtain the land cover map of the watershed. As explained in more detail in Section 3.2., Land Change Modeler for ArcGIS was used to predict the land cover pattern based on the previous change trend; only 4 classes were identified through the image classification.

Table 4.6.1. Satellite images applied

No.	Path/Row	Data Set	Acquisition Date	Land Cloud Cover
1	129/057	Landsat 7 ETM C1 Level 1	19/05/2003	1%
2	129/058	Landsat 7 ETM C1 Level 1	19/05/2003	0%
3	129/057	Landsat 8 OLI/TIRS C1 Level 1	21/02/2015	12.87%
4	129/058	Landsat 8 OLI/TIRS C1 Level 1	21/02/2015	2.54%

4.6.2.3 Population growth

To estimate the effect of population growth (one of our two key drivers) on water quality status, the entire study area was divided into different demand sites that mainly represent the populations of different cities on both sides of the Deli River within our study area and that directly impact the river through the discharge of their domestic sewerage water. The future population was estimated by the ratio method using projected growth data from UN DESA (2015). The total population of

2,200,001 was considered for base year, i.e., 2010 in our study area, and for the future population projection, the annual growth rates were 0.96, 1.58, 2.25 and 2.04 during the 2011-2015, 2016-2020, 2021-2025, and 2025-2030 periods, respectively. Henceforth, the populations considered for the current year (2015) and target year (2030) were 2,307,648 and 3,085,883, respectively.

4.6.2.4 Urban flooding

There are three river systems under the administration of Medan city: the Belawan, Deli and Percut watersheds. The Deli River has great potential for causing flood inundation; it flows through the center of Medan city, the provincial capital of North Sumatra Province, and due to its small river flow capacity, flooding has frequently occurred. The flood events have been reported to be increasing due to urbanization of the city and its surrounding area as well as the changing climate. This study aims to contribute to the reduction of flood damage, the stabilization and enhancement of human livelihoods, and the promotion of the local economy through an improved city flood risk management plan. The Medan floodway was constructed at Titi Kuning to connect the Deli River to the Percut River, and it is currently designed to discharge 70 m^3/s. It is planned that this will be increased to 120 m^3/s and beyond.

Flood modeling consists of two components: hydrologic modeling (peak discharge estimation) and hydraulic modeling (flood inundation simulation). The total catchment area of the Deli river basin is approximately 400 km^2, of which the upper catchment area (u/s of the floodway) is approximately 160 km^2. HEC-HMS was run to simulate peak discharge in the upper catchment region with an outlet at the floodway diversion point, and the FLO2D model was run for the lower watershed boundary. Topography data (DEM) were extracted from SRTM with a 30-m resolution (Figure 4.6.6).

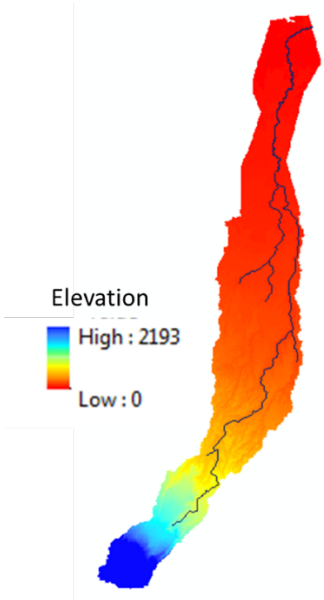

Figure 4.6.6. Deli River basin, Medan

4.6.2.5 Water quality

Basic information regarding the model and data requirements

As explained in Section 3.6, the WEAP model was used to simulate future water quality variables in the year 2030 to assess alternative management policies in the Deli River basin. Apart from our main objective, the model also simulates river flow, storage, pollution generation, treatment and discharge while considering different users and environmental flows. For water quality modeling, a wide range of input data is used including point and nonpoint pollution sources, their locations and concentrations, past spatiotemporal water quality, wastewater treatment plants, population, historical rainfall, evaporation, temperature, drainage networks, river flow-stage-width relationships, river length, groundwater, surface water inflows and land use/land cover.

The WEAP model was developed for the Deli River basin for four command areas with interbasin transfers. Hydrologic modeling requires that the entire study area be split into smaller catchments with consideration of the confluence points and physiographic and climatic characteristics (Figure 4.6.7). The hydrology module within the WEAP tool enables the catchment runoff and pollutant transport processes into the river to be modeled; pollutant transport from a catchment accompanied by rainfall-runoff is enabled by ticking the water quality modeling option. Pollutants that accumulate on catchment surfaces during nonrainy days reach water bodies through surface runoff, and the WEAP hydrology module computes the catchment surface pollutants generated over time by multiplying the runoff volume by the concentration or intensity for different types of land use.

During the simulation, the land use information was broadly categorized into three areas, viz., agricultural, forest, and built-up. The soil data parameters were identified using secondary data and the literature.

Daily rainfall has been collected at Sampali meteorological station for the period from 1990 to 2010, and daily average stream flow data from 2005-2014 were measured at five stations, namely, Mangonsidi, Raden Saleh, Unibis, Simpang Kantor and Medan Labuhan, on the Deli River and utilized to calibrate and validate the WEAP hydrology module simulation. Data for the water quality indicators (BOD and *E. coli*) were also collected at four of the above five stations and used for water quality modeling. The resulting population distributions and their future trends in these four command areas were calculated by the ratio method using the UN DESA projection rate as explained in Section 4.6.2.3. Regarding the future precipitation data, a different GCM output was used after bias correction, which is explained in detail in Section 4.6.2.1.

Model setup

The entire problem domain and its different components were divided into four catchments considering the influent locations of major tributaries (Figure 4.6.7), and other major considerations in representing the problem domain were the five demand sites and one wastewater treatment plant. Here, demand sites are meant to identify domestic populations whose attributes explain

water consumption and wastewater pollution loads per capita, water supply sources and wastewater return flows; these dynamic attributes are described as functions of time and include population and industries. Wastewater treatment plants are pollution-handling facilities with design specifications that include total capacity and pollutant removal rates. The flow of wastewater into the Deli River and its tributaries mainly occurs through domestic, industrial and stormwater runoff routes. In the absence of any precise information about the type of currently operational WWTP, the UASB-SBR type of wastewater treatment plant was considered in the modeling, and its treatment efficiency was assumed to be 97% for BOD, 77% for TN and 99.69% for fecal coliform (Khan et al., 2013). No precise data were available regarding the total volume of wastewater production from domestic sources, so in the absence of detailed information, the daily volume of domestic wastewater generation was estimated as 130 liters of average daily consumption per capita based on a literature review. Future projection were performed to determine the water quality of the Deli River in 2030 considering the effects of climate change, population growth and the existing WWTPs with a capacity of 18 MLD.

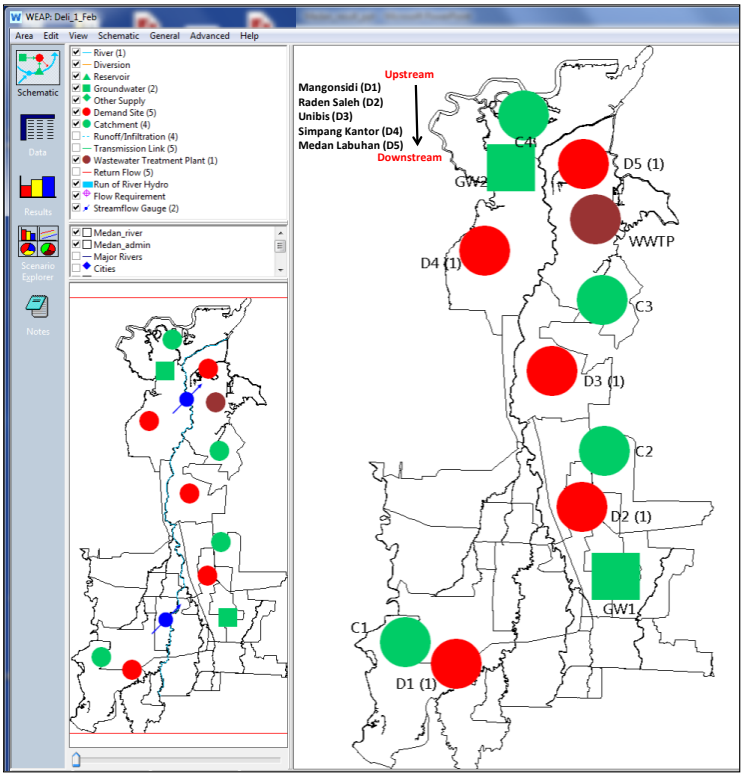

Figure 4.6.7. Schematic diagram showing the problem domain for water quality modeling in Medan using the WEAP interface

4.6.2.6 Floodwater-borne infectious diseases

Following the methodology in Section 3.8, the risk assessment model for floodwater-borne infectious gastroenteritis was developed to evaluate the number of cases of gastroenteritis caused

by noroviruses in the flooded area in Medan. Two scenarios were developed, one to simulate the current situation (current scenario) and the other to simulate the future situation as of 2030 without mitigation measures (business-as-usual scenario). The results of the flood inundation and water quality models corresponding to each scenario were used to represent the current or future urban flooding and surface water quality situations. For the business-as-usual scenario, the resulting flood simulation with MRI-CGCM3 at RCP 4.5 was used to represent the moderate climate scenario. Current and future population in each FLO-2D grid (29,304 grids in total) was calculated using the current and future population of the city as described in Section 4.6.2.3, the area of the city, and the area of the FLO-2D grid (8,100 m^2). The total population in the study area was 1,122,474 for 2015 and 1,501,018 for 2030 (34% increase).

4.6.3 Results and discussion

4.6.3.1 Precipitation change

Using bias-corrected rainfall data, the daily maximum rainfall for different return periods was estimated, Table 4.6.2 provides a comparison of the daily rainfall for the 50- and 100-year return periods. However, in this study, the 50-year daily maximum rainfall was employed to assess the flood inundation simulation, and a 17.5 and 43 percent increase was found for the RCP 4.5 and RCP 8.5 emission scenarios, respectively, relative to the baseline period. This significant increase in the daily maximum indicates that climate change should be considered in future flood risk management plans for Medan to ensure a sustainable urban water environment.

Table 4.6.2. Comparison of daily maximum rainfall for the 50- and 100-years return periods

Return period, year	Current climate	Future climate (MRI-CGCM3)	
		RCP 4.5	RCP 8.5
50	177.7	208.8	252.9
100	193.6	220.4	275.4

Using bias-corrected GCM data for the 1985–2004 and 2020–2039 periods, the climate change impacts on precipitation over the Deli River basin were assessed. First, the quantile-based bias corrections were used to identify the bias pattern in the GCM precipitation data by comparing the observations with the corresponding GCM data. A comparison of the daily precipitation values indicated that peaks in the GCM values were significantly smaller than the peaks in the observation values, and the GCM precipitation data had significantly more wet days than the observed precipitation data. The performance of the quantile-based correction technique was evaluated by comparing the monthly average number of rainy days and daily precipitation amounts, and plots indicated a similar number of rainy days and extreme rainfall magnitudes, thereby demonstrating the effectiveness of the quantile-based bias-correction technique.

Rainfall IDF curves can be used to estimate rainfall intensities for different durations and return periods. Frequency analysis using the Gumbel extreme value method enabled the generation of rainfall IDF curves and an assessment of the change in extreme precipitation for the present and future climate scenarios over the Deli River watershed. In this study, the 1-day maximum precipitation for the 50- and 100-year return periods was determined for the current and future precipitation data sets, and these values clearly indicated that extreme precipitation events will be more frequent and intense in the future for all return periods and all durations (Table 4.6.3)

Table 4.6.3. Comparison of 1-day maximum rainfall for current and future climate conditions

Return period, years	One-day maximum rainfall, mm		
	Current	Future average of three GCMs	Future extreme among three GCMs
50	207	227	330
100	228	249	365

4.6.3.2 Land cover change

The comparison of the current and predicted land cover maps shows an increase in urban growth (Figure 4.6.8). The predicted expansion of built-up areas was approximately 20%, which may lead to increased runoff and reduced infiltration. Consequently, flood risk could be more significant in the future, so a suitable land-use plan is required to avoid increasing the vulnerability of people and buildings.

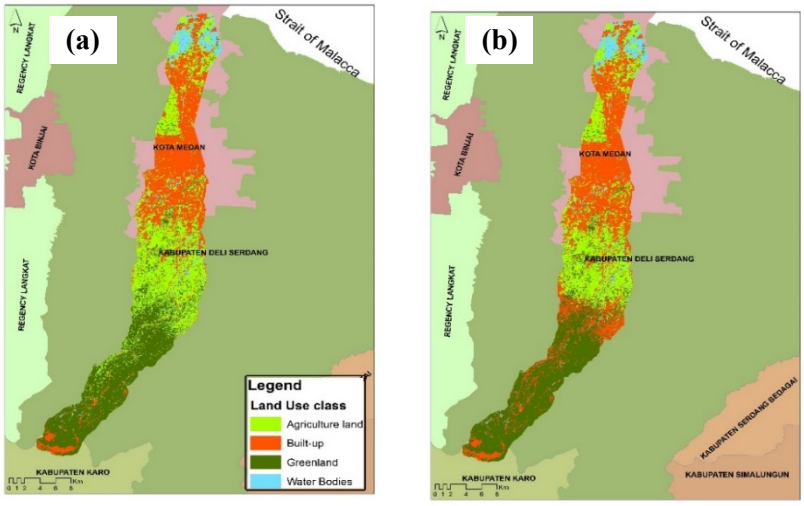

Figure 4.6.8. Land cover change map: (a) 2015 land cover and (b) 2030 land cover

4.6.3.3 Urban flooding

Although river improvement and drainage projects, including a floodway connecting the Deli and Percut Rivers, have been undertaken, flooding still occurs in Medan city. The HEC-HMS was calibrated to the November 2001 flood event, during which a peak discharge of 290 m^3/s was reported (JICA, 2010). On the other hand, the simulated flood discharge was 314 m^3/s, which can be considered acceptable. After diverting a discharge of 70 m^3/s via the floodway, the inundation simulation was performed for the current climate condition. Figure 4.6.9 provides a spatial comparison of the flood inundation simulation for the lower region under current and future conditions, and Table 4.6.4 indicates that there will be a significant increase in flood inundation despite the increased flood diversion. Flood inundation is expected to increase in 2030, especially inundation of 3-4.5 m in depth in the central and northern part of Medan and in the south along the Sungai Deli River. Therefore, the flood risk master plan for Medan must focus more attention on addressing the problem of increased flooding.

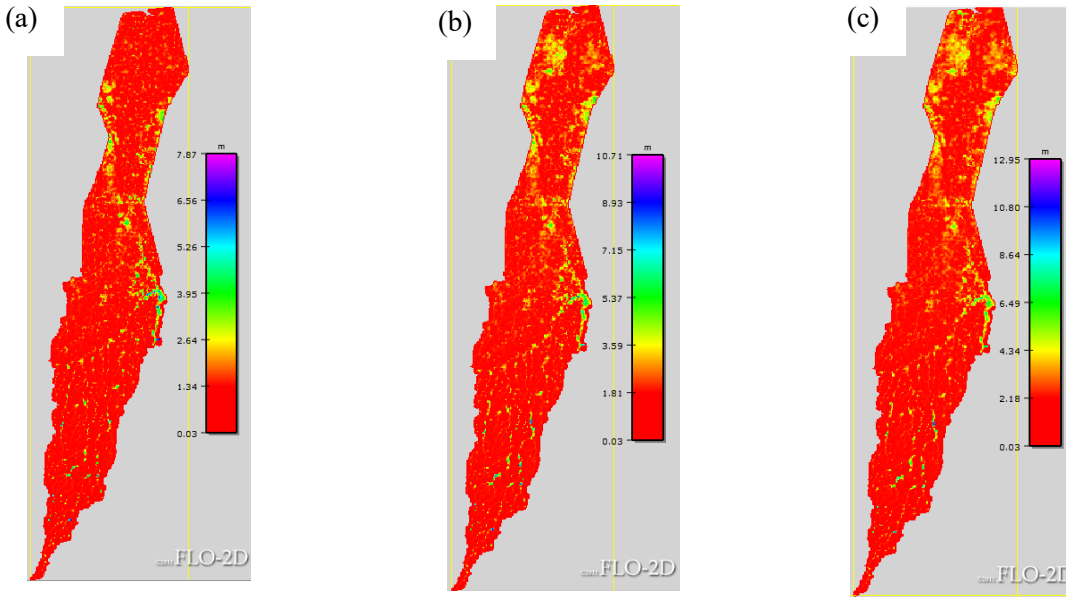

Figure 4.6.9. (a) Maximum flow depth in the current climate (2015) for the 50-year return period; (b) maximum flow depth (m) in 2030 with MRI RCP 4.5 for the 50-yr return period; and (c) maximum flow depth (m) in 2030 for MRI RCP 8.5 for the 50-yr return period

Table 4.6.4. Comparison of flood inundation under current and future climate conditions

Inundation depth, m	Inundation area, km^2	
	Current	Future
0.2-0.5	17.4	23.8
0.5-1.5	21.3	32.6
>1.5	8.2	16.6

4.6.3.4 Water quality

Future simulation of water quality using the selected parameters (BOD and *E. coli*) was conducted under the business-as-usual scenario including the effects of population growth and climate change while considering that the existing wastewater treatment plant (capacity of 18 MLD and coverage of a mere 16% of the total population in the study area) will continue to the year 2030. The results are shown in Figure 4.6.10, and it can be observed that the current water quality status throughout the river is very poor compared with the local guidelines for class 2 water (BOD < 5 mg/L; *E. coli* < 1000 CFU/100 mL), and the downstream locations of the river are even worse because of the cumulative effect of waste disposal and an excess of untreated waste coming from upstream. Under the business as usual scenario, the effects of both climate and population changes are prominent in the status water quality, which will be further deteriorated in 2030 relative to the current situation. Due to climate and population changes combined, the water quality parameters BOD and *E. coli* will further deteriorate by 54.2% and 12.4% on average, respectively, by 2030 compared to the current situation, whereas the individual contributions from population and climate change to the change in BOD and *E. coli* were 86% and 14% and 92% and 8%, respectively. Explaining water quality more precisely, a high concentration of nitrate indicates untreated sewerage input. The value for BOD varied from 5.2 to 22.6 mg/L, which clearly indicates that most of the water samples were moderately to extremely polluted relative to the BOD value required for a safe aquatic system. The *E. coli* value, a commonly used biological indicator of water quality status, also exhibited no significant improvement in the future, possibly because of a lack of available data such as the chlorination rate. The above result suggests that current management policies and near-future water resources management plans are not sufficient to maintain pollution within the desirable limit, and it calls for transdisciplinary research into more holistic approaches for sustainable management.

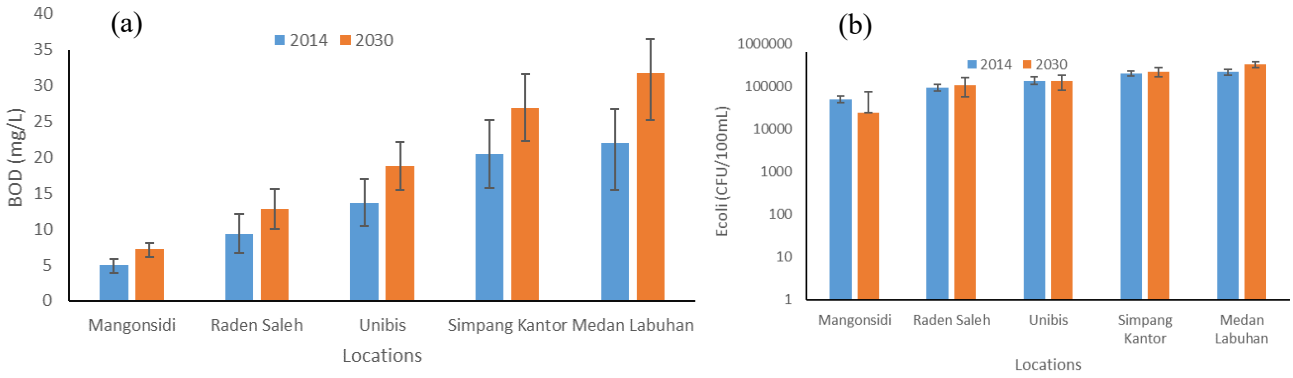

Figure 4.6.10. Simulated annual average values of (a) BOD and (b) *E. coli* for five different locations in 2014 and 2030 under different scenarios (current situation and business as usual)

4.6.3.5 Floodwater-borne infectious diseases

The simulated risk of floodwater-borne gastroenteritis under the two scenarios, expressed as number of gastroenteritis cases caused by noroviruses per grid, is shown in Figure 4.6.11. The yellow grids represent low-risk areas (less than 0.01 cases per grid), and the white represent no risk (areas with no flooding). The estimated risk was low compared to other cities, and no high-risk (more than 0.1 cases per grid) or medium-risk (0.01 – 0.1 cases per grid) grids were observed because the simulated flood (see Figure 4.6.9) and the water pollution situations (Figure 4.6.10) were relatively mild in the study area. It is still noteworthy that the risk was projected to increase significantly with the business-as-usual scenario with a 239% increase compared to the current scenario, which was the highest increase among the studied cities. Thus, it is recommended that stakeholders in the water management sector consider the health aspects of damages, including infectious diseases caused by urban flooding, when they develop future water infrastructure development plans.

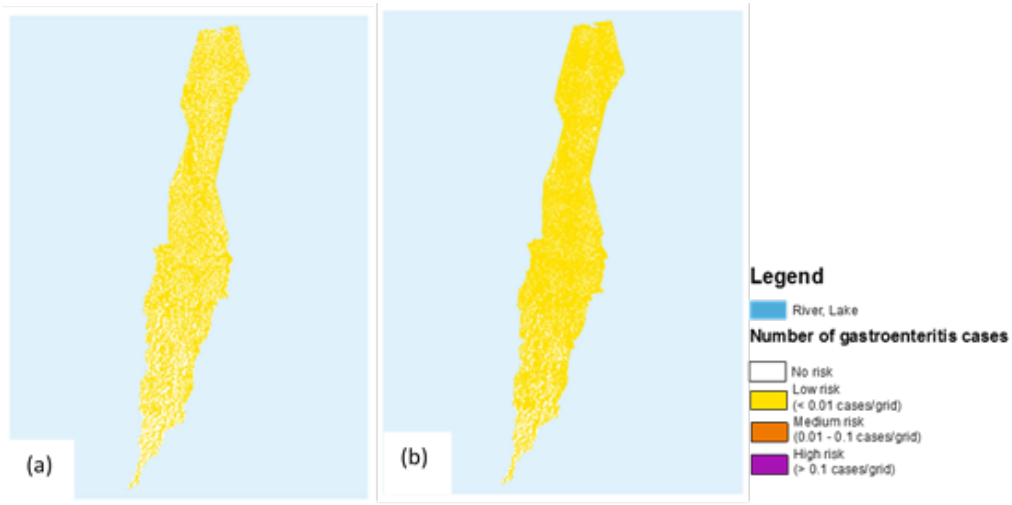

Figure 4.6.11. Simulated health risk (number of cases of gastroenteritis due to floodwater-borne noroviruses) for Medan under the (a) current scenario and (b) business-as-usual scenario

References

Elshamy, M.E.; Seierstad, I.A.; Sorteberg, A. Impacts of climate change on Blue Nile flows using bias-corrected GCM scenarios. *Hydrol. Earth Syst. Sci.* **2009**, 13: 551–565.

Intergovernmental Panel on Climate Change. *Climate Change 2014: Synthesis Report*. Core Writing Team; Pachauri, R.K., Meyer, L.A., Eds.; IPCC, Geneva, Switzerland, 2014.

Japan International Cooperation Agency (JICA). *Ex-post evaluation of Japanese ODA loan "Medan flood control project"*; 2010. https://www2.jica.go.jp/en/evaluation/pdf/2010_IP-495_4.pdf [Accessed on 18th October, 2018]

Khan A.A.; Gaur R.Z.; Diamantis V.; Lew B.; Mehrotra I.; Kazmi A.A.; Continuous fill intermittent decant type sequencing batch reactor application to upgrade the UASB treated sewage. *Bioprocess Biosyst. Eng.* **2013**, 36: 627–634.

Sunyer, M.A.; Hundecha, Y.; Lawrence, D.; Madsen, H.; Willems, P.; Martinkova, M.; Vormoor, K.; Bürger, G.; Hanel, M.; Kriauciuniene, J.; et al. Inter-comparison of statistical downscaling methods for projection of extreme precipitation in Europe. *Hydrol. Earth Syst. Sci.* **2015**, 19: 1827–1847.

United Nations Department of Economic and Social Affairs, Population Division *World Urbanization Prospects: The 2014 Revision*; ST/ESA/SER.A/366; United Nations: New York, NY, 2015.

4.7 Kathmandu

4.7.1 Introduction

With a population of approximately 3 million people, Kathmandu is the capital city of Nepal, and it extends between 27°48′00″N and 27°34′30″N latitude and between 85°12′30″E and 85°29′30″E longitude. Kathmandu Valley has been transformed almost beyond recognition due to rapidly expanding urban sprawl, and it faces problems of constantly growing traffic congestion, polluted air from vehicles and brick factories, streams and rivers that too often resemble sewers, piles of garbage and a shortage of drinking water. Water resources are being increasingly polluted by domestic, agricultural and industrial wastes, and municipal and industrial effluents are often directly discharged into natural water bodies without any treatment. Surface water sources such as rivers and ponds have received tremendous pressure from the increasing population and economic activities, whereas ground water sources are also under immense pressure as they are heavily used for drinking and other purposes. There is a sewerage system in the city, but it is inadequate and poorly maintained and usually directly connected to the rivers of the valley. Although there are some wastewater treatment systems, most do not function well. The quality of both the surface and ground water has deteriorated, so it has become essential to scientifically study the urban water environment of the Kathmandu Valley.

This research reviewed the water quality management frameworks and spatial relationships between land uses and the urban water quality of the Bagmati River in Kathmandu Valley (Figure 4.7.1), which is highly significant for drinking, agriculture, recreation, religion and several other uses, but river pollution has been a challenging problem for Kathmandu residents in recent years (Figure 4.7.2). Pollution in the Bagmati River is a serious concern for the sustainable development of the Kathmandu Valley (Mishra et al., 2017, Regmi et al., 2016, Shrestha et al., 2015, International Center for Integrated Mountain Development, 2007); the quantity and quality of the river water, particularly during the dry season, is alarming along most of the course of the river through the valley. The water quality problems affecting the Bagmati River include low dissolved oxygen concentrations, bacterial contamination, and metal toxicity, and uncoordinated rapid urban expansion, inadequate wastewater treatment facilities, low levels of awareness, a lack of regulations and insufficient adherence to municipal and industrial wastewater generation laws are considered the primary reasons for the pollution. Some sewer lines connect directly to the Bagmati River and its tributaries, and wastewater management in the valley is largely limited to the collection of wastewater that originates from different sources through open and underground sewer lines as well as the disposal of untreated wastewater into the rivers (Regmi et al., 2014). Although several large-scale wastewater treatment plants have been constructed in the Kathmandu Valley over the years, only the Guheshwori wastewater treatment plant is currently functional.

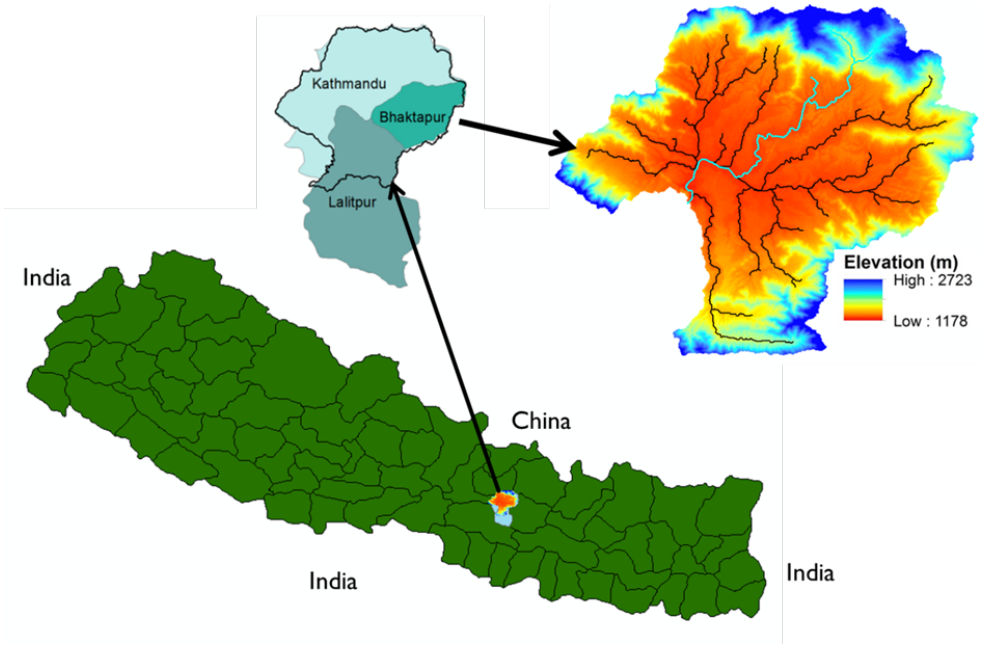

Figure 4.7.1. Location of the Bagmati River basin, Kathmandu Valley, Nepal

Figure 4.7.2. Polluted Bagmati River (downstream of the Pashupati area)

4.7.2 Methodology

4.7.2.1 Population growth

The amount of water required for drinking as well as domestic, industrial, and recreational uses has increased over time with the increase in the population, quality of life, economic activities, and development activities in Kathmandu. The standard method of projected population growth is the

cohort-component method, and the population was projected at the national level using this method. However, because of the lack of reliable demographic parameters at subnational levels, the ratio method was used instead of the cohort-component method. Ratio trend or step-down techniques assume that the relationship between a locality and some larger geographic entity (county or state) will prevail in the future and that larger-scale population projections represent degrees of reliability and components of details that cannot be achieved at a smaller analytical scale. The cohort-component method (i) uses the components of demographic change to project population growth, (ii) projects the population by age groups, (iii) and is based on the components of demographic change including births, deaths, and migration. Information necessary for the cohort-component method, including the sex ratio at birth, life expectancy at birth, life table survival ratios for males and females, age-specific fertility rates and net migration, was taken from UN DESA (2013).

4.7.2.2 Water quality

This research simulated and compared the spatial and temporal variations in two important water quality variables to explore pollution management options for the Bagmati River in Kathmandu Valley. This study focused on a 25-km length of the Bagmati River inside Kathmandu Valley (Figure 4.7.3), and dissolved oxygen (DO) and BOD were simulated along sections of the Bagmati River to identify problems related to the degradation of the water environment. Examining the DO and BOD values along different sections of the Bagmati River could help to determine acceptable maximum pollution loads for the river, so an in-depth review of the Bagmati River basin was conducted to understand its physiography, hydroclimatology, wastewater generation and management systems to simulate the DO and BOD values. The water quality and hydrology modules of the WEAP tool enabled DO and BOD to be simulated along sections of the Bagmati River. Considering the wastewater generation and treatment systems likely to be in place by 2030, DO and BOD values were simulated to analyze current conditions and the future outlook of the urban water environment. Finally, simulated current and future DO and BOD values were compared to explore alternative wastewater management options to enhance the urban water environment.

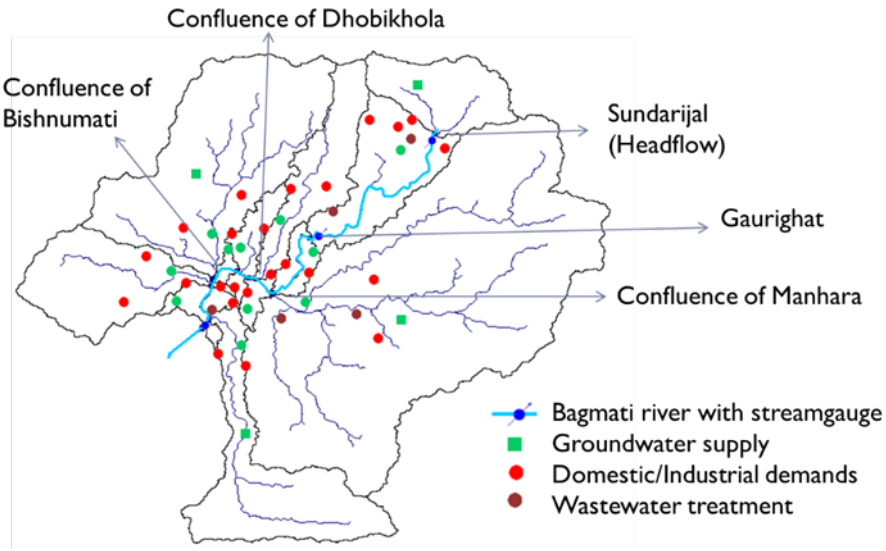

Figure 4.7.3. Bagmati River network and the locations of wastewater treatment plants, water quality stations, and streamflow measurement stations in Kathmandu Valley

4.7.3 Results and discussion

4.7.3.1 Population growth

Figure 4.7.4 provides a spatial graph of the current and projected population over the Kathmandu Valley. The ratio method was used to estimate the current (2014) and 2030 population inside the area, and Figure 4.7.5 illustrates the spatial distribution of population growth for the study area (the Bagmati River basin upstream of Chovar). The growth of the population in the Kathmandu Valley is above the average for other urban areas of Nepal, and a more than 50% increase is projected by 2030. Consequently, the volume of wastewater will greatly increase, and the growth of the transient and migrant population in Kathmandu could lead to haphazard urbanization of the Kathmandu Valley, resulting in further degradation of the urban water environment.

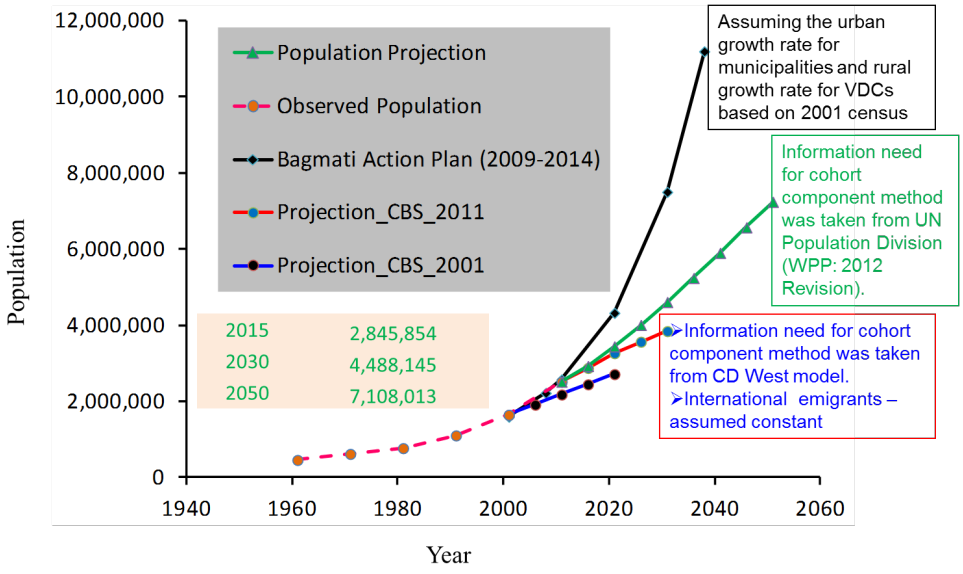

Figure 4.7.4. Population projections for Kathmandu Valley, Nepal

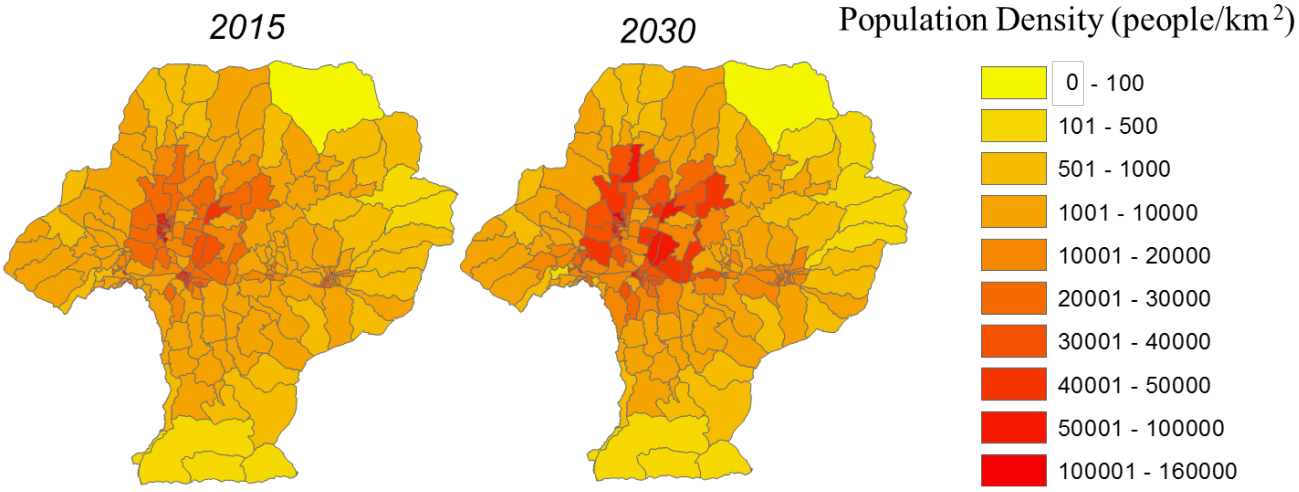

Figure 4.7.5. Population distribution over the study area (Bagmati River basin upstream of Chovar)

4.7.3.2 Water quality

With 2014 as the baseline year, BOD and DO values were simulated and compared for 2020 and 2030 considering wastewater generation and new/rehabilitated WWTPs. A sample of the DO and BOD levels generated by the WEAP model is presented to describe the pollution of the surface water in the Bagmati River in terms of flow variability, spatial extent, future trends and alternative water quality management options. Figures 4.7.6 and 4.7.7 show fluctuations in DO and BOD along the Bagmati River in January 2014; the Bagmati River was found to be most polluted near Teku Dovan, with simulated monthly DO and BOD values of nearly 0 mg/l and 190 mg/l, respectively. DO decreases and BOD increases as the river flows towards the center of the city; in most parts of the river, DO is less than 5 mg/l and BOD is greater than 15 mg/l, indicating that the quality of the river

water is extremely poor and not suitable for aquatic life or agricultural use. The water quality of the Bagmati River was found to improve significantly due to increased monsoon river flow. However, a comparison of the simulated DO and BOD values for 2020 and 2030 with those of 2014 indicated that the water quality of the Bagmati River within the Kathmandu Valley will not significantly improve as a result of the planned wastewater treatment plants.

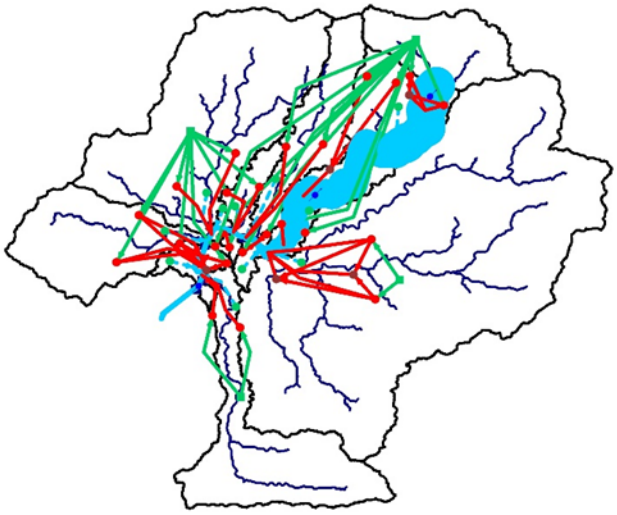

Figure 4.7.6. Variation in DO (8.5 to 0 mg/l) along the Bagmati River in January 2014

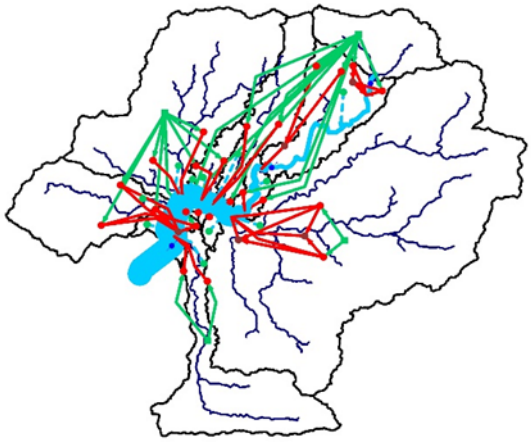

Figure 4.7.7. Variation in BOD (2.4 to 190 mg/l) along the Bagmati River in January 2014

The extent of pollution caused by releasing untreated sewage into the river system and the impact of the two management plans were also determined, and the simulation results showed that the current practice of discharging untreated sewage into the river system is causing widespread pollution that escalates to an alarmingly hazardous state during drier periods. The proposed countermeasures were found to be largely ineffective at reducing the extent and duration of surface

water pollution due to the increasing urban growth. Furthermore, the results indicate that water quality is largely unsuitable for any practical use from the Gaurighat area to the Chovar section. In summary, the severe deterioration of water quality in the Bagmati River requires immediate and effective action; it is essential to integrate water quality management and land use planning to protect water quality and maintain ecologically and economically healthy land development in the Kathmandu Valley.

References

International Center for Integrated Mountain Development. *Kathmandu valley environment outlook*; International center for integrated mountain development (ICIMOD): Kathmandu, Nepal; 2007.

Mishra, B.K.; Regmi, R.K.; Masago, Y.; Fukushi, K.; Kumar, P.; Saraswat, C. Assessment of Bagmati River pollution in Kathmandu Valley: Scenario-based modeling and analysis for sustainable urban development. *Sustainability of Water Quality and Ecology* **2017**, 9-10: 67-77.

Regmi, R.K.; Mishra, B.K.; Luo, P.; Toyozumi, A.; Fukushi, K; Takemoto, K. A preliminary trend analysis of DO and BOD records in Kathmandu, Nepal: Towards improving urban water environment in developing Asian countries. In *Proceedings of 11th International Symposium on Southeast Asian Water Environment*, 2014, pp. 371-376.

Regmi, R.K.; and Mishra, B.K. *Current water quality status of rivers in the Kathmandu Valley*. Water and Urban Initiative Working Paper Series, No. 06; United Nations University: Tokyo, Japan; 2016.

Shrestha, N.; Lamsal, A.; Regmi, R.K.; Mishra, B.K. *Current status of water environment in Kathmandu Valley, Nepal*. Water and Urban Initiative Working Paper Series, No. 03; United Nations University: Tokyo, Japan; 2015.

United Nations, Department of Economic and Social Affairs, Population Division. *World Population Prospects: The 2012 Revision*; ESA/P/WP.228; United Nations: New York, NY, 2013.

4.8 Nanjing

4.8.1 Introduction

Nanjing city, which is the capital of Jiangsu province, is located in eastern China (31°14'N, 118°22'E) in the lower Yangtze River drainage basin and the Yangtze River Delta economic zone (Figure 4.8.1). The city is surrounded by hills on three sides with the Yangtze River to the northwest, and the typical topographic features are hills, rivers, plains, and islands. The name of the city means "Southern Capital," and it has a history of more than 2,400 years.

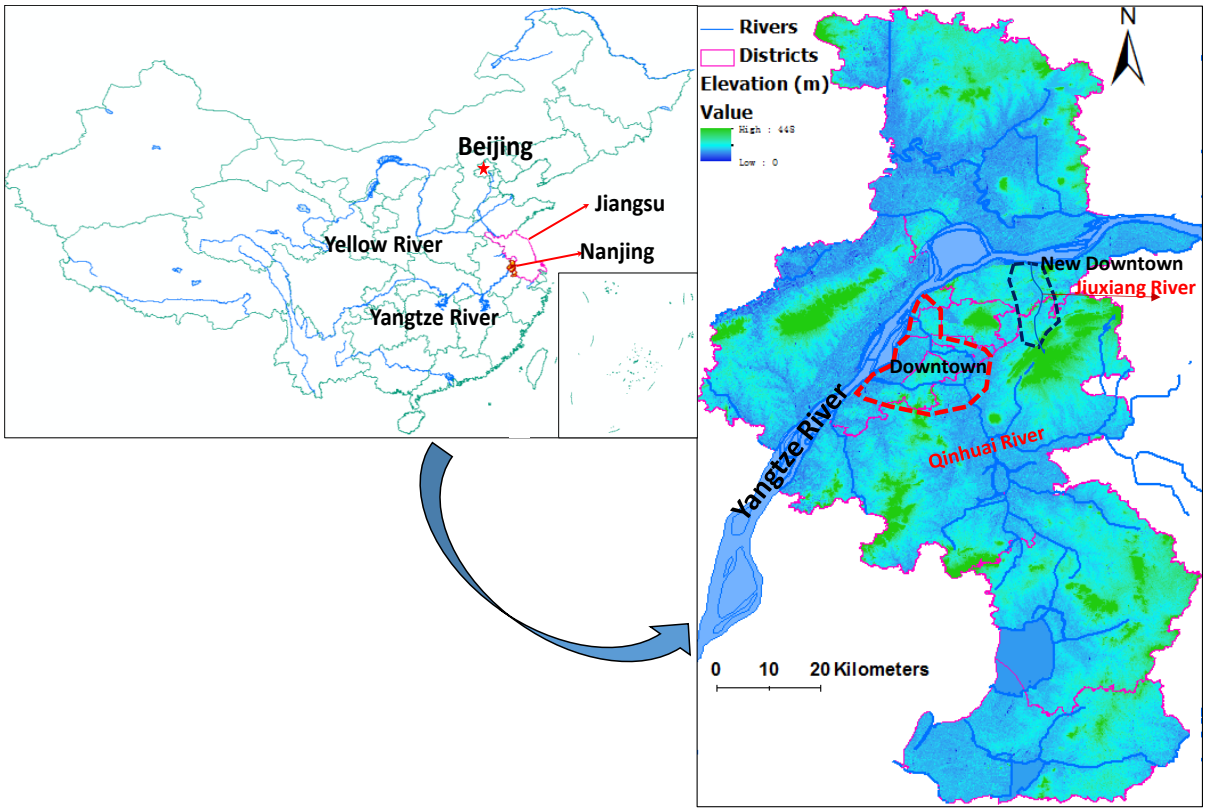

Figure 4.8.1. Location of Nanjing.

With a total land area of 6,598 km^2, Nanjing comprises 11 districts and is strategically located at the confluence of the Qinhuai and Yangtze Rivers, or the Yangtze River basin, in eastern China. The city is 300 km west-northwest of Shanghai, 1,200 km south-southeast of Beijing, and 1,400 km east-northeast of Chongqing. In 2013, the municipality of Nanjing had a population of 8.2 million and an urban population of 6.6 million.

Nanjing has a humid subtropical climate and is influenced by the East Asian monsoon. The plum blossom blooming season lasts from mid-June to the end of July, during which the city experiences a period of mild rain as well as dampness. However, high-intensity rainfall stresses the urban drainage system; sewers overflow and become major sources of water pollution. Flooding in urban areas is often serious because of the inadequately maintained drainage network as well as pumping

stations with insufficient capacity. Historically, the tributaries of the Qinhuai River were interconnected with sufficient flow capacity, but siltation has greatly reduced flows from these waterways. Additionally, there is no consistent sludge treatment and disposal scheme for the Jiuxiang River. At some locations, the water flow of these two rivers is completely blocked, aggravating flooding and water pollution. Therefore, it is urgent that river flow augmentation and improved flood control and water quality be accomplished through 1) river dredging, 2) river bank stabilization and erosion control, 3) river water diversion and replenishment, and 4) restoration of the degraded urban wetland area.

4.8.2 Methodology

4.8.2.1 Population growth

To estimate the effect of population growth on water quality status, the entire study area was divided into different demand sites that mainly represent the populations of different cities on both sides of the Qinhuai River within our study area and that directly impact the river by discharging domestic sewerage water. The future population was estimated by the ratio method using projected growth rate data from UN DESA (2015). The total population of 6,488,900 was considered the base year, i.e., 2013 in our study area, and for the future population projection, the annual growth rate was considered 3.54, 2.84, 1.97 and 1.32 during the 2014-2015, 2016-2020, 2021-2025, and 2025-2030 periods, respectively. Henceforth, the populations considered for the current year (2015) and the target year (2030) were 6,956,446 and 9,419,671 respectively.

4.8.2.2 Water quality

Basic information regarding the model and data requirements

The WEAP model greatly supports scenario formation functionalities through which policy alternatives can be considered for current and future conditions. The WEAP hydrology module enables the estimation of rainfall-runoff and pollutant travel from a catchment to water bodies, and scenarios can be developed based on population growth, land use/land cover, the capacity and status of treatment plants and climate change as well as several other factors that can significantly impact wastewater levels. WEAP provides a GIS-based interface to graphically represent wastewater generation and treatment systems, and a variety of WEAP applications have been reported for water quality modeling and ecosystem preservation. The model can simulate several conservative water quality variables (which follow exponential decays) as well as nonconservative water quality variables in addition to pollution generation and removal at different sites. In this study, the WEAP model was used to simulate future water quality variables in the year 2030 to assess alternative management policies in the Qinhuai River basin. Apart from our main objective, it can also simulate river flow, storage, pollution generation, treatment and discharge while considering different users and environmental flows. For water quality modeling, wide range of input data was provided including point and nonpoint pollution sources, their locations and concentrations, past spatiotemporal water quality, population, historical rainfall, evaporation, temperature (Department

of Hydrology and Meteorology), wastewater discharge and treatment facilities (Department of Drinking Water Supply and Sewerage), river flow-stage-width relationships, river length, groundwater, surface water inflows and land use/land cover (Department of Hydrology and Meteorology), water use data (Bureau of Statistics) and water quality (Department of Drinking Water Supply and Sewerage).

The WEAP model was developed for the Qinhuai River basin for four command areas with interbasin transfers. Hydrologic modeling requires that the entire study area be split into smaller catchments with consideration of the confluence points and physiographic and climatic characteristics (Figure 4.8.2), and the hydrology module within the WEAP tool enables the catchment runoff and pollutant transport processes into the river to be modeled. Pollutant transport from a catchment accompanied by rainfall-runoff is enabled by ticking the water quality modeling option. Pollutants that accumulate on catchment surfaces during nonrainy days reach water bodies through surface runoff, and the WEAP hydrology module computes the catchment surface pollutants generated over time by multiplying the runoff volume by the concentration or intensity for different types of land use.

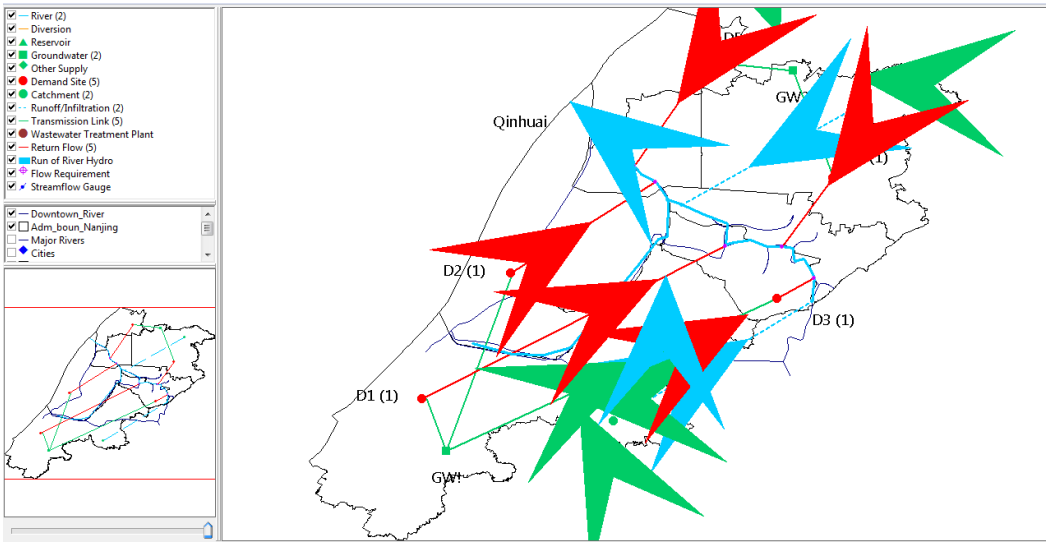

Figure 4.8.2. Schematic diagram showing the problem domain for water quality modeling in Nanjing using the WEAP interface

During simulation, the land use information was broadly categorized into three areas, viz., agricultural, forest, and built-up. The soil data parameters were identified using secondary data and the literature.

Daily rainfall was collected at the Q3 meteorological station for the 1995-2010 period, and daily average stream flow data from 2010-2016 were measured at four stations, namely, Q3, Q1, Q6 and Q9 of the Qinhuai River, and were utilized to calibrate and validate the WEAP hydrology module simulation. Data for the water quality indicators (BOD and *E. coli*) were also collected at the above four stations and used for water quality modeling (Figure 4.8.2).

The resulting population distributions and their future trends at these four command areas were calculated by the ratio method using the UN DESA projection rate as explained in Section 4.2.2.3.

Model setup

The entire problem domain and its different components were divided into two catchments considering the influent locations of the major tributaries (Figure 4.8.2), and other major considerations in representing the problem domain were the four demand sites. Here, the demand sites are meant to identify domestic (population) and industrial centers whose attributes explain water consumption and wastewater pollution loads per capita, the water supply source and wastewater return flow, and these dynamic attributes are described as functions of time and include population and industries. In the absence of detailed information, the daily volume of domestic wastewater generation was estimated as 130 liters of average daily consumption per capita based on a literature review.

The future projection was made using a business-as-usual scenario to determine the water quality of the Qinhuai River in 2030. This scenario is represented by selecting all the existing elements as currently active, which is hereafter termed the current stage. Information about each object can be easily retrieved by clicking the corresponding graphical element, and the baseline year under the current reference scenario in this study was 2013.

4.8.3 Results and discussion

4.8.3.1 Water quality

Model performance evaluation

Before conducting the future scenario analysis, the performance of the WEAP simulation was validated with observed and simulated values of hydrological and water quality parameters (mainly effective precipitation and runoff/infiltration), which were adjusted using the trial and error method during the simulation to reproduce the observed BOD value at Q1 (Table 4.8.1). The water quality simulation part was validated by comparing the simulated and observed BOD concentrations at the Q1 location; this location and time, i.e., the year 2014, were selected based on the consistent availability of the observed water quality data. The results showed a strong relationship between

these two datasets (Figure 4.8.3, with an error of 13%), confirming the suitability of the model performance in this problem domain.

Table 4.8.1. Summary of parameters and steps used for calibration

Parameter	Initial value	Step
Effective precipitation	100%	±0.5%
Runoff/infiltration ratio	50/50	±5/5

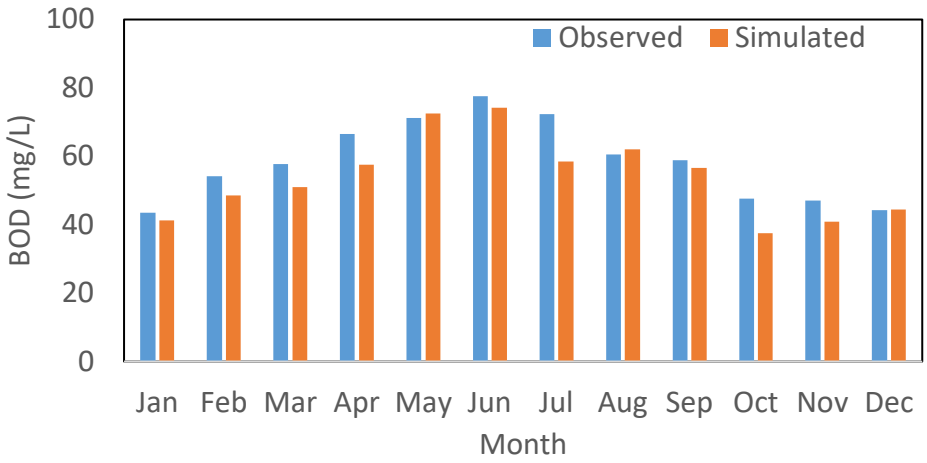

Figure 4.8.3. Validation of the model output by comparing simulated and observed BOD values for the year 2014 at Q1

Future Water Quality simulation and scenario analyses

Future simulation of water quality using selected parameters (BOD and *E. coli*) was conducted under the business-as-usual scenario, which considered the effects of population growth and the existing wastewater treatment facility in the area, for the year 2030. The simulation results for the water quality parameters using this scenario are shown in Figure 4.8.4, and the current water quality status throughout the river, as shown by the blue bar, was found to be very poor relative to the local guidelines for class 2 water (BOD < 5 ml/L, *E. coli* < 1000 CFU/100 mL), and the downstream locations of the river were even worse because of the cumulative effect of waste disposal and an excess of untreated waste coming from upstream, which also matched our observation well. Water quality will further deteriorate in 2030 compared to the current situation; due to population changes, the water quality (expressed as BOD) will further deteriorate by 40.1% on average. The value for BOD varied from 54.2 to 77.6 mg/L, which clearly indicates that all the water samples were moderately to extremely polluted relative to the BOD value required for a safe aquatic system, i.e., 5 mg/L (Department of Hydrology and Meteorology). The *E. coli* value, a commonly used biological indicator of water quality status, also exhibited no significant improvement in the future, possibly because of a lack of available data such as the chlorination rate. The above result suggests that current management policies and near-future water resources management plans are not sufficient

to maintain the pollution level within the desirable limit, and it calls for transdisciplinary research into more holistic approaches for sustainable management.

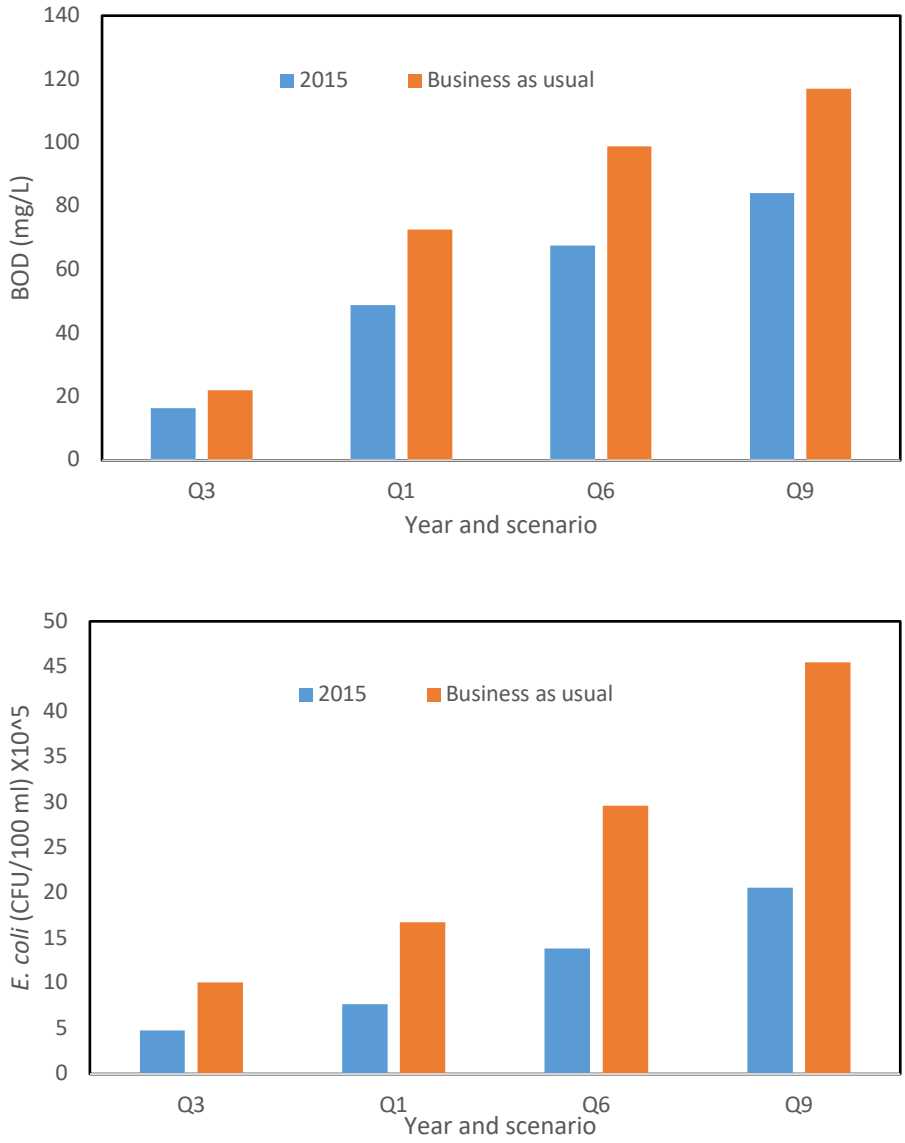

Figure 4.8.4. Simulated annual average values of (a) BOD and (b) *E. coli* for four different locations in 2015 and 2030 under different scenarios (current and business as usual)

References

Khan A.A.; Gaur R.Z.; Diamantis V.; Lew B.; Mehrotra I.; Kazmi A.A.; Continuous fill intermittent decant type sequencing batch reactor application to upgrade the UASB treated sewage. *Bioprocess Biosyst. Eng.* **2013**, 36: 627–634.

United Nations Department of Economic and Social Affairs, Population Division *World Urbanization Prospects: The 2014 Revision*; ST/ESA/SER.A/366; United Nations: New York, NY, 2015.